

## **General Disclaimer**

### **One or more of the Following Statements may affect this Document**

- This document has been reproduced from the best copy furnished by the organizational source. It is being released in the interest of making available as much information as possible.
- This document may contain data, which exceeds the sheet parameters. It was furnished in this condition by the organizational source and is the best copy available.
- This document may contain tone-on-tone or color graphs, charts and/or pictures, which have been reproduced in black and white.
- This document is paginated as submitted by the original source.
- Portions of this document are not fully legible due to the historical nature of some of the material. However, it is the best reproduction available from the original submission.

**SPACE  
DIVISION**

NASA CR-134714  
1P80-5G4-170



## MODELING AND ANALYSIS OF POWER PROCESSING SYSTEMS

by Dr. K. A. Fegley, J. H. Hayden, and D. W. Rehmann

(NASA-CR-134714) MODELING AND ANALYSIS  
OF POWER PROCESSING SYSTEMS (General  
Electric Co.) 365 p HC \$10.00 CSCL 09C

N75-11155

Unclas  
G3/33 53828

GENERAL ELECTRIC COMPANY

prepared for

NATIONAL AERONAUTICS AND SPACE ADMINISTRATION

NASA Lewis Research Center

Contract NAS 3-17783



GENERAL  ELECTRIC

1. Report No. NASA CR 134714		2. Government Accession No.		3. Recipient's Catalog No.	
4. Title and Subtitle  MODELING AND ANALYSIS OF POWER PROCESSING SYSTEMS				5. Report Date 28 October 1974	
				6. Performing Organization Code IP80	
7. Author(s)  Dr. K.A. Fegley, J.H. Hayden, D.W. Rehmann				8. Performing Organization Report No. IP80-564-170	
				10. Work Unit No.	
9. Performing Organization Name and Address  General Electric Company Space Systems, P.O. Box 8555 Philadelphia, Pennsylvania 19101				11. Contract or Grant No. NAS 3-17783	
				13. Type of Report and Period Covered Contractor Report	
12. Sponsoring Agency Name and Address National Aeronautics and Space Administration Lewis Research Center Cleveland, Ohio 44135				14. Sponsoring Agency Code	
15. Supplementary Notes Project Manager: Irving G. Hansen Lewis Research Center Cleveland, Ohio 44135					
16. Abstract <p>This report describes the interim results of a program to investigate the feasibility of formulating a methodology for the modeling and analysis of aerospace electrical power processing systems. The object is to develop a flexible engineering tool to allow the power processor designer to effectively and rapidly assess and analyze the tradeoffs available by providing, in one comprehensive program, a mathematical model, an analysis of expected performance, simulation, and a comparative evaluation with alternative designs. This requires an understanding of electrical power source characteristics and the effects of load control, protection, and total system interaction.</p> <p>Power processing systems are usually designed by a trial-and-error process. Components are selected which appear to be appropriate and a paper design based on the selected components is completed, then modeled, simulated and analyzed to determine its adequacy. If the design specifications are not met, the paper design is modified by selecting different components and/or by redesigning the system. The modified design is then analyzed. This iterative procedure continues until a satisfactory design is achieved.</p> <p>These methods are time consuming and generally do not lead to an optimal system. There is need for a method which will permit the design to be completed more expeditiously. This report presents such a method. It shows how a digital computer may be used in an interactive mode for the design, modeling, analysis and comparison of power processing systems.</p>					
17. Key Words (Suggested by Author(s)) Power Processing, Optimization, Modeling, Analysis, Computer Techniques			18. Distribution Statement  Unclassified - Unlimited		
19. Security Classif. (of this report) Unclassified		20. Security Classif. (of this page) Unclassified		21. No. of Pages	
				22. Price*	

MODELING AND ANALYSIS OF  
POWER PROCESSING SYSTEMS

BY DR. K.A. FEGLEY, J.H. HAYDEN, AND D.W. REHMANN

GENERAL ELECTRIC COMPANY

PREPARED FOR  
NATIONAL AERONAUTICS AND SPACE ADMINISTRATION

NASA LEWIS RESEARCH CENTER

CONTRACT NAS3-17783



## FOREWARD

This study program was sponsored under contract NAS3-17783 from the National Aeronautics and Space Administration.

This is a report of work performed by Space Systems Organization, Space Division, General Electric Company; and the Department of Systems Engineering, Moore School of Electrical Engineering, University of Pennsylvania. The Literature Search and Power Processing Methodology was completed principally by Mr. Peter Blair, assisted by Mohammed El-Nowehi and Hou-Shing Shu, all graduate students at the Moore School of Electrical Engineering, University of Pennsylvania, under the direction of Dr. Kenneth A. Fegley.

## TABLE OF CONTENTS

<u>SECTION</u>		<u>PAGE</u>
	SUMMARY	
	INTRODUCTION	
1.0	Selection of Power Processing Systems	1-1
1.1	Available Electric Power Sources	1-1
1.2	Projected Electric Power Levels	1-4
2.0	System Documentation and Trade Studies	2-1
2.1	Applications Technology Satellite F	2-1
2.2	Mariner Jupiter/Saturn 1977	2-5
2.3	Three-Phase, 400 Hertz Aircraft Electrical Systems	2-8
2.4	Fuel Cell or Primary Battery Systems	2-10
2.5	Solar Array and Secondary Battery Systems	2-11
3.0	Existing Technique Documentation	3-1
3.1	Computer Aided Design Procedures	3-3
3.2	Simulation and Analysis Languages and Programs	3-3
3.2.1	Mathematical Programming	3-4
3.2.2	System Simulation	3-6
3.2.3	Analysis and Synthesis	3-8
3.3	Design Factors	3-18
3.4	Design Procedures	3-18
3.5	Component Design	3-18
3.6	Complete System Examples	3-18
3.7	Power Sources	3-18
3.9	Summary and Conclusions	3-19

<u>SECTION</u>		<u>PAGE</u>
4.0	Formulation of a Methodology	4-1
4.1	Design Procedure	4-1
4.1.1	Input Information (Block No.1)	4-4
4.1.2	Search Procedure	4-5
4.1.2.1	The Filing System	4-7
4.1.2.2	The Search Algorithm	4-9
4.1.2.3	Pre-Analysis	4-11
4.1.2.4	Pre-Analysis without Hits	4-11
4.1.2.5	Pre-Analysis with Hits	4-11
4.1.2.6	Concluding the Search	4-12
4.1.3	Subsystem Synthesis	4-12
4.1.4	System Assembly	4-12
4.1.4.1	Sorting Available Designs of Subsystems (Hits) (Block No.4)	4-12
4.1.4.2	Assembly of the PPS (Block No.5)	4-13
4.1.5	System Evaluation	4-14
4.1.6	Modeling and Analysis	4-15
4.1.6.1	Stability Analysis	4-22
4.1.6.2	Transformer Optimization	4-23
4.1.6.3	Transformer Design	4-28
4.2	The Management Program	4-43
4.2.1	Choosing A System Implementation Language	4-44
4.2.2	System Profile	4-44
4.2.2.1	Subsystems Data Base Facility	4-45

<u>SECTION</u>		<u>PAGE</u>
4.2.2.2	Registrar	4-47
4.2.2.3	Editor (Lexical Analyzer)	4-47
4.2.2.4	User's Library	4-47
4.2.2.5	Language Processor	4-48
4.2.2.6	Error Message Handling Routine	4-48
4.2.2.7	Dispatcher	4-49
4.2.2.8	Subprogram Library	4-49
4.2.2.9	Power Processing Subsystems Data Base Facility	4-50
4.2.3	Implementation Strategy	4-50
4.2.4	File Design	4-52
4.3	Summary	4-53
5.0	Plan For Phase II	5-1
5.1	Introduction	5-1
5.2	Scope of Work	5-3
5.3	Task Descriptions	5-5
5.3.1	Task 1 - Design of the Management Computer Program	5-5
5.3.2	Task 2 - Design of a Library of Power Processing System Components	5-6
5.3.3	Task 3 - Methodology of Optimization	5-8
5.3.4	Task 4 - Computerized Design Routine	5-9
5.4	Phase II Implementation Plan	5-19
5.5	Milestone Schedule	5-20
5.6	Required Resources	5-20

# LIST OF TABLES

<u>TABLE</u>		<u>PAGE</u>
1-1	Electric Power Source State of the Art Summary	1-2
1-2	Shuttle Payload Power Source Requirements	1-5
1-3	Representative Future Mission Power Source Requirements	1-6
1-4	Radioisotope Thermoelectric Generator Power	1-7
1-5	Shuttle Automated Payload Solar Power Requirements	1-7
3-1	Features of Languages used as a System Implementation Tool	3-21
4-1	Power Processor Criteria	4-6
4-2	The Ordering of the Subsystems	4-13
4-3	General Information on Circuit Analysis Programs	4-18
4-4	Analysis Details	4-20
4-5	Input Details	4-20
4-6	Outputs	4-21
4-7	Design Formulae	4-29
4-8	Transformer Analysis Printout	4-32
4-9	Transformer Analysis Program	4-35
5-1	Memory Required to Store Characteristics	5-7
5-2	Transformer Optimization Computer Program	5-10
5-3	Computer Program for the Design of Toroidal Transformers	5-10
5-4	Interactive Transformer Design	5-12
5-5	Technical Work Allocation	5-21

# LIST OF ILLUSTRATIONS

<u>ILLUSTRATION</u>	<u>PAGE</u>
1-1 NASA Mission Model	1-5
2-1 Direct Energy Transfer System Block Diagram	2-3
2-2 Operating Mode Bus Voltage	2-3
2-3 Mariner Jupiter/Saturn Power Subsystem Block Diagram	2-6
4-1 Power System Block Diagram	4-1
4-2 Design Process Block Diagram	4-3
4-3 Block No.1 Schematic	4-4
4-4 The Search Procedure	4-8
4-5 The File Structure	4-8
4-6 Examples of Inverted Files	4-9
4-7 The Search Algorithm	4-9
4-8 Subsystem Nodes and Branches	4-15
4-9 Combined Circuit	4-16
4-10 Shape of Scrapless EI Laminations	4-23
4-11 Operating Characteristics for Typical Materials	4-24
4-12 Family of Variable Primary Turns Transformers	4-25
4-13 Typical Minimum Loss Transformer Designs	4-26
4-14 Watts/Weight Transformer Tradeoff	4-28
4-15 Transformer Physical Characteristics	4-29
4-16 Optimized Minimum Dissipation Supermalloy Transformers	4-30
4-17 Characteristics of Orthonol Toroidal Transformers	4-39
4-18 Characteristics of Supermalloy Toroidal Transformers	4-39
4-19 Characteristics of Silectron Cut Core Transformers	4-39

# LIST OF ILLUSTRATIONS

<u>ILLUSTRATION</u>		<u>PAGE</u>
4-20	Characteristics of Supermalloy Cut Core Transformers	4-40
4-21	Locus of Orthonol Toroidal Transformers	4-40
4-22	Locus of Supermalloy Toroidal Transformers	4-40
4-23	Locus of Silectron Cut Core Transformers	4-42
4-24	Locus of Supermalloy Cut Core Transformers	4-42
4-25	Composite of Optimized 18 Watt Transformers	4-42
4-26	Submodule (Service Programs) of The Management Program	4-46
5-1	Program Milestone Schedule	5-21

## SUMMARY

This report describes the interim results of a program to investigate the feasibility of formulating a methodology for the modeling and analysis of aerospace electrical power processing systems. The object of the total program is to develop a flexible engineering tool which will allow the power processor designer to effectively and rapidly assess and analyze the trade-offs available by providing, in one comprehensive program, a mathematical model, an analysis of expected performance, simulation, and a comparative evaluation with alternative designs. This requires an understanding of electrical power source characteristics and the effects of load control, protection, and total system interaction.

Power processing systems are usually designed by a trial-and-error process. Components are selected which appear to be appropriate and a paper design based on the selected components is completed, then modeled, simulated and analyzed to determine its adequacy. If the design specifications are not met, the paper design is modified by selecting different components and/or by redesigning the system. The modified design is then analyzed. This iterative procedure continues until a satisfactory design is achieved.

The currently used methods for designing power processing systems are time consuming and generally do not lead to an optimal system. There is need for a method which will permit the design to be completed more expeditiously. This report presents such a method. It shows how a digital computer may be used in an interactive mode for the design, modeling, analysis and comparison of power processing systems.



The project was sponsored by NASA-Lewis Research Center. The General Electric Company-Space Systems and the University of Pennsylvania-National Center for Energy Management and Power cooperated in performing the tasks. This union of the industrial and academic worlds was established to combine unfettered scientific curiosity with the experience and knowledge gained from design, production, and test of hardware.

## INTRODUCTION

This report covers a nine month Phase I program to investigate the feasibility of formulating a methodology for the modeling and analysis of power processing systems. The program, initiated on 22 August 1973, was organized into the following tasks:

1. Survey, screen, and recommend five representative power processing systems.
2. Characterize the selected systems with all the internal and external features which enter into engineering evaluations relative to utilization.
3. Survey, screen, and evaluate available modeling and analysis techniques and approaches.
4. Formulate a methodology for the modeling and analysis of power processing concepts.
5. Prepare a Phase II implementation plan.

SECTION 1  
INTRODUCTION

REPRODUCIBILITY OF THE  
ORIGINAL PAGE IS POOR

## 1.0 SELECTION OF POWER PROCESSING SYSTEMS

This task resulted in an assessment of present and planned power processing system requirements applicable to high power spacecraft and aircraft power sources and loads. Power processing systems were found to be more identified with the power source than the load, so principal attention was focused on the variety of sources considered as viable candidates to satisfy mission requirements for the next decade.

### 1.1 Available Electric Power Sources

The available basic sources for spacecraft electrical power listed in order of increasing lifetime are primary battery, fuel cell, nuclear, radioisotope, and solar. A representative state of the art summary of electrical power systems is given in Table 1-1, extracted from NASA Contract NAS-9-13401. All these electrical power source systems are long life, durable, space qualified, and viable contenders for use on missions in the next decade.

Aircraft electrical power is provided from a 400 Hertz alternator that is mechanically driven from the engine power plants, either directly in wild frequency systems, or thru a constant speed drive. Electronic variable speed, constant frequency cyclo-converters have been developed for aircraft, but are not in general use.

Dynamic isotope and reactor Brayton, Rankine, and Sterling cycle systems have been proposed, and could be made available within the decade if a specific application makes one attractive from a cost standpoint.

Table 1-1  
Electric Power Source State of the Art Summary

TYPE	TYPICAL SYSTEMS	MISSION	STATUS	POWER CAPABILITY
SOLAR ARRAY/ SECONDARY BATTERY	FIXED ARRAY	SKYLAB	FLOWN	7200 WATTS
	ORIENTED ARRAY	EARTH RESOURCES TECHNOLOGY SATELLITE	FLOWN	250 WATTS
RADIOISOTOPE THERMOELECTRIC GENERATOR	SNAP 19	NIMBUS III	FLOWN	25 WATTS
	SNAP 27	LUNAR STATION	FLOWN	70 WATTS
	MULTI-HUNDRED WATT	LINCOLN EXPERIMENTAL SATELLITE 8 MARINER JUPITER SATURN	IN DEVELOPMENT AVAILABLE 1975	150 WATTS
	MULTI-KILOWATT	STATION BASE	PAPER STUDIES AVAILABLE POST 1980	1000 WATT MODULES
RADIOISOTOPE HEAT SOURCE	BRAYTON, RANKINE, STERLING, THERMAL ELECTRIC	ADVANCED	PAPER STUDIES AVAILABLE 1977	400 WATTS
FUEL CELL	SINGLE STACK	BIOSATELLITE	FLOWN	300 WATTS
	TRIPLE STACK	GEMINI	FLOWN	1000 WATTS
	SEVEN STACK	APOLLO	FLOWN	2500 WATTS
PRIMARY BATTERY	SILVER ZINC	CLASSIFIED MILITARY	FLOWN	400 WATTS

A magnetohydrodynamic generator is analogous to the rotating aircraft generator, except that the electrical current, in the form of hot ionized gasses or plasma, is forced through a magnetic field, producing a potential difference between two electrodes which is perpendicular to the magnetic field and the gas flow. Because of the high temperature, the magnetic field that is required, and the need for high velocity gas flow, the MHD technique is most efficient in large power ratings. The MHD generator is in the proof of feasibility stage, is under active development by the General Electric Company and others, but is not considered to be available at this time. The phenomenon was first recorded in 1910, and efforts are still underway to make it practical for terrestrial use. The major problem is to find materials that will not corrode at the 5000<sup>0</sup> Farenheit temperatures involved and in the presence of two thousand miles per hour ionized gas flow. The MHD can be discarded as an active contender for a long life system because of its high development risk.

The conventional dynamic or rotating turbine-generator unit mentioned above is by no means completely out of the race as a compact, portable, and efficient device for space. It may suffer from inherent reliability problems and operational difficulties because of the mechanical motion, but it is the reference against which other systems have to compete and be proved superior before their operational use is assured. However, even this system cannot be considered where the power requirements are below the kilowatt range.

A more detailed consideration of electrical power sources in general use is given in the next paragraphs to permit source selection for a specific mission.

## 1.2 Projected Electric Power Levels

Power requirements and future spacecraft power levels can be derived from the NASA Mission Model, Shuttle System Payload Data Activity, Contract NAS-8-29462. Table 1-2 summarizes these power needs ranging from 140 to 2600 watts. Table 1-3 was obtained from the August 1971 report on Electric Power Processing Technology prepared by the subcommittee on Power Conditioning, NASA Research and Technology Advisory Committee on Power and Electric Propulsion. All of these electrical power requirements can be met with today's technology. The selection of power sources for a given mission will be primarily a performance/cost trade for that particular mission.

There are 986 non-DOD space missions thru 1991 identified in NASA's October 1973 mission model. Figure 1-1 shows a histogram of 798 of these spacecraft distributed between sortie and automated systems. Sortie payloads will interface with the shuttle fuel cell, and have no power system of their own. Radioisotope thermoelectric generators have been identified for outer planet missions only. Table 1-4 shows the planned missions and power requirements. Solararray/battery systems satisfy all other automated missions, and Table 1-5 shows some typical mission power requirements. No other power sources are required during the next two decades.

Table 1-2

## Shuttle Payload Power Source Requirements

MISSION	POWER REQUIREMENTS, WATTS		
	BEGINNING OF LIFE	END OF LIFE	AVERAGE (WATTS)
GEOSYNCHRONOUS OPERATIONAL METEOROLOGICAL SATELLITE (GOMS)	-	140	-
FOREIGN SYNCHRONOUS METEOROLOGICAL SATELLITE (FSMS)	-	140	-
EARTH RESOURCES SURVEY OPERATIONAL SATELLITE (ERSOS)	550	-	-
SYNCHRONOUS EARTH OBSERVATION SATELLITE (SEOS)	557	402	-
EARTH OBSERVATORY SENSOR DEVELOPMENT LABORATORY	-	-	2600 (4500 PEAK)
TRACKING AND DATA RELAY SATELLITE (TDRS)	466	400	-
EARTH OBSERVATORY SATELLITE (EOS)	-	-	1000
TIROS O	-	-	1000
ENVIRONMENTAL MONITORING SATELLITE	-	-	1000
SYNCHRONOUS METEOROLOGICAL SATELLITE (ADVANCED) (SMS)	900	650	-
SMALL APPLICATION TECHNOLOGY SATELLITE (SATS)	-	-	490 (1000 PEAK)

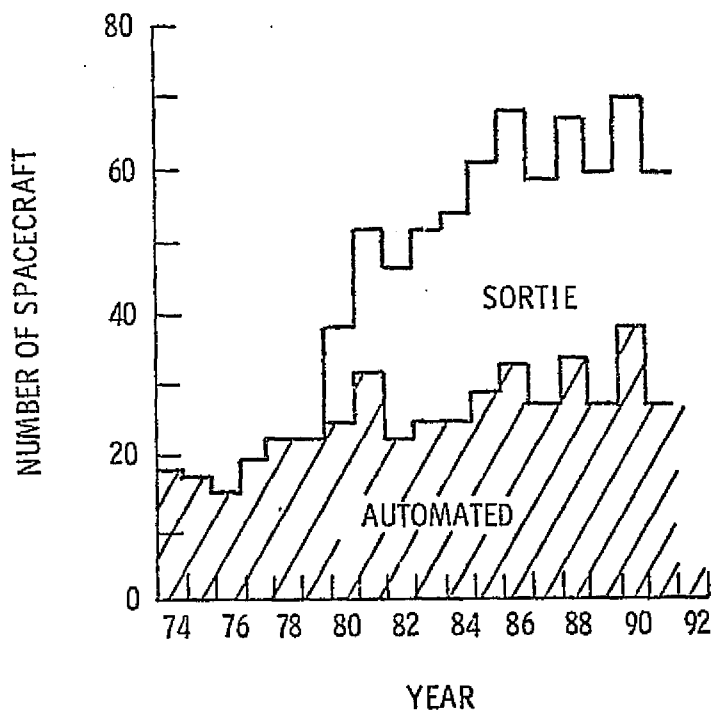


Figure 1-1. NASA Mission Model



Table 1-3

## Representative Future Mission Power Source Requirements

			MANNED VEHICLES				UNMANNED VEHICLES		
			AIR BREATHING	EARTH ORBITAL			SOLAR ORBITAL		
			AIRCRAFT	SHUTTLE	STATION	BASE	SCIENCE	NEAR PLANET	OUTER PLANET
			40	1,000	20,000	100,000	7,500	25,000	100,000
MISSION DURATION, HOURS									
POSTULATED ENERGY SOURCES	NUCLEAR	STATIC	THERMO-ELECTRIC	ARRAY CAPABILITY		SUBSYSTEM CAPACITY		BUS POWER, WATTS	
				80,000		500,000		1,250	
				50,000		500,000		1,000	
		DYNAMIC	BRAYTON	25,000		200,000		500	
				SYSTEM CAPACITY		250,000		600	
				25,000		200,000		500	
	CHEMICAL	STATIC	THERMIONIC	SUBSYSTEM CAPACITY		250,000		150,000	
				BUS POWER, WATTS		200,000		75,000	
		DYNAMIC	FUEL CELL	SUBSYSTEM CAPACITY		250,000		90,000	
				BUS POWER, WATTS		200,000		75,000	
	CHEMICAL	STATIC	BATTERY	BUS POWER, WATTS		5,000			
		DYNAMIC	TURBINE GENERATOR	BUS POWER, WATTS		270,000		10,000	

Table 1-4

## Radioisotope Thermoelectric Generator Power

MISSION	POWER REQUIREMENTS, WATTS
MARS SURFACE SAMPLE RETURN	70 WATTS "A" LANDER
VENUS RADAR MAPPER	(3) 400 WATTS TOTAL
PIONEER SATURN/URANUS FLYBY	(2) 140 WATTS TOTAL
MARINER JUPITER ORBITAL	(3) 400 WATTS TOTAL
PIONEER JUPITER PROBE	(2) 140 WATTS TOTAL

( ) QUANTITY PER S/C

NO REQUIREMENTS FOR RTG OUTSIDE PLANETARY DISCIPLINE
---

Table 1-5

## Shuttle Automated Payload Solar Power Requirements

DISCIPLINE	NUMBER OF FLIGHTS *	SOLAR ARRAYS NO./TYPE	POWER RANGE (WATTS)	ORBIT LIFE (YEARS)
ASTRONOMY & SOLAR PHYSICS	11	11/ROTATING (2 PANELS)	150-1500	2-3
HIGH ENERGY ASTROPHYSICS	8	8/ROTATING (2 PANELS)	150-1200	2-5
ATMOSPHERIC & SPACE PHYSICS	24	2/ROTATING (4 PANELS) 22 BODY MOUNTED	200-500	1-3
EARTH OBSERVATIONS	87	69/ROTATING (2 PANELS) 18 BODY MOUNTED	140-960 140	2-5
EARTH & OCEAN PHYSICS	15	13 BODY MOUNTED 2 NO ELECT. S/S	90-620	0.5-5
COMMUNICATIONS/NAVIGATION	69	34 ROLL-OUT 7 BODY MOUNTED 28/ROTATING (2 PANELS)	300-500	5-10
TOTALS:		116 ROTATING (2 PANELS) 2 ROTATING (4 PANELS) 60 BODY MOUNTED 34 ROLL-OUT ARRAYS		

\* NUMBER OF FLIGHTS BASED ON JUNE 1973 MISSION MODEL

## SECTION 2

### SYSTEM DOCUMENTATION AND TRADE STUDIES

REPRODUCIBILITY OF THE  
ORIGINAL PAGE IS POOR

## 2.0 SYSTEM DOCUMENTATION AND TRADE STUDIES

A cursory study of potential power sources and expected mission requirements has resulted in the selection of the following five systems as representative of evolving standard power processing systems or a survey of present practice. More detailed information can be found in Appendix A thru E of this report

### 2.1 APPLICATIONS TECHNOLOGY SATELLITE F.

This is a 28 volt, photovoltaic power source with nickel-cadmium electrochemical energy storage incorporated in a direct energy transfer system that utilizes dissipative partial shunt regulation of the solar array and pulse-width-modulation of battery discharge power to provide a constant voltage bus without in-line processing of power from the source. This system appears to be the optimum solar array-battery combination for earth orbiting satellite systems.

Utilization of power is decided autonomously by the central power processor. The first priority is that the electrical loads of the system must be satisfied, and power for the loads may be supplied directly from the solar array or by electronic boosting of the battery. If the loads can be satisfied by the solar array, any additional array power is used to charge the battery as a second priority. However, the battery charge rate is additionally constrained to a constant current limit, and may be further reduced by an end-of-charge temperature compensated constant voltage limit. As a third priority, any excess array power over that required by the load and the battery charger is dissipated by a shunt regulator which maintains the solar array at a constant voltage point on its volt-ampere characteristic.

When uniformly illuminated by the sun, the solar array is a constant power source for any specific load. Maximum power is obtained at the knee of the volt-ampere characteristic. In a Direct Energy Transfer System, the solar array is designed so that peak power is available at the bus voltage level. The shunt regulator is turned on only when the available array power at the constant voltage operating point exceeds the needs of the spacecraft to satisfy load demand and battery charging. If efficiency is defined as the ratio of power required by the load and the battery charger divided by the power supplied by the source to satisfy this demand, then the system efficiency approaches 100 per cent.

Since the solar array current is limited by area and light intensity, partial shunt regulation can be employed to reduce the thermal burden in the shunt elements. This is accomplished by determining the minimum number of solar cells necessary to satisfy the minimum load condition at the maximum array condition, and by shorting out the remaining solar cells necessary to satisfy the maximum load condition at the minimum array condition. Each solar array string is tapped at this point, and the partial shunt regulator is attached between the tap point and the negative bus.

The gravity gradient test satellite was designed with a partial shunt regulator by General Electric. The vehicle was launched on 29 June 1966, and continued to operate until contact was lost in August 1972.

The principal elements of DETS are shown in Figure 2-1. Power from the solar array is transferred directly to the loads, accounting for the name applied to the approach. Power to and from the battery is processed

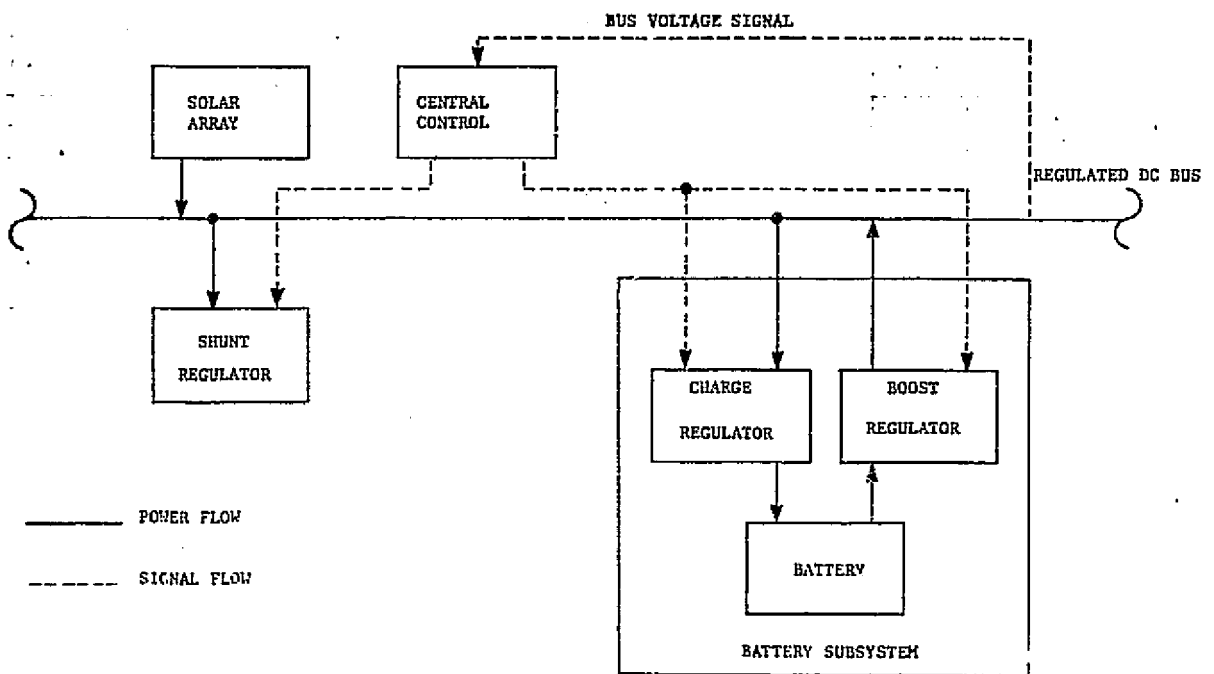


Figure 2-1. Direct Energy Transfer System Block Diagram

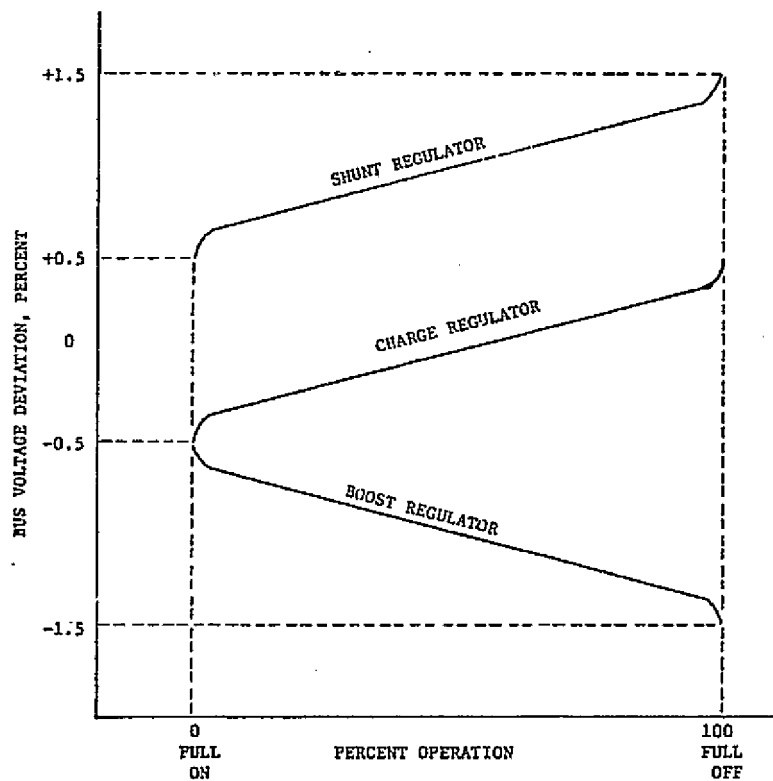


Figure 2-2. Operating Mode Bus Voltage

by the charge and boost regulators, respectively. A shunt regulator dissipates any excess power from the solar array, once load and charging demands are satisfied. The relative processing of power in the charge regulator, boost regulator and shunt regulator by a central control is indicated in Figure 2-2. The central control provides a signal proportional to the bus voltage deviation. The range of acceptable voltage deviation is nominally selected to be  $\pm 1.5$  percent of the bus voltage. At the upper limit of voltage deviation the shunt regulator is turned full on; full charge demands are satisfied depending on the battery status; and the load demands are met. With higher load demands or decreased array power, the shunt regulator dissipation is decreased, and completely turned off when the deviation is around  $+0.5$  percent. With further load demands, the array power is preferentially supplied to the load by gradually decreasing the available charge power to a point where charging is totally inhibited at a voltage deviation of around  $-0.5$  percent. At this particular condition, the array power just satisfies the load demand. Further load demands are supplied by the boost regulator, which is at a full-on condition at a voltage deviation around  $-1.5$  percent.

In the sequence of operation just described, the voltage deviation signal serves to establish the operating condition of the various power processing elements. In the ATS implementation, the voltage deviation signal is amplified and each power processor is set to respond to nonoverlapping regions of the amplified error signal. In this way the possibility of simultaneous shunting and boosting is avoided.

The principal advantages of the DETS approach are: 1. array power is used directly, and therefore, most efficiently; 2. the power output is voltage regulated, minimizing the need for downstream regulation; 3. with charge power taken from a regulated bus, the range of operating conditions for the charge regulator is narrowed, permitting a more optimum design; and 4. limitations on battery voltage variations are less stringent; the boost regulator can easily be designed to accept low battery discharge voltages.

## 2.2 MARINER JUPITER/SATURN 1977.

This is a 29 volt, radioisotope thermoelectric generator power source with a limited amount of nickel-cadmium electrochemical energy storage incorporated in a direct energy transfer system that utilizes dissipative full shunt regulation of the radioisotope thermoelectric generator and pulse-width-modulation of battery discharge power to provide a constant voltage bus without in-line processing of the power from the source. This system appears to be the leading contender for outer planet satellite systems, and has the added unique feature of central inversion and distribution of 2.4 KHz, 50 VAC square wave power to loads.

The functional block diagram of Figure 2-3 shows the primary power source of three radioisotope thermoelectric generators (RTG's) coupled by the power source and logic unit to form a dc power bus.

The power source and logic contains the circuitry necessary to interconnect the RTG's to the power conditioning equipment. This would include such things as isolation diodes and RTG shorting switches.

The dc power bus is regulated to 29 vdc  $\pm 1\%$  by a shunt regulator. The shunt regulator senses the common RTG voltage and maintains it by dissipating



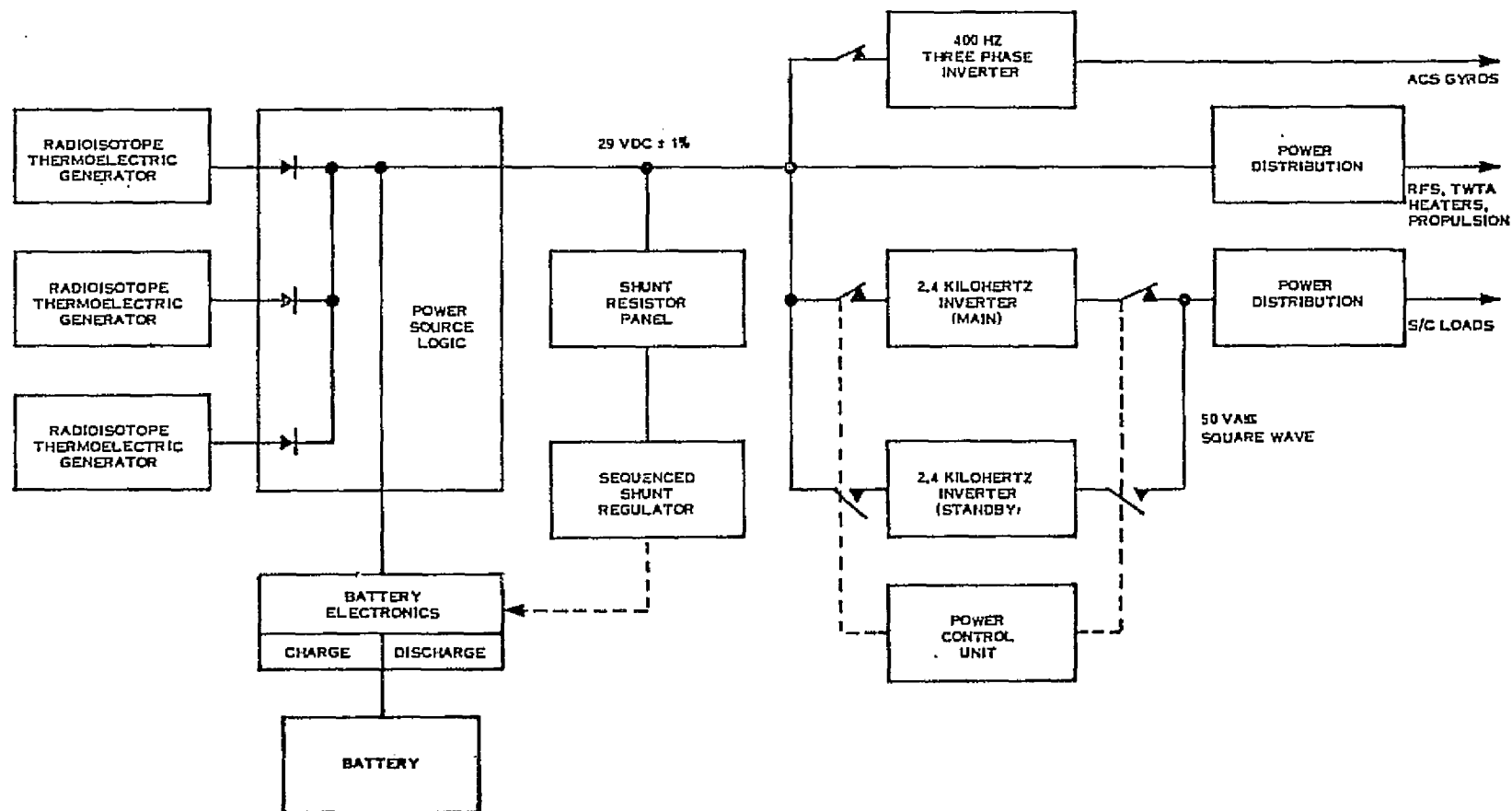


Figure 2-3. Mariner Jupiter/Saturn Power Subsystem Block Diagram

the difference between RTG power available at 29 vdc and the spacecraft load demand. Voltage regulation of the RTG's provides relatively constant loading and serves to maintain the RTG internal temperature near the design point.

Power from the dc bus is transformed to 50 volts, rms, 2.4 KHz, single-phase, square-wave power by the main inverter for all spacecraft ac loads. An identical inverter in standby serves as a backup to the main inverter. Switch-over is controlled by inverter failure detection circuitry located within the power control unit.

The power distribution assembly is designed to provide the required switching and control functions for the effective management and distribution of power to user loads. Power switching circuitry is designed to operate in response to commands from the computer command subsystem which can execute stored or real time commands.

A 400 Hz, 3 phase inverter provides conditioned power to the attitude control subsystem gyros.

A battery, with its associated charge and discharge electronics, will provide the large magnitude, short duration power required by a propulsion module during injection into interplanetary cruise.

During planet encounter, the power margin between spacecraft load demands and RTG capability is minimal. It is intended that the battery be used to supply load turn-on transient power at this time. The battery energy that is removed during discharge is replaced when there is excess RTG power being dissipated in the shunt regulator. A control signal from the shunt limits the charge rate so that some power remains in the shunt to keep it active and

able to maintain dc power bus voltage regulation. When spacecraft load demands deplete the power in the shunt, the shunt signals the battery discharge electronics to supply battery power to maintain dc bus voltage regulation.

### 2.3 THREE-PHASE 400 HERTZ AIRCRAFT ELECTRICAL SYSTEMS

This is a prime-mover, rotating generator system used on most aircraft and on the space shuttle during some mission modes. It is a multi-kilowatt system and the power processing equipment principally converts the AC power to user needs.

Generally, each aircraft engine drives an ac generator. These generators are tied into the ac mains thru circuit breakers that are activated when a phase sequencer confirms the correct phase relationship and when a voltage differential indicator shows that the generator and the bus are approximately in-phase. This instrumentation is located on an instrumentation panel in the cockpit, and is usually accomplished manually.

Some of the ac power is applied thru approximately coordinated circuit breakers into converters that consist of input line filters, a step-down transformer, a rectifier stack, and output filtering. Various rectifier circuits are utilized for this ac to dc conversion. Single-way circuits have found general acceptance for high power applications since they require that load current flow thru only one rectifier; and the six-phase, double-wye with interphase gives the best overall performance in terms of minimum transformer volt-ampere rating, low output ripple, and rectifier rms current.

The transformer-rectifier is tied into the dc bus thru a reverse current relay. This is a hand-down from dc generator practice, but does protect the dc bus from a faulted rectifier. This relay has a main contactor coil, a reverse current coil, a bus voltage coil, and a voltage differential coil. When the output of the transformer-rectifier rises to approximately 22 volts, the bus voltage coil closes a set of contacts that energizes the voltage difference coil. When the transformer-rectifier output voltage is at least one volt higher than the bus, the main contactor operates, closing the transformer-rectifier into the bus. This protects against high transient currents when two low impedance devices are tied together. The reverse current coil will open the main contactor if the current flows from the bus into the transformer-rectifier, and the trip point is approximately 3% of rated current.

The reverse current relay also has provision for a failure indicator that is energized when the main contactor is open. Unfortunately, this failure indicator is ambiguous when used with a solid-state converter rather than a rotary dc generator. The dc generator, if not energized, would draw reverse current and trip the relay. The reverse resistance of the transformer-rectifier is too high, however, and the transformer-rectifier failure light does not come on, even when the input circuit breaker is tripped.

A nickel-cadmium battery floats on the dc bus, absorbs charge current (and continuous overcharge current) when the transformer-rectifier output voltage is higher than the battery float voltage, and supplies power to essential equipment when ac power fails for any reason. No other charge control method is utilized except initial voltage matching.

Two or more transformer-rectifier units are operated in parallel, with no forced sharing. The inherent regulation of the converter causes the units to share to within ±10% typically.

Fault coordination is provided such that downstream dc feeder fuses blow first, the transformer-rectifier input circuit breaker trips second, and the rectifiers within the transformer-rectifier fail short only if neither one of the two protective devices operates.

#### 2.4 FUEL CELL OR PRIMARY BATTERY SYSTEMS

This class of electrical power systems is characterized by a time or load variant DC source voltage that results in series power processors to maintain constant voltage for user loads.

Pure energy source systems that are the result of chemical reactions are typified by short duration silver-zinc battery systems of up to seven days duration, and fuel cell systems such as Gemini, Apollo, and Biosatellite. These vehicles distribute the unregulated source voltage directly without in-line power processing, unless a number of loads have specific common requirements such as AC voltage.

Power processing to condition the unregulated voltage into a constant DC level is accomplished at each user load, and each user performs his own trade study to determine the form of conditioning to be employed. These trade studies result in different conclusions, based on power level, required reliability, relative sophistication, cost, and the capability of the user to provide the optimum design.

Every electrically actuated event that occurs in the system requires some minimum amount of power to guarantee that the event will occur. Since the event must occur equally as well at low input voltage as at high input voltage, the volt-ampere characteristic of each individual load is selected to insure that at minimum voltage an adequate amount of current will flow to power the event.

## 2.5 SOLAR ARRAY AND SECONDARY BATTERY SYSTEMS

As part of this investigation, all present or planned solar array systems were investigated to document concepts of intermediate voltage levels such as the Canadian Communications Technology Satellite, 120 volt systems, 200 to 400 volt systems proposed for the Solar Electric Propulsion Stage, and kilovolt array systems matched to user loads such as high power transmitters and ion propulsion.

Although most spacecraft have been designed to operate at nominally 28 volts dc and can benefit from the power system described in paragraph 2.1, various systems have been proposed or are being designed and developed to operate at higher voltage. The driving force to higher voltage is the weight of the distribution system at high power levels and at low power to weight figure of merit systems.

The operating current density of the conductors for minimum vehicle total weight is determined by the watts per pound for the power system.

The resistance of a conductor can be expressed as:

$$R = \sigma l / A \quad \text{where}$$

$R$  = resistance in ohms

$\sigma$  = resistivity of the material, ohm-inches<sup>2</sup>/inch

$l$  = length of the conductor, inches

$A$  = cross-sectional area, inches<sup>2</sup>

The electrical losses in a length of conductor at a current level  $I$  are then:

$$\text{Watts} = I^2 R = \sigma l I^2 / A$$

and the weight of this same piece of conductor can be expressed as:

$$\text{Weight} = \rho l A \quad \text{where}$$

$\rho$  = specific weight pounds per cubic inch

$l$  = length, inches

$A$  = cross-sectional area, inches<sup>2</sup>

Obviously the loss in watts can be reduced by adding cross-sectional area, and consequently weight. When the watts saved by adding one pound of conductor are equal to the ratio of total available watts to total power system weight for the vehicle, then the optimum operating current density has been determined.

$$\text{New Watts} = \sigma l I^2 / (A + dA)$$

$$\text{delta watts} = \frac{\sigma l I^2 (A + dA - A)}{A(A + dA)} = \frac{\sigma l I^2 dA}{A(A + dA)}$$

$$\text{new weight} = \rho l (A + dA)$$

$$\text{delta weight} = \rho l (A + dA - A) = \rho l dA$$

$$\frac{\text{delta watts}}{\text{delta weight}} = \frac{\sigma l I^2 dA}{\rho l A dA (A + dA)} = \frac{\sigma I^2}{\rho A (A + dA)} \quad \text{and rearranging,}$$

$$\frac{\sigma I^2}{\rho (A^2 + AdA)} = \frac{\text{delta watts}}{\text{delta weight}} \quad \text{and in the limit as } dA \text{ approaches zero,}$$

$$\frac{I}{A} = \sqrt{\frac{\rho \text{ delta watts}}{\sigma \text{ delta weight}}} = \text{optimum operating current density,}$$

in amperes per square inch of cross sectional area of conductor, where delta watts/delta weight is the watts per pound trade-off figure for the vehicle.

When the weight of the 28 volt distribution system becomes excessive, its weight can be reduced proportional to an increase in operating voltage. As part of JPL Contract 953387 it was determined that the weight of the solar array distribution harness for a 10 kilowatt system could be reduced from 13 pounds to 3 pounds if the bus voltage was raised from 100 volts to 400 volts. Studies by Wilson and O'Connor of the Naval Research Laboratory have also shown that aircraft electrical systems could benefit from a proposed standard 230 volt dc distribution system.

A second consideration in bus voltage selection is the requirement of the load. When a significant portion of the available power is utilized by one load, the vehicle design is most efficient when the voltage is supplied in a form in which it can be used directly by the load. This was the objective of NASA Lewis contracts NAS 3-8995, NAS 3-8996, and NAS 3-8997. These studies defined solar array electrical configurations which regulate and reconfigure, by switching, a 16 kilovolt, 15 kilowatt array with electronics integrally mounted to the array substrate. The anticipated advent of satellites incorporating ion thrusters and high frequency electron tubes has created a need for 2,000 to 16,000 volt power. The present thrusters require from 2,000 to 5,000 volts DC at the accelerator electrodes. The near future tubes may require up to 16,000 volts DC.

The DC power required for the thrusters and tubes is expected to be derived from solar arrays. For many satellites where thrusters and tubes are involved, a major portion of the total solar array power will be used by these systems and used at relatively constant power levels during steady state operations.



Conventional solar arrays are wired to deliver power at less than 100 volts. For the present low voltage solar arrays to meet the high voltage requirements noted above, it is necessary to transform the low voltage into a higher voltage through the use of heavy and complex power conditioning equipment. Typically, each one kilowatt of regulated power is delivered with 15 to 30 pounds of power processing equipment.

Systems tradeoff studies have eliminated conventional series and shunt regulator systems and maximum power tracker systems in comparison to a system which achieves regulation by a binary-coded switching system. The selected discrete switching system (1) appropriately short circuits series connected solar cell groups to achieve voltage regulation and (2) reduces problems of rejecting excess array power and unneeded array power (when loads are off) by operating the solar cells in a shorted mode, which produces considerably less total heat dissipation than other techniques.

SECTION 3  
EXISTING TECHNIQUE DOCUMENTATION

REPRODUCIBILITY OF THE  
ORIGINAL PAGE IS POOR

### 3.0 EXISTING TECHNIQUE DOCUMENTATION

Power Processing Systems are usually designed by a trial-and-error method. Components are selected which appear to be appropriate and a paper design based on the selected components is completed, then modeled, simulated and analyzed to determine its adequacy. If the design specifications are not met, the paper design is modified by selecting different components and/or by re-designing the system. The modified design is then analyzed. This iterative procedure continues until a satisfactory design is achieved.

The currently used methods for designing power processing systems are time consuming and generally do not lead to an optimal system. There is need for a method which will permit the design to be completed more expeditiously. This report presents such a method in Section 4. It shows how a digital computer may be used in an interactive mode for the design, modeling, analysis and comparison of power processing systems.

This section of this report summarizes the results of a literature search for available design, analysis, and modeling techniques applicable to power processing systems. These techniques consist of simulation, circuit analysis, and circuit synthesis programs. There is extensive reference to the literature in the areas of power processing design procedures, design criteria, and complete systems applications. In addition, power source information is included since power processing systems are highly dependent upon the power source.

The following literature source files of data from 1967 to the present were consulted in the compilation of this data:

The Institute of Electrical and Electronics Engineers  
Engineering Index  
Moore School Library Listings  
Moore School Master's Theses and Dissertations  
General Electric Space Center Document File  
General Electric Space Center Library  
NASA Computer Program Abstracts  
University of Pennsylvania Computer Documents Library  
Department of Defense Listings  
Computing Reviews Journal  
Datamation  
Proceedings of International Symposia on Computer Aided Design  
Defense Documentation Center - Space Power Processing Report Bibliography

A literature search and a survey of industry, university, and governmental agencies was initiated in October, and continued during the next two reporting periods to identify existing modeling and analysis techniques. A standard reporting format has been prepared, and was used to document approximately 385 pertinent existing programs.

NASA Literature Search Number 24412 yielded 178 open references to space power electrical processing, conditioning, and conversion systems, and 11 additional limited distribution references. The Defense Documentation Center Search Number 010358 produced 18 additional references to Space Power Processing. A report on the results of this literature search, Modeling and Analysis Techniques, dated 26 March 1974, was published and was distributed.

This task was completed principally by Mr. Peter Blair, assisted by Mohammed El-Nowehi and Hou-Shing Shu, all graduate students at the Moore School of

Electrical Engineering, University of Pennsylvania, under the direction of Dr. Kenneth A. Fegley.

### 3.1 Computer Aided Design Procedures

A survey yielded 23 reports of applicable specific power processing design procedures that utilize computer oriented techniques for at least some portion of the design process. The information from these procedures will provide input for the formulation of a management program. Seventeen additional sources were identified for background reference. These items were documented in a Task 3 Report, "Modeling and Analysis Techniques".

### 3.2 Simulation and Analysis Languages and Programs

A review of computer program languages in which the design management program can be written is presented. The most important feature of the language that is finally selected is the availability of interactive programming. However, a variety of other factors must be considered as well. The information from these sources will provide input for the organization of the computer based management program. More specifically, it will help define the access procedure to use the management program, and the options that are available to the user in terms of interaction, display, storage, and information handling capabilities.

The analysis programs will be accessed by the management program at the option of the user in the design process. Use of available analysis programs at both the system level and specific design level would be attractive and are included here. This includes programs involving circuit analysis, circuit synthesis, and system simulation.

The following are examples of programs available for mathematical programming, system simulation, and analysis and synthesis.

### 3.2.1 Mathematical Programming (Compiled from UNICOLL Newsletters)

#### MATHEMATICAL PROGRAMMING

PROGRAM NAME: MPS 360

MPS/360 is a linear programming package which performs linear, parametric, and separable programming. In addition, MARVEL, the file processor for MPS/360, may be used for data preparation and matrix generation. The Report Generator Program RPG, may be used for output analysis and management report writing.

#### LINEAR PROGRAMMING

PROGRAM NAME: MFOR/360

This program uses the revised simplex method with product form of the inverse to solve linear programming problems. The program can handle problems with variables up to 2000, subject to constraints up to 511, with total entries not more than 12,000.

#### LINEAR PROGRAMMING

PROGRAM NAME: LINPROG

This program solves linear programming problems using the simplex method. Possible degeneracies are taken into account via the method of Charnes. The program is written in double precision and can handle problems of moderate size.

#### SEQUENTIAL UNCONSTRAINED MINIMIZATION TECHNIQUE FOR NON-LINEAR PROGRAMMING

PROGRAM NAME: SUMT

This program solves nonlinear programming problems by solving a sequence of unconstrained minimization problems. The algorithm is based on the method of Fiacco and McCormick.

#### LINEAR AND QUADRATIC PROGRAMMING

PROGRAM NAME: LQPROG

This program solves linear and quadratic programming problems using Lemke's complementary pivot algorithm. The program can handle problems of medium size.

## ZERO-ONE INTEGER LINEAR PROGRAMMING WITH HEURISTICS

PROGRAM NAME: ZERØØNE

This program is designed to solve linear programming problems whose variables are restricted to the values zero or one. The program utilizes the well-known additive algorithm of Egon Balas, combined with a group of user-selected heuristic test options designed to speed solution time by taking advantage of individual problem characteristics.

## WOLFE QUADRATIC PROGRAMMING

PROGRAM NAME: WOLFEQP

This program solves quadratic programming problems using the WOLFE algorithm. The program is written in double precision and can handle problems of limited size.

## BRANCH AND BOUND MIXED INTEGER PROGRAMMING

PROGRAM NAME: BBMIP

This program employs a branch and bound algorithm based upon the Land and Doig method to solve mixed and pure integer programming problems of limited size. The region of integer variables to be restricted must be specified by the user of this program.

## INTEGER AND MIXED INTEGER LINEAR PROGRAMMING

PROGRAM NAME: INTEGER

This program solves integer and mixed integer linear programming problems via the Land-Doig branch and bound method. The program provides information for drawing the branch and bound network so that the behavior of the search process can be followed.

## JOB SCHEDULING AND OPTIMIZATION FOR MINIMUM TIME, OR MINIMUM DISTANCE

PROGRAM NAME: JOBSCH

This program is designed to solve the general case of the Job Sequence Optimization or the Traveling Salesman Problem. This program will find the minimum or near-minimum distance required to travel to specific locations and return. It will also solve both symmetric and non-symmetric problems. Non-symmetric problem applications may include setup and grade-changes, and military reconnaissance flight planning. Symmetric problem applications may include pin assignment, traveling salesman, and truck routing.

## GENERAL NON-LINEAR LEAST SQUARES PROGRAM

PROGRAM NAME: GNLLS

UNI-COLL has significantly improved the performance of the General Non-Linear Least Squares program (GNLLS). On October 15, 1973, VIMI will supercede VIMO (documentation dated: 7/26/71) and will be available to UNI-COLL customers. This program provides an arbitrary function fit to a set of data points. The new version provides a reduction in run time, larger program capacity (parameter estimates and number of independent variables), more accurate results, a CPU execution time report, and more readable listings of control card parameters and output results. GNLLS is written in FORTRAN IV (G1).

## CONSTRAINED OPTIMIZATION VIA MOVING EXTERIOR TRUNCATION

PROGRAM NAME: COMET

COMET (Constrained Optimization via Moving Exterior Truncation) is designed to solve the general nonlinear programming (NLP) problem. The program uses a new penalty function which controls convergence to a constrained solution. Specifically designed to be easily executed by those with limited NLP experience, COMET is able to solve a wide variety of problems with varying numbers of inequality and equality constraints and having as many as 100 variables.

COMET may also be used for unconstrained minimization and provides an option for using a numerical differencing technique to approximate partial derivatives. The program is written in double precision in FORTRAN IV (G1) and is due to R. L. Staha and D. M. Himmelblau of the University of Texas, at Austin.

### 3.2-2. System Simulation (Compiled from UNICOLL Newsletters)

- GPSS V is an IBM Program Product particularly well suited for modeling discrete systems which involve scheduling and queues. It offers ease in describing systems whose logic is extremely complex or which defy mathematical description and has been used to solve problems in information system design, communications networking, and advanced management planning. Particle or material-oriented, GPSS V employs a variable time-incrementing method and a specialized block diagram flowcharting convention. It offers the capability to interface with routines written in Assembler, FORTRAN, and PL/1.



- SIMSCRIPT 11.5 is a powerful, versatile, general-purpose language. It provides excellent facilities for discrete system simulation and a wide choice of statistical distribution functions. Event-oriented and employing a variable time-incrementing method, SIMSCRIPT 11.5 interfaces with routines in FORTRAN or Assembler Language. The programmer uses a free-form English-like language which offers many optional words and synonyms for clarity of expression. The UNI-COLL implementation is Release 7 of a proprietary product from Consolidated Analysis Centers, Inc.
- GASP II is a FORTRAN-based programming language for discrete system simulation, relying on pre-programmed FORTRAN subroutines. Simple and easily learned, GASP II is event-oriented and uses a variable time-incrementing method. Its programs are easily debugged. The UNI-COLL implementation includes a graph routine for plotting histograms.
- DYNAMO II is a programming language for continuous system simulation, developed originally for studying the closed loop feedback systems typical of industrial dynamics, in which systems are modeled as sets of differential equations. Useful for any continuous system, DYNAMO II has been widely employed to study business, social, economic, biological, psychological, and engineering systems. The version implemented at UNI-COLL is a proprietary release from Pugh Robert Associates, Cambridge, Massachusetts; it employs a fixed time-incrementing method and a specialized flowcharting convention.
- CSMP is an IBM Application Program for the modeling of continuous systems, accepting problems expressed in the form of an analog block diagram or as a set of ordinary differential equations. Problem-oriented control statements facilitate input and output; the CSMP program interfaces with FORTRAN, enabling the user to handle complex non-linear or time-variant problems with ease. CSMP utilizes a fixed time-incrementing method; the UNI-COLL implementation includes an option for graphic representation of output on the CalComp plotter.
- GASP IV, a recently announced extension to GASP II developed at Purdue University, is in effect a new simulation language comprising a set of FORTRAN subroutines for preparing discrete, continuous, or combined simulation models. Experience with GASP IV has been limited to date; in its development stage, it has been used to code a number of dynamic models from the systems dynamics literature, a mechanical impact, slip-clutch problem, and a chemical engineering problem involving hydrogeneration reactions in four reactors.

- SAAM25 is a simulation, analysis, and modeling program developed at the National Institutes of Health primarily for simulation of biological systems - more specifically, for kinetic models. Permitting both simulation and curve fitting, it differs from other programs in that its language is oriented to the biomedical system investigator; its elements and computational procedures, likewise, are counterparts of the conceptualizations and experimental methodologies used by this breed of researcher. Any set of mathematical functions or equations (differential, integral, or algebraic) may serve as a model, provided that a numerical or analytical procedure exists for their solution. A library of model types is incorporated within the program as modular components for routine use. Made possible by the use of a single set of computational parameters and variables throughout the program, a common data input format is used for all model types. By minimizing the number of entries required to specify a model and its constraints, its designers have further simplified the use of this large, complex FORTRAN IV program, which comprises more than 25,000 statements.

### 3.2.3 Analysis and Synthesis (Compiled from NASA Computer Program Abstracts 7/71)

#### NIMBUS ENERGY BALANCE COMPUTER PROGRAM

SOURCE: Radio Corporation of America, New York

FORTRAN IV 1,342 cards  
IBM 360

The program performs an electrical energy balance analysis of each power system on a per-orbit basis. The purpose is to simulate the operation of various power subsystems as the spacecraft passes through a complete orbital cycle. The simulation is accomplished by combining the known electrical characteristics of the solar array, battery, source control devices, load power conditioning devices, charge controller, system power losses, and spacecraft load profiles. A running tally of the various power system operating parameters is provided throughout the simulated orbit; these parameters are printed out at user-specified time increments during the orbit.

#### CIRCUS: A DIGITAL COMPUTER PROGRAM FOR TRANSIENT ANALYSIS OF ELECTRONIC CIRCUITS

SOURCE: Boeing Co., Seattle Washington

FORTRAN H (93%), ASSEMBLER (7%) 6,987 cards  
IBM 360, Release 11

This program is designed to simulate the time domain response of an electronic circuit to an arbitrary forcing function. CIRCUS uses a charge-control parameter model to represent each semiconductor device. When given the primary

photocurrent induced in the semiconductor devices, the transient behavior of a circuit in a radiation environment can be determined. The program initially sets up time-domain circuit equations from a topological description of the network. Steady-state initial conditions are found by setting the differential equations to zero, then evaluating the transient solution by numerical integration of the differential equations. The program output includes the input data and columnar listings of network variables vs time. Virtually any circuit variable including currents and voltages internal to the semiconductor devices, may be displayed. Although no plotting capability is ordinarily supplied with CIRCUS, provisions have been made for saving variables on tape for subsequent plotting or further analysis by other programs.

#### ANALYSIS PROGRAM

SOURCE: General Dynamics Corporation, San Diego, Calif.

FORTRAN IV 1,421 cards  
CDC 6400; IBM 7094

Determination can be made of the Laplace transform of linear electronic networks. The corresponding poles and zeros, as well as the frequency and/or time domain response of a network can also be found. Input requirements are a list of elements (described by their terminal node numbers, element types, and elemental values), the input and output node numbers, and the type of desired network function (driving point impedance, voltage transfer function, etc). The program then calculates the coefficients of the required network function, the poles and zeros, frequency response, and transient response to an arbitrary input. Allowed element types are resistors, capacitors, inductors, non-ideal transformers, and voltage-controlled current sources in arbitrary configuration. Network size is limited to 12 - 15 nodes, 25 - 30 elements.

#### DC CIRCUIT ANALYSIS

SOURCE: Boeing Co., Seattle, Washington

FAP 4,260 cards  
IBM 7094 with Boeing FORMON Monitor

This program analyzes any number of linear direct current circuits per run, giving detailed results for each circuit. The program accepts as input the topological description of the circuit to be analyzed. From this description, tables are formed, and topological matrices are formed from the tables. The topological matrices describe the circuit geometry and can be used throughout an analysis of one particular circuit configuration. Matrices containing the parameter values are manipulated with the topological matrices to form the

system matrix. The system matrix represents a set of  $n$  independent simultaneous equations which are solved for the voltages at the dependent and first-order dependent nodes. From these voltages, the voltage at each second-order dependent node is found along with the value of the connecting voltage source. The program next finds the voltage drop across, the current through and the power dissipated by each circuit element. Partial derivatives of any circuit variable can be taken to determine the parameter value necessary to create the desired worst-case condition and the sensitivity of a solution variable with respect to all the circuit parameters.

#### A LINEAR CIRCUIT ANALYSIS PROGRAM (CIRCS)

SOURCE: Jet Propulsion Lab., Calif. Inst. of Tech., Pasadena

FORTRAN IV 6,782 cards  
IBM 1620/1311

The program can solve a linear network containing a maximum of 15 nodes (excluding ground) and 45 branches. Transistors and diodes can be included in the network as linear models and a special data card allows the user to describe the base, collector, and  $g$  or  $G_m$  characteristics of the transistor. Mutual inductance is not considered. A Mandex Worst Case is available with the dc program. The sensitivities computations in CIRCS gives the user a perspective as to the percentage effect that a particular input parameter has on a particular node voltage with respect to the remaining input parameters. Linear approximations for the differentials and integrals in the transient program are substituted, thereby reducing the system of differential equations to a system of algebraic equations.

#### GERT: SIMULATION PROGRAM FOR GERT NETWORK ANALYSIS

SOURCE: National Aeronautics and Space Administration, Electronics Research Center, Cambridge, Mass.

FORTRAN IV 1,359 cards  
IBM 1130

This program can accommodate GERT networks which have EXCLUSIVE-OR, INCLUSIVE-OR and AND logical operations associated with the input side of a node. The branches of the GERT network are described in terms of a probability that the branch is realized and a time to perform the activity represented by the branch. The time associated with a branch can be a random variable. The results obtained from the GERT simulation program are: (1) The probability that a node is realized; (2) The average time to realize a node; (3) An estimate of the standard deviation of the time to realize a node; (4) The minimum time observed to realize a node; (5) The maximum time observed to realize a node; and (6) A histogram of the times to realize a node. Normally this information is obtained for each sink node of the network. The program is written to permit the information to be obtained for any node specified in the input data. A comparison report is available which describes in detail the required input data.

## ALTERNATING CURRENT CIRCUIT ANALYSIS

SOURCE: Boeing Co., Seattle, Wash.

FORTTRAN IV (91%), MAP (9%) 1,341 cards

IBM 7094

The ac analysis program is used by an electronic design engineer to aid in designing and analyzing linear ac circuits. The program automatically sets up nodal equations from a description of linear ac circuit. Topological descriptions of the circuits to be analyzed are input. All parameter units are assumed to be in volts, ohms, amps, and watts, although a consistent scaled system may be used. Various matrices are generated from the nodal description. The equations are solved for the node voltages which in turn are used to calculate the voltage drop, current, and power dissipation in each circuit component. It also checks the integrity of the network and its function. There is no limit to the number of circuits that may be analyzed in a single computer run. Since the program can analyze any number of circuits per run and gives very detailed results for each circuit, the program will result in a very significant tool for automated circuit design.

## GERT EXCLUSIVE OR PROGRAM: COMBINING PATHS AND LOOPS OF ELECTRICAL NETWORKS

SOURCE: National Aeronautics and Space Administration, Electronics Research Center, Cambridge, Mass

FORTTRAN IV 849 cards

IBM 1130

The program reduces an electrical network with multi-parameter branches to a network which has only a single branch connecting source nodes to sink nodes. It calculates the probability, mean and variance of the time to go from each source node to each sink node of the GERT network. It also determines the paths and loops associated with the network and combines the values associated with paths and loops according to a topology equation which obtains the parameters associated with the equivalent.

## A HEURISTIC FOR COMPUTER-AIDED SYNTHESIS OF MULTIPLE-OUTPUT ALL NAND COMBINATIONAL-LOGIC CIRCUITS

SOURCE: Sandia Corp., Albuquerque, N. Mex.

FORTTRAN II 846 cards

SDS 930, CDC 3600

Logic circuits consist of two primary types: combinational and sequential. The combinational logic circuit derives its output from inputs that are present at a given time, while the sequential-logic circuit contains memory elements such that its output is determined by the inputs present at a given time plus the time history of these inputs. Using the heuristic, this program performs the necessary operations for evaluating the heuristic and synthesizing combinational-logic circuits. In addition to three-input,

one-output circuits that are synthesized, four-, five-, and six-input, one-output circuits have been attempted to determine if the heuristic fails as the complexity of the desired circuit increases. Only six-input circuits with memory overflow do not complete. Because of the computer memory size, no more than six input circuits can be synthesized with the program. Seven inputs could be handled with more efficient use of memory, but, beyond that, more than one core loading would be required.

#### PERFORMANCE ANALYSIS OF ELECTRICAL CIRCUITS (PANE)

SOURCE: Boeing Co., Seattle, Wash.

FORTRAN H (66%), ASSEMBLER (34%) 5,600 cards

IBM 360, Release 11

An automated statistical and worse case IBM system 360 computer program performs dc and ac steady state circuit analyses. The program writes a set of real (dc analysis) or complex (ac analysis) circuit equations in matrix form from a topological description of the circuit components and their interconnections. The program determines the worse case circuit performance by solving the circuit equations with each input toleranced to produce the minimum and maximum value of each output parameter. It also performs a Monte Carlo statistical analysis by solving the circuit equations repeatedly, using random selections of the input parameter values, according to user specified density distributions, thereby producing a statistical variation of each output parameter. The program handles 60 dependent nodes (other than ground or those connected to independent voltage sources). The ac program accepts resistors, capacitors, inductors, independent voltage and current sources, voltage dependent current sources, any ac equivalent transistor model using voltage dependent current sources, and diodes represented by their ac equivalent.

#### GENERAL FREQUENCY RESPONSE PROGRAM

SOURCE: Boeing Co., Seattle, Wash.

FORTRAN IV (95%), MAP (5%) 1,071 cards

IBM 7094/7044 DCS

In recent years, perhaps due to early successes in military applications, the analysis of automatic control systems has become an important problem in many diverse disciplines. A central question is that of stability: Do the dependent variables describing a dynamic system remain bounded under the perturbations arising from the physical environment? Because of its ease of application, the frequency response method is a natural tool for stability investigations. This computer program provides the frequency response of any linear feedback control system. The General Frequency Response Program enables computation of the open loop frequency response of a closed loop control system. The system characteristic matrix, obtained from the Laplace transformations of the dynamic and control equations, is input to the program. A variety of outputs is available, including a detailed print, a summary print, and Nyquist and Bode plots. Other program features of interest are parameter variation, amplitude to decibel conversion, and linear interpolation of amplitudes and phases at critical points.

## SOLUTION OF NONLINEAR ALGEBRAIC EQUATIONS CHARACTERISTIC OF FILTER CIRCUITS

SOURCE: Northrop Space Labs., Hawthorne, Calif.

FORTRAN IV (99%), MAP (1%) 6,160 cards

IBM 7094, SC 4020 Plotter

This program is designed to solve sets of nonlinear algebraic equations, which are characteristic of filter circuits. The unknowns in the equations are the values of resistances, inductances, and reciprocals of capacitances which occur in a filter circuit. Each equation consists of a sum of terms with each term consisting of the product of several unknowns and with the coefficient of each term equal to unity. This program has been used successfully to solve sets of equations in 6 unknowns and 13 unknowns. The program utilizes a combination of Kizner's method and the Freudenstein Roth technique in solving for the roots of the equation. After obtaining the roots, the program selects standard circuit components whose values approximately match the actual roots.

## PROGRAM FOR IMPROVED ELECTRICAL HARNESS DOCUMENTATION AND FABRICATION

SOURCE: General Electric Co., Philadelphia, PA

FORTRAN IV(98.4%), MAP (1.6%) 5,594 cards

IBM 7094

A package of programs produces an automated printout of the electrical harness interconnection wiring table, necessary subsequent to the establishment of electrical harnessing requirements for the Nimbus Spacecraft. The programs provide an automated crosscheck of reciprocal pin/connector assignments, and improve the accuracy and reliability of final documented data. The interconnection wiring table stipulates wire size and type, connector identification and type, pin identification, shielding, splicing and bussing requirements, special harness fabrication and test requirements, and identifies reciprocal pin/connector assignments for all wiring within a harness segment. The interconnection table provides the basic information for the preparation of harness parts listings, mockup harness development, harness drawings, harness boards, and fabrication and testing of prime harnesses.

## ANALYSIS OF DC CIRCUITS (R1113)

SOURCE: National Aeronautics and Space Administration, Langley Research Center, Langley Station, Va.

FORTRAN IV (82%), MAP (15%), OBJECT (3%) 8,023 cards

IBM 7090/7094

ASAP (Automated Statistical Analysis Program) is a D. C. circuit analysis program. In contrast to previous programs, ASAP does not require that the

circuit equations be written and solved to produce a Monte Carlo statistical analysis. By using a nodal description of the circuit in English text free-format style, ASAP will write circuit equations, solve them algebraically, write and compile a FORTRAN subroutine, and run the statistical analysis. A considerable amount of programmer time can be saved and careless errors eliminated by this method. The ASAP 11 program is designed and programmed to accept the user's simple topological description on his circuit, and the component parameter information, such as their nominal values, the tolerances and the type of densityfunction that characterizes each component. The output of this program is another computer program which contains all the statistical information and mathematical models of the circuit and its non-linear components. The second part of this program, STRESS, performs the statistical analysis.

DETERC

SOURCE: Rocketdyne, Canoga Park, Calif.

FORTRAN IV 510 cards

IBM 7094

Laplace transfer functions of networks are determined. Inputs to the program are of determinants of second-order expressions, usually containing L, C, and R of electrical networks or analogous quantities. The program expands the determinants by minors to obtain the numerator and denominator polynomials of the transfer functions. These polynomials are then factored using BROOT as a subroutine. (See MFS-1502, M69-10348, Volume 1, Numbers 1 and 2, July 15, 1969 of this publication.) Determinants up to the tenth-order ( $10 \times 10$ ) can be used.

#### A DIGITAL COMPUTER PROGRAM FOR PASSIVE NETWORK SYNTHESIS SUBJECT TO A QUANTIZED VALUE CONSTRAINT

SOURCE: International Business Machines Corp. New York

FORTRAN IV, E-Level Subset 626 cards

IBM 360, Release 11

This program synthesizes an electrical network. It determines that combination of element values which yields a close approximation to a desired transfer function denominator for one of several network configurations from which any element(s) may be deleted. It is the responsibility of the user to determine the tank circuit values which give the desired numerator, and to determine the resistor values which give the desired resistance. These determinations can be made using conventional network analysis techniques. The criterion for the selection of a particular set of component values is the summation of the squared differences between the coefficients of the desired transfer function and the corresponding coefficients for the specified component values. In order to minimize the total error, an organized search is made on the undetermined component values. This is done by perturbing individual elements and determining the effect on the total error.



## REALIZATION PROGRAM

SOURCE: General Dynamics/Convair, San Diego, Calif

FORTRAN IV (100%) 1,244 cards

IBM 7090; CDC 6400

Frequency selective networks are designed when the network configuration or topology is given. The element values are perturbed until the final design (if possible) is achieved. The program specifies the final design by prescribing element values and/or a network function  $T(S)$ . It is assumed that the approximation problem has been solved and that the coefficients of the desired network functions are known. The principal features of the program are its abilities to accept arbitrary topologies, to grow new elements, and to converge rapidly. It is possible to generate filters with prescribed loss from lossless filters or to design bandpass amplifiers to accommodate transistors with prescribed small signal equivalent circuits. Also, the frequency characteristics of networks can be altered by adjusting certain elements. For example, passive or active linear phase filters can be transformed from a design originally having a Tchebysheff amplitude response.

## DIGITAL FILTER SYNTHESIS PROGRAM

SOURCE: National Aeronautics and Space Administration, Ames Research Center, Moffett Field, Calif.

FORTRAN IV (33%), MAP (67%) 1,557 cards

IBM 7040/7094

This program allows any continuous function of a complex variable to be expressed in approximate form as a computational algorithm or difference equation. Once the difference equation has been developed, digital filtering can be performed by the program on any input data. The bilinear transform method of digital filter synthesis originated by Steiglitz is automatically implemented by the program. The method allows synthesis of the difference equation for digital filtering with the initial specifications for filter performance given in terms of the analog prototype in the frequency domain. Thus, the digital filter can be derived from the transfer function for the real time analog equivalent network. Documentation for this program is also available as NASA TM X-62000 from the National Technical Information Service (NTIS). Springfield, Virginia 22151.

## ELECTRICAL FILTER SYNTHESIS PROTOTYPE

SOURCE: Lockheed Electronics Co., Plainfield, NJ

FORTRAN IV 1,746 cards

IBM 360/44

Synthesis of one of three different types of electrical filters is provided; the maximally flat or Butterworth filter, the equal-ripple or Chebyshev filter, or the linear-phase or Bessel Filter. The filter may have one of four possible pass-band characteristics; low pass, high pass, band pass, or band reject. The

program is designed for use with two digital cathode ray tube screens. One tube displays instructions for the operator's selection, and the other displays the results of the frequency response analysis for the synthesized filter.

#### PASSIVE NETWORK DIGITAL PROGRAM

SOURCE: Boeing Co., Seattle, Wash.

FORTRAN II (44%) FAP (55%), OBJECT (1%) 5,791 cards

IBM 7094

This general purpose program is designed to perform the analysis of any linear lumped-parameter passive electrical network. The network is described to the program by listing elements and the direction of loop currents flowing through them. The program also calculates the poles and zeroes of input impedance and transfer admittance, and the frequency response of both. The passive network program is written in FORTRAN 2. However, some of the subroutines are coded in FORTRAN assembly language (FAP) and are not available on the source level. Therefore, all production is done using a binary version of this program. This binary deck has been generated on an IBM 7094 computer operating under a FORTRAN 2-version 3IBSYS monitor. It is doubtful that the binary deck will function properly under any other system than the one mentioned above.

#### IBM ELECTRONIC CIRCUIT ANALYSIS PROGRAM (ECAP) VERSION 1

SOURCE: Boeing Co., Seattle, Wash.

FORTRAN H 5,649 cards

IBM 360, Release 11

The Electronic Circuit Analysis Program (ECAP) is an integrated system of programs to aid in the design and analysis of electronic circuits. Dc, ac, and transient analyses of electrical networks can be produced from a description of the connections of the network (the circuit topology), a list of corresponding circuit element values, a selection of the type of analysis desired, a description of the circuit excitation, and a list of the output desired. ECAP recognizes standard electrical circuit elements. Any electrical network that can be constructed from the different elements in the set can be analyzed by ECAP. There is almost no limit to the number of ways that the circuit elements can be arranged in the network. The set of standard circuit elements does not include electronic components, but in many cases, these components are easily simulated by means of equivalent circuits constructed of standard elements. Examples are included in this manual that involve the use of equivalent circuits.

BELAC

SOURCE: General Electric Co., Philadelphia, PA

FORTRAN IV 11,117 cards

IBM 7040; GE 635

A method of quickly simulating a linear, time-invariant, lumped-constant network is provided. Input consists of the component values and their interconnections. Components recognized by the program include resistors, capacitors, inductors, independent voltage and current generators, voltage or current generators dependent on voltage or current, transformers, 2-part parameters, transfer functions, and gyrators. Output can be currents, voltages, impedance, gain, etc. One run produces any or all of the following concerning the output variables: frequency or time response tabulated and plotted, ac/dc sensitivities to parameter variations, ac/dc worse case analysis, optimizing to a frequency domain or dc specification, poles and zeros, etc. The most important assets of this program are its simple input format and its flexibility.

#### PASSIVE NETWORK PROGRAM

SOURCE: Boeing Co., Seattle, Wash.

FORTRAN IV (100%) 1,128 cards

IBM 360

Calculations are made of the input impedance and transfer function of an electrical network composed of such components as capacitors, resistors, and inductors. The poles and zeros of the input impedance and network transfer function are computed. A user description of the network is provided using a problem-oriented input data sheet, and the input impedance and transfer function are expressed as ratios of real polynomials  $P(s)/Q(s)$ . The roots of  $P(s)$  and  $Q(s)$  are also expressed. The program can be used for any R-L-C filter network with a maximum of 40 components and 20 current loops.

### 3.3 Design Factors

A multitude of factors influence design decisions both directly and indirectly. Twenty-four reports were identified that provide information that will describe the nature of the interaction points in the management program (e.g., relative trade-off parameters). These documents were identified in a Task 3 Report, "Modeling and Analysis Techniques". (See references)

### 3.4 Design Procedures

This section deals with conventional methods of power processing system design. Computerized design procedures have normally evolved from such conventional procedures. Information from these references shed light on what assumptions, decisions, and conclusions were made in the past computerizations of design procedures, and twenty such references were documented in the Task 3 Report.

### 3.5 Component Design

The nature of components influences the nature of a design procedure. Sixty-three examples of specific subsystem characteristics that will dictate the nature of the format of computerized storage of a large number of subsystems were documented in the Task 3 Report to provide the significant key words to be used in a random access memory information storage system.

### 3.6 Complete System Examples

Twenty-nine examples of complete power processing systems that have evolved from both conventional and computerized design procedures were documented in the Task 3 Report. They will indicate the nature of final requirements of a completed system and hence the goals of the design process.

### 3.7 Power Sources

The nature of the power source greatly affects power processing system design.

All viable electrical power sources were reviewed from a system characteristics point of view to account for the processing system dependency on power sources. The information that resulted from this review of available data was documented in the Task 3 Report, and was divided into the following subheadings:

1. Power System Comparison (15)
2. Brayton Cycle Systems (24)
3. Rankine Cycle Systems (13)
4. Magnetohydrodynamic Systems (4)
5. Thermionic Power Systems (7)
6. Thermoelectric Systems (24)
7. Systems for Nuclear Auxiliary Power (SNAP): Applications (10)
8. Solar Arrays (28)
9. Storage Batteries (4)
10. Power Source Applications (35)

Numbers in parentheses indicate the number of topics documented.

### 3.9 Summary and Conclusions

Three computer languages that possessed sufficient interactive capabilities were reviewed. Table 3-1 shows their relative features used as a system implementation tool. A choice will be made from these three alternatives for implementation as the management program language. The final choice will be the one best suited to the design methodology in terms of:

1. Independence of subprograms
2. Variety of data structures
3. Method of storage management
4. Debugging capability
5. Proven reliability of language

6. Documentation method
7. Speed of language processor
8. Operation cost
9. Arithmetic features
10. File handling capability
11. Linkage capability

Table 3-1

## Features of Languages used as a System Implementation Tool

	FORTRAN	APL	PL/I
Speed of the language processor	Fortran H and G compiler Very fast (in the sense running object code)	APL is an interpreter Slow No way to get object code	PL/I optimizer Very Fast PL/I checker Used for one-shot program
Price of using the language	Very economical	Relatively expensive	Economical
Arithmetic in the language	Double precision available Complex operation	Precision up to 14 digits. Complex Operation	Double precision available Complex Operation
File handling capability	Files handled by the operating system READ, PRINT statement allows user to create and retrieve data	Variable name used as a file name There is no difference between a variable and a file	READ, GET, WRITE, PUT statements allow user to create and retrieve data There are two kinds of input/output operations, one is RECORD the other is STREAM
Linkage to other programs	Use linkage editor		Use linkage editor
Independence of subprograms	Variable cannot be the same	Function structure language	Block structure language
Variety of data structure	Integer, real number, array, etc. No list processing capability. Character string handled poorly	Integer, real, complex, array, etc. Vector & array handled very efficiently	Integer, real, complex, character string, array, & structure Has list processing capability
Method of storage management	Static	Static, controlled	Static, controlled & automatic
Debugging tools	Trace	Trace	Trace, "ON" statement
State of language	Stable, widely used, good service - may be phased out within ten years	Growing, going to be widely used	Stable, widely used, good service
Maintenance of the program.	Easy to read the code	Code is very compact	Easy to read the code Partially self-documentable

SECTION 4  
FORMULATION OF A METHODOLOGY

PRECEDING PAGE BLANK NOT FILMED

REPRODUCIBILITY OF THE  
ORIGINAL PAGE IS POOR ...



## 4.0 FORMULATION OF A METHODOLOGY

The program as envisioned specifies power processing subsystems based on mission objectives that determine primary and secondary characteristics, system constraints that may modify these characteristics, and a data file of existing equipment for comparison. Additionally, routines could be prepared to synthesize a power processing subsystem if no data existed, and this combination of historical data and simulation would permit configuring a system from the optimum combination of power processing subsystems.

### 4.1 Design Procedure

The main function of a power processing system (PPS) in a space vehicle is to supply the energy generated by an energy source to the loads (see Figure 4-1).

The load equipment includes units essential to the operation of the space vehicle itself as well as units essential to the fulfillment of the mission

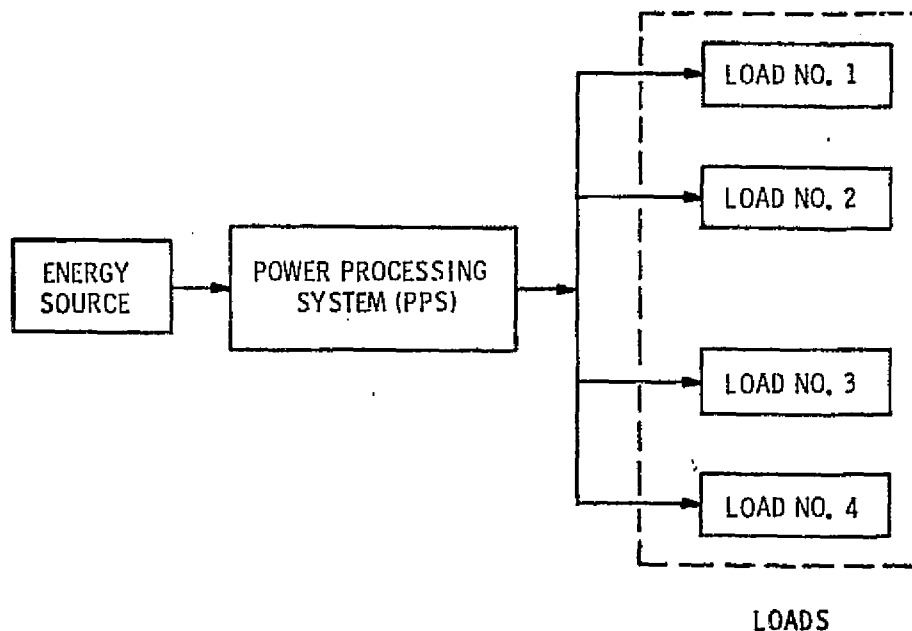


Figure 4-1. Power System Block Diagram

objectives. This equipment has various energy requirements and operating conditions such as voltage level, voltage type (ac or dc), voltage wave shape, frequency, regulation characteristics, etc. All these characteristics must be generated within the PPS and then supplied to the respective loads. The PPS demands some energy and has its own operating characteristics as well. It consists of subsystems which are made of several components. A PPS may include, for example, the following subsystems: energy storage devices (batteries or capacitors), charge-discharge controller, converters, inverters, regulators, etc.

Figure 4-2 is a block diagram of the procedure developed for the design, modeling, simulation, analysis and evaluation of power processing systems. Block No. 1 receives all data and information available related to: (1) mission objectives, (2) mission constraints, (3) space vehicle type, functions and environment, (4) load unit specifications and operating characteristics, and (5) energy sources available and their capabilities. These data and information are organized, classified and utilized to construct a set of criteria used to search for applicable power processing subsystems. In Block No. 2, these criteria are used to search for readily available subsystems (hits) which satisfy the required characteristics and specifications.

In Block No. 3, any required subsystem which is not located by the search process will be conceptually synthesized to conform with the specification information given in Block No. 1

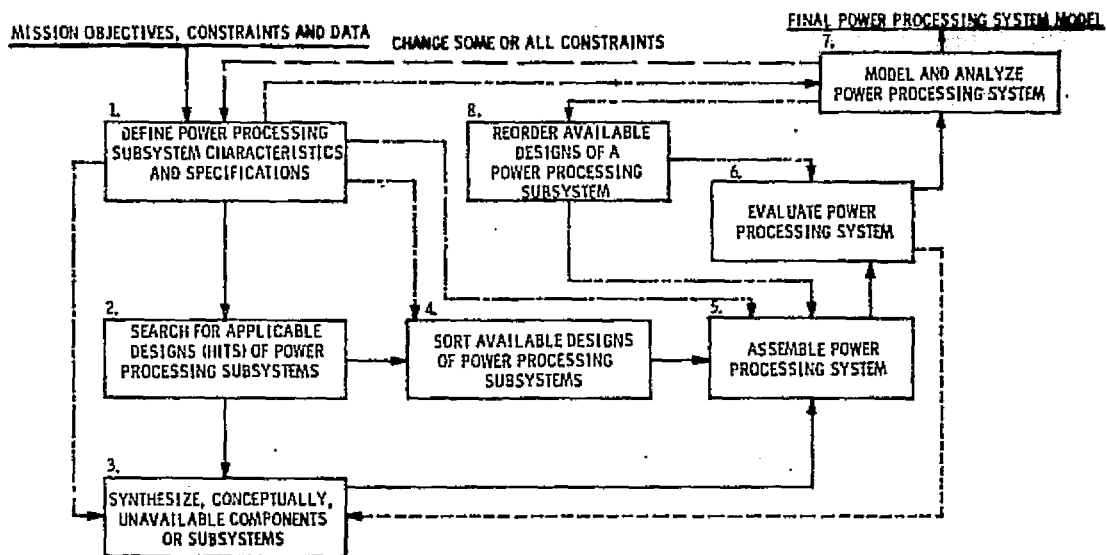


Figure 4-2. Design Process Block Diagram

After completing the search, all subsystems obtained from Block No. 2 are sorted in Block No. 4 according to a priority list (from the most to the least desirable for the PPS) guided by the information in Block No. 1.

In Block No. 5, an assembly of the PPS is made from the most desirable systems as selected in Block No. 4 and using conceptually synthesized subsystems from Block No. 3, if needed.

In Block No. 6, the assembled PPS will be evaluated to determine whether or not system constraints such as total weight, volume, cost, etc., are met. After evaluation, the resultant PPS will be modeled and analyzed in Block No. 7 to determine whether performance criteria are met. The data and information of Block No. 1 provide the several criteria for the evaluation, modeling, and analysis processes.

If the model does not satisfy the design objective of Block No. 1, the available subsystem designs are reordered in Block No. 8 and other assemblies from

the other hits of available designs of subsystems are evaluated, modeled and analyzed.

#### 4.1.1 Input Information (Block No. 1)

Mission objectives, mission constraints, and space vehicle function requirements data are collected. These data are processed to develop the specifications of the several subsystems and the criteria which will be the basis for the search and synthesis processes in Block Nos. 2 and 3.

Figure 4-3 shows a schematic construction of Block No. 1. Note that the mission objectives (e.g., Mercury scan, Venus scan, interplanetary, atmosphere and surface data collection) and the mission data and constraints (e.g., mission duration of both transit and orbit, mission budget, mission control system, orbit characteristics of period and size, etc.) will determine the spacecraft design requirements including: type, injected weight, configuration, energy

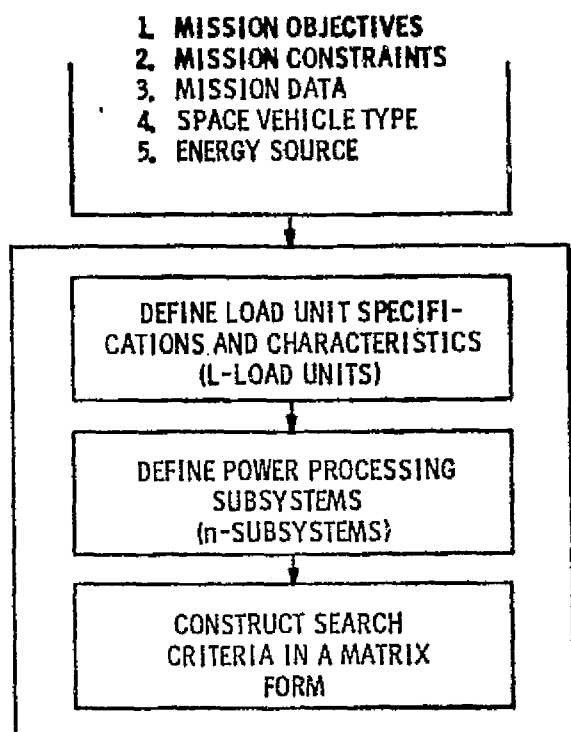


Figure 4-3. Block No. 1 Schematic

source capability and configuration, control system, stabilization system, communication system, launch vehicle, etc. Having defined the mission objectives and constraints and having selected the spacecraft, the various load units required to achieve those objectives within the mission constraints and to operate the spacecraft within its power capability, can be decided upon. Load units may include: gyros, sensors, TV systems, transmitters, receivers, control systems, instruments, tape recorders, heaters, valves, data handling system, etc.

Each of these load units has its operation characteristics and requirements which can be identified (e.g., voltages, current, frequency, power, priority with respect to mission objectives, reliability, etc.).

The priority level of each load unit with regard to its importance and necessity for the mission objectives and spacecraft operation is given a priority index of 1 to 5, with 1 being the highest priority.

The data and information are classified and categorized according to common criteria among the load units (e.g., ac voltage, dc voltage, 26 volts, 120 volts, 400 Hz, 3 phase, etc.).

With the mission objectives and constraints known and with the spacecraft functions and energy sources known, the characteristics and specifications of the required subsystems of the PPS can be identified. These characteristics and specifications are grouped in a search matrix which may take the form shown in Table 4-1.

#### 4.1.2 Search Procedure

Table 4-1 has been constructed from load unit requirements and characteristics

Table 4-1. Power Processor Criteria

CRITERION																				
C1	C2	C3	C4	C5	C6	C7	C8	C9							C10	C11	C12	C13		
VOLTAGE TYPE	VOLTAGE MAGNITUDE			SUBSYSTEM NAME	WEIGHT (LB.)	COST (\$)	RELIABILITY	MISSION PHASE POWER (WATT)							PRIORITY LEVEL	VOLTAGE REGULATION		ALLOWED VOLTAGE TOLERANCE		
								1	2	3	4	5	6	7						
CRITERION																				
C1	C2	C3	C4	C5	C6	C7	C8	C9							C10	C11	C12	C13		
VOLTAGE TYPE	VOLTAGE MAGNITUDE	FREQUENCY HERTZ	NUMBER OF PHASES(Φ)	SUBSYSTEM NAME	WEIGHT (LB.)	COST (\$)	RELIABILITY	MISSION PHASE POWER (VA OR WATT)							PRIORITY LEVEL	VOLTAGE REGULATION	FREQUENCY REGULATION	ALLOWED VOLTAGE TOLERANCE		
								1	2	3	4	5	6	7						
DC	AC	28 V	6000	1	ABLE	1.20	5000	.98	250	250	250	250	250	250	250	1	± 2	± 0.01	± 4	
					BAKER	.75	1050	.97	75	75	0	75	75	0	75	2	± 3	± 0.02	± 6	
					CHARLIE	.30	250	.97	50	0	50	50	0	50	0	2	± 3	± 0.02	± 4	
					DOG	2.10	7500	.95	200	200	200	200	200	200	200	1	± 1	± 0.01	± 2	
					.	1.35	6010	.98	150	0	0	150	150	0	150	3	± 3	± 0.03	± 4	
		400	3		.	.55	570	.97	70	70	70	0	0	0	70	2	± 2	± 0.02	± 4	
					.	1.35	2580	.97	120	120	0	0	0	120	0	2	± 3	± 0.03	± 6	
					.	.85	790	.96	95	0	0	0	95	95	95	3	± 2	± 0.05	± 2	
					.	3.25	8000	.98	270	270	0	0	270	270	270	1	± 1	± 0.03	± 4	
					.	2.30	7900	.98	200	0	200	0	0	200	200	2	± 2	± 0.03	± 4	
	22 V	400	1		.	.45	850	.97	25	0	0	0	25	0	0	3	± 2	± 0.03	± 6	
					.	2.75	5800	.94	180	180	180	180	180	180	180	2	± 3	± 0.05	± 4	
					.	1.80	4900	.95	200	0	0	0	200	200	200	2	± 2	± 0.03	± 2	
					.	.75	890	.98	40	40	40	40	0	0	0	3	± 3	± 0.01	± 4	
					.	.95	1080	.98	50	0	0	0	50	50	50	2	± 2	± 0.02	± 2	
					.	2.00	4670	.97	170	170	0	170	0	170	170	3	± 2	± 0.02	± 2	

and provides the basis for search of the power processing subsystems data file for applicable subsystems.

After Table 4-1 was constructed, a combination of all common requirements of the several loads requiring processed power must be performed. This leads to a specification of the number of characteristics of the subsystems required to deliver processed power to the loads. There is, however, no unique number of subsystems which should be used in the power processing system. For example, a centralized voltage regulator may be used or the voltage regulation may be performed by a number of relatively small regulators. The number and characteristics of the power processing subsystems also depend upon the type of energy source. Characteristically, solar arrays are used for earth-orbital missions and for inner-planetary missions, while radioisotope thermoelectric generators are used for outer-planetary missions. Also, in specifying the number and characteristics of the subsystems, it should be recognized that not all loads are used simultaneously and the total power rating of the power processing system will frequently be far less than the sum of the power ratings of the several loads.

Figure 4-4 shows a flow diagram for the search procedure. The several blocks in this figure are discussed in the following paragraphs.

#### 4.1.2.1 The Filing System

The structure of the Power Processing Subsystem Data File is shown in Figure 4-5. This data file contains descriptions of power processing subsystem designs in terms of the criteria listed in Table 4-1. The file is placed in secondary storage, probably disk storage. At the front of this secondary storage (i.e., in the initial records), a directory will assist in interpreting

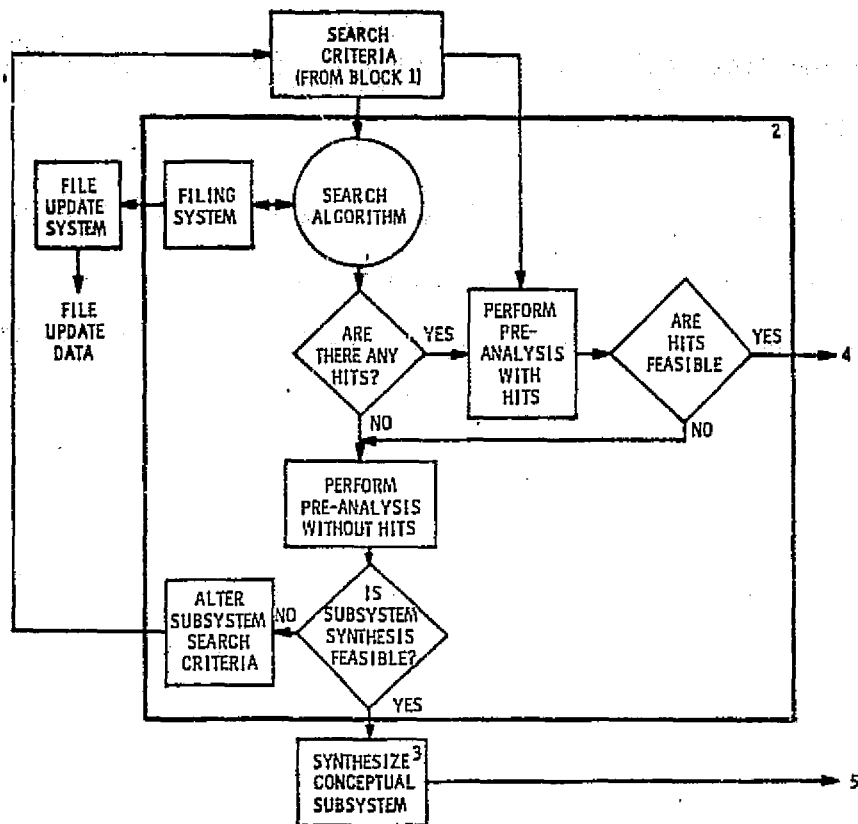


Figure 4-4. The Search Procedure

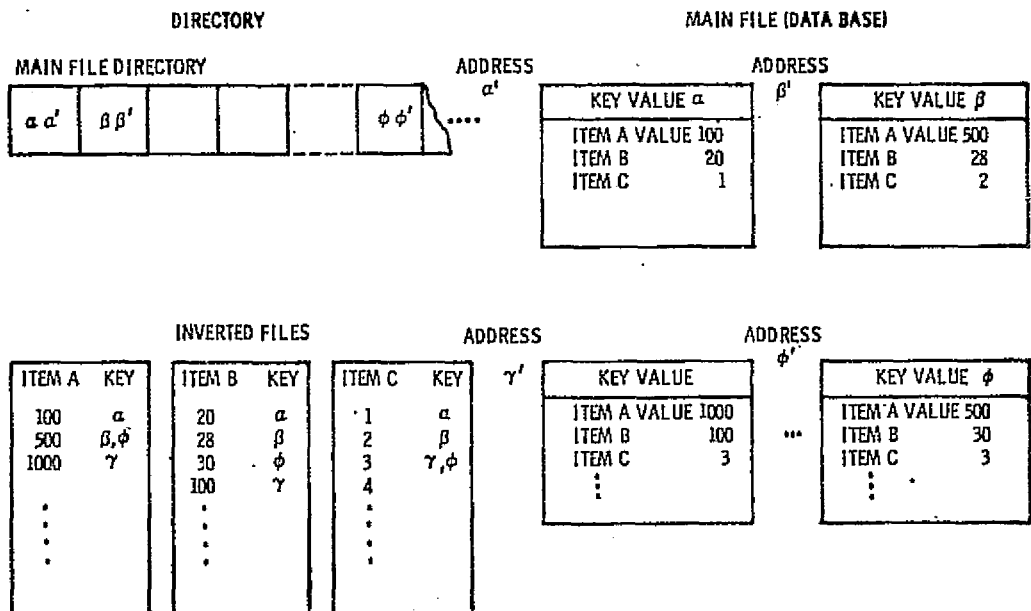


Figure 4-5. The File Structure



the content of the files. The directory contains the key to the main file and to several inverted files which correspond to particular search criteria. A frequency inverted file would contain the key to file storage based on the frequency of the subsystems, as shown in Figure 4-6.

FREQUENCY	KEYS TO THE MAIN FILE
100 Hz	A, B,
500 Hz	C, D, E, F,
1000 Hz	G,

VOLTAGE	KEYS TO THE MAIN FILE
20 V	C, D
28 V	E, F, G, H,
30 V	A,
100 V	B,
.	
.	
.	

Figure 4-6. Examples of Inverted Files

#### 4.1.2.2 The Search Algorithm

Figure 4-7 shows a flow diagram for the search algorithm. The search for applicable subsystems proceeds in two modes: (1) the directory mode, and (2) the file mode.

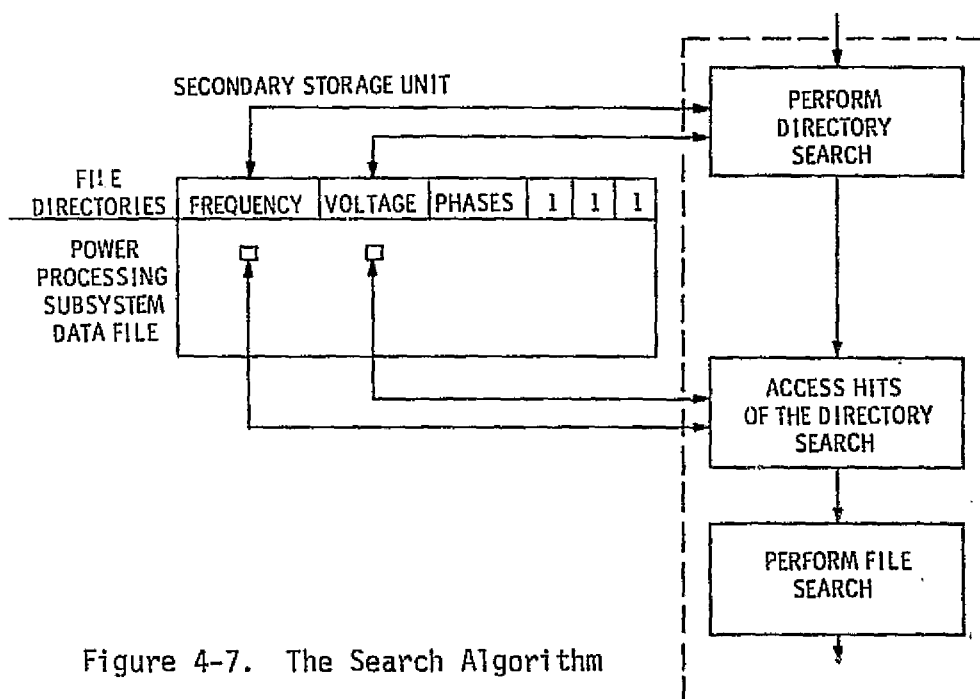


Figure 4-7. The Search Algorithm

In the directory-mode search, the operator/designer will specify several criteria for which the directory contains a key to the main file. For example, an initial search might be used upon a voltage criterion. The keys corresponding to all suitable subsystems are determined. The next search might then be based upon a frequency criterion. Again the keys corresponding to the current criterion are determined. Any common keys resulting from these two searches are retained as "hits" from the directory-mode search.

In file-mode search, the "hits" from directory-mode search are used as a reduced sample space for a search for "hits" conforming to the remaining criteria, i.e., phase, reliability, cost, weight, etc.

The file-mode search proceeds in passes, one pass for each criterion, using the results of the previous pass as a reduced sample space.

In file-mode search, there is active interfacing between the operator/designer and the computer. This active interfacing permits the operator/designer to select the options which will expedite the task. One option available is to provide a display of the closeness of non-hits on each pass. An example of this option is the following command:

DISTRIBUTION m(p)k

This command would display the number of non-hits in pass number m that are within p increments of the criterion, where k is the size of each increment. For example, in the command:

DISTRIBUTION 4(3)10

4 indicates the 4th pass, which could be the voltage range pass; 3 indicates that we wish to see the voltage non-hits within 3 increments of ten volts each from the desired voltage level. The command might yield:

9 non-hits within 10 volts

17 non-hits within 20 volts

51 non-hits within 30 volts

During file-mode search, the operator/designer also has the options of: (1) altering subsystems requirements to obtain more hits, and (2) adding arbitrary hits independent of the search.

#### 4.1.2.3 Pre-Analysis

After the search has been completed (and the operator/designer has perhaps exercised his options of altering subsystem requirements to obtain more hits or has added subsystems independent of the search), a number of hits for each subsystem results. A pre-analysis phase is then entered, the type of pre-analysis being dependent upon whether or not the number of hits for a desired subsystem is finite or zero.

#### 4.1.2.4 Pre-Analysis Without Hits

If no hits are obtained in the search for a particular subsystem, synthesis is implied. Pre-analysis then determines: (1) the feasibility of the required subsystem (cost, weight, etc.), and (2) the complexity of the required system. If the subsystem appears feasible, the subsystem is "conceptually" synthesized in Block No. 3. If the subsystem does not appear feasible, the subsystem search criteria are altered and the search for this subsystem is repeated and, if necessary, the pre-analysis is repeated as well.

#### 4.1.2.5 Pre-Analysis With Hits

If there are hits in the search for a particular subsystem, pre-analysis determines: (1) whether or not the operator/designer's options have altered the system constraints, and (2) the compatibility of the subsystem with the

other subsystems which have been selected.

#### 4.1.2.6 Concluding the Search

Referring again to Figure 4-4, it is seen that the search concludes, for a particular subsystem, after a design has been located in the file that is then found to be feasible, or if no feasible design is found, after the subsystem has been "conceptually" synthesized. The search continues until all required subsystems have been found or have been conceptually synthesized.

#### 4.1.3 Subsystem Synthesis

If the criteria for a particular subsystem cannot be satisfied by an entry in the Power Processing Subsystem Data File, then that subsystem is "conceptually" synthesized. That is, the power processing subsystem that is unavailable is replaced by a constructed set of parameters that satisfy the criteria established for the subsystem. The "conceptual" subsystem is regarded as a "hit", and the constructed parameters are included in the system assembly (Block No. 5). The dynamic characteristics of the conceptual subsystem are modeled so that the total power processing system can be analyzed (Block No. 7). Should the system perform well and meet all of the system constraints while using these dynamic characteristics, circuit synthesis can be justified.

#### 4.1.4 System Assembly

##### 4.1.4.1 Sorting Available Designs of Subsystems (Hits) (Block No. 4)

After completing the search for available designs of subsystems and the conceptual synthesis of unavailable subsystems, the sorting of these subsystem designs takes place. According to some criteria (e.g., power rating, weight, cost, reliability, etc.), the most desirable design is given the highest rank. The least desirable design is placed at the bottom of the stack. Thus, for the n

subsystems of the power processing system each having one or more available designs, the order of the available designs may take the form of Table 4-2. Note in Table 4-2 that Subsystem No. 1 has  $k$  available designs, Subsystem No. 2 has only one, and that the highest number of hits is  $m$ . For synthesized subsystems, the number of hits will normally be only one.

Table 4-2. The Ordering of the Subsystems

Available Designs	Subsystem					
	1	2	3	4...L....n		
1	$d_{11}$	$d_{21}$	$d_{31}$	$d_{41}$	$d_{l1}$	$d_{n1}$
2	$d_{12}$		$d_{32}$	$d_{42}$	$d_{l2}$	$d_{n2}$
3	$d_{13}$		$d_{33}$	$d_{43}$	$d_{l3}$	
4	$d_{14}$			$d_{44}$	$d_{l4}$	
.	.			.		
.	.			.		
.	.			.		
k	$d_{1k}$			$d_{4k}$		
.				.		
.				.		
.				.		
m				$d_{rm}$		

#### 4.1.4.2 Assembly of the PPS (Block No. 5)

Having ordered the available designs of the subsystems according to their degree of desirability for the most desirable subsystems, the system is assembled from the most desirable systems. This assembly is a complete design of the power processing system if no synthesized subsystems need to be included. A block diagram presenting the power processing system is constructed to show the interrelationship between the various subsystems and to show their functions. The assembly and the block diagram are evaluated and modeled and analyzed in Block Nos. 6 and 7, respectively.

#### 4.1.5 System Evaluation

The assembled power processing system has a set of characteristics and specifications which are the result of the aggregate sum of the characteristics and specification of its subsystems. These characteristics and specifications are evaluated (see Block No. 6 of Figure 4-2) with respect to mission objectives and constraints. For example, there may be limitations on the weight, power rating and cost of the PPS. Hence, it is necessary to compute:

$$\text{Total Weight} = W_t = \sum_{i=1}^n W_i \text{ lbs}$$

$$\text{Total Power Rating} = P_t = \sum_{i=1}^n P_i \text{ watts}$$

$$\text{Total Cost} = C_t = \sum_{i=1}^n C_i \text{ dollars}$$

where  $n$  is the total number of subsystems in the PPS. If the constraint is violated, the operator/designer selects an alternative design for a subsystem which has more than one available design and which is a promising candidate to remove the violation. For example, if the weight constraint is violated, the subsystem that normally has a great weight but for which some available designs have substantially less weight than average merits consideration. The available designs for this subsystem would be reordered such that the design with the least weight would be at the top of the stack. With the new subsystem replacing the old design, the PPS is again evaluated. This process continues until a PPS design is obtained which meets the objectives and constraints.

In case all of the available designs are exhausted for the subsystems having multi-alternate designs, either a modification of the synthesized subsystem(s) must be made or the system constraints must be modified.

If the evaluation carried out in Block No. 6 proves satisfactory, modeling and analysis is carried out in Block No. 7, which is described below. Note, however, that if the modeling and analysis reveals that a functional characteristic of the PPS is unsatisfactory, another design of the subsystem, whose nature is relevant to the functional characteristic, is chosen to improve the performance. The reordering procedure mentioned above is used to select the required design of the subsystem.

#### 4.1.6 Modeling and Analysis

The power processing system which was assembled in Block No. 5 (see Figure 4-2) and evaluated in Block No. 6 is modeled and analyzed in Block No. 7. For a particular analysis, the procedure might include the following steps:

1. The circuit description (probably an admittance matrix) is retrieved from the PPS data file for the final subsystem choices. Each subsystem will have its own index of nodes and branches as in Figure 4-8.

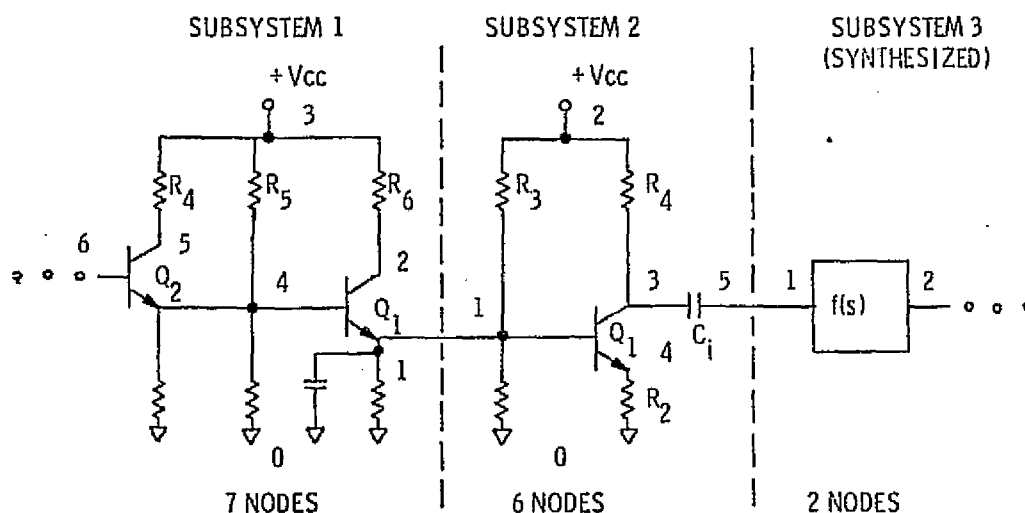


Figure 4-8. Subsystem Nodes and Branches

2. A synthesis routine develops dynamic characteristics for any subsystems that were "conceptually" synthesized in Block No. 3.
3. The subsystem descriptions, admittance matrices in the case of stored subsystems and transfer functions (dynamic characteristics) in the case of synthesized subsystems, are combined onto one matrix with a common index of nodes and branches as in Figure 4-9. This combination could involve: first a simple matrix formulation (e.g., four  $n \times n$  matrices combine to form a  $4n \times 4n$  matrix), followed by a node suppression scheme. This will yield the basis or linearly independent set of row vectors of the admittance matrix by eliminating redundant nodes.

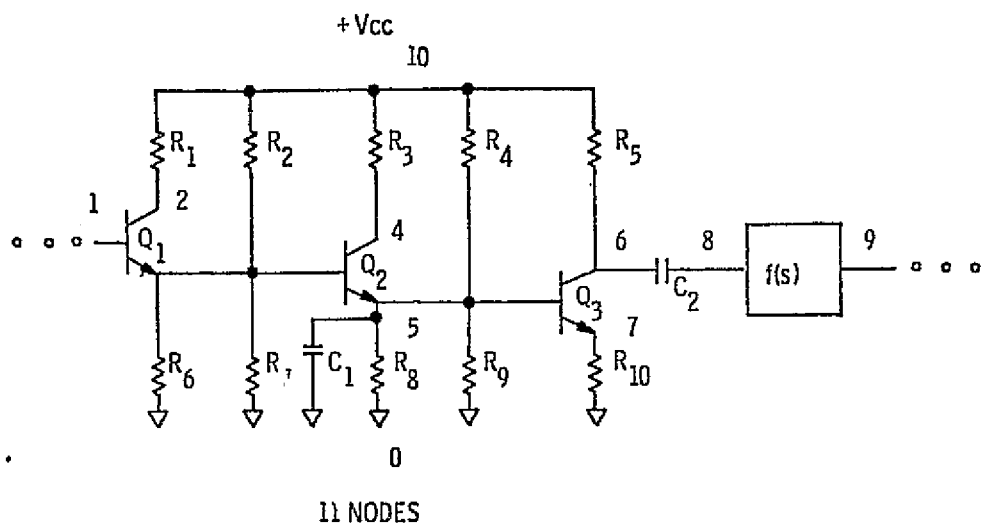


Figure 4-9. Combined Circuit

4. "First order" simplifications of the system circuit are performed by a branch suppression scheme. For instance, both  $R_6$  and  $R_7$ , and  $R_8$  and  $R_9$  of Figure 4-9 would combine to reduce the branch dimension



of the admittance matrix (as it turns out, also the weight and cost of the system are reduced) by one each. The extent of simplification could be controlled by the operator. He may wish to combine all parallel resistances, RC combinations, etc. "Higher order" simplifications could be handled interactively, e.g., elimination of redundant or unnecessary networks. The "higher order" simplifications demand that the circuit diagram be available so that the operator can "see" the circuit and then make suitable changes.

At any time, the option will be available for the operator to change any component in the circuit, or even "go back to the beginning" and introduce a new subsystem.

At some point, a final admittance matrix will result and the various analysis options are now ready to be accessed. The available options could include: transient response, stability analysis, sensitivity analysis, overload analysis, steady state analysis, etc.

The management program will enable the operator to access any circuit analysis program in the "system library". The routines may be stored as sub-programs. (Tables 4-3 through 4-6 compare a number of circuit analysis programs that may be used in the modeling and analysis.)

An important part of the management program will be a set of format conversion routines that can convert the circuit description (admittance matrix) of the management routine to the input formats of the analysis programs.

Table 4-3

GENERAL INFORMATION ON CIRCUIT  
ANALYSIS PROGRAMS

Program Name	Type Of Analysis		Approx. No. Of Statements	Core Requirements (Bytes)	Computers On Which Operating	Time In Use (Years)	Debug Status	Topological Limits	Documentation	Program Availability	Unique Program Features
	Linear	Nonlinear									
ANPS	X		4 K	80 K to 135 K	1,2,3,4,5,7,8 <sup>(1)</sup>	2	Complete	100 Branches 40 Nodes	Good	No Restrictions	Excellent Teaching Program Written in FORTRAN and ALGOL
BELAC	X		10 K	120 K	4	5	Complete	None <sup>(5)</sup>	Good	No Restrictions <sup>(2)</sup>	Available on Time Share, Batch, and Remote Batch
COMPACT	X		2 K	64 K	2,6,7	2	Complete	1 and 2 Port Topologies	Good	No Restrictions <sup>(3)</sup>	Microwave Design and Optimization
FORMAP	X		3 K	80 K to 110 K	2,4,6,7	6	Complete	50 Elements to 70 Elements	Good	No Restrictions	State Equation Oriented Completely ANSI and FORTRAN 4
LISA	X		-	140 K	7	5	Complete	125 Elements 50 Nodes	Good	No Restrictions	Provides Poles and Zeros and Block Diagram
MARTIA	X		-	32 K	7	3	Complete	2 Port Topologies	Good	No Restrictions	Simple, Open Ended Library of Elements, Responses, Fast, Built-in Functions and Frequency Transformations
PTFA	X		1.5 K	115 K	7	2	Complete	50 Elements <sup>(6)</sup>	Good	No Restrictions	Primarily Suited to Instruction of Undergraduates
SCAP	X		1.4 K	125 K	7	0.5	Complete	200 Nodes 500 Branches 100 Coupled Elements	Good	No Restrictions	Response Evaluated by Loopless Code
SNAP	X		1.6 K	26 K	2	3	Complete	35 Nodes 100 Branches	Good	No Restrictions	Symbolic Transistor Function

Table 4-3

## GENERAL INFORMATION ON CIRCUIT ANALYSIS PROGRAMS (CONTINUED)

Program Name	Type of Analysis		Approx. No. of Statements	Core Requirements (Bytes)	Computer On Which Operating	Time in Use (Years)	Debug Status	Topological Limits	Documentation	Program Availability	Unique Program Features
	Linear	Nonlinear									
ADA-74	X	X	4 K	64 K	4	8	Complete	None ⑤	Good	No Restrictions ③	Optimized for Most Efficient Use of CPU Time and Memory
ASTAP	X	X	60 K	200 K	7	4	Complete	None ⑤	Good	No Restrictions ③	Statistical Transient Analysis
DACSLP	X	X	-	1200 K	2	0.5	Complete	200 Nodes	None	Restricted	Models Large Microwave Transistor
CURE2000	X	X	9 K	600 K	2	0.5	Complete	200 Elements	Good	Restricted	Convergence Features, Large Signal Sensitivities
IMAG2	X	X	10 K	100 K	4, 5, 7, 10	3	Complete	None ⑤	Good	No Restrictions ③	3rd Generation Features
IL-CAP	X	X	3 K	200 K	0	2.5	Complete	-	Good	Restricted	3rd Generation Features
CIRCUITS-2	X	X	13 K	160 K, 600 K, 400 K	4 ③, 7, 2	3	Complete	None ⑤	Good	No Restrictions	Convolution Integral Modeling of Linear Systems 3rd Generation Features
SAP2		X	6.5 K	104 K or 250 K	7	1	80%	200 Branches 50 Nodes or 1500 Branches 500 Nodes	Preliminary Users Manual	No Restrictions	3rd Generation Features Well Suited for Shift Systems
SCEPTRE	X	X	16 K	130 K	7, 4 ③	5	Complete	300 Nodes	Good	No Restrictions	FFT and Monte Carlo Added to GE Version
SYSCAP	X	X	12 K ⑥	240 K ⑥	2	4	Complete	255 Nodes	Good	No Restrictions ③	

① ALGOL version of program

② GE system has time share and remote batch

③ Available commercially

④ Adjustable

⑤ None implies computer memory limited

⑥ SYSCAP consists of three separate analysis programs; each requires indicated quantities

⑦ LEGEND: 1 = Burroughs, 2 = CDC, 3 = ICL, 4 = GE/Honeywell, 5 = UNIVAC, 6 = PDP, 7 = IBM, 8 = RC4000, 9 = SPECTRA, 10 = C.I.L.

Table 4-4  
ANALYSIS DETAILS

Program Name	AC	DC	Sensitivity	Worst Case	Monte Carlo	Time	Optimization	Fourier Analysis	FFT	Other
ANFS	X	X*				X				Semi-Symbolic
BEIAC	X	X*	X	X	X	X	X			LaPlace Equations
COMPACT	X		X				X			Noise Figure - Stability Factor
CORNAP	X					X				
LISA	X	X	X			X				Root Locus
MAINTMA	X									
PTNA	X	X								Topological
SCAP	X	X								
SNAP										Symbolic
ADA-74	X	X	X				X			
ASTAP	X	X			X	X				
DACSEP	X	X				X				
CURE2000	X	X	X							
IMAG2	X	X					X			
II-CAP	X	X	X	X		X				
CHICLS-2		X				X				
NAI12	X	X	X	X			X	X		Tolerance
SCPTRE		X			X**	X			X**	
SYSCAP	X <sup>①</sup>	X	X	X	X <sup>①</sup>	X				Failure, Stress, Analyses

Table 4-5  
INPUT DETAILS

Elements		Controlled Sources	Equations	Library Elements	Tables	Transmission Lines	Arbitrary Input Signal	Other
Active	Passive							
X	X	X	X*		X		X	
X	X	X	X*	X	X			
X	X							S, Y, Z, and Noise
X	X	X						
X	X	X						
X	X	X	X	X	X	X		Wave- guides
	X							
X	X	X				X		
X	X	X						
			X	X				
X	X	X	X	X	X		X	
X	X	X	X	X	X		X	
X	X	X		X				
X	X	X	X	X	X		X	
X	X	X		X	X		X	
X	X	X	X	X				

\* Frequency = 0 Hz

\*\* Not on all versions

① To be available early in 1974

\*Equations for signals - polynomials, poles, zeros, LaPlace transforms, FORTRAN subroutines

\*\*Equations for elements - values are a function of time, frequency, signals, other element tracking, etc.

Table 4-6

## OUTPUTS

Data Format							Details												
Program Name	Lists	Printer Plots	Histograms	Scatter Plots	Envelope Plots	Miscellaneous	Element Volts	Node Volts	Element Current	Voltage Differences	Poles And Zeros	Transfer Function	Gain	Driving Point Function	Group Delay	Phase	User Specified	LaPlace Equation	Trees, Etc.
ANPS	X	X									X	X	X	X	X	X			
RELAC	X	X	X				X	X	X	X	X	X	X	X	X	X	X	X	
COMPACT	X												X			X	X		
COMNAP	X	X*					X	X	X	X	X	X	X	X	X	X			
LTSA	X	X					X	X	X	X	X	X							
NOBLEIA	F	X				Smith Charts	X	X	X	X		X	X	X		X	X		
PCSA	X	X					X	X	X	X		X	X						X
SCAP	X	X					X	X	X	X									
SCAP	X	X										X		X					
ADV-11	X	X															X		
ANLAP	X	X	X	X	X		X	X	X	X	X	X	X	X			X		
DIAGNOLP	X	X					X	X	X	X							X		
CLIM 2000	X	X					X	X		X									
PIAG2	X	X	X				X	X		X		X	X			X	All User Parameters		
IL-CAD	X	X						X	X			X							
CIRCUITS-2	X	X					X	X	X	X							X		
NAP2	X	X					X	X	X	X		X	X	X		X	X		
SC EPTHE	X	X					X	X	X	X							X		
SASCAP	X	X	X**				X	X	X	X			X				X		

\*Not on all versions

\*\*To be available early in 1974

REPRODUCIBILITY OF THE  
ORIGINAL PAGE IS POOR

4.1.6.1 Stability Analysis - Frequency performance and loop stability are determined empirically by use of a phase-gain meter on a breadboard configuration of a circuit implementation. This test data can be used to create a simple Fourier equivalent circuit that matches the actual circuit performance without access to the specific details of the schematic, the devices used, their variations with temperature, and distributed parameters that are not easily determined but may effect circuit performance. An example of this is a pulsewidth modulated regulator that is extremely difficult to analyze, but the transform of which will permit detailed simulation of its interactive effects with other circuits.

Test results from phase-gain measurements are used presently to determine compensation necessary to provide sufficient phase margin for stability under expected variation in part parameters with temperature and life. The same data can be utilized in a computer program much more extensively to predict circuit performance under a wide range of conditions.

4.1.6.2 Transformer Optimization - Block 7 can be used in an additional way to optimize or synthesize a particular device such as a power transformer. For example, consider a computer routine to provide a minimum-weight design.

To simplify calculations, the program uses a shell type transformer design utilizing scrapless shape laminations with a square center leg to simplify calculations. This choice fixes the form factor of the transformer and allows routine calculations varying only flux density, frequency, total transformer weight, and total watts. A typical lamination has a shape as shown in Figure 4-10, normalized on the width of the outer leg.

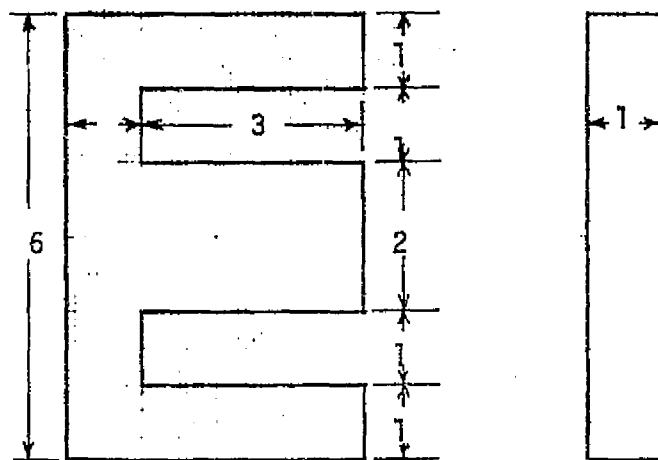


Figure 4-10 Shape of Scrapless EI Laminations

To provide a range of flux densities and operating frequencies, information on three distinctly different core materials is supplied to the computer program. The first of these core materials is a non-oriented 80% nickel-iron alloy that is especially useful where circuit losses must be minimized. It

will yield high weight, low loss, voltage transformation. The second material is a grain-oriented 50% nickel-iron alloy with nominal core loss and weight. The third material is a highly refined 50% cobalt-iron alloy, designed for extreme high temperature operation and miniaturization. Figure 4-11 shows the relative operating ranges for these three materials and core loss data in watts per pound.

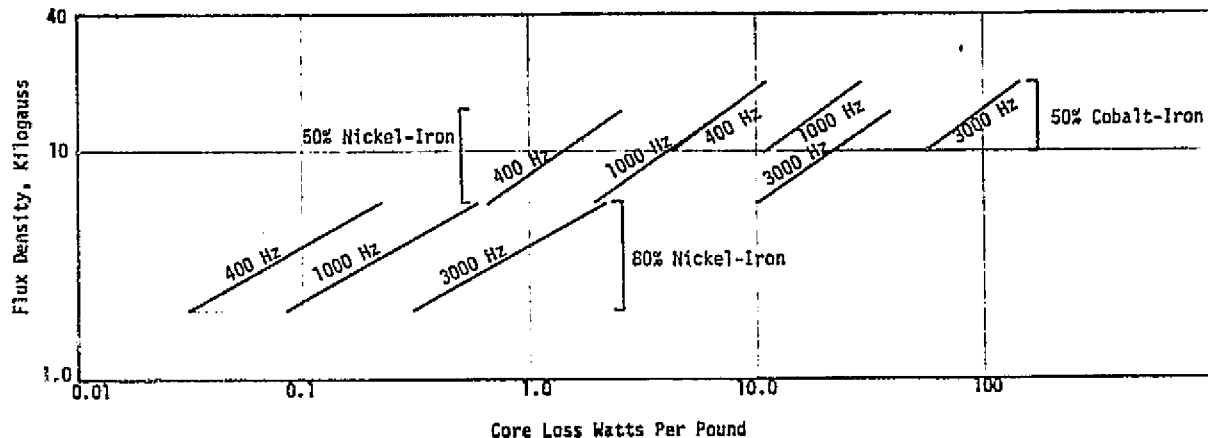


Figure 4-11 Operating Characteristics for Typical Materials

It should be noted here again that this approach to computer design of power transformers is highly simplistic, laminations do not come in an infinite range of sizes, copper is not available in all diameters but only discrete gage sizes, and grain oriented low loss core material should be used in tape wound toroids or cut cores.

The advantage of this program is that no advance knowledge or experience is required to determine the optimum transformer physical characteristics.



The computer program envisioned designs a group of transformers at a given frequency and flux density with a given core material, and starts with a single turn primary winding and sufficient iron cross-section to satisfy the flux density at the operating frequency. The copper is assumed to fill the window completely with an appropriate stacking factor, and is evenly divided between primary and secondary. The computer program then repeats the design process with two primary turns, then three, and so on. At each step, it computes iron weight, iron losses, copper weight, and copper losses. The design with a one turn primary will obviously have a large core, and a heavy iron weight. The weight of the iron will decrease and the copper losses increase with an increasing number of primary turns. If this data is plotted on log-log paper, the general results are as shown on Figure 4-12. The process is then repeated at incremental steps of frequency, flux density, and core material.

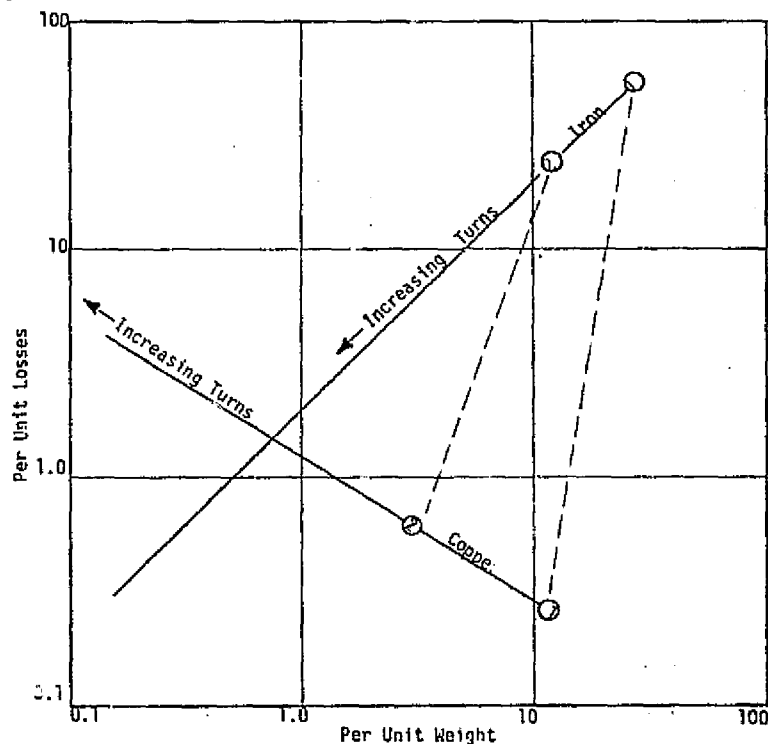


Figure 4-12 Family of Variable Primary Turns Transformers

The typical results of such a transformer optimization study on three core materials operating at three different flux levels for each material are displayed graphically in Figure 4-13.

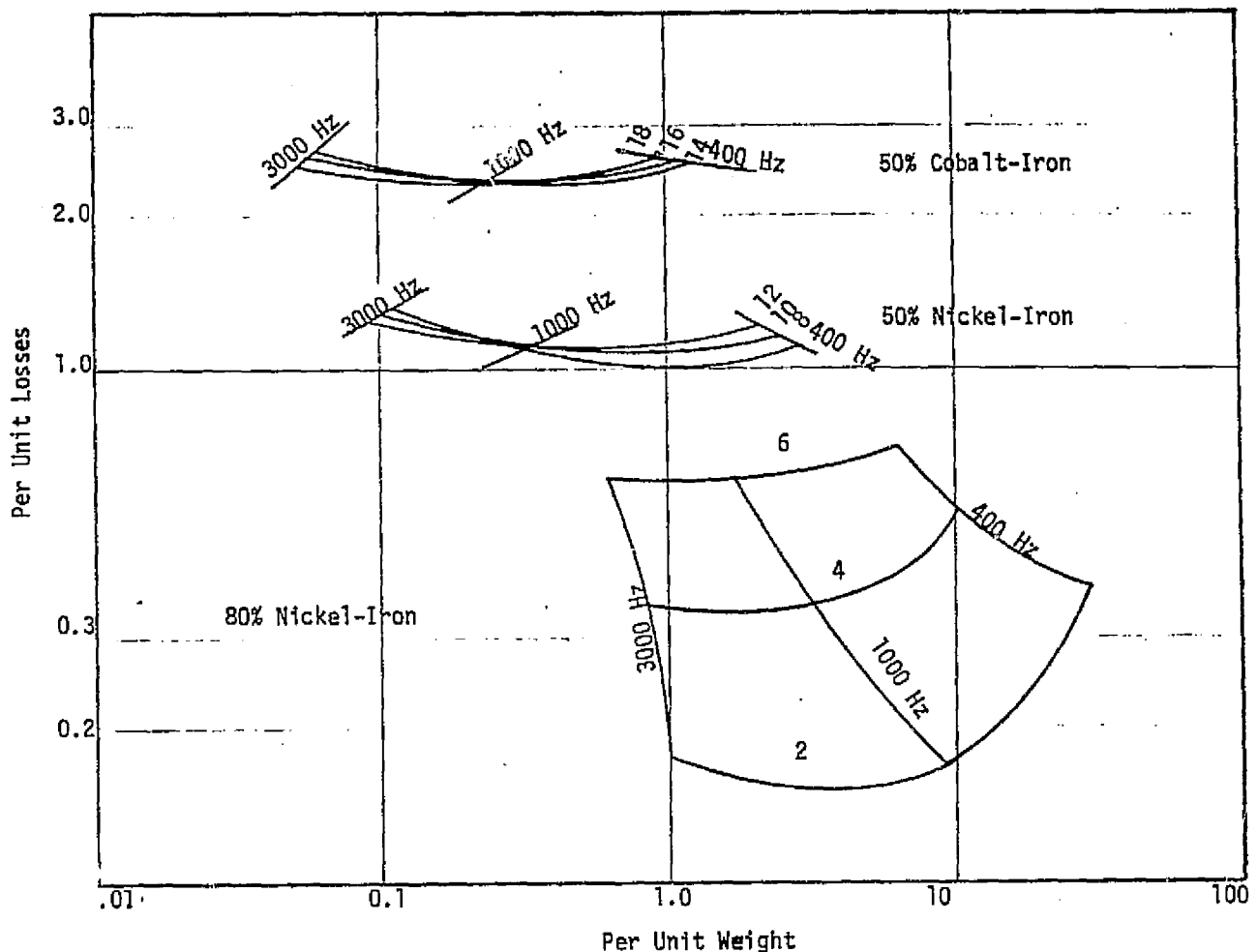


Figure 4-13 Typical Minimum Loss Transformer Designs

The 50% cobalt-iron alloy obviously yields the minimum weight transformer since it can operate in excess of twenty kilogauss. However, at three kilohertz, the core loss is greater than one hundred watts per pound, compared to the 80% nickel-iron alloy that, at ten kilogauss and three kilohertz, has a core loss of only three hundred milliwatts per pound. The transformer must weigh ten times as much to process the same power at the lower flux density, but the losses will be considerably less.

Although Figure 4-13 shows typical power loss and weight for minimum loss designs, it does not provide total information to size the optimum power processor. To allow for the proper choice of magnetic material and operating point, it is also necessary to know the total weight cost in pounds per watt of the power generation and auxiliary equipment necessary to provide raw electrical power. This allows an increase in dissipation at the power processor with a decrease in weight. If the rate at which the power processor weight is decreasing is greater than the rate at which the source weight is increasing to furnish the additional watts, then the total vehicle weight is being minimized with constant electrical power delivered to the load. Therefore, the watts per pound figure of merit for the mission is a constraint that is added at block 1, and is used to iterate other designs.

The transformer designs shown are minimum loss, but still are not optimum. Figure 4-14 shows there is a minimum loss, and that the weight can be increased or decreased, with a corresponding increase in total watts dissipated. Increasing both dissipation and weight is obviously not desirable, so the locus of points in that direction has been shown dotted. There is a useful range of designs with increasing watts of dissipation and decreasing weight, and this is true of all the typical designs although this figure shows calculated values for the single case of 50% nickel-iron core material operated at twelve kilogauss and at three kilohertz.

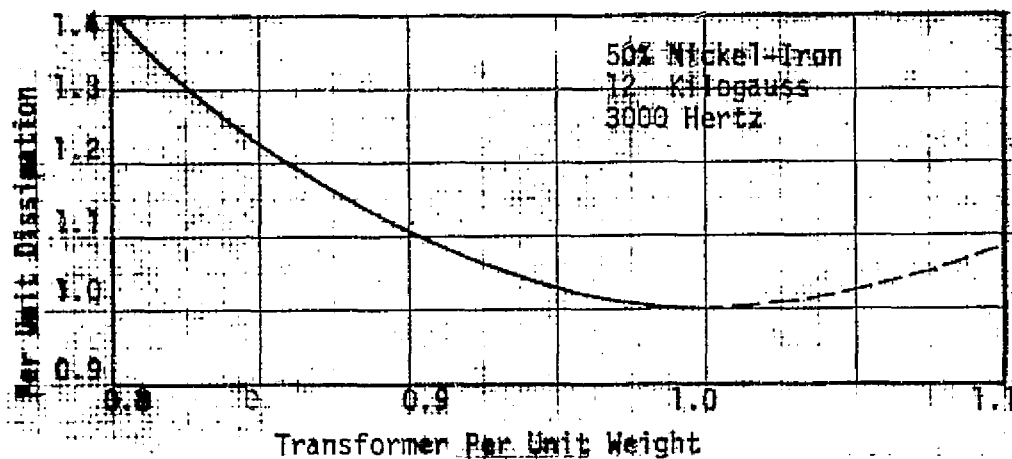


Figure 4-14 Watts/Weight Transformer Tradeoff

It can be seen from this example that transformer design is a tedious and iterative process to optimize, even in this simple case. In practice, laminations come in discrete sizes, wire comes in specific gages, and primary and secondary turns come in integral numbers that may not be compatible with the voltage ratios required. All these factors combine to make transformer design one of the first computer programs in any power processing library.

**4.1.6.3 Transformer Design** - Practical transformer designs utilize either cut cores or toroids. A computer program was written to study four transformer types: Orthonol and Supermalloy toroids, and Sillectron and Supermalloy cut cores. Figure 4-15 shows the physical construction of the transformers. Core dimension  $D$  was slowly increased and the window area completely filled with wire using the same amperes per square inch (ASI) for all windings and allowing very high ratings (24000 ASI) to start with small cores. As the iron area increased, the turns decreased and the window area increased, allowing the ASI to decrease rapidly. The program thus calculated sets of curves for different fluxes and frequency as illustrated in Figure 4-16.

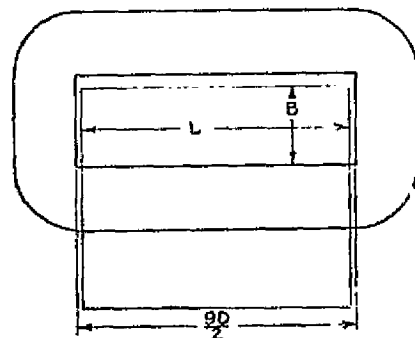
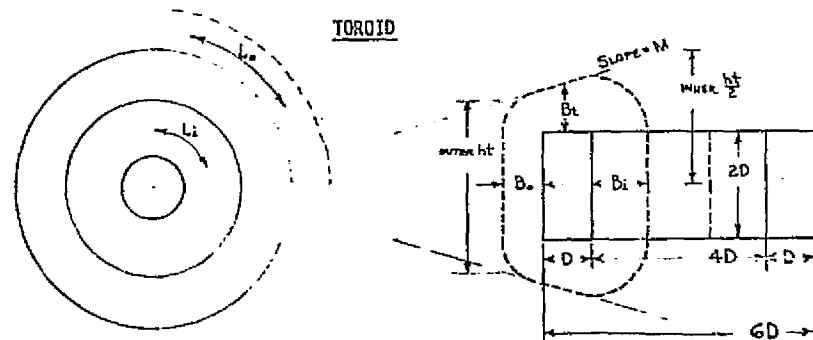


Figure 4-15 Transformer Physical Characteristics

Table 4-7 Design Formulae

Usable Window = window x % Usable (WF) x Copper Stacking Factor (SF)

$$\text{Area Current} = \sum_{i=1}^{N \text{ windings}} K_i N_i A_i$$

$K = 2$  for Center Tap  
 $N$  = Number of turns  
 $A$  = Current  
 $i$  = Winding Index

ASI = Current Area / Usable Window

$$\text{Copper Power Dissipation} = \sum_{i=1}^{NW} \frac{\sigma \times \text{Mean length} \times (A_i N_i)^2}{N_i A_i / \text{ASI}}$$

$$\text{Winding Build} = \frac{\text{Area Current}}{\text{ASI} \times \text{WF} \times \text{SF}} \div \text{length for the winding (L)}$$

Toroid:

Winding Length (L) =  $2 \pi \times$  Radius from center for that winding

$$\text{Core Volume} = 10 \pi D^3$$

$$\text{Winding Volume} = \pi [(ht_{inner} + M \times R_i) (R_o^2 - R_i^2) - M/3 (R_o^3 - R_i^3)] - 10 \pi D^3$$

Where  $R_o$  = radius to outside of winding

$R_i$  = radius to inside of winding

C-Core:

$$\text{Core Volume} = 24 D^3$$

$$\text{Winding Volume} = h \times w \times 4.5D - 6.75D^3$$

Frequencies of 5 and 10 kilohertz were selected for close study. The effect of switching losses in the transistors was included to get a better tradeoff versus frequency. Specific formulas used are listed in Table 4-7.

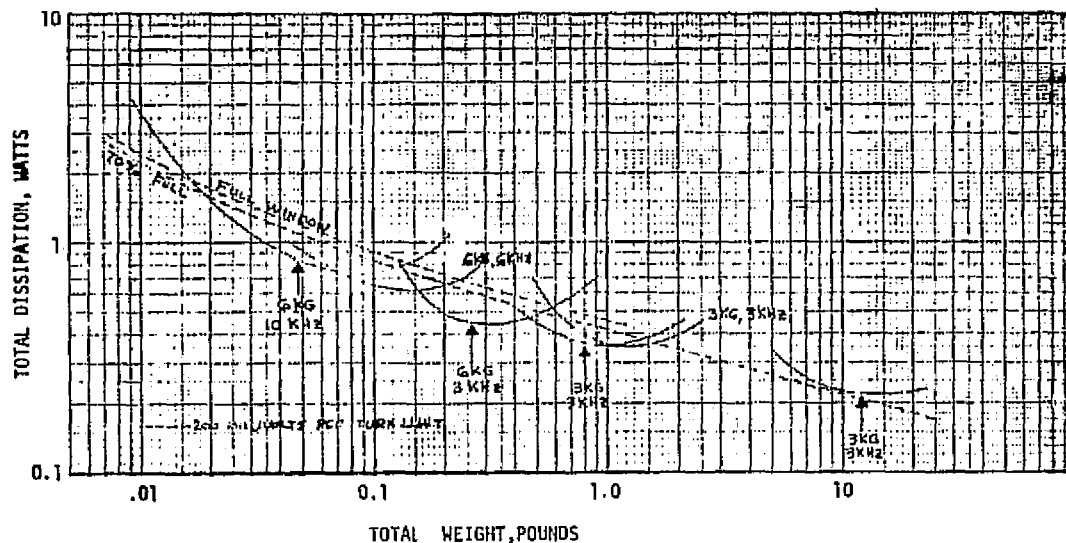


Figure 4-16 Optimized Minimum Dissipation Supermalloy Transformers

An additional limitation on realistic transformer design is the granularity with which voltage ratios can be adjusted. Low voltage converters typically must power logic requiring plus and minus five volts and plus and minus fifteen volts. The transformer will have a specific volts per turn rating which increases as flux density and operating frequency are increased and the required number of turns is decreased. The number of volts per turn cannot be increased above some arbitrary limit or it becomes impossible to adjust the number of turns for each winding to achieve the desired output voltage.

To get results most applicable to the expected requirements, a limit of 200 millivolts per turn (maximum) was imposed since five volt outputs are often required, and this granularity is required to adjust the output voltage level.

The computer program then calculated transformers by incrementally increasing the iron area (at a given flux and frequency) and filling the resulting window area with turns. The first transformer design accepted is when the ampere turns divided by the window area results in an acceptable ASI. The wire, core, and switching losses are then calculated along with weight, and "remembered". Additional designs are then calculated (by increasing the iron) until the total power loss exceeds that of the first acceptable design or until the volts per turn limit is reached. The program then calculates and prints a number of designs in the interval between the first acceptable design and the terminating design. Table 4-8 is a copy of one printout, and Table 4-9 is a copy of the program.

The results of the previously described computer runs generate curves like those of Figures 4-17, 4-18, 4-19, and 4-20. The cutoff which determines the bottom "horizontal" line was the 200 millivolt per turn maximum. Figures 4-21, 4-22, 4-23, and 4-24 show the resulting "bottom line" for each core material. Smaller (lighter) transformers could be made with Orthonal and Sil-ectron, for example, by using higher flux densities, but the 200 millivolt per turn limit forces high ASI, hence high copper loss. In general the volt per turn limit stops the designs to the left of the bottom of the convex curves shown in Figure 4-16 which corresponds to higher copper loss than core loss. The minimum "bottom line" for the different materials are shown together in

Table 4-8 Transformer Analysis Printout

TRANSFORMER ANALYSIS-WEIGHT, POWER, EFFICIENCY MATRIX  
 RUN I.D.=HI WY ORTH & SUPPLY TOROIDS & SUPCIL C CORE

DO YOU WANT DETAILED PRINTOUT?=YES

PUT IN UP TO 6 WINDINGS, IN ORDER FROM CORE OUTWARD  
 NUMBER OF WINDINGS, WHICH WINDING IS PRIMARY?= 3, 2

VOLTS, AMPS, KIND(2=CT) OF ALL WINDINGS  
 = 6.4, 3.15, 2, 29.56, 0, 2, 32.64, 0.1, 1

PUT IN 4 FLUXES FOR EACH CORE TYPE, 0 MUST BE USED IF REAL FLUX NOT  
 (1) ORTHANOL, (2) 48 ALLOY, (3) SUPERMALLOY, (4) C CORE  
 FLUXES=2000, 1000, 0, 0, 0, 0, 0, 2000, 1000, 500, 0, 1500, 1000, 500, 0,

FREQUENCIES NOT DESIRED(1, 2, 3, &/OR 4)=1, 2, 3, 4

MINIMUM CORE DIMENSION=.12

% WINDOW AREA USABLE FOR EACH MATERIAL= 70, 70, 70, 90

COPPER-STACKING FACTOR, RESISTIVITY(MICRO-OHM IN2/IN), WEIGHT(LBS/IN3),  
 AND MAX CURRENT DENSITY(AMPS/IN2)= 0.6, 0.68, 0.32, 3000

SWITCH DATA- VSAT, RISE, & FALL TIME(MICRO SECONDS)= 0.25, 1, 1

WATTS/POUND FACTOR(0 FOR MATRIX), MAX VOLTS/TURN= 2, 0.2

\*\*\*\*\* 2 MIL ORTHONOL \*\*\*\*\*  
 WINDOW AREA USED 70. %

GAUSS= 2000. FREQUENCY= 6000. CORE LOSS= 7.656 WATTS/LB  
 FINAL D= 0.220 IN. D1= 0.174 IN. XD= 0.0231

WT	POW	EFF	CORWT	CUWT	CPOW	CUPOW	ASI	D	
0.122	1.334	0.946	0.044	0.078	0.335	0.765	2998.	0.174	0.187
0.131	1.256	0.949	0.047	0.084	0.360	0.665	2700.	0.178	0.196
0.140	1.227	0.950	0.050	0.090	0.385	0.607	2493.	0.182	0.205
0.150	1.203	0.951	0.054	0.096	0.413	0.554	2300.	0.187	0.215
0.161	1.149	0.953	0.058	0.103	0.443	0.475	2056.	0.191	0.225
0.173	1.138	0.954	0.062	0.111	0.474	0.430	1890.	0.196	0.236
0.185	1.133	0.954	0.066	0.119	0.509	0.388	1736.	0.200	0.247
0.198	1.133	0.954	0.071	0.127	0.545	0.351	1593.	0.205	0.259
0.213	1.137	0.954	0.076	0.136	0.584	0.315	1459.	0.210	0.271
0.228	1.148	0.953	0.082	0.146	0.626	0.283	1335.	0.215	0.284
0.244	1.134	0.954	0.088	0.157	0.671	0.233	1169.	0.220	0.297



Table 4-8 (continued) Transformer Analysis Printout

\*\*\*\*\* 1 MIL SELECTRONIC C CORE \*\*\*\*\*  
 WINDOW AREA USED 90. Z

GAUSS= 1500. FREQUENCY= 5000. CORE LOSS= 3.480 WATTS/LB  
 FINAL D= 0.291 IN. DI= 0.231 IN. XD= 0.0231

WT	POW	EFF	CORWT	CUWT	CPOW	CUPOW	ASI	D	
0.217	1.920	0.924	0.068	0.149	0.235	1.490	2986.	0.231	0.154
0.232	1.828	0.928	0.072	0.160	0.252	1.379	2776.	0.236	0.161
0.249	1.684	0.933	0.078	0.171	0.270	1.217	2518.	0.242	0.169
0.267	1.554	0.938	0.083	0.184	0.290	1.070	2281.	0.247	0.177
0.286	1.440	0.942	0.089	0.197	0.310	0.936	2059.	0.253	0.185
0.307	1.386	0.944	0.096	0.211	0.333	0.858	1905.	0.259	0.194
0.329	1.292	0.948	0.103	0.226	0.357	0.742	1711.	0.265	0.203
0.352	1.254	0.949	0.110	0.242	0.382	0.676	1578.	0.271	0.213
0.378	1.224	0.950	0.118	0.260	0.410	0.616	1456.	0.278	0.223
0.405	1.158	0.953	0.126	0.278	0.439	0.525	1297.	0.284	0.234
0.434	1.141	0.954	0.135	0.298	0.471	0.475	1192.	0.291	0.245

GAUSS= 1000. FREQUENCY= 5000. CORE LOSS= 1.585 WATTS/LB  
 FINAL D= 0.323 IN. DI= 0.256 IN. XD= 0.0231

WT	POW	EFF	CORWT	CUWT	CPOW	CUPOW	ASI	D	
0.297	2.336	0.909	0.293	0.204	0.147	1.995	2951.	0.256	0.127
0.318	2.146	0.916	0.099	0.219	0.157	1.793	2703.	0.262	0.133
0.341	1.972	0.922	0.106	0.235	0.169	1.608	2473.	0.269	0.139
0.366	1.814	0.928	0.114	0.252	0.181	1.438	2259.	0.275	0.146
0.392	1.669	0.933	0.122	0.270	0.194	1.279	2058.	0.281	0.152
0.420	1.538	0.938	0.131	0.289	0.208	1.135	1872.	0.288	0.160
0.450	1.419	0.943	0.140	0.310	0.223	1.001	1699.	0.295	0.167
0.483	1.313	0.947	0.151	0.332	0.239	0.881	1538.	0.301	0.175
0.517	1.262	0.949	0.161	0.356	0.256	0.810	1426.	0.308	0.183
0.554	1.174	0.952	0.173	0.382	0.274	0.705	1284.	0.316	0.192
0.594	1.136	0.954	0.185	0.409	0.294	0.645	1187.	0.323	0.201

GAUSS= 500. FREQUENCY= 5000. CORE LOSS= 0.413 WATTS/LB  
 FINAL D= 0.456 IN. DI= 0.304 IN. XD= 0.0403

WT	POW	EFF	CORWT	CUWT	CPOW	CUPOW	ASI	D	
0.497	3.644	0.865	0.155	0.342	0.264	3.386	2972.	0.304	0.089
0.561	3.074	0.884	0.175	0.386	0.072	2.807	2547.	0.317	0.097
0.633	2.577	0.901	0.198	0.436	0.032	2.300	2171.	0.330	0.105
0.715	2.151	0.916	0.223	0.492	0.092	1.864	1839.	0.344	0.114
0.807	1.842	0.927	0.252	0.555	0.104	1.542	1575.	0.358	0.123
0.911	1.575	0.937	0.284	0.627	0.117	1.262	1341.	0.372	0.134
1.028	1.347	0.946	0.321	0.707	0.132	1.019	1134.	0.388	0.145
1.160	1.195	0.951	0.362	0.795	0.149	0.849	975.	0.404	0.157
1.309	1.029	0.958	0.408	0.901	0.169	0.667	813.	0.420	0.170
1.478	0.958	0.961	0.461	1.017	0.190	0.570	708.	0.438	0.185
1.668	0.869	0.964	0.520	1.148	0.215	0.458	597.	0.456	0.200

Table 4-8 (continued) Transformer Analysis Printout

\*\*\*\*\* 2 MIL SUPERMALLOY \*\*\*\*\*  
 WINDOW AREA USED 70. %

GAUSS= 2000. FREQUENCY= 6000. CORE LOSS= 0.822 WATTS/LB  
 FINAL D= 0.220 IN. DI= 0.174 IN. XD= 0.0231

WT	POW	EFF	CORWT	CUWT	CPOW	CUPOW	ASI	D	
0.125	1.037	0.958	0.046	0.078	0.038	0.765	2998.	0.174	0.137
0.134	0.938	0.962	0.050	0.084	0.041	0.665	2700.	0.178	0.196
0.143	0.886	0.964	0.053	0.090	0.044	0.607	2493.	0.182	0.205
0.154	0.838	0.965	0.057	0.096	0.047	0.554	2300.	0.187	0.215
0.165	0.757	0.969	0.061	0.103	0.050	0.475	2050.	0.191	0.225
0.176	0.718	0.970	0.066	0.111	0.054	0.430	1890.	0.196	0.236
0.189	0.682	0.972	0.070	0.119	0.058	0.388	1706.	0.200	0.247
0.203	0.650	0.973	0.076	0.127	0.062	0.351	1593.	0.205	0.259
0.217	0.619	0.974	0.081	0.136	0.067	0.315	1459.	0.210	0.271
0.233	0.593	0.975	0.087	0.146	0.071	0.283	1335.	0.215	0.284
0.250	0.539	0.977	0.093	0.157	0.076	0.233	1169.	0.220	0.297

GAUSS= 1000. FREQUENCY= 6000. CORE LOSS= 0.219 WATTS/LB  
 FINAL D= 0.261 IN. DI= 0.207 IN. XD= 0.0231

WT	POW	EFF	CORWT	CUWT	CPOW	CUPOW	ASI	D	
0.210	1.535	0.939	0.078	0.131	0.047	1.285	2998.	0.207	0.132
0.225	1.404	0.943	0.084	0.141	0.048	1.150	2743.	0.212	0.139
0.241	1.283	0.948	0.090	0.151	0.050	1.029	2504.	0.217	0.145
0.258	1.172	0.952	0.096	0.162	0.051	0.916	2282.	0.222	0.152
0.276	1.069	0.956	0.103	0.173	0.053	0.812	2076.	0.227	0.159
0.296	0.974	0.960	0.110	0.186	0.054	0.718	1884.	0.232	0.167
0.318	0.925	0.962	0.118	0.199	0.056	0.662	1749.	0.238	0.175
0.340	0.843	0.965	0.127	0.214	0.058	0.580	1581.	0.243	0.183
0.365	0.767	0.968	0.136	0.229	0.060	0.505	1425.	0.249	0.191
0.391	0.729	0.970	0.146	0.245	0.062	0.462	1317.	0.255	0.200
0.419	0.666	0.972	0.156	0.263	0.064	0.399	1181.	0.261	0.210

GAUSS= 500. FREQUENCY= 6000. CORE LOSS= 0.058 WATTS/LB  
 FINAL D= 0.360 IN. DI= 0.246 IN. XD= 0.0379

WT	POW	EFF	CORWT	CUWT	CPOW	CUPOW	ASI	D	
0.353	2.407	0.907	0.132	0.222	0.008	2.165	2997.	0.246	0.094
0.396	2.031	0.920	0.148	0.243	0.009	1.789	2574.	0.256	0.101
0.444	1.752	0.930	0.165	0.278	0.010	1.507	2232.	0.266	0.109
0.497	1.463	0.941	0.185	0.312	0.011	1.219	1896.	0.276	0.118
0.557	1.251	0.949	0.208	0.350	0.012	1.006	1627.	0.287	0.127
0.624	1.102	0.955	0.233	0.392	0.014	0.852	1415.	0.298	0.137
0.699	0.938	0.961	0.261	0.439	0.015	0.690	1203.	0.309	0.148
0.784	0.825	0.966	0.292	0.492	0.017	0.574	1036.	0.321	0.159
0.878	0.726	0.970	0.327	0.551	0.019	0.473	889.	0.334	0.172
0.984	0.639	0.973	0.367	0.617	0.021	0.386	758.	0.347	0.185
1.103	0.586	0.976	0.411	0.692	0.024	0.327	660.	0.360	0.200

```

00010 * TRANSFORMER ANALYSIS
00020 * STATEMENTS 6-30
00030 *
00040 * FORMATS 99-107, 111-114
00050 DIMENSION KM(4,4),KK(4,4),FLUX(4,4),WF(4),APWK(5),AK1(5),AVE(4),
00060 AMZ(4),NFSKIP(4),CRD(4),VC(5),AC(6),IN(6),KIND(6)
00070 ASU1 ASC(10),DATE(2)
00080 PI=3.14159
00090 CALL DATE*TIM(DATE, HOUR) ; PRINT 99, DATE, HOUR
00100 PRINT: " TRANSFORMER ANALYSIS-WEIGHT, POWER, EFFICIENCY MATRIX"
00110 PRINT: " RUN 1-B." ; READ:ASC(10)
00120 PRINT: " *PRINT: " DO YOU WANT DETAILED PRINTOUT?" ; READ:ASC(1)
00130 PRINT: "PUT IN UP TO 6 WINDINGS, IN ORDER FROM CORE OUTWARD"
00140 PRINT: " NUMBER OF WINDINGS, WHICH WINDING IS PRIMARY?" ; READ:IN, N1
00150 PRINT: " VOLTS, AMPS, KIND(2=0) OF ALL WINDINGS" ; PRINT: " "
00160 READ:(VC(K), AK(K), KIND(K), AP1(K))
00170 PRINT: "PUT IN 4 FLUXES FOR EACH CORE TYPE, 0 MUST BE USED IF
00180 A REAL FLUX NOT DESIRED"
00190 PRINT: " (1) ORIHANUL, (2) 45 ALLOY, (3) SUPERHALLUL, (4) C CORE"
00200 PRINT: " FLUXES" ; READ:(FLUX(1,K), K=1,4), I=1,4)
00210 PRINT: " FREQUENCIES NOT DESIRED(1,2,3, & /OR 4)" ; READ:(NFSKIP(1), I=1
,4)
00220 PRINT: " MINIMUM CORE DIMENSION" ; READ:00
00230 PRINT: " X WINDOW AREA USABLE FOR EACH MATERIAL" ; READ:(WF(1), I=1,4
)
00240 PRINT: " COPPER-STICKING FACTOR, RESISTIVITY(MICRO-OHM IN2/IN),
00250 & WEIGHT(LBS/IN3)," ; PRINT: " AND MAX CURRENT DENSITY(AMPS/IN2)"

```

```

00260 READ:SF, SIGMA, CURD, ASIMAX ; SIGMA=SIGMA*1.0E-6
00270 PRINT: " SWITCH DATA-VSAT, RISE, & FALL TIME(MICRO SECONDS)"
00280 READ:IR, IF ; TH=IR*1.0E-6 ; IF=IF*1.0E-6
00290 PRINT: " WAIT/POUND FACTOR(0 FOR MATRIX), MAX VOLTS/TURN"
00300 READ:VF, VPMAX
00310 * SLOPES AND INTERCEPTS FOR CORE LOSSES
00320 KM(1,1)=1.32; KM(1,2)=1.23; KM(1,3)=1.11; KM(1,4)=1.63
00330 KK(1,1)=-.73; KK(1,2)=-.03; KK(1,3)=.55 ; KK(1,4)=.875
00340 KM(2,1)=1.62; KM(2,2)=1.61; KM(2,3)=1.58; KM(2,4)=1.45
00350 KK(2,1)=-1.17; KK(2,2)=-.41; KK(2,3)=.00; KK(2,4)=.53
00360 KM(3,1)=2.00; KM(3,2)=1.96; KM(3,3)=1.91; KM(3,4)=1.78
00370 * CORE DENSITIES(LB/IN3)
00380 KK(3,1)=-1.76; KK(3,2)=-1.15; KK(3,3)=-.66; KK(3,4)=-.35
00390 KM(4,1)=1.80; KM(4,2)=1.77; KM(4,3)=1.94; KM(4,4)=2.00
00400 KK(4,1)=-.46; KK(4,2)=-.22; KK(4,3)=.20 ; KK(4,4)=.55
00410 CRD(1)=8.2*.03613*.89
00420 CRD(2)=8.2*.03613*.89
00430 CRD(3)=8.7*.03613*.89
00440 CRD(4)=.276*.83
00450 AMZ(1)=1000 ; AMZ(2)=3000 ; AMZ(3)=6000 ; AMZ(4)=10000
00460 POUT=0 ; DO 14 J=1,NK ; IF(J.EQ.NP) GO TO 14
00470 POUT=POUT+AC(J)*VC(J) ; 14 CONTINUE
00480 NPRINT=11
00490 DO 15 I=1,4
00500 IF(I.EQ.4) AMZ(2)=2000 ; IF(I.EQ.4) AMZ(3)=5000
00510 IF(I.EQ.1) PRINT 111
00520 IF(I.EQ.2) PRINT 112 ; IF(I.EQ.3) PRINT 113 ; IF(I.EQ.4) PRINT 114

```

Table 4-9 (continued) Transformer Analysis Program

```

00530 PRINT 105, WF(1)
00540 CORRO=CRO(1)
00550 DO 17 M=1,4
00560 H=FLUX(I,M)
00570 IF(B-EO,K) GO TO 17
00580 DO 16 K=1,4
00590 IF(K.EQ.NFSKIP(1)) GO TO 16 ; IF(K.EQ.NFSKIP(2)) GO TO 16
00600 IF(K.EQ.NFSKIP(3)) GO TO 16 ; IF(K.EQ.NFSKIP(4)) GO TO 16
00610 XLJGCL=XN(I,K)*(0.43429*ALOG(B)-3.6)+XN(I,K)
00620 WPLH=EXP(2.302585*XLJGCL)
00630 FREU=HZ(K)
00640 PRINT 1,4,F,FREU,WPLH
00650 A(K)=1 ; K(K)=W ; INVE=0 ; K(K)=W
00660 T(K)=L ; T(K)=W ; TWO=2.00
00670 U=0 ; U1=W ; UA=W
00680 V=CON(1+U)
00690 U=SQRT(1+U)*U
00700 IF(UA.EQ.U) U=SQRT(U*U*(1+.049/1.001))
00710 K1=2.4*U ; K2=3.6*U
00720 AURE=U*2*U=6.425 ; IF(1.EQ.4) AURE=U*.5*U=6.425
00730 CONVOL=1F*(1+U*U) ; IF(1.EQ.4) CONVOL=24.*U*U
00740 CORW1=CONVOL*CORRO ; CORP1=CONW1*WPLH
00750 VPI=(AURE+B/1000.+FREU/1000.)/25. ; N(NP)=VNP/VPI
00760 IF(VPI.GT.VPIMAX) K(K)=1
00770 A(NP)=0 ; LA=0
00780 IF(N(NP).LT.2) GO TO 12
00790 DO 3 J=1,NK
00810 IF(J.EQ.NP(K)) TJ=3

```

```

00810 XN=V(J)*N(NP)/V(NP) ; N(J)=XN
00820 IF((XN-IFIX(XN)).GT.0.5) N(J)=N(J)+1
00830 A(NP)=A(NP)+N(J)=A(J)/N(NP)
00840 IF(N(J).LT.2) GO TO 12
00850 8 CONTINUE
00860 AW=PI*R1*R1*SF*WF(1)/100.
00870 IF(1.EQ.4) AW=1.5*U*4.5*U*SF*WF(1)/100.
00880 DO 10 J=1,NK
00890 L0=CA+KIND(J)*N(J)*A(J)
00900 ASI=CA/AW
00910 1919 FORMAT(1H,18,F6.2,18,E13.5,2F8.3,E13.5)
00920 ASI=CA/AW ; IF(ASI.GT.ASIMAX) GO TO 9 ; CUMW=0
00930 IF(DA.NE.U) GO TO 22
00940 U=SQRT(U*U+.957) ; UA=U ; GO TO 9
00950 22 IF(U1.EQ.U) U1=.999999*U ; AL1=U
00960 XL1=U ; ALL1=1.5*U ; KLI1=2.*U ; KLU1=2.*U
00970 DO 11 J=1,NK
00980 CADEL=KIND(J)*N(J)*A(J)/ASI
00990 ADEL=CADEL/SF
01000 IF(1.EQ.4) GO TO 27
01010 K2=SQRT(K1=K1-ADEL/H1) ; K02=SQRT(K0=K0+ADEL/H1)
01020 XL2=XL1+K1-K2+K02-K0
01030 KLU2=KLU1+2.*(K02-K0) ; KLI2=KLI1+2.*(K1-K2)
01040 KHLT=(KLI1+KLI2+KLU1+KLU2)/2.+KLI+KLE2
01050 KLI=KLE2 ; KLI1=KLI2 ; KLU1=KLU2 ; K1=K2 ; K0=K02
01060 GO TO 28
01070 27 KLE2=KLI+2.*ADEL/(4.5*U) ; KLI2=KLI1+2.*ADEL/(4.5*U)
01080 KML1=KLI+KLE2+KLI1+KLE2

```

```

01090 XL1=XL2 / ALL1*ALL2
01100 20 CONTINUE
01110 CUPW=CUPW+SLPWA*(XL1*(ACJ)+N(CJ))*2./(CABEL/XIND(CJ))
01120 11 CONTINUE
01130 SLOPE=(XL12-XL02)/XL2
01140 CUWL=PI*((XL12+K2*SLOPE)*(K02+KJ2-K2*K2)-2.*SLOPE/3.*(K0)*3.
01150 (K2**3.))-16.*PI*D*D*D
01160 IF(1.EQ.4) CUWL=AL2*ALL2=4.5*D-6.75*D*D
01170 CUKI=CUWL*SF*CUKO
01180 SLPW=2./3.*2.*V(NP)*A(NP)*(1+1K)*FREQ+VCEBAT*A(NP)
01190 TKT=CORW1+CUKI / IPW=CORPOW+CUPW+SLPW
01200 IF(TKT.GT.90) GO TO 12
01210 IF(TW10.EQ.0) T10=T1 / IF(TW1.GT.1.EQ.1) T10=TKT/KIKKI=1
01220 IF(IPW0.EQ.0) IPW0=IPW / IF(IPW.GT.1.EQ.1) IPW0=IPW/KIKKI=1
01230 IF(D.GT.100*D1) GO TO 12
01240 IF(PF.EQ.0) GO TO 25
01250 IAVE=IAVE+1 / IF(IAVE.EQ.0) IAVE=1
01260 HPWK(IAVE)=IPW / AKI(IAVE)=1K1
01270 IF(KIKPF.EQ.0) GO TO 23
01280 11=IAVE+1
01290 KAVE=K
01300 10 24 KAVE=1.4
01310 11=11-1 / IF(11.EQ.0) 11=0
01320 12=11-1 / IF(11.EQ.1) 12=0
01330 AVE(MAVE)=(HPWK(11)+HPWK(12))/(AKI(12)+AKI(11))
01340 24 KAVE=KAVE+AVE(MAVE)
01350 IF(KAVE/4..LT.PF) D=D*1.002+0.1/1.004000
01360 IF(KAVE/4..LT.PF) D1=D

```

```

01370 23 IF(IAVE.EQ.4) KIKPF=1
01380 NPRINT=1
01390 IF(KIKPW.EQ.1) D1=D
01400 IF(D1.EQ.0) GO TO 12
01410 GO TO 9
01420 25 CONTINUE
01430 IF(KIKPW.EQ.0) GO TO 9
01440 IF(D.L1.1.26*D1) D=1.26*D1
01450 12 IF(D1.EQ.0) GO TO 13 / XD=ALOG(D/D1)/16.
01460 IF(ASCII).EQ."YES") PRINT 107 ,D,D1,XD
01470 IF(PF.EQ.0) PRINT 106,KAVE/4.
01480 13 JF=1,NPRINT
01490 IF(JF.GT.1) GO TO 26
01500 PRINT 102 / IF(ASCII).EQ."YES") PRINT 103
01510 26 D=EXP(ALOG(D1)+JF-1)*XD
01520 K1=2.*D / K0=3.*D
01530 ACORR=D*2.*D*.8.425 / IF(1.EQ.4) ACORR=D*1.5*D*.425
01540 CORVOL=10.*PI*D*D*D / IF(1.EQ.4) CORVOL=24.*D*D*D
01550 CUKI=CORVOL*CORW / CORPO=CORW1*WFLH
01560 VPT=(ACORR*H/1000.*FREQ/1000.)/25. / N(NP)=V(NP)/VPT
01570 A(NP)*6 / C=0
01580 10 18 J=1,NK
01590 IF(J.EQ.NP) GO TO 18
01600 KN=V(CJ)+N(NP)/V(NP) / N(CJ)=KN
01610 IF((KN-1E+KN).GT.0.5) N(CJ)=N(CJ)+1
01620 A(NP)=A(NP)+N(CJ)*A(CJ)/N(NP)
01630 IF(N(CJ).LT.1) PRINT 11,"N",N(CJ), / JF="JF
01640 IF(N(CJ).LT.1) N(CJ)=1

```

Table 4-9 (continued) Transformer Analysis Program

```

01650 18 CONTINUE
01660 AW=PI*R1*R1*ST*WF(1)/100.
01670 IF(1.E6-4)AW=1.5*D*4.5*D*ST*WF(1)/100.
01680 DO 20 J=1,NK
01690 20 CA=CA+KIND(J)*N(J)*A(J)
01700 ASI=CA/AW ; CUPOW=0
01710 XL1=0 ; XLL1=1.5*D ; XLI1=2.*D ; XLO1=2.*D
01720 DO 21 J=1,NK
01730 CADEL=KIND(J)*N(J)*A(J)/ASI
01740 ADEL=CADEL/ST ; IF(1.E6-4)GO TO 29
01750 K2=SQRT(K1*K1-ADEL/F1) ; KJ2=SQRT(KJ*KJ+ADEL/F1)
01760 XL2=XL1+K1-K2+KJ2-KJ
01770 XLI2=XLI1+2.*(K1-K2) ; XLI2=XLI1+2.*(KJ2-KJ)
01780 XLL1=(XLI1+XLI2+XLO1+XLO2)/2.+XLI1+XL2
01790 XLI=XLI2 ; XLL1=XLI2 ; XLI1=XLI2 ; K1=K2 ; KJ=KJ2
01800 GO TO 30
01810 29 XL2=XL1+2.*ADEL/(4.5*D) ; XLL2=XLL1+2.*ADEL/(4.5*D)
01820 XLL1=XLI+XL2+XLL1+XLL2
01830 XLI=XLI2 ; XLL1=XLL2
01840 30 CONTINUE
01850 CUPOW=CUPOW+SI*AW*XLI*(A(J)*N(J))*20./(CADEL/KIND(J))
01860 21 CONTINUE
01870 SLOPE=(XLI2-XLO2)/XL2
01880 CUWL=PI*((XLI2+K2*SLOPE)*(KJ2+KJ2-K2-K2)-2.*SLOPE/3.*(KJ2+3.
01890 (K2+3.))-11.*PI*D*D*D
01900 IF(1.E6-4)CUWL=XLL2*XLL2*4.5*D*6.75*D*D*D
01910 CUB1=CUWL*ST*CUW
01920 SLPW=2./3.*2.*V(NP)*A(NP)*(TH*1)*FNEW*VCSAT*A(NP)
01930 TWT=CORWT+CUWT ; THW=CORPOW+CUPOW+SLPW
01940 EFF=POUT/(POUT+THW)
01950 PRINT 100,TWT,THW,EFF ; IF(ASC(1).EQ."YES")PRINT 101,CORWT,CUWT,
01960 2CORPOW,CUPOW,ASI,D,VPT
01970 13 CONTINUE
01980 16 CONTINUE
01990 17 CONTINUE
02000 15 CONTINUE
02010 CALL DATE*TIME(DATE, HOUR) ; PRINT 99,DATE,HOUR
02020 99 FORMAT(1H,24H,F7.3)
02030 100 FORMAT(1H,3F6.3)
02040 101 FORMAT(1H,4F6.3,F7.0,2F6.3)
02050 102 FORMAT(1H," WT POW EFF")
02060 103 FORMAT(1H," CORWT CUWT CPOW CUPOW ASI D")
02070 104 FORMAT(1H," JSS=",F8.0," FREQUENCY=",F8.0," CORE LOSS
",
02080 4F7.3," WATTS/LB")
02090 105 FORMAT(1H," WINDOW AREA USED",F5.0," IN")
02100 106 FORMAT(1H," D WATTS/D POUNDS AVE",F7.3," WATTS/POUND")
02110 107 FORMAT(1H," FINAL D=",F7.3," IN. DI=",F7.3," IN.
02120 4 KJ=",F7.4)
02130 111 FORMAT(1H-," 1H-,"20(1H)," 2 MIL ORTHONOL ",20(1H))
02140 112 FORMAT(1H-," 1H-,"20(1H)," 2 MIL 48 ALLOY ",20(1H))
02150 113 FORMAT(1H-," 1H-,"20(1H)," 2 MIL SUPERMALLOY ",17(1H))
02160 114 FORMAT(1H-," 1H-,"20(1H)," 1 MIL SELECTRONIC C CORE ",16(1H))
02170 STOP

```

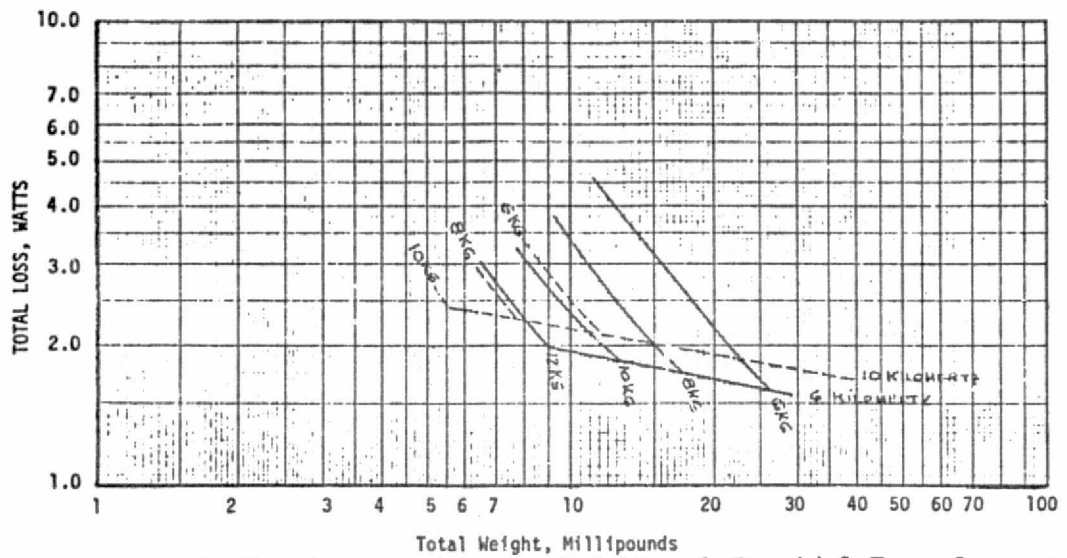


Figure 4-17 Characteristics of Orthonol Toroidal Transformers

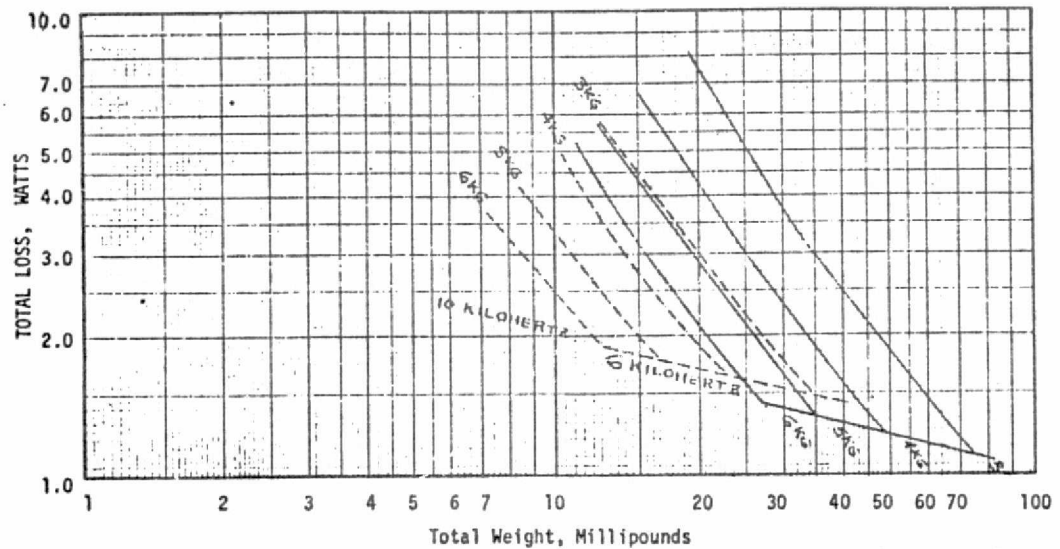


Figure 4-18 Characteristics of Supermalloy Toroidal Transformers

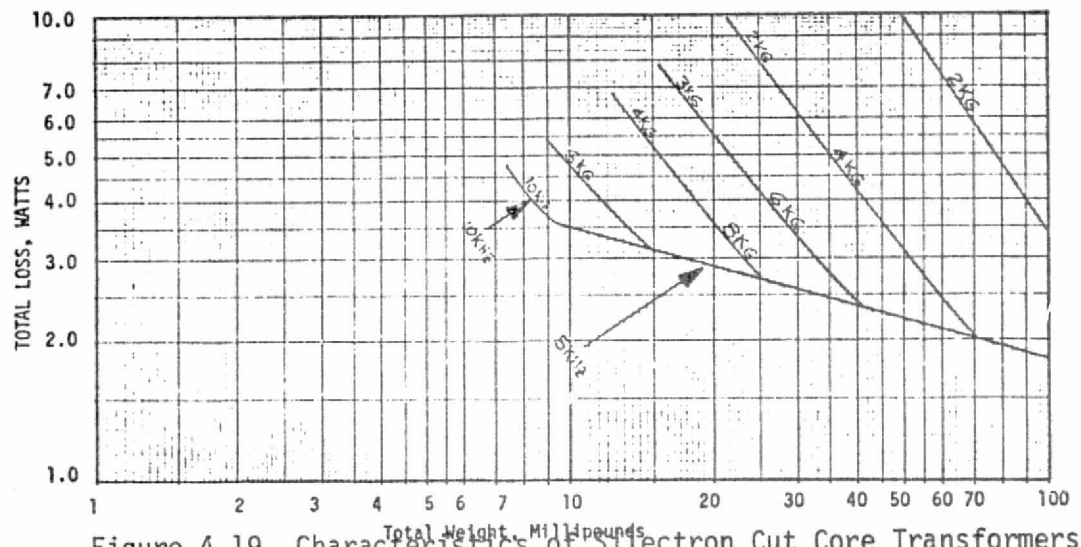


Figure 4-19 Characteristics of Sillectron Cut Core Transformers

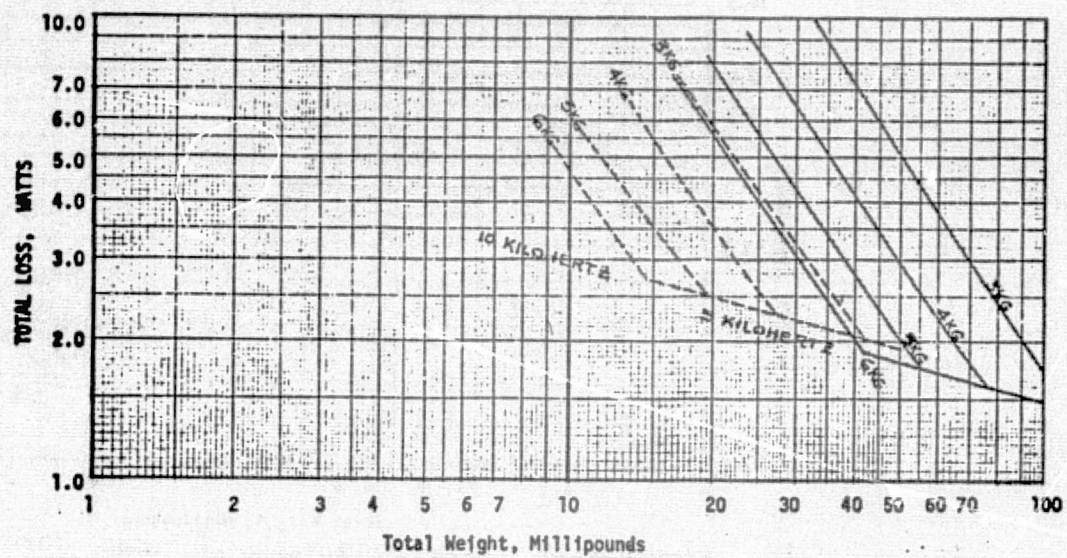


Figure 4-20 Characteristics of Supermalloy Cut Core Transformers

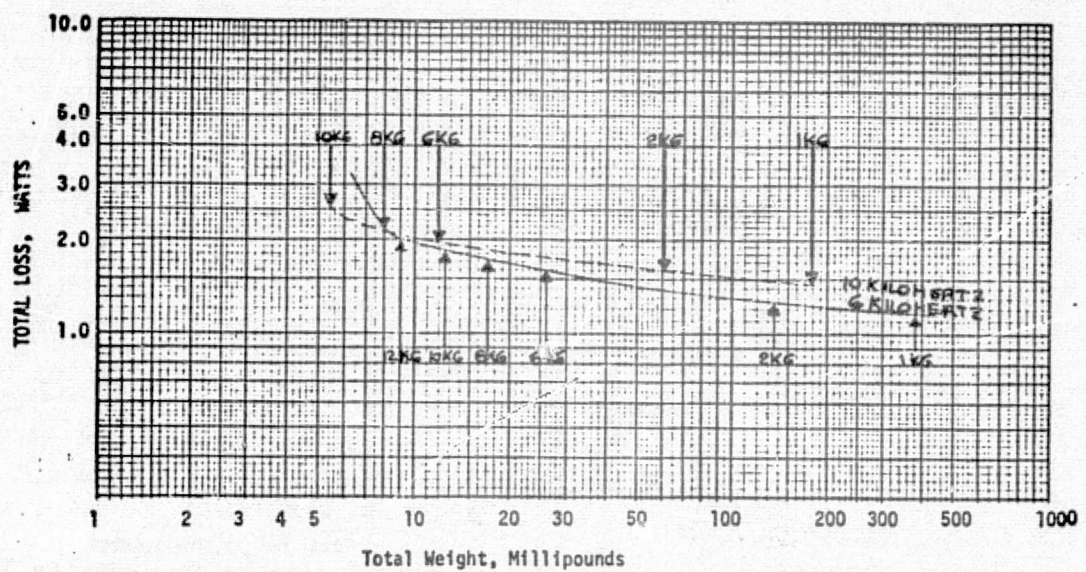


Figure 4-21 Locus of Orthonol Toroidal Transformers

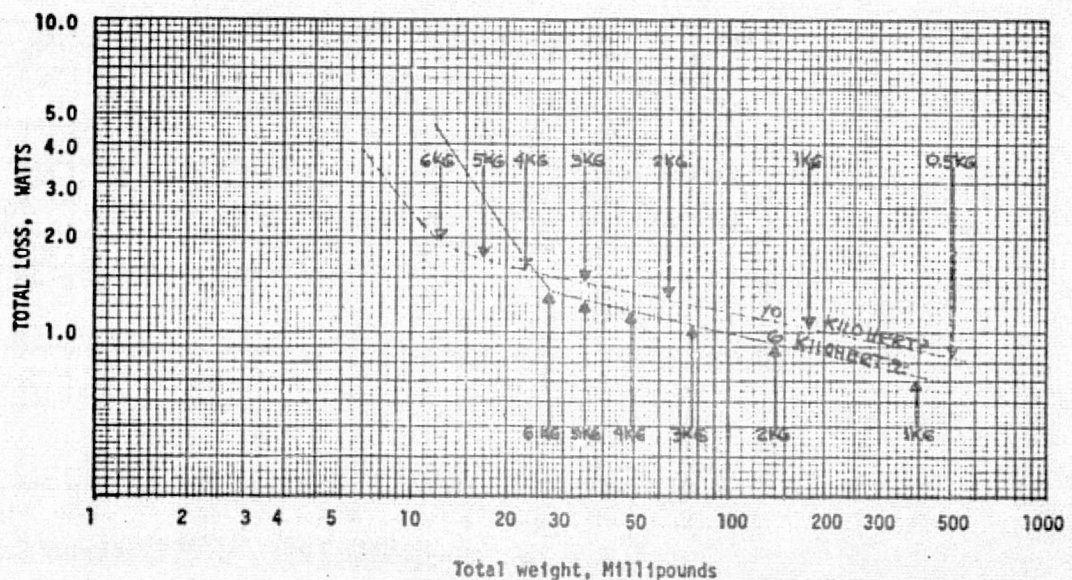


Figure 4-22 Locus of Supermalloy Toroidal Transformers



Figure 4-25. The assumed mission 1.7 watt per pound point was determined by calculating the slope for small lengths of the curve. Since the axes are logarithmic, the linear slope changes rapidly along the curve so the area indicated is approximately the location of the 1.7 watt per pound slope.

The "best" 1.7 watt per pound point is the supermalloy toroid. It must be noted, however, that power loss due to saturation spikes is not included and the difference in power loss between the toroid and cut core is less than 1.4% of the transformer output power. The power loss difference for a cut core at the same weight as the 1.7 watt per pound point of the toroid is less than 2.5% of the output power. It is also impossible to say whether the physical constraints selected are near optimum. It is also impossible to get cores in such incremental sizes as computed.

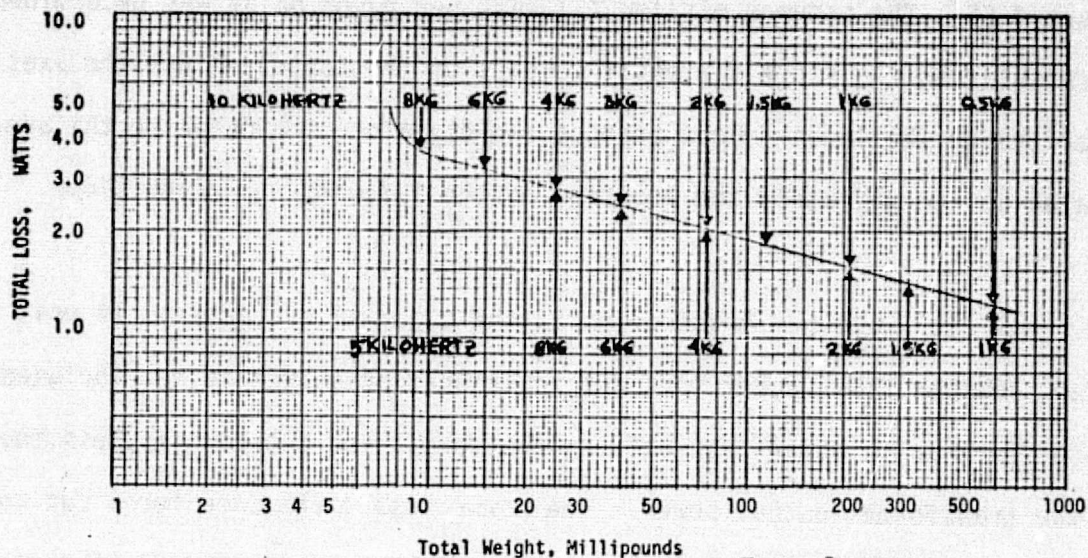


Figure 4-23 Locus of Silectron Cut Core Transformers

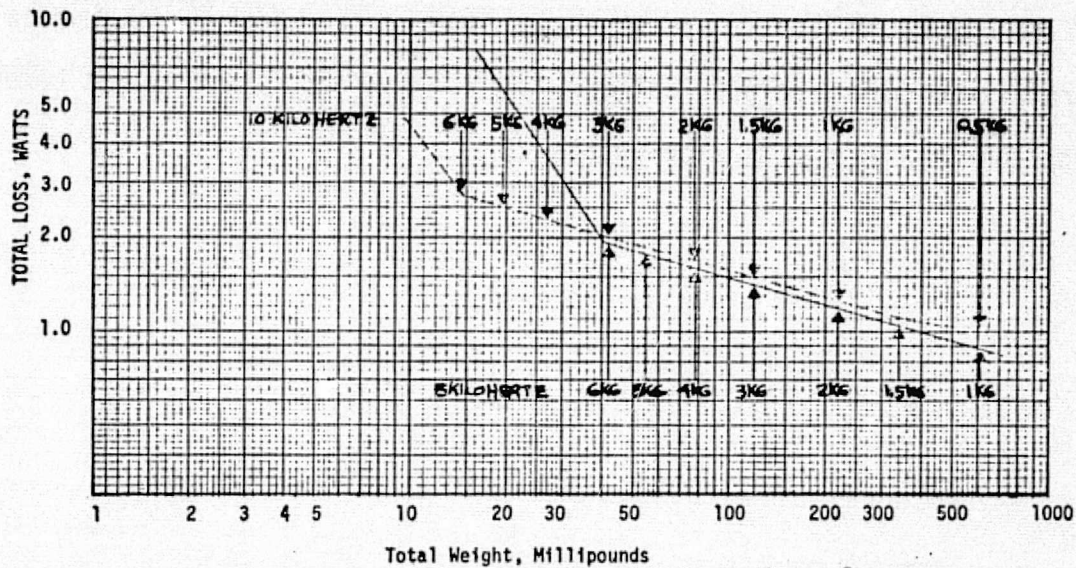


Figure 4-24 Locus of Supermalloy Cut Core Transformers

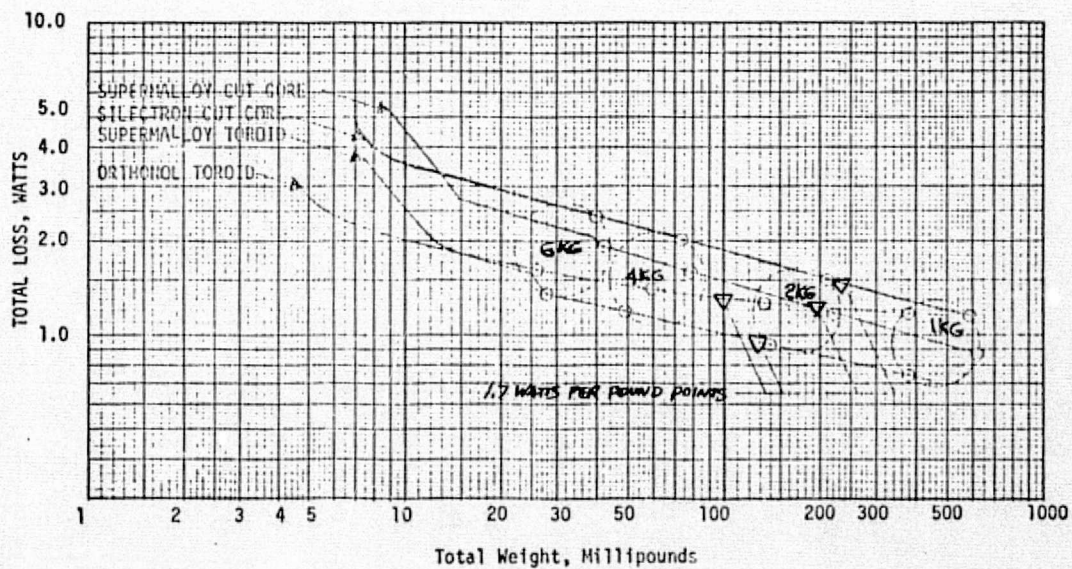


Figure 4-25 Composite of Optimized 18 Watt Transformers

## 4.2 The Management Program

The major goal of the management program is to enable the user to design a power processing system in a natural manner, as if he were communicating with a specialist. Such a management program makes the designing procedure logical and concise. It frees the user from having to concern himself with many details and permits him to concentrate on the essential features of his design.

Whether or not it is worthwhile to develop an entirely new management program for a special purpose application such as the design of power processing systems has been a subject of much controversy. To develop a new management program takes a great deal of time, trouble and expense, and the resultant program can be used only for the purpose of designing power processing systems. One may argue that it is easier to develop the program as an extension of some well-known program. However, in order to develop a management program with the immediate interactive response which will permit man and computer to work as partners, it appears best to avoid limitations imposed by extending another program.

The major part of the management program will be an engineering tool used to execute a defined, well-instructed procedure. However, in a good interactive system, the user and the program will not only exchange the information but also control the exchange exercised by either party, such as key word explanation, future step guidance, error recovery, etc. To achieve such control of information exchange requires careful development of the management program.



#### 4.2.1 Choosing A System Implementation Language

For a management program which is to have the capabilities of data storage and retrieval, mathematical calculation and immediate interactive response, APL, FORTRAN and PL/I are three languages representative of the current art.

APL is an interpretive system specially designed for classes of mathematical operation (such as matrix manipulation) and for dynamic data structure operations (such as forming a matrix from vectors). However, it is normally relatively difficult to understand the work of another person written in APL language. FORTRAN, the first language that has received wide use, is not a concise language. PL/I is selected as the most suitable language for implementing a computer based power processing design facility.

#### 4.2.2 System Profile

In designing the management program, the following questions are of importance:

1. Is the system intended to be used for fast "production" type operations, or as a general experimental tool?
2. What is to be the prime method of storing the input data?
3. If user specified functions are to be added, how are they to be stored?
4. Is an input statement to be retained in such a fashion that it can later be displayed to the user in a form identical to his input?
5. How far should the internal representation differ from a fully parsed form?
6. How versatile should the command language be? Does it contain debugging aids? Are function (macros) and command language modifiable

by the user?

These questions are addressed in the management program design now described. One requirement of the management program is a definition of the operators, variables, statements and macros\* in the user's syntax. To implement this requirement the syntactic information is arranged in internal lists (to be described later). The heart of the program consists of the operator, variable statement and macro definition programs, which produce, as data of the system, the internal lists. Another requirement of the system is to provide a means of parsing input expressions. Special delimiters (such as blanks, carriage return) are used to break up an input expression into its component parts. In order to use a macro, an EDITOR "translates" the macro into a suitable form, making error checks, and producing an internal macro representation list. Once a macro has been written, it may be desirable to save it for future re-use in order to avoid reprogramming. To implement this, a library of programs is accumulated at a computer installation.

The management program consists of the following submodules (service programs): REGISTRAR, EDITOR, USER'S LIBRARY, LANGUAGE PROCESSOR, ERROR MESSAGE, HANDLING ROUTINE, DISPATCHER, SUBPROGRAM LIBRARY, AND POWER PROCESSING.

#### 4.2.2.1 Subsystems Data Base Facility

The functions and features of each submodule (service program) are shown in Figure 4-26 and are described in the following paragraphs.

---

\*Because simple statements are not sufficient to do complex manipulations, a means is necessary for concatenating these statements into a "macro". Thus, a macro consists of a string of statements that are executed in sequence.

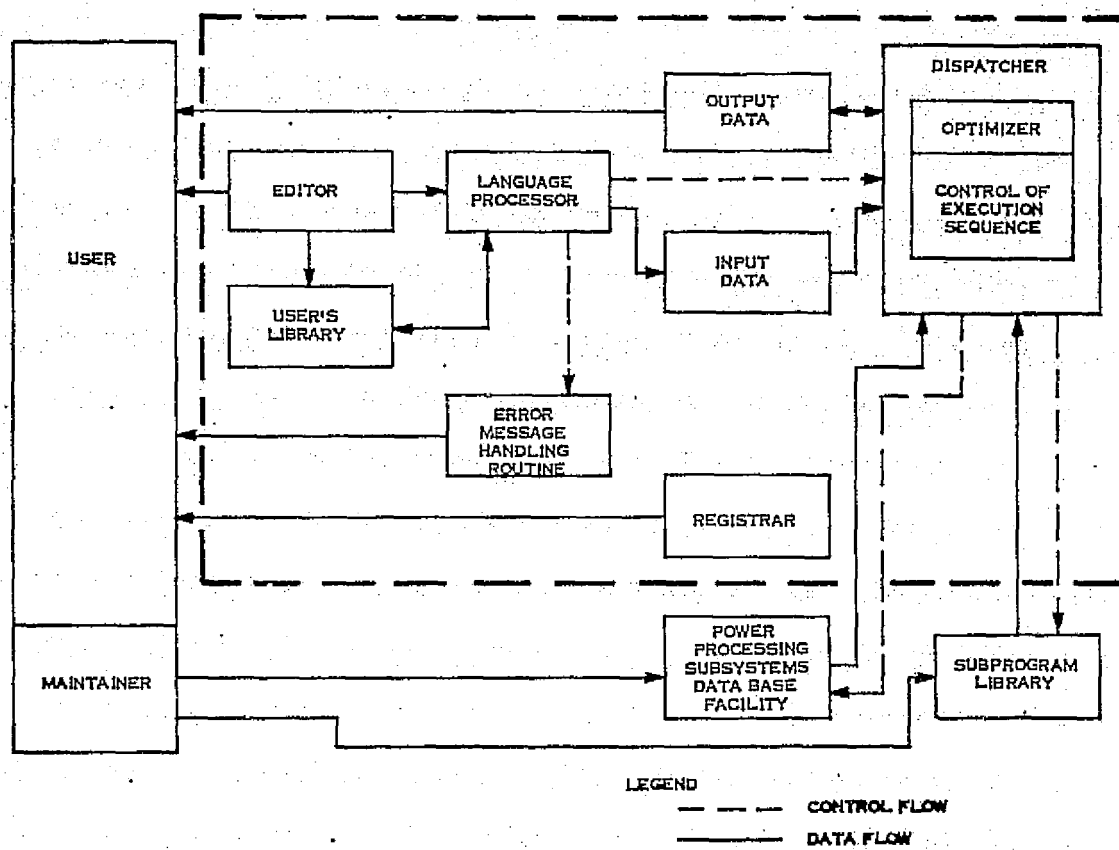


Figure 4- 26 Submodule (Service Programs) of the Management Program

#### 4.2.2.2 Registrar

This module (service program) is used to check the user's identification, account balance, etc., and to gather statistics on the system's performance.

#### 4.2.2.3 Editor. (Lexical Analyzer)

This module has two modes: 1) a macro definition mode and 2) an executive mode. In the macro definition mode, a macro may be defined or edited and then placed in the user's library. The executive mode provides for executing a command or an instruction.

#### 4.2.2.4 User's Library

This module provides for saving user's macros and variables and provides working space for the user during the period he is at the terminal. The user can load a library and then use it, update it and save it. The user's library commands will:

1. Provide a workspace.
2. Terminate a work session and store the active workspace.
3. Copy all the macros and variables from a stored workspace.
4. List names of defined macros.
5. Activate a copy of a stored workspace.
6. Restore a copy of the active space.
7. List names of defined variables.
8. List values of defined variables.
9. List macros.
10. Name a workspace.
11. Find the name of the current workspace.

#### 4.2.2.5 Language Processor

This module accepts: 1) system commands, 2) subprogram instructions, 3) system information inquiries, and 4) programming statements.

System commands include user's library commands and specification commands. Specification commands include both components and total system specifications. Subprogram instructions provide the information to use a particular subprogram which is stored in the Subprogram Library. Systems Information Inquiries provide system information and messages. The functions of the language processor include:

1. As an interpreter, it accepts inputs, statement by statement, from the message buffer and puts the data into a common place so that the executed program can access these data.
2. If an input is a macro, the processor will execute that macro, statement by statement.
3. If an input is a Subprogram Instruction, the processor will call the Dispatcher. Upon return of control to the processor it will continue to examine the input.
4. If there is any illegal statement, the processor will call the Error Message Handling Routine, and terminate the current execution mode, clearing the common data area.

#### 4.2.2.6 Error Message Handling Routine

This module will issue an error message to the user whenever there is an illegal input statement. The messages should include an error code, problem explanation, and corrective action. Recovery from user-program errors involves immediate



discontinuation of execution, cutting back the execution stack to the level of the most recently called macro, and requesting typewriter input. Recovery from system errors is accomplished by the PL/I compiler and operating monitor. Infinite loops are forcibly terminated by the interval timer routine.

#### 4.2.2.7 Dispatcher

This module will set up the information regarding what parameters to expect from the user and what subprogram to call to execute the instruction. If necessary, it will guide the user on how to proceed.

#### 4.2.2.8 Subprogram Library

This module stores the object code of the programs for modeling, simulating and analyzing power processing systems.

#### 4.2.2.9 Power Processing Subsystems Data Base Facility

This module provides the following capabilities:

1. A means of accessing, and maintaining, variable-length applications data.
2. A means of cross-referencing or interrelating the data within two or more data bases.
3. A means to restructure and expand an established data base without modifying application programs that use it.
4. A means to ensure that information is available only to those entitled to it and that only eligible persons may update the data base.
5. Checkpoint, restart, data recovery, and statistical information collection capabilities.

Essentially, this module is a generalized program that assists the user in the creation and organization of a data base, provides an efficient dump restore program for data bases, and provides a means for collecting data base modifications which are to be used in data base reconstruction. This module can be used to create and maintain data bases, and to accomplish data storage and access.

#### 4.2.3 Implementation Strategy

The basic organizational unit of the management program is the workspace. The workspace consists of 1) system variables, 2) a symbol table, 3) a syntax analyses stack, 4) a user's data area, and 5) an execution stack.

The system variables contain various pointers and workspace constants. The symbol table contains entries and each entry has a pointer, a type indicator, symbol length indicator, and symbol point-name. The pointer points to the

data area where the value of the symbol is stored. The type indicator indicates whether the associated item is a variable or a macro. The point-name of a symbol may be a symbol itself or a pointer to the actual symbol, depending on the length of the symbol. Syntax analysis is essentially done by the Conway Transition Diagram method, and the syntax analysis stack is used to maintain a record of the syntax analysis path being traced. The information in a record may include: 1) name and current line number of the macro being executed, 2) status information necessary to resume parsing of the internal form from the point it was interrupted, 3) pointers to the symbol table for all local variables and their previous pointers to data. The user data area contains user defined data items, such as macro definitions, variables values (may be boolean, character, integer, real, complex), and list data entries (used for each macro, it contains a pointer to the beginning of each of the macro's lines). Flags tell whether or not the data entry is a list data entry and whether or not the data entry is useful.

The string of input commands and instructions will be scanned by the EDITOR which generates the internal form of the language. The internal form is essentially produced by a one to one mapping of the input string. Negligible syntax checking is done during internal form generation; and once the internal form is produced, the input string is discarded. From the internal form it is easy to reproduce the corresponding input string and also the internal form is readily parsed by the LANGUAGE PROCESSOR.

Once the internal form has been generated, it may be executed by calling the LANGUAGE PROCESSOR (at the execution mode) which can then generate output and/or create data entry in the user's data area to store the results of the

calculation. If the internal form was created in the macro definition mode, then instead of calling the LANGUAGE PROCESSOR, the internal form is added to the directory of the currently active macro definition. The list data entry is essentially a description which characterizes the particular macro, followed by a series of pointers and line counters which describe each line of the macro.

#### 4.2.4 File Design

The power processing subsystem data should be organized so that a search can be conducted in an efficient manner, based on the criteria listed in Table 4-1. It is desirable also that the filing system be designed so that the data base can be maintained easily.

To achieve an efficient search the main file is organized in index random form and surrounded by several inverted files. Because the file is index random organized, the user can easily search for a particular range of values or for a particular value of say voltage or power or frequency. The inverted file assists the user in retrieving a file efficiently based on several key words of interest such as voltage, power and frequency.

To achieve low cost file maintenance, batched updating rather than on-line updating is used. Batched updating can be accomplished at a much lower cost than on-line updating and carries essentially no negative aspects for this application since there is no need for instantaneous addition to the file of data on new subsystems.

#### 4.3 SUMMARY

This section has presented a computer management program that can, with suitable available catalog data on existing power processing subsystems, and with defined mission objectives, constraints and data; select suitable candidate designs to assemble a complete system.

The program can be expanded by additional analysis and synthesis routines as they become available to permit the operator to create the optimum design by an interactive procedure which compares the results of modeling, analysis and synthesis with the data base of existing designs.

## SECTION 5

### PLAN FOR PHASE II

## 5.0 Plan for Phase II

### 5.1 INTRODUCTION

Phase 1 of this project for the formulation of a methodology for the modeling and analysis of power processing systems investigated the feasibility of the mathematical modeling, simulation and analysis. The result of Phase 1 is a methodology for the development of a flexible engineering tool which allows the power processor designer to effectively and rapidly assess and analyze the tradeoffs available, and this management program has been described in section 4 of this report.

In Phase 2 of this project, a detailed plan for formulation of this methodology will be developed and portions of the plan will be implemented. The detailed plan includes a logic flow diagram, and when completed will provide the vehicle for modeling, simulating and analyzing power processing systems. This computer program when fully implemented will also provide for design and optimization. For each power processing system to be designed, the program will provide: 1) a mathematical model, 2) an analysis of expected performance, 3) simulation, and 4) a comparative evaluation with alternative designs.

A power processing system generally includes 1) an energy source, such as a solar array, fuel cells, or a thermoelectric generator; 2) energy storage devices such as batteries or capacitors; 3) power processing equipment such as converters, inverters, and voltage regulators; and 4) control and distribution equipment such as distribution lines, switches, relays and breakers.

To initiate the design of a power processing system it is necessary to know or

to assume performance specifications. Typical specifications may include: 1) the required power level; 2) the required voltage(s); 3) regulation and ripple voltage limitations, 4) electrical compatibility requirements, and 5) mission constraints such as size, weight, or power limits. With these specifications set, the power processing system may be designed to meet the requirements at minimum cost, with minimum weight, or with maximum reliability; or the design can optimize an objective function that is a composite of several factors. Limitations on weight, volume and thermal heating, if included as design specifications, may obviate a satisfactory design.

Power processing systems are usually designed by a trial-and-error process. Components are selected which appear to be appropriate, and a paper design based on the selected components is completed and then modeled, simulated and/or analyzed to determine its adequacy. If the design specifications are not met, the paper design is modified, and then analyzed again. This iterative procedure continues until a satisfactory design is achieved.

The currently used trial-and-error methods for designing power processing systems are time consuming and generally do not lead to an optimal system. An engineering tool or vehicle which will permit the expeditious design, modeling, simulation, analysis and comparison of power processing systems is needed.

There are several ways to implement a long term, low level of effort program to achieve the final goal of a complete power processing design and analysis tool. It can be achieved by generating a series of computer routines for specific elements of the power processing design task with the thought that these eventually would be combined in a master program, or the management program can be designed first, and these routines can be added as they evolve to flesh



out the skeleton which is the management program.

The risk in the first approach is that there is no common interface description, computer language, format, and instructions to permit integration and combination at a later date. The risk of the latter approach is that a great deal of time and effort is required before visible results are achieved. However, the myriad of routines that already exist without a means of combining them in a common system leads to the conclusion that the management program and language must be developed first, and that is the recommendation of this section.

## 5.2 Scope of Work

The work outlined herein consists of developing a detailed plan for formulating a methodology for the modeling and analysis of power processing systems to allow the power processor designer to effectively and rapidly assess and analyze the tradeoffs available. The detailed plan to be developed will include a logic flow diagram which, when implemented as an operational computer program, will provide the vehicle for modeling, simulating, designing, optimizing, and analyzing power processing systems. For each power processing system to be designed, the program will provide 1) a mathematical model, 2) an analysis of the expected performance, 3) simulation, and 4) a comparative evaluation with alternative designs.

The many capabilities of the total program will be called into play through a management program. It is the management program which will establish the sequence in which the several parts of the program are called, in order to

accomplish a desired function such as the comparison of two candidate systems or the initiation of a new design which meets a set of specifications. The management program will embrace a command language of action verbs such as DESIGN, OPTIMIZE, COMPARE, PLOT, CORRELATE, ADD, DELETE.

Features of the computer program will include:

1. A file handling capability so that any file generated by a management program command can be used by any subsequent command.
2. MACROS - the ability to read and save a sequence of commands (the set of commands is called a MACRO and is given a name). Later use of the name of the MACRO with appropriate file names as arguments, will invoke the entire sequence.
3. A general data input program to read and store input data appropriately.
4. Interaction - providing the user with the ability to rapidly interact with the program.
5. Machine independence - the program will be written either in Fortran IV or in APL so that it can be used on most large scale digital machines. The interaction feature will be somewhat limited for machines which do not have teletype or display terminals.

Previous studies and comparisons of existing computer languages resulted in a recommendation to use Programming Language 1 for the Management Program. This International Business Machine product is in common usage at most universities

and is familiar to all new entrants to the profession. Table 3-1 has presented a comparison of languages. This information will be reviewed early in Phase 2 and a final selection made.

6. Error recovery - when the user does something wrong, the program will report the problem and continue or abort as appropriate.
7. Self documentation - the users manual for the program will be available for printout. Only a very short set of instructions on how to access the program will be required in addition to a tape of the program.
8. Open endedness - the program will permit the addition of additional capabilities as the need arises.

### 5.3 Task Descriptions

#### 5.3.1 Task 1 - Design of the Management Computer Program

A computer program will be the vehicle which shall permit the rapid design, modeling, simulation, analysis and comparison of power processing systems. The framework shall be a management program which ties together a system of programs.

This management program and parts of the program will be developed. In particular;

1. The language to be used will be selected (either Fortran IV, APL, or PL1).
2. The management program command language will be developed.
3. The management program will be developed and implemented as a computer program.

### 5.3.2 Task 2 - Design of a Library of Power Processing System Components

At any point in time there is an array of power processing system components that are readily available and whose characteristics are well known. To facilitate the design of power processing systems the computer program will:

1) provide for the storage of data on a relatively large number of power processing system components, 2) provide a search mechanism to retrieve data on those components which have potential for the particular system to be designed and 3) provide a mechanism to select from the potentially suitable components that complement of components which provide the best design.

During this task;

1. Data on an array of power processing systems will be collected and prepared for computer storage.
2. A methodology for retrieving data on suitable power processing system components will be developed and implemented as a computer program.
3. A methodology for selecting the complement of available components which best satisfy a set of design specifications will be developed and implemented by a computer program.

As a first useful product of the Management Program, it is proposed that a catalog of existing power processors be computerized to facilitate a search on any of a number of parameters. Table 5-1 summarizes the amount of memory required to store characteristics of power processors. Refer to Table 4-1 for typical format of this data.

Table 5-1

## Memory Required to Store Characteristics

DESCRIPTION	REQUIRED DIGITS	DIGITAL BYTES
Voltage Type	1	1
Voltage Magnitude	5	3
Frequency	4	3
Number of Phases	2	1
Name	12	12
Weight	Full Word	4
Cost	5	3
Reliability	Full Word	4
Mode Power	30	18
Priority	2	1
Voltage Regulation	Full Word	4
Voltage Tolerance	1	1
Frequency Regulation	Full Word	4
Size	3 Full Words	12
TOTAL MEMORY REQUIRED		71

These characteristics can be recorded on punched cards, with two cards required for each power processor. If the NASA inventory of spacecraft totals 200, with an average of ten power processors per spacecraft type, then data should be available on 2000 different pieces of equipment.

If 80 bytes of data fully characterizes a power processor, and if 2000 different pieces of equipment exist, then 1280 kilobits of storage would be required to place all these characteristics in direct access to a computer program.

Other methods of sorting are certainly available and more economical to sort and file on any one characteristic. However, if the intent is to make the program interactive on a computer with display, then all parameters must be accessible either in active memory or on magnetic tape.

### 5.3.3 Task 3 - Methodology of Optimization

The total computer program, upon completion, will have the following capabilities:

1. To store data on many power processing system components.
2. To retrieve data on components suitable for particular designs.
3. To select the "best" set of components for a particular system.
4. To indicate when system specifications cannot be met by currently available components.
5. To design needed components.
6. To model system components and the complete system.
7. To compare two or more systems.

8. To simulate components of power processing systems or the complete system.

This task will culminate in a demonstration of the total program at the contractor's facility.

#### 5.3.4 Task 4 - Computerized Design Routine

In order to provide immediate useful results, one design task will be methodized in a computer routine in concert with the language, format, and the nomenclature of the management program.

In section 4 of this report two examples of computerized transformer design routines were given. The first of these took a purely theoretical approach to transformer optimization, using a scrapless lamination shape, square leg, and continuous core and copper sizes to generate a family of transformer designs. No interaction with the designer was required, and no practical constraints, such as wire gages, were imposed.

The second transformer optimization considered both cut core and toroidal shapes, but imposed no limits on actual available cores and wire sizes. Practical considerations such as maximum volts per turn and transistor switching losses were considered, but the routine went thru a series of designs with no human intervention to determine minimum loss transformer designs.

The objective of this task is to generate a computer program for a design procedure that is usually accomplished manually, requires much time or iteration to achieve optimum results, but does utilize the prior knowledge and

experience of the design engineer. Table 5-2 and Table 5-3 list data on two computer programs for transformer design, the second of which appears to have the desirable attributes to satisfy the objectives of this task.

Table 5-2 Transformer Optimization Computer Program

<p>A computer program has been developed for performing transformer optimization. In using this program, values of flux density, frequency, primary and secondary voltage and current, materials constants, and input volts per turn ratio must be known or assumed. Given these parameters, the program computes:</p>	<p>Results are computed versus volts per turn ratio. Since frequency and flux density are not included in the transformer optimization routine, the program is not complete. In its present condition, it would make a good subroutine in a more general transformer optimization program.</p> <p>Language: FORTRAN IV</p> <p>Machine Requirements: IBM-7094</p> <p>Source: P. Ramirez and H. Dove of Electro-Optical Systems, Inc. under contract to Lewis Research Center (LEW-3299)</p>
<ol style="list-style-type: none"> <li>1. primary and secondary turns, resistance, length of windings, and losses;</li> <li>2. core size, volume, weight, and losses;</li> <li>3. voltage regulation; and</li> <li>4. overall transformer efficiency.</li> </ol>	

Table 5-3 Computer Program for the Design of Toroidal Transformers

<p>A computer program has been developed which carries out the necessary calculations for the design of toroidal transformers for use in parallel inverters. Any magnetic tape material may be used in the core and any standard round metal wire may be used in the coil.</p> <p>In most inverter circuits, the transformer is the heaviest component and usually accounts for a significant fraction of the power loss. Therefore, careful attention to transformer design can have an important effect on system weight and efficiency, but, because transformer calculations tend to be tedious and time consuming, a detailed analysis of the effects of various parameters can be a formidable task. This program relieves the designer of most of the computational details, while he maintains control over most engineering decisions. The number of specifications that must be supplied by the user allows for considerable flexibility and for the exercise of engineering judgment. Furthermore, the speed of the program makes it possible to run a great many cases, economically determining the effect of various parameter changes.</p>	<p>This program has been applied to the design of 2- and 4-kilovolt-ampere transformers and, over a range of frequency from 200 to 3200 hertz, a class of transformers of nearly equal efficiency has been designed. The variation in characteristics of transformers wound on heavy and light cores can also be examined.</p>
<p>The information supplied to the computer is the input voltage, input current, output voltage, frequency of operation, desired fill factor, maximum <math>I^2R</math> loss in a coil, maximum magnetic flux density, density of the magnetic material, specific core loss, specific apparent excitation power, ambient temperature, desired current density in the windings, and relative resistance and density of the wire if a metal other than copper is used.</p>	<p>Notes:</p> <ol style="list-style-type: none"> <li>1. The program is written in FORTRAN IV language for use on an IBM 7094 and the calculation time is approximately 0.0011-minute per transformer.</li> <li>2. Inquiries concerning this program should be directed to:</li> </ol> <p>COSMIC Information Services 112 Barrow Hall University of Georgia Athens, Georgia 30602 Reference: LEW-11878</p>
<p>The computer output consists of the input and output currents and voltages, excitation current, core identification number, core weight, core loss, approximate regulation, total losses, efficiency, total mass, fill factor, ambient and operating temperatures, final height, diameter, and surface area, frequency, power lost per unit surface area, and, for each coil, the number of turns, size of wire, number of parallel windings, resistance, power dissipated, and mass.</p>	<p>Source: James A. Dayton, Jr. Lewis Research Center (LEW-11878)</p>
<p>The program contains information on 48 sizes of wire and 90 sizes of magnetic cores, equally divided into two groups called light (high-gain) and heavy (low-gain) cores.</p>	



To illustrate the kind of program intended, Table 5-4 gives an example of the type of design engineer-computer program interaction to achieve an economical, practical, and optimum result.

The first column lists the information required from the operator by the computer, such as number and kind of winding, operating frequency, flux density, input voltage, and input current. It also requires information on physical characteristics, such as insulation thickness between the core and the windings, between windings, and between layers. Ambient temperature must be given, as well as the operator's choice of a core size to start the design procedure.

At this point the computer prints the core dimensions and tolerances if a standard core (available in computer memory) has been selected, or the operator inserts the dimensions he has chosen with tolerances.

For the example given, an AM-3 core was selected, operated at 20,000 Hertz and 1500 Gauss, with 13 volts on the primary. The program calculated the nearest number of primary turns to operate near 1500 Gauss, and it was found to be 65 turns at 1494 Gauss. The nearest approach to the secondary was 14.0 volts rather than 13.9, with an error of -0.719%, and a total of 70 turns. This established an operating point of 200 millivolts per turn.

REPRODUCIBILITY OF THE  
ORIGINAL PAGE IS POOR

Table 5-4 Interactive Transformer Design

5-12

1  
SUPPLY THE FOLLOWING DATA:  
NUMBER OF TURNS, KIND OF WINDING(1OR2), 1,NUIND  
OPERATING FREQ.(HZ) INDUCTION(GAUSS)= 2, 1,2, 20000, 1500  
TYPE CONSTRUCTION- 1=SINGLE SIDE, 2=EQUAL SPLIT TWO SIDES= 2

SUPPLY FOLLOWING DATA IN WINDING ORDER:  
SUPPLY PER SIDE VOLTAGE AND CURRENT DATA  
VOLTS(PK.)= 13, 13.9  
AMPERES(PK.)= .077, .057  
DO YOU WISH TO USE STANDARD INS.& STACKING DATA? YES  
CORE BOX INS. THICKNESS, LAYER INS. THICKNESS  
MAJOR INS. THICKNESS, COPE STACKING FACTOR =0.010,0.001,0.002,0.830  
AMBIENT TEMP.(DEG.C)= 25  
WIRE SIZE (0 FOR MANUAL)= 3  
D= 0.25000 E= 0.12500 F= 0.25000 G= 0.50000  
TOLERANCES D=0.0312 E=0.0156 F=0.0156 G=0.0156

CONTROL W DG. NO.= 1  
ACTUAL FLUX DENSITY= 1494. GAUSS CORE LOSS= 0.3644 WATTS

WDG.NO.	VOLTS SPEC'D	VOLTS ACTUAL	ERROR NO.	TURNS
1	13.000000	13.000000	0.000	65
2	13.900000	14.000000	-0.719	70

VOLTS PER TURN= 0.20000  
NEW FLUX DESIRED? NO  
NEW CORE DESIRED? NO  
>>>> WINDING NUMBER= 1 WIRE SIZE (AWG)= 25  
3.421 LAYERS FILLED. DO YOU WISH TO CHANGE WIRE SIZE? YES  
>>>> WINDING NUMBER= 1 WIRE SIZE (AWG)= 27  
2.709 LAYERS FILLED. DO YOU WISH TO CHANGE WIRE SIZE? YES  
>>>> WINDING NUMBER= 1 WIRE SIZE (AWG)= 26  
3.095 LAYERS FILLED. DO YOU WISH TO CHANGE WIRE SIZE? NO  
TURNS/LAYER= 21.0 WINDING WIDTH= 0.407 WINDABLE WIDTH= 0.424  
DO YOU WISH TO CHANGE TURNS/LAYER? YES  
IF TURNS/LAYER= 22.  
2.755 LAYERS FILLED. DO YOU WISH TO CHANGE WIRE SIZE? NO  
TURNS/LAYER= 22.0 WINDING WIDTH= 0.425 WINDABLE WIDTH= 0.424  
DO YOU WISH TO CHANGE TURNS/LAYER? NO  
>>>> WINDING NUMBER= 2 WIRE SIZE (AWG)= 27  
6.364 LAYERS FILLED. DO YOU WISH TO CHANGE WIRE SIZE? YES  
>>>> WINDING NUMBER= 2 WIRE SIZE (AWG)= 26  
7.000 LAYERS FILLED. DO YOU WISH TO CHANGE WIRE SIZE? NO  
TURNS/LAYER= 10.0 WINDING WIDTH= 0.407 WINDABLE WIDTH= 0.424  
DO YOU WISH TO CHANGE TURNS/LAYER? NO

2  
CHECK FIT: 192.80 % FULL BUILD= 0.22 IN. PER SIDE  
NEW FLUX? NO  
NEW CORE? NO  
PER SIDE DATA

WDG.NO.	AMPS	AMPS/SQ.IN.	MLT(IN.)	LENGTH(FT.)	% OF FILL
1	0.0730000	392.	1.177	6.6241	29.031
2	0.0570000	203.	2.042	12.1614	67.326

WDG.	WIRE	NO. OF TURNS/	WDG.	RESISTANCE		
NO.	Gauge	LAYERS	LAYER WIDTH	OHMS/LEG	LEG WT.	LEG I R
1	26	3.00	22.0	0.425	0.2769	0.0051
2	26	7.00	10.0	0.407	0.5083	0.0093

TRANSFORMER TOTALS

	COPPER	COPE	TOTAL	
LOSSES	0.0067	0.3644	0.3711	WATTS
WEIGHT	0.0473	0.0130	0.0603	POUNDS

LENGTH(G)= 0.8169 HEIGHT(F)= 0.9995 WIDTH(D)= 0.7333

SPECIFY PRIMARY WINDING NO.= 1/2  
PER SIDE DATA

WDG.	IND CT	REACT	E(X)	E(R)P	E(F)S	E(TOT)
NO.	MICRO H	OHMS	VOLTS	VOLTS	VOLTS	VOLTS
1	35.78	4.4961	0.2233	0.0135	0.0216	0.2583

WDG. NO.	TURNS	VOLTS SPEC'D	VOLTS ACTUAL	VOLTS OUTPUT
1	65	13.000000	12.9999996	12.7416918
2	70	13.9000000	13.9999996	13.9999996

REPEATS= NO 'ALL', 'CORE', OR 'FLUX' = FLUX  
NEW FLUX= 1600

CONTROL W DG. NO.= 1  
ACTUAL FLUX DENSITY= 1592. GAUSS CORE LOSS= 0.4161 WATTS

WDG.NO.	VOLTS SPEC'D	VOLTS ACTUAL	ERROR NO.	TURNS
1	13.000000	13.000000	0.000	61
2	13.900000	13.852459	0.342	65

Table 5-4 (continued) Interactive Transformer Design

5-13

3		4																																																																																																				
VOLTS PER TURN= 0.21311 NEW FLUX DESIRED? = NO NEW CORE DESIRED? = NO >>>> WINDING NUMBER= 1 WIRE SIZE (AVG)= 30 1.794 LAYERS FILLED. DO YOU WISH TO CHANGE WIRE SIZE? = YES >>>> WINDING NUMBER= 1 WIRE SIZE (AVG)= 32 1.452 LAYERS FILLED. DO YOU WISH TO CHANGE WIRE SIZE? = NO TURNS/LAYER= 42.0 WINDING WIDTH= 0.417" WINDABLE WIDTH= 0.424" DO YOU WISH TO CHANGE TURNS/LAYER? = NO >>>> WINDING NUMBER= 2 WIRE SIZE (AVG)= 32 3.250 LAYERS FILLED. DO YOU WISH TO CHANGE WIRE SIZE? = NO TURNS/LAYER= 26.0 WINDING WIDTH= 0.407" WINDABLE WIDTH= 0.424" DO YOU WISH TO CHANGE TURNS/LAYER? = NO  CHECK FIT: 64.55 % FULL BUILD= 0.07 IN. PER SIDE NEW FLUX? = YES 1400 CONTROL W DG. NO.= 2 ACTUAL FLUX DENSITY= 1403. GAUSS CORELOSS= 0.3197WATTS  <table border="1"> <thead> <tr> <th>WDG.NO.</th> <th>VOLTS SPEC'D</th> <th>VOLTS ACTUAL</th> <th>ERROR</th> <th>NO. TURNS</th> </tr> </thead> <tbody> <tr> <td>1</td> <td>13.000000</td> <td>12.960811</td> <td>0.301</td> <td>69</td> </tr> <tr> <td>2</td> <td>13.900000</td> <td>13.900000</td> <td>0.000</td> <td>74</td> </tr> </tbody> </table> VOLTS PER TURN= 0.18734 NEW FLUX DESIRED? = NO NEW CORE DESIRED? = NO >>>> WINDING NUMBER= 1 WIRE SIZE (AVG)= 29 2.360 LAYERS FILLED. DO YOU WISH TO CHANGE WIRE SIZE? = NO TURNS/LAYER= 30.0 WINDING WIDTH= 0.415" WINDABLE WIDTH= 0.424" DO YOU WISH TO CHANGE TURNS/LAYER? = NO >>>> WINDING NUMBER= 2 WIRE SIZE (AVG)= 30 4.675 LAYERS FILLED. DO YOU WISH TO CHANGE WIRE SIZE? = NO TURNS/LAYER= 16.0 WINDING WIDTH= 0.408" WINDABLE WIDTH= 0.424" DO YOU WISH TO CHANGE TURNS/LAYER? = NO  CHECK FIT: 107.62 % FULL BUILD= 0.12 IN. PER SIDE NEW FLUX? = YES 1500 CONTROL W DG. NO.= 2 ACTUAL FLUX DENSITY= 1505. GAUSS CORELOSS= 0.3700WATTS  <table border="1"> <thead> <tr> <th>WDG.NO.</th> <th>VOLTS SPEC'D</th> <th>VOLTS ACTUAL</th> <th>ERROR</th> <th>NO. TURNS</th> </tr> </thead> <tbody> <tr> <td>1</td> <td>13.000000</td> <td>13.094203</td> <td>-0.725</td> <td>65</td> </tr> <tr> <td>2</td> <td>13.900000</td> <td>13.900000</td> <td>0.000</td> <td>69</td> </tr> </tbody> </table>		WDG.NO.	VOLTS SPEC'D	VOLTS ACTUAL	ERROR	NO. TURNS	1	13.000000	12.960811	0.301	69	2	13.900000	13.900000	0.000	74	WDG.NO.	VOLTS SPEC'D	VOLTS ACTUAL	ERROR	NO. TURNS	1	13.000000	13.094203	-0.725	65	2	13.900000	13.900000	0.000	69	VOLTS PER TURN= 0.20145 NEW FLUX DESIRED? = YES NEW FLUX= 1550 CONTROL W DG. NO.= 2 ACTUAL FLUX DENSITY= 1550. GAUSS CORELOSS= 0.3934WATTS  <table border="1"> <thead> <tr> <th>WDG.NO.</th> <th>VOLTS SPEC'D</th> <th>VOLTS ACTUAL</th> <th>ERROR</th> <th>NO. TURNS</th> </tr> </thead> <tbody> <tr> <td>1</td> <td>13.000000</td> <td>13.070149</td> <td>-0.540</td> <td>63</td> </tr> <tr> <td>2</td> <td>13.900000</td> <td>13.900000</td> <td>0.000</td> <td>67</td> </tr> </tbody> </table> VOLTS PER TURN= 0.20746 NEW FLUX DESIRED? = YES NEW FLUX= 1575 CONTROL WDG. NO.= 2 ACTUAL FLUX DENSITY= 1573. GAUSS CORELOSS= 0.4060WATTS  <table border="1"> <thead> <tr> <th>WDG.NO.</th> <th>VOLTS SPEC'D</th> <th>VOLTS ACTUAL</th> <th>ERROR</th> <th>NO. TURNS</th> </tr> </thead> <tbody> <tr> <td>1</td> <td>13.000000</td> <td>13.057575</td> <td>-0.443</td> <td>62</td> </tr> <tr> <td>2</td> <td>13.900000</td> <td>13.900000</td> <td>0.000</td> <td>66</td> </tr> </tbody> </table> VOLTS PER TURN= 0.21061 NEW FLUX DESIRED? = NO NEW CORE DESIRED? = NO >>>> WINDING NUMBER= 1 WIRE SIZE (AVG)= 29 2.667 LAYERS FILLED. DO YOU WISH TO CHANGE WIRE SIZE? = NO TURNS/LAYER= 30.0 WINDING WIDTH= 0.415" WINDABLE WIDTH= 0.424" DO YOU WISH TO CHANGE TURNS/LAYER? = YES NEW TURNS/LAYER= 31 2.000 LAYERS FILLED. DO YOU WISH TO CHANGE WIRE SIZE? = NO TURNS/LAYER= 31.0 WINDING WIDTH= 0.429" WINDABLE WIDTH= 0.424" DO YOU WISH TO CHANGE TURNS/LAYER? = NO >>>> WINDING NUMBER= 2 WIRE SIZE (AVG)= 30 4.125 LAYERS FILLED. DO YOU WISH TO CHANGE WIRE SIZE? = NO TURNS/LAYER= 16.0 WINDING WIDTH= 0.405" WINDABLE WIDTH= 0.424" DO YOU WISH TO CHANGE TURNS/LAYER? = YES NEW TURNS/LAYER= 17 3.032 LAYERS FILLED. DO YOU WISH TO CHANGE WIRE SIZE? = NO TURNS/LAYER= 17.0 WINDING WIDTH= 0.432" WINDABLE WIDTH= 0.424" DO YOU WISH TO CHANGE TURNS/LAYER? = NO  CHECK FIT: 80.33 % FULL BUILD= 0.09 IN. PER SIDE NEW FLUX? = NO NEW CORE? = NO PER SIDE DATA  <table border="1"> <thead> <tr> <th>WDG.NO.</th> <th>AMPS</th> <th>AMPS/50 IN.</th> <th>MLT(IN.)</th> <th>LENGTH(FT.)</th> <th>% OF FILL</th> </tr> </thead> <tbody> <tr> <td>1</td> <td>0.0780000</td> <td>39.</td> <td>1.046</td> <td>5.6547</td> <td>14.520</td> </tr> <tr> <td>2</td> <td>0.0570000</td> <td>513.</td> <td>1.409</td> <td>7.9933</td> <td>25.874</td> </tr> </tbody> </table> <table border="1"> <thead> <tr> <th>WDG.</th> <th>WIRE NO.</th> <th>NO. OF TURNS/LAYER</th> <th>WIRE WIDTH</th> <th>RESISTANCE OHMS/LEG</th> <th>LEG LT.</th> <th>LEG I F</th> </tr> </thead> <tbody> <tr> <td>1</td> <td>29</td> <td>2.00</td> <td>31.0</td> <td>0.429</td> <td>0.4632</td> <td>0.0022</td> </tr> <tr> <td>2</td> <td>30</td> <td>4.00</td> <td>17.0</td> <td>0.432</td> <td>0.8473</td> <td>0.0024</td> </tr> </tbody> </table>		WDG.NO.	VOLTS SPEC'D	VOLTS ACTUAL	ERROR	NO. TURNS	1	13.000000	13.070149	-0.540	63	2	13.900000	13.900000	0.000	67	WDG.NO.	VOLTS SPEC'D	VOLTS ACTUAL	ERROR	NO. TURNS	1	13.000000	13.057575	-0.443	62	2	13.900000	13.900000	0.000	66	WDG.NO.	AMPS	AMPS/50 IN.	MLT(IN.)	LENGTH(FT.)	% OF FILL	1	0.0780000	39.	1.046	5.6547	14.520	2	0.0570000	513.	1.409	7.9933	25.874	WDG.	WIRE NO.	NO. OF TURNS/LAYER	WIRE WIDTH	RESISTANCE OHMS/LEG	LEG LT.	LEG I F	1	29	2.00	31.0	0.429	0.4632	0.0022	2	30	4.00	17.0	0.432	0.8473	0.0024
WDG.NO.	VOLTS SPEC'D	VOLTS ACTUAL	ERROR	NO. TURNS																																																																																																		
1	13.000000	12.960811	0.301	69																																																																																																		
2	13.900000	13.900000	0.000	74																																																																																																		
WDG.NO.	VOLTS SPEC'D	VOLTS ACTUAL	ERROR	NO. TURNS																																																																																																		
1	13.000000	13.094203	-0.725	65																																																																																																		
2	13.900000	13.900000	0.000	69																																																																																																		
WDG.NO.	VOLTS SPEC'D	VOLTS ACTUAL	ERROR	NO. TURNS																																																																																																		
1	13.000000	13.070149	-0.540	63																																																																																																		
2	13.900000	13.900000	0.000	67																																																																																																		
WDG.NO.	VOLTS SPEC'D	VOLTS ACTUAL	ERROR	NO. TURNS																																																																																																		
1	13.000000	13.057575	-0.443	62																																																																																																		
2	13.900000	13.900000	0.000	66																																																																																																		
WDG.NO.	AMPS	AMPS/50 IN.	MLT(IN.)	LENGTH(FT.)	% OF FILL																																																																																																	
1	0.0780000	39.	1.046	5.6547	14.520																																																																																																	
2	0.0570000	513.	1.409	7.9933	25.874																																																																																																	
WDG.	WIRE NO.	NO. OF TURNS/LAYER	WIRE WIDTH	RESISTANCE OHMS/LEG	LEG LT.	LEG I F																																																																																																
1	29	2.00	31.0	0.429	0.4632	0.0022																																																																																																
2	30	4.00	17.0	0.432	0.8473	0.0024																																																																																																

Table 5-4 (continued) Interactive Transformer Design

5

TRANSFORMER TOTALS

	COPPER	COPE	TOTAL		
LOSSES	0.0112	0.4060	0.4172	WATTS	0.702
WEIGHT	0.0141	0.0130	0.0271	POUNDS	

LENGTH(S)= 0.8169 HEIGHT(F)= 0.7492 WIDTH(D)= 0.4826

SPECIFY PRIMARY WINDING NO.= 2

PER SIDE DATA

Wdg.	INDUCT	REACT	E(X)	E(R)P	E(P)S	E(TOT)
NO.	MICRO H	OHMS	VOLTS	VOLTS	VOLTS	VOLTS
1	10.19	1.2310	0.0636	0.0227	0.0365	0.1223

Wdg. NO.	TURNS	VOLTS SPEC'D	VOLTS ACTUAL	VOLTS OUTPUT
1	62	13.000000	13.057575	12.9347469
2	66	13.900000	13.999997	13.8999997

REPEATS=NO, 'ALL', 'CORE', OR 'FLUX'=FLUX  
NEW FLUX= 1375  
CONTROL Wdg. NO.= 2  
ACTUALFLUX DENSITY= 1366. GAUSS CORELOSS= 0.3024WATTS

Wdg. NO.	VOLTS SPEC'D	VOLTS ACTUAL	ERROR NO. TURNS
1	13.000000	12.935526	0.111 71
2	13.900000	13.900000	0.000 76

VOLTS PER TURN= 0.15879  
NEW FLUX DESIRED?= NO  
NEW CORE DESIRED?= NO  
>>>>WINDING NUMBER= 1 WIRE SIZE (AVG)= 30  
2.034 LAYERS FILLED. DO YOU WISH TO CHANGE WIRE SIZE?= NO  
TURNS/LAYER= 34.0 WINDING WIDTH= 0.420" WINDABLE WIDTH= 0.424"  
DO YOU WISH TO CHANGE TURNS/LAYER?= YES  
NEW TURNS/LAYER= 36  
1.270 LAYERS FILLED. DO YOU WISH TO CHANGE WIRE SIZE?= NO  
TURNS/LAYER= 36.0 WINDING WIDTH= 0.444" WINDABLE WIDTH= 0.424"  
DO YOU WISH TO CHANGE TURNS/LAYER?= NO  
>>>>WINDING NUMBER= 2 WIRE SIZE (AVG)= 31  
4.222 LAYERS FILLED. DO YOU WISH TO CHANGE WIRE SIZE?= YES  
>>>>WINDING NUMBER= 2 WIRE SIZE (AVG)= 30  
4.750 LAYERS FILLED. DO YOU WISH TO CHANGE WIRE SIZE?= NO  
TURNS/LAYER= 16.0 WINDING WIDTH= 0.408" WINDABLE WIDTH= 0.424"  
DO YOU WISH TO CHANGE TURNS/LAYER?= NO

CHECK FIT: 90.83 % FULL BUILD= 0.10 IN. PER SIDE

6

NEW FLUX?= YES  
1300  
CONTROL Wdg. NO.= 2  
ACTUALFLUX DENSITY= 1298. GAUSS CORELOSS= 0.2717WATTS

Wdg. NO.	VOLTS SPEC'D	VOLTS ACTUAL	ERROR NO. TURNS
1	13.000000	13.051250	-0.240 75
2	13.900000	13.900000	0.000 80

VOLTS PER TURN= 0.17375  
NEW FLUX DESIRED?= NO  
NEW CORE DESIRED?= NO  
>>>>WINDING NUMBER= 1 WIRE SIZE (AVG)= 29  
2.590 LAYERS FILLED. DO YOU WISH TO CHANGE WIRE SIZE?= NO  
TURNS/LAYER= 30.0 WINDING WIDTH= 0.415" WINDABLE WIDTH= 0.424"  
DO YOU WISH TO CHANGE TURNS/LAYER?= NO  
>>>>WINDING NUMBER= 2 WIRE SIZE (AVG)= 30  
5.000 LAYERS FILLED. DO YOU WISH TO CHANGE WIRE SIZE?= NO  
TURNS/LAYER= 16.0 WINDING WIDTH= 0.408" WINDABLE WIDTH= 0.424"  
DO YOU WISH TO CHANGE TURNS/LAYER?= NO

CHECK FIT: 107.69 % FULL BUILD= 0.12 IN. PER SIDE  
NEW FLUX?= YES  
1200  
CONTROL Wdg. NO.= 2  
ACTUALFLUX DENSITY= 1193. GAUSS CORELOSS= 0.2281WATTS

Wdg. NO.	VOLTS SPEC'D	VOLTS ACTUAL	ERROR NO. TURNS
1	13.000000	12.941379	0.451 31
2	13.900000	13.900000	0.000 37

VOLTS PER TURN= 0.15977  
NEW FLUX DESIRED?= YES  
NEW FLUX= 1395  
CONTROL Wdg. NO.= 2  
ACTUALFLUX DENSITY= 1334. GAUSS CORELOSS= 0.3109WATTS

Wdg. NO.	VOLTS SPEC'D	VOLTS ACTUAL	ERROR NO. TURNS
1	13.000000	12.973333	0.205 70
2	13.900000	13.900000	0.000 75

VOLTS PER TURN= 0.13533  
NEW FLUX DESIRED?= NO  
NEW CORE DESIRED?= NO  
>>>>WINDING NUMBER= 1 WIRE SIZE (AVG)= 30  
2.059 LAYERS FILLED. DO YOU WISH TO CHANGE WIRE SIZE?= NO  
TURNS/LAYER= 34.0 WINDING WIDTH= 0.420" WINDABLE WIDTH= 0.424"

Table 5-4 (continued) Interactive Transformer Design

7										8									
DO YOU WISH TO CHANGE TURNS/LAYER? = YES										REPEATS = 'NO', 'ALL', 'CORE', OR 'FLUX' = FLUX									
NEW TURNS/LAYER = 35										NEW FLUX = 1795									
3.900 LAYERS FILLED. DO YOU WISH TO CHANGE WIRE SIZE? = NO										CONTROL "DG." NO. = 2									
TURNS/LAYER = 35.0 WINDING WIDTH = 0.432" WINDABLE WIDTH = 0.424"										ACTUAL FLUX DENSITY = 1731 GAUSS CORE LOSS = 0.4953 WATTS									
DO YOU WISH TO CHANGE TURNS/LAYER? = NO										NO. NO. VOLTS SPEC'D VOLTS ACTUAL XERFOR NO. TURNS									
>>> WINDING HEIGHT = 2 WIRE SIZE (AWG) = 31										1 13.000000 12.973333 0.205 56									
4.167 LAYERS FILLED. DO YOU WISH TO CHANGE WIRE SIZE? = NO										2 13.900000 13.900000 0.000 60									
TURNS/LAYER = 15.0 WINDING WIDTH = 0.407" WINDABLE WIDTH = 0.424"										VOLTS PER TURN = 0.23167									
DO YOU WISH TO CHANGE TURNS/LAYER? = YES										NEW FLUX DESIRED? = NO									
NEW TURNS/LAYER = 10										NEW CORE DESIRED? = NO									
3.247 LAYERS FILLED. DO YOU WISH TO CHANGE WIRE SIZE? = NO										>>> WINDING HEIGHT = 1 WIRE SIZE (AWG) = 28									
TURNS/LAYER = 10.0 WINDING WIDTH = 0.423" WINDABLE WIDTH = 0.424"										2.074 LAYERS FILLED. DO YOU WISH TO CHANGE WIRE SIZE? = NO									
DO YOU WISH TO CHANGE TURNS/LAYER? = NO										TURNS/LAYER = 27.0 WINDING WIDTH = 0.414" WINDABLE WIDTH = 0.424"									
CHECK FIT: 72.95 % FILL BUILD = 0.03 IN. PER SIDE										DO YOU WISH TO CHANGE TURNS/LAYER? = YES									
NEW FLUX? = NO										NEW TURNS/LAYER = 20									
NEW CORE? = NO										3.000 LAYERS FILLED. DO YOU WISH TO CHANGE WIRE SIZE? = NO									
PER SIDE DATA										TURNS/LAYER = 25.0 WINDING WIDTH = 0.429" WINDABLE WIDTH = 0.424"									
NO. NO. AMPS AMPS/SC. IN. MLT (IN.) LENGTH (FT.) % OF FILL										DO YOU WISH TO CHANGE TURNS/LAYER? = NO									
1 0.0730000 224. 1.034 0.2302 13.145										>>> WINDING HEIGHT = 2 WIRE SIZE (AWG) = 29									
2 0.0570000 143. 1.361 3.757 23.345										4.250 LAYERS FILLED. DO YOU WISH TO CHANGE WIRE SIZE? = NO									
NO. WIRE NO. OF TURNS/ NO. GAUGE LAYERS LAYER WIDTH										TURNS/LAYER = 14.0 WINDING WIDTH = 0.402" WINDABLE WIDTH = 0.424"									
1 30 2.00 35.0 0.432										DO YOU WISH TO CHANGE TURNS/LAYER? = YES									
2 21 4.00 15.0 0.423										NEW TURNS/LAYER = 15									
RESISTANCE 2										4.000 LAYERS FILLED. DO YOU WISH TO CHANGE WIRE SIZE? = NO									
OHMS/LEG LEG WT. LEG I F										TURNS/LAYER = 15.0 WINDING WIDTH = 0.429" WINDABLE WIDTH = 0.424"									
1 0.6657 0.0619 0.0041										DO YOU WISH TO CHANGE TURNS/LAYER? = NO									
2 1.1736 0.0021 0.0019										CHECK FIT: 59.07 % FILL BUILD = 0.10 IN. PER SIDE									
TRANSFORMER TOTALS										NEW FLUX? = NO									
LOSSES COPPER 0.0157 CORE 0.3109.048 TOTAL 0.3266 WATTS .6637										NEW CORE? = NO									
WEIGHT 0.0122 0.0130 0.0252 POUNDS										PER SIDE DATA									
LENGTH(G) = 0.6169 HEIGHT(F) = 0.7306 WIDTH(D) = 0.4650										NO. NO. AMPS AMPS/SC. IN. MLT (IN.) LENGTH (FT.) % OF FILL									
SPECIFY PRIMARY WINDING NO. = 2										1 0.0730000 224. 1.053 5.1592 15.393									
PER SIDE DATA										2 0.0570000 143. 1.453 7.5403 23.640									
NO. DIRECT FACT E(X) E(C) P E(R) S F(TOT)										NO. WIRE NO. OF TURNS/ NO. GAUGE LAYERS LAYER WIDTH									
NO. WIRE NO. 0.715 VOLTS VOLTS VOLTS VOLTS										1 28 2.00 25.0 0.429									
1 11.4" 1.4420 0.0717 0.5312 0.0512 0.1543										2 29 4.00 15.0 0.429									
RESISTANCE 2										OHMS/LEG LEG WT. LEG I F									
1 0.3456 0.0025 0.0021										2 0.6243 0.0029 0.0010									
TRANSFORMER TOTALS										LOSSES COPPER 0.0093 CORE 0.4953 TOTAL 0.5046 WATTS									
NO. NO. TURNS VOLTS SPEC'D VOLTS ACTUAL VOLTS OUTPUT										WEIGHT 0.0167 0.0130 0.0297 POUNDS									
1 70 13.000000 12.973333 12.973333										LENGTH(G) = 0.6169 HEIGHT(F) = 0.7667 WIDTH(D) = 0.5011									
2 75 13.900000 13.900000 13.900000																			

Table 5-4 (continued) Interactive Transformer Design

9

SPECIFY PRIMARY WINDING NO.= 2  
PER SIDE DATA

WDG. NO.	INDUCT	REACT	E(X)	E(R)P'	E(R)S	E(TOT)
	HICRO H	OHMS	VOLTS	VOLTS	VOLTS	VOLTS
1	9.41	1.1819	0.0587	0.0166	0.0270	0.1023

WDG. NO.	TURNS	VOLTS SPEC'D	VOLTS ACTUAL	VOLTS OUTPUT
1	56	13.0000000	12.9733330	12.8710784
2	60	13.9000000	13.3999996	13.3999996

REPEATS='NO', 'ALL', 'CORE', OR 'FLUX'= FLUX

NEW FLUX= 1250

CONTROL WDG. NO.= 2

ACTUAL FLUX DENSITY= 1251. GAUSS CORE LOSS= 0.2516 WATTS

WDG. NO.	VOLTS SPEC'D	VOLTS ACTUAL	ERROR NO. TURNS
1	13.000000	13.062650	-0.462 78
2	13.900000	13.900000	0.000 83

VOLTS PER TURN= 0.16747

NEW FLUX DESIRED?= NO

NEW CORE DESIRED?= NO

>>>> WINDING NUMBER= 1 WIRE SIZE (AWG)= 31  
2.058 LAYERS FILLED. DO YOU WISH TO CHANGE WIRE SIZE?= NO  
TURNS/LAYER= 38.0 WINDING WIDTH= 0.417" WINDABLE WIDTH= 0.424"  
DO YOU WISH TO CHANGE TURNS/LAYER?= YES

NEW TURNS/LAYER= 39  
2.090 LAYERS FILLED. DO YOU WISH TO CHANGE WIRE SIZE?= NO  
TURNS/LAYER= 39.0 WINDING WIDTH= 0.425" WINDABLE WIDTH= 0.424"  
DO YOU WISH TO CHANGE TURNS/LAYER?= NO

>>>> WINDING NUMBER= 2 WIRE SIZE (AWG)= 32  
4.150 LAYERS FILLED. DO YOU WISH TO CHANGE WIRE SIZE?= NO  
TURNS/LAYER= 20.0 WINDING WIDTH= 0.407" WINDABLE WIDTH= 0.424"  
DO YOU WISH TO CHANGE TURNS/LAYER?= YES

NEW TURNS/LAYER= 21  
3.952 LAYERS FILLED. DO YOU WISH TO CHANGE WIRE SIZE?= NO  
TURNS/LAYER= 21.0 WINDING WIDTH= 0.427" WINDABLE WIDTH= 0.424"  
DO YOU WISH TO CHANGE TURNS/LAYER?= NO

CHECK FIT: 66.51 % FULL BUILD= 0.07 IN. PER SIDE

NEW FLUX?= NO

NEW CORE?= NO

10

PER SIDE DATA

WDG. NO.	AMPS	AMPS/SQ. IN.	MLT(IN.)	LENGTH(FT.)	% OF FILL
1	0.0730000	1254.	1.022	6.8950	11.873
2	0.0570000	801.	1.321	9.3855	21.354

WDG. NO.	WIRE GAUGE	NO. OF LAYERS	TURNS/ LAYER	WDG. WIDTH	RESISTANCE OHMS/LEG	LEG WT.	LEG 1 R
1	31	2.00	39.0	0.423	0.9239	0.0017	0.0056
2	32	4.00	21.0	0.427	1.5486	0.0013	0.0025

TRANSFORMER TOTALS

	COPPER	CORE	TOTAL	LOSSES	WEIGHT
	0.0213	0.2516	0.2729	WATTS	.0603
	0.0106	0.0130	0.0236	POUNDS	

LENGTH(G)= 0.5169 HEIGHT(F)= 0.7161 WIDTH(D)= 0.4505

SPECIFY PRIMARY WINDING NO.= 2

PER SIDE DATA

WDG. NO.	INDUCT	REACT	E(X)	E(R)P'	E(R)S	E(TOT)
	HICRO H	OHMS	VOLTS	VOLTS	VOLTS	VOLTS
1	12.82	1.6111	0.0800	0.0415	0.0721	0.1935

WDG. NO.	TURNS	VOLTS SPEC'D	VOLTS ACTUAL	VOLTS OUTPUT
1	78	13.0000000	13.0626502	12.8691075
2	83	13.9000000	13.3999996	13.3999996

REPEATS='NO', 'ALL', 'CORE', OR 'FLUX'= FLUX

NEW FLUX= 650

CONTROL WDG. NO.= 2

ACTUAL FLUX DENSITY= 651. GAUSS CORE LOSS= 0.1126 WATTS

WDG. NO.	VOLTS SPEC'D	VOLTS ACTUAL	ERROR NO. TURNS
1	13.000000	12.933524	0.088 114
2	13.900000	13.900000	0.000 122

VOLTS PER TURN= 0.11393

Table 5-4 (continued) Interactive Transformer Design

11											12																																																																																										
<p>NEW FLUX DESIRED? = YES            NEW FLUX = 525            CONTROL V Dg. NO. = 1/2            ACTUAL FLUX DENSITY = 824. GAUSS      CORE LOSS = 0.1053 WATTS</p>											<p>PER SIDE DATA</p>																																																																																										
<p>VDG. NO. VOLTS SPEC'D VOLTS ACTUAL      ERROR NO. TURNS</p> <table border="1"> <tr> <td>1</td> <td>13.000000</td> <td>13.017466</td> <td>-0.134</td> <td>118</td> </tr> <tr> <td>2</td> <td>13.900000</td> <td>13.900000</td> <td>0.000</td> <td>126</td> </tr> </table> <p>VOLTS PER TURN = 0.11032            NEW FLUX DESIRED? = YES            NEW FLUX = 530            CONTROL V Dg. NO. = 2            ACTUAL FLUX DENSITY = 831. GAUSS      CORE LOSS = 0.1070 WATTS</p>											1	13.000000	13.017466	-0.134	118	2	13.900000	13.900000	0.000	126	<table border="1"> <tr> <th>VDG. NO.</th> <th>AMPS</th> <th>AMPS/50. IN.</th> <th>WLT (IN.)</th> <th>LENGTH (FT.)</th> <th>% OF FILL</th> </tr> <tr> <td>1</td> <td>0.0780000</td> <td>1254.</td> <td>1.074</td> <td>10.7195</td> <td>17.069</td> </tr> <tr> <td>2</td> <td>0.0570000</td> <td>801.</td> <td>1.518</td> <td>16.0616</td> <td>31.375</td> </tr> </table>											VDG. NO.	AMPS	AMPS/50. IN.	WLT (IN.)	LENGTH (FT.)	% OF FILL	1	0.0780000	1254.	1.074	10.7195	17.069	2	0.0570000	801.	1.518	16.0616	31.375																																																				
1	13.000000	13.017466	-0.134	118																																																																																																	
2	13.900000	13.900000	0.000	126																																																																																																	
VDG. NO.	AMPS	AMPS/50. IN.	WLT (IN.)	LENGTH (FT.)	% OF FILL																																																																																																
1	0.0780000	1254.	1.074	10.7195	17.069																																																																																																
2	0.0570000	801.	1.518	16.0616	31.375																																																																																																
<p>VDG. NO. VOLTS SPEC'D VOLTS ACTUAL      ERROR NO. TURNS</p> <table border="1"> <tr> <td>1</td> <td>13.000000</td> <td>13.010400</td> <td>-0.030</td> <td>117</td> </tr> <tr> <td>2</td> <td>13.900000</td> <td>13.900000</td> <td>0.000</td> <td>125</td> </tr> </table> <p>VOLTS PER TURN = 0.11120            NEW FLUX DESIRED? = NO            NEW CORE DESIRED? = NO            &gt;&gt;&gt;&gt; WINDING NUMBER = 1      WIRE SIZE (AWG) = 31            3.072 LAYERS FILLED. DO YOU WISH TO CHANGE WIRE SIZE? = NO            TURNS/LAYER = 39.0      WINDING WIDTH = 0.417"      WINDABLE WIDTH = 0.424"            DO YOU WISH TO CHANGE TURNS/LAYER? = YES            NEW TURNS/LAYER = 39            3.000 LAYERS FILLED. DO YOU WISH TO CHANGE WIRE SIZE? = NO            TURNS/LAYER = 39.0      WINDING WIDTH = 0.423"      WINDABLE WIDTH = 0.424"            DO YOU WISH TO CHANGE TURNS/LAYER? = NO            &gt;&gt;&gt;&gt; WINDING NUMBER = 2      WIRE SIZE (AWG) = 32            6.250 LAYERS FILLED. DO YOU WISH TO CHANGE WIRE SIZE? = NO            TURNS/LAYER = 20.0      WINDING WIDTH = 0.407"      WINDABLE WIDTH = 0.424"            DO YOU WISH TO CHANGE TURNS/LAYER? = YES            NEW TURNS/LAYER = 21            5.952 LAYERS FILLED. DO YOU WISH TO CHANGE WIRE SIZE? = NO            TURNS/LAYER = 21.0      WINDING WIDTH = 0.427"      WINDABLE WIDTH = 0.424"            DO YOU WISH TO CHANGE TURNS/LAYER? = NO</p>											1	13.000000	13.010400	-0.030	117	2	13.900000	13.900000	0.000	125	<p>VDG. WIRE NO. OF TURNS/ VDG. RESISTANCE</p> <table border="1"> <tr> <th>NO.</th> <th>GAUGE</th> <th>LAYERS</th> <th>LAYER WIDTH</th> <th>OHMS/LEG</th> <th>LEG WT.</th> <th>LEG I R</th> </tr> <tr> <td>1</td> <td>31</td> <td>3.00</td> <td>39.0</td> <td>0.428</td> <td>1.4364</td> <td>0.0026</td> </tr> <tr> <td>2</td> <td>32</td> <td>6.00</td> <td>21.0</td> <td>0.427</td> <td>2.6502</td> <td>0.0031</td> </tr> </table> <p>TRANSFORMER TOTALS</p> <table border="1"> <tr> <th>LOSSES</th> <th>COPPER</th> <th>CORE</th> <th>TOTAL</th> <th>WATTS</th> <th>PERCENT</th> </tr> <tr> <td>WEIGHT</td> <td>0.0347</td> <td>0.1070</td> <td>0.1417</td> <td>0.027</td> <td></td> </tr> <tr> <td></td> <td>0.0176</td> <td>0.0130</td> <td>0.0306</td> <td>POUNDS</td> <td></td> </tr> </table> <p>LENGTH (G) = 0.3169      HEIGHT (F) = 0.7889      WIDTH (D) = 0.5233</p> <p>SPECIFY PRIMARY WINDING NO. = 2</p> <p>PER SIDE DATA</p> <table border="1"> <tr> <th>VDG.</th> <th>INDUCT</th> <th>REACT</th> <th>ECN</th> <th>ECORP</th> <th>ECTS</th> <th>ECTOT</th> </tr> <tr> <th>NO.</th> <th>MICRO H</th> <th>OHMS</th> <th>VOLTS</th> <th>VOLTS</th> <th>VOLTS</th> <th>VOLTS</th> </tr> <tr> <td>1</td> <td>47.07</td> <td>5.9148</td> <td>0.2937</td> <td>0.6707</td> <td>0.1120</td> <td>0.4764</td> </tr> </table> <p>VDG. NO. TURNS VOLTS SPEC'D VOLTS ACTUAL      VOLTS OUTPUT</p> <table border="1"> <tr> <td>1</td> <td>117</td> <td>13.0000000</td> <td>13.0103797</td> <td>12.5339565</td> </tr> <tr> <td>2</td> <td>125</td> <td>13.9000000</td> <td>13.8999997</td> <td>13.8999997</td> </tr> </table> <p>REPEATS - 'NO', 'ALL', 'CORE', OR 'FLUX' = NO</p>											NO.	GAUGE	LAYERS	LAYER WIDTH	OHMS/LEG	LEG WT.	LEG I R	1	31	3.00	39.0	0.428	1.4364	0.0026	2	32	6.00	21.0	0.427	2.6502	0.0031	LOSSES	COPPER	CORE	TOTAL	WATTS	PERCENT	WEIGHT	0.0347	0.1070	0.1417	0.027			0.0176	0.0130	0.0306	POUNDS		VDG.	INDUCT	REACT	ECN	ECORP	ECTS	ECTOT	NO.	MICRO H	OHMS	VOLTS	VOLTS	VOLTS	VOLTS	1	47.07	5.9148	0.2937	0.6707	0.1120	0.4764	1	117	13.0000000	13.0103797	12.5339565	2	125	13.9000000	13.8999997	13.8999997
1	13.000000	13.010400	-0.030	117																																																																																																	
2	13.900000	13.900000	0.000	125																																																																																																	
NO.	GAUGE	LAYERS	LAYER WIDTH	OHMS/LEG	LEG WT.	LEG I R																																																																																															
1	31	3.00	39.0	0.428	1.4364	0.0026																																																																																															
2	32	6.00	21.0	0.427	2.6502	0.0031																																																																																															
LOSSES	COPPER	CORE	TOTAL	WATTS	PERCENT																																																																																																
WEIGHT	0.0347	0.1070	0.1417	0.027																																																																																																	
	0.0176	0.0130	0.0306	POUNDS																																																																																																	
VDG.	INDUCT	REACT	ECN	ECORP	ECTS	ECTOT																																																																																															
NO.	MICRO H	OHMS	VOLTS	VOLTS	VOLTS	VOLTS																																																																																															
1	47.07	5.9148	0.2937	0.6707	0.1120	0.4764																																																																																															
1	117	13.0000000	13.0103797	12.5339565																																																																																																	
2	125	13.9000000	13.8999997	13.8999997																																																																																																	
<p>CHECK FIT: 98.97 % FULL      BUILD = 0.11 IN. PER SIDE            NEW FLUX? = NO            NEW CORE? = NO</p>																																																																																																					

The details of transformer design are now established between the operator and the computer. The operator selects AWG 25 for the primary. The computer says this fills 3.421 layers. This is not a desirable form, since all layers should be filled. The operator says, try AWG 27. The computer says 2.708 layers filled. The operator says, try AWG 26. The computer says 3.095 layers filled. This appears to be achievable in the judgment of the operator, and he proceeds to tell the computer to place an additional turn on each layer, exceeding the minimum windable width by 0.001 inches. This process is repeated for the secondary.

In column 2, it is determined that the core window is 192.8% full, indicating an impossible design. However, the operator wants to know all the particulars before he proceeds. The computer prints out current, current density, mean length of turn, total length, number of layers, turns per layer, resistance, winding weight, copper loss, copper weight, core loss, core weight, and over all dimensions. The program also calculates the winding inductance, reactance, and actual winding voltage on each winding.

At this point the operator inserts his judgment on what to try next, and chooses a higher operating flux density, 1600 gauss, and this drops the primary to 61 turns (from 65), and the secondary to 65 turns (from 70), with a +0.342% error on the actual secondary voltage.

At the top of column 3, the wire fit is checked, and much smaller wire sizes are selected, this time utilizing only 64.55% of the core window. The operator now selects a flux of 1400 gauss, and determines wire fit. The nearest full layer wire size again exceeds the core window, and the flux is changed



back to the initial 1500 gauss, but this time the voltage error is put with the primary.

This iterative process is repeated for a total of fifteen different flux densities, until a winding fit is established which fills each layer, fills the core window, and achieves an acceptable design in terms of weight and losses.

#### 5.4 Phase II Implementation Plan

All aspects of power processing methodology are to be brought together under the management computer program described in detail in Section 4 of this report. This activity will serve as the common structure on which to develop design, modeling, analysis, optimization, and simulation techniques; and the language, format, and consistent nomenclature to permit a variety of power processing design routines to be operated in sequence.

Three types of information can be developed to add to the total management program. The first of these is the physical characteristics and details on existing equipment described under Task 2 of this section. This data will also serve as the baseline against which simulated systems are measured and against which analyzed systems can be compared. The second type of data to be utilized is electrical performance characteristics determined from phase-gain measurements on circuits that cannot be modeled or analyzed by other means. The mathematical transform of the Bode Diagram resulting from the phase-gain measurement will permit detailed analysis within the content of the management computer program, and the effects of interaction with other circuit elements whose characteristics are already available. The third source of information is computer routines for tedious and iterative design procedures

that can be handled directly and adequately by a computer. The transformer design procedure is the best example of this type. Three different routines have been detailed in this report, two additional programs at NASA Lewis have been referenced, and other computer techniques were listed in the Task 3 Report.

#### 5.5 Milestone Schedule

The Phase II task schedule and program milestones are shown in Figure 5-1.

#### 5.6 Required Resources

The allocation of manpower resources is shown on Table 5-5. This includes the number of hours and type of personnel by labor category to be assigned to each task of work. Estimated computer costs in dollars by task are also shown on Table 5-5, based on a composite billing rate for a variety of data processing services. Average computer charges for the power processing design group at Valley Forge have been \$300 per month over the past several years. The interactive routines envisioned do not result in open loop computer processing, and consequently do not result in high computer expense.

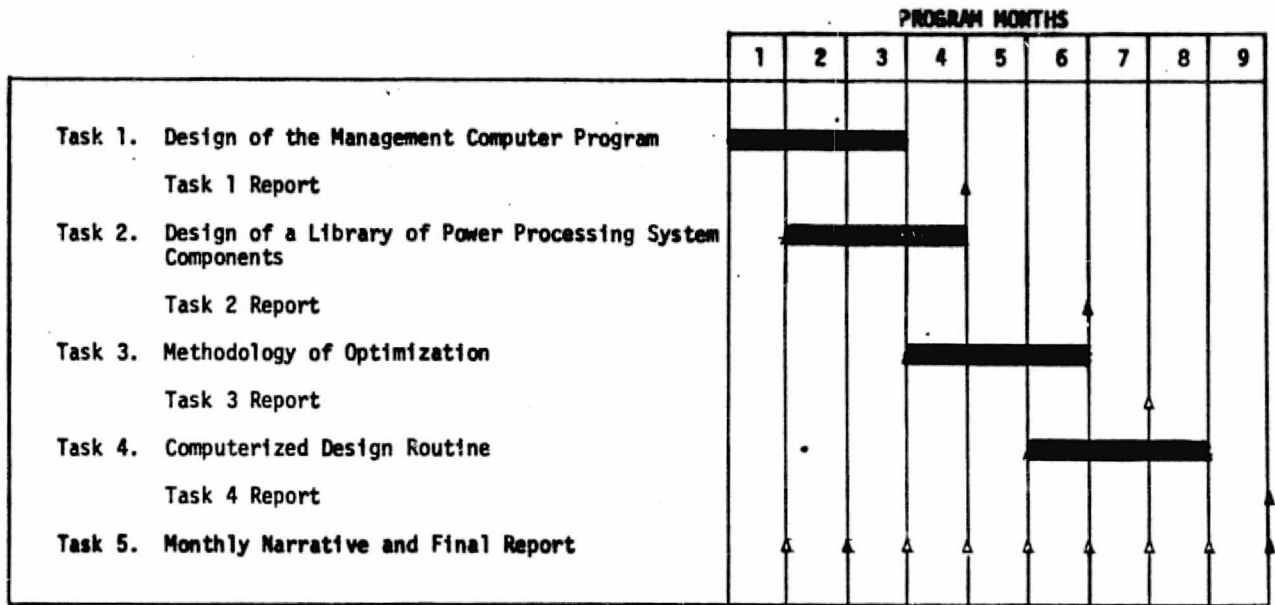


Figure 5-1. Program Milestone Schedule

Table 5-5. Technical Work Allocation

	Task 1	Task 2	Task 3	Task 4	Task 5	Total
<u>Man Hours</u>						
Engineers	400	130	200	200	100	1030
Technicians	120	180	20	0	50	370
Total Program	520	310	220	200	150	1400
Computer Dollars	\$1500	\$600	\$1200	\$800	---	\$4100

SECTION 6  
CONCLUSIONS

## CONCLUSIONS

This report has presented a computer management program that can, with suitable available catalog data on existing power processing subsystems, and with defined mission objectives, constraints and data, select suitable candidate designs to assemble a complete system.

The program can be expanded by additional analysis and synthesis routines as they become available to permit the operator to create the optimum design by an interactive procedure which compares the results of modeling, analysis and synthesis with the data base of existing designs.

APPENDIX A

MARINER JUPITER/SATURN 1977

Appendix A  
Mariner Jupiter/Saturn 1977

TABLE OF CONTENTS

<u>SECTION</u>		<u>PAGE</u>
1.0	INTRODUCTION	A-1
2.0	SYSTEM OVERVIEW	A-2
3.0	VEHICLE CONFIGURATION	A-4
4.0	POWER SYSTEM FUNCTIONAL DESCRIPTION	A-8
5.0	POWER SOURCE EQUIPMENT DESCRIPTION	A-11
5.1	Multi-Hundred Watt Radioisotope Thermoelectric Generator	A-11
5.1.1	RTG Internal Impedance	A-13
5.1.2	RTG Radiation	A-15
5.1.3	RTG Life Characteristics	A-15
5.2	Battery	A-15
6.0	POWER PROCESSING EQUIPMENT	A-18
6.1	Main Inverter	A-18
6.2	Sequenced Shunt Regulator	A-20
6.3	Three-Phase, 400 Hertz Inverter	A-25
6.4	Battery Charge/Discharge Electronics	A-27
6.5	Power Control	A-29
6.6	Power Distribution	A-29
7.0	POWER SYSTEM PERFORMANCE CHARACTERISTICS	A-30
7.1	Power Profile	A-30
7.2	Electromagnetic Compatibility	A-30
7.3	Radiation Effects	A-32

LIST OF TABLES

TABLE

PAGE

A-1      Design Requirements

A-24



## LIST OF ILLUSTRATIONS

<u>FIGURE</u>		<u>PAGE</u>
A-1	Mariner Jupiter/Saturn Vehicle Configuration	A-5
A-2	Electronic Packaging Arrangement	A-6
A-3	Electronic Assembly Number 2	A-7
A-4	Electronic Assembly Number 9	A-7
A-5	Power Subsystem Block Diagram	A-9
A-6	RTG Cutaway View	A-12
A-7	RTG Heat Source Cutaway View	A-14
A-8	Equivalent Circuit-RTG Internal Impedance	A-13
A-9	Gamma Radiation Flux Map	A-16
A-10	Neutron Radiation Flux Map	A-16
A-11	RTG Performance in Vacuum	A-17
A-12	Main Inverter Schematic	A-19
A-13	Efficiency and Voltage Regulation	A-21
A-14	Sequenced Shunt Regulator Block Diagram	A-22
A-15	Three-Phase, 400 Hertz Inverter Block Diagram	A-26
A-16	Boost Regulator Block Diagram	A-28
A-17	Power Profile by Mission Mode	A-31

## 1.0 INTRODUCTION

The Mariner Jupiter/Saturn vehicle (MJS77) is an outgrowth of the previously flown Mariner-class spacecraft for outer planet missions.

Previous Mariners used a solar cell power source for missions out to one and one-half years. The Jupiter/Saturn mission is nearly three times as long, and involves interplanetary distances to 9.5 astronomical units, and thus requires a solar independent power source.

Two identical vehicles will be launched during the 1977 Jupiter/Saturn launch opportunity. Their mission is to conduct exploratory investigations of the planetary systems of Jupiter and Saturn and of the interplanetary medium out to Saturn. Primary emphasis will be placed on comparative studies of Jupiter and Saturn by obtaining measurements of the environment, atmosphere and physical characteristics of the planets, and one or more satellites of each planet; studies of the nature of the rings of Saturn; and exploration of the interplanetary medium of increasing distance from the sun.

Engineering objectives of this mission are to demonstrate the use of Mariner class spacecraft for operational periods of four years. The second objective is to demonstrate the use of radioisotope thermoelectric generators (RTG's) as a primary spacecraft power source for long duration interplanetary missions. A third objective is to demonstrate interplanetary communication and navigation accuracy for distances in the order of one million miles.

## 2.0 SYSTEM OVERVIEW

The Mariner Jupiter/Saturn spacecraft system has the basic mission of supporting scientific experiments for at least four years and of collecting outer planetary data and transmitting it back to earth.

Representative instruments and experiments are of the following types: energetic particles, imaging, infrared, Lyman alpha, magnetic field, meteoroid science, photometry polarimetry, plasma, plasma wave, radio astronomy, radio science, ultraviolet spectroscopy and X-ray.

These experiments place various demands on the spacecraft and supporting subsystems, such as pointing accuracy for imaging and scanning devices, and control of radiation and thermal levels for the nuclear power sources to prevent interference with energy measuring and infrared experiments. Still other experiments are electro-mechanical and optical in nature and as such will demand short duration, high current, fast rise time pulses with the resulting EMI effects, all of which must be considered in the electrical and power subsystem design.

Spacecraft power management, fault detection, and fault removal are of significance since ground communications to the spacecraft in deep space can require considerable time. Reaction time is of critical importance near mission end, where system power has decayed and there is a high power demand to support collection and transmission. Autonomous power management was considered for system implementation under these operational conditions.

Three radioisotope thermoelectric generators are installed on the vehicle during the typical pre-launch phase sequence of events. The next phase is ascent with

its many events of boost and spacecraft separation, but of significance to the power system is the firing of pyrotechnics for venting and deploying the power sources. At this time the science scan platform is unlatching and science booms are deployed. Within two hours of launch, the sun and Canopus are acquired for guidance. Science instruments are sequentially turned on to gather data from the earth's magnetic field and trapped radiation belts. The subsequent cruise phase encompasses all the mission time that is not included in the ascent, trajectory correction maneuver, or the Jupiter/Saturn encounter phases which are not detailed here.

The power subsystem must be capable of enduring the hazardous environments of the near-earth and solar magnetic and electro-magnetic radiation, Van Allen Belt protons and electrons, solar wind protons, and galactic cosmic rays. The environments peculiar to Jupiter and Saturn include planetary radiation belts, the interplanetary meteoroid and asteroid belts beyond the Earth-Mars region, and the rings of Saturn. Information on these environments is presented in the Outer Planets Natural Space Environmental Estimates Document. An assessment and description of these environments is available in the Mariner Jupiter/Saturn 1977 Mission Requirements Document, JPL Project Document No. 618-4, and was modified based on interpretation of data accumulated from the Pioneer 10 mission.

### 3.0 VEHICLE CONFIGURATION

The spacecraft has a design mass of approximately 737.5 kilograms or 1625.8 pounds, including the adapter and a 4 percent contingency. Figure A-1 is an assembly drawing of the vehicle.

The power system is expected to weigh 516 pounds or 31.7 percent of the spacecraft weight. This power system weight includes both electrical and mechanical support items such as the three radioisotope thermoelectric generators; their deployment boom, mechanisms, squibs, latches, thermal heaters, and radiation shielding; and all regulators and converters used in the power processing. Also included are 113 pounds of vehicle harnessing and an estimated weight of 40 pounds for the spacecraft loads which must provide their own 2.4 KHz converters.

The four major structural elements of the spacecraft are the radioisotope thermoelectric generator boom, the high gain dish antenna, the science boom, and the bus structure with nine bays of electronics. Bays 2 and 9 are dedicated to the power subsystem as shown in Figures A-2, A-3 and A-4.

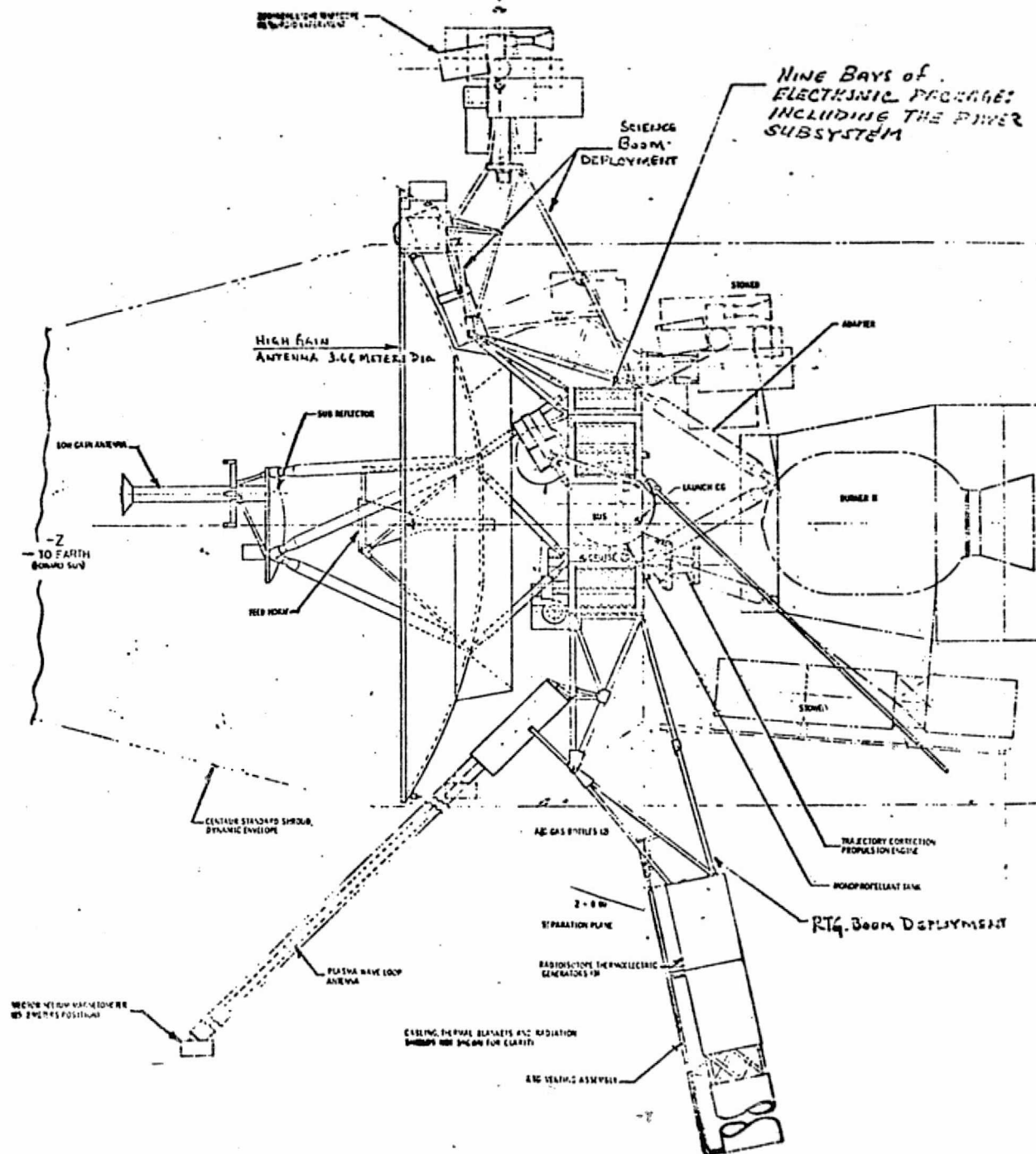


Figure A-1. Mariner Jupiter/Saturn Vehicle Configuration

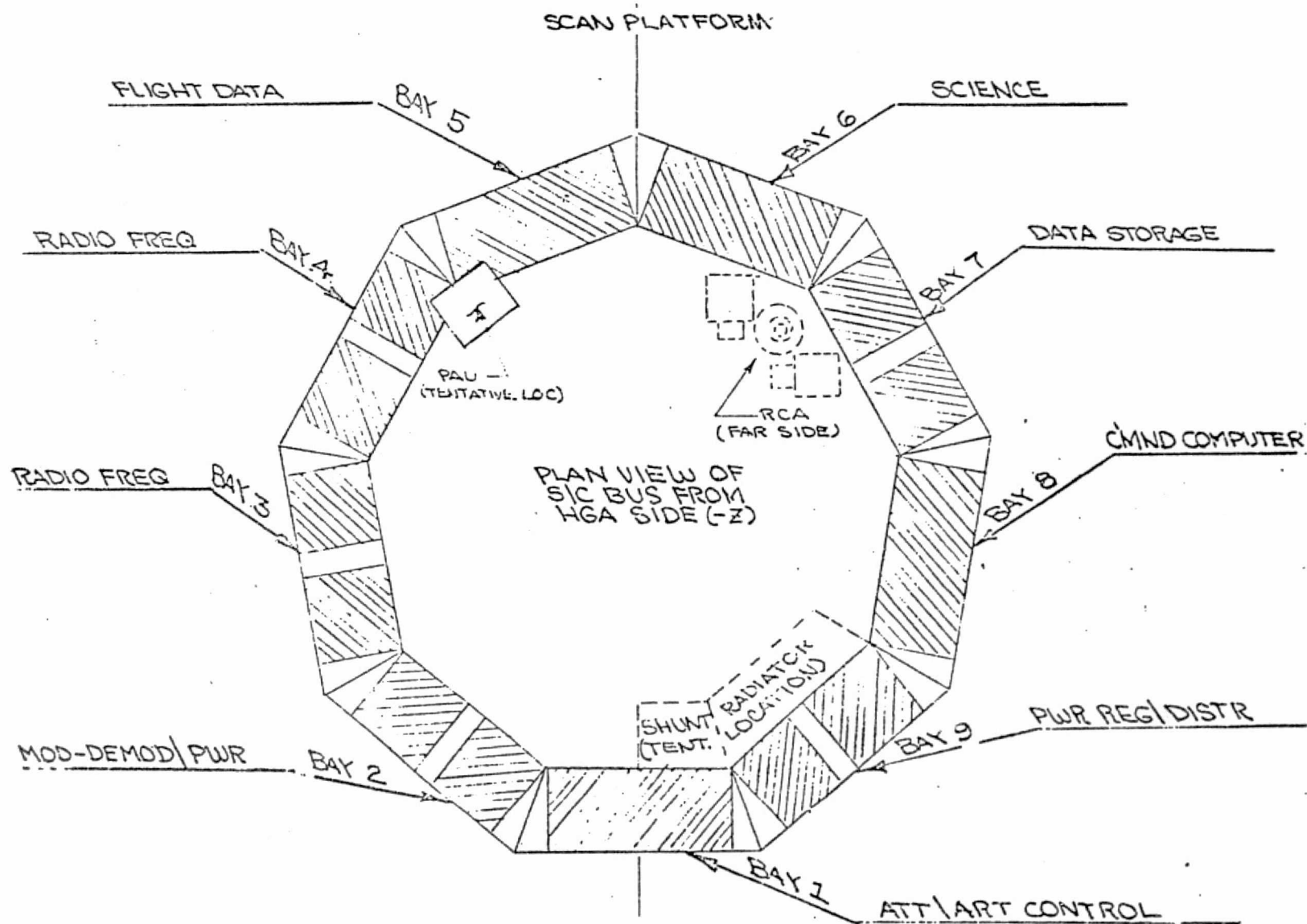


Figure A-2. Electronic Packaging Arrangement

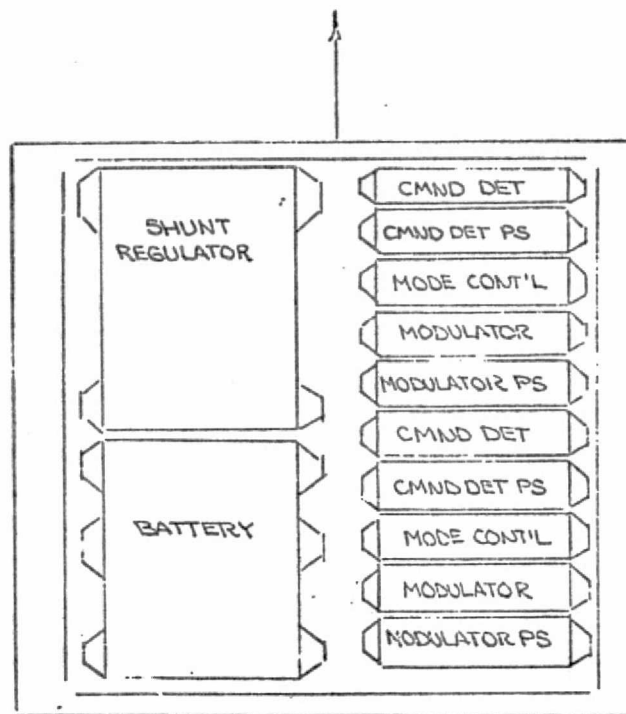


Figure A-3. Electronic Assembly Number 2

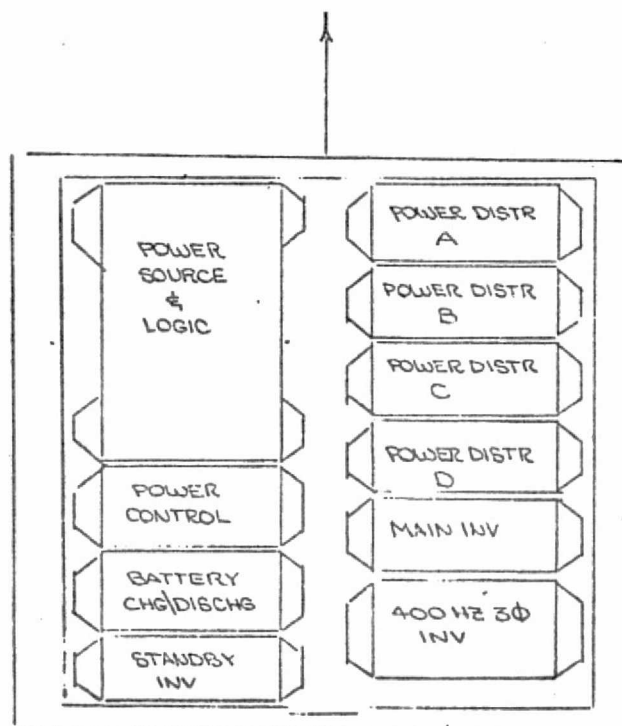


Figure A-4. Electronic Assembly Number 9



#### 4.0 POWER SYSTEM FUNCTIONAL DESCRIPTION

The power system has two primary functions. First, it must provide a central supply of electrical power to operate the spacecraft electrical equipment. Second, it must provide the required sensing, switching and control functions for the effective management and distribution of electrical power.

Three Multi-Hundred Watt Radioisotope Thermoelectric Generators provide the primary power source as shown in the functional block diagram of Figure A-5.

The power source logic unit contains the circuitry necessary to interconnect the RTG's to the power conditioning equipment. This includes isolation diodes and shorting switches.

The dc power bus is regulated to 29 vdc  $\pm 1\%$  by a shunt regulator. The shunt regulator senses the common RTG voltage and maintains it by dissipating the difference between RTG power available at 29 vdc and the spacecraft load demand. Voltage regulation of the RTG's provides relatively constant loading and serves to maintain the RTG internal temperature near the design point.

Power from the dc bus is transformed to 50 volts rms, 2.4 KHz, single-phase, square-wave power by the main inverter for most spacecraft ac loads. An identical inverter in standby serves as a backup to the main inverter.

Switchover is controlled by inverter failure detection circuitry located within the power control unit.

The power distribution assembly is designed to provide the required switching and control functions for the effective management and distribution of power to user loads. Power switching circuitry is designed to operate in response

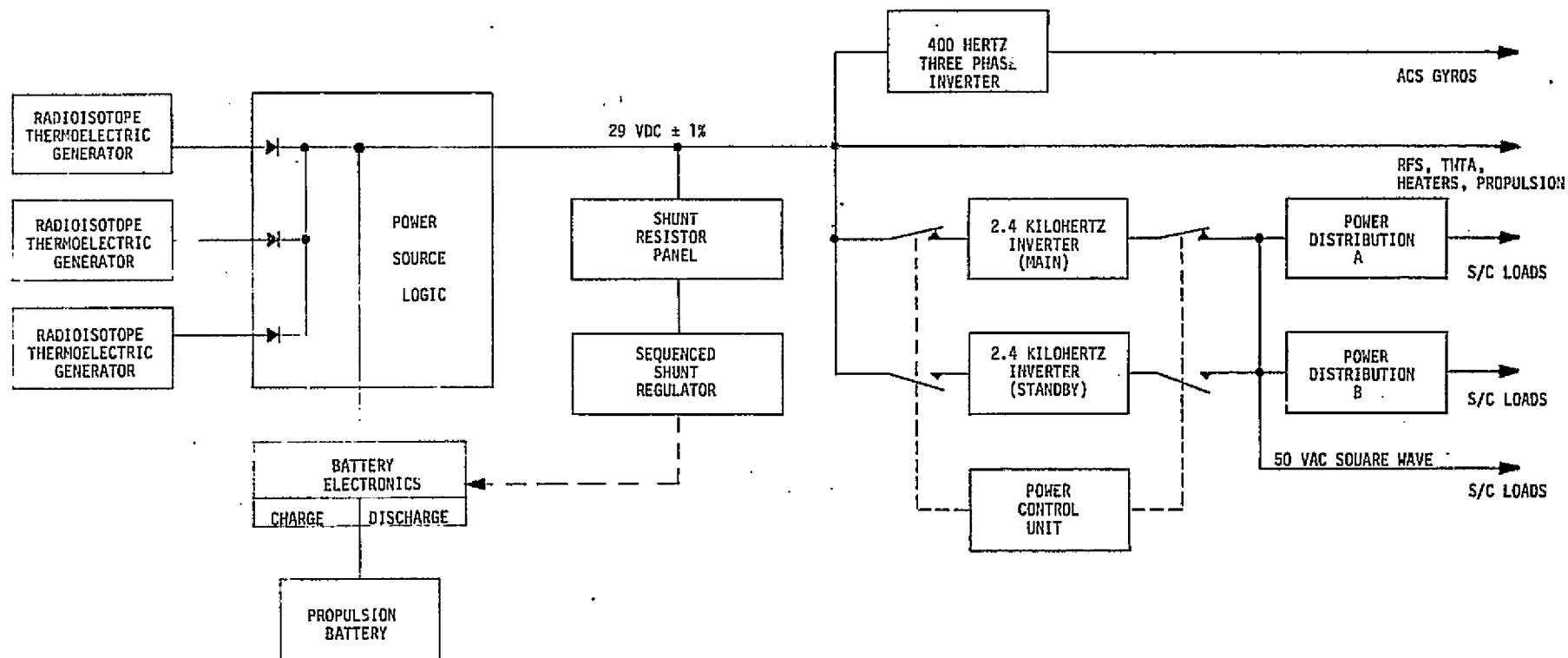


Figure A-5 Power Subsystem Block Diagram

to stored or real time commands from the computer command subsystem.

A 400 Hz, three phase inverter provides conditioned power to the attitude control subsystem gyros.

A battery, with its associated charge and discharge electronics, will provide the large magnitude, short duration power required by a propulsion module during the ascent phase. During planet encounter, the power margin between spacecraft load demands and RTG capability is minimal. It is intended that the battery be used to supply load turn-on transient power at this time. The battery energy that is removed during discharge is replaced when there is excess RTG power being dissipated in the shunt regulator. A control signal from the shunt limits the charge rate so that some power remains in the shunt to keep it active and able to maintain dc power bus voltage regulation. When spacecraft load demands deplete the power in the shunt, the shunt signals the battery discharge electronics to supply battery power to maintain dc bus voltage regulation.

Some components of the power system such as the power distribution units, the power control unit, the battery, and the charge/discharge electronics are presently in the design phase. Therefore, breadboard data, analysis, and researched estimates will be used in their descriptions.

## 5.0 POWER SOURCE EQUIPMENT DESCRIPTION

### 5.1 Multi-Hundred Watt Radioisotope Thermoelectric Generator (MHW-RTG)

The Multi-Hundred Watt Radioisotope Thermoelectric Generator (MHW-RTG) has been designed and developed by the General Electric Company for the Atomic Energy Commission to be used on NASA's Mariner Jupiter/Saturn vehicles. The generator shown in Figure A-6 uses a 2400 watt plutonium 238 heat source and has been designed to produce 125 watts of electrical power at 30 volts at the end of five years of operation. Initially, it will produce 150 watts at 30 volts. The power output drops about 17 percent over five years. The converter consists of 312 silicon-germanium (SiGe) thermoelectric elements and a multi-layer molybdenum foil astroquartz insulation system housed within a sealed beryllium outer shell which serves as the RTG primary structure and external waste heat radiator. The SiGe thermoelectric material was selected because of its high conversion efficiency and for its ability to operate in air or vacuum at high temperatures---a prime consideration for long duration missions. During normal operation, the nominal hot and cold junction temperatures are 1000° and 300°C, respectively. An inert cover gas is provided for ground operations to prevent exposure of the oxidizable foil insulation to air. This gas is vented to space after launch.

To contain the cover gas, the outer shell of the RTG is pneumatically sealed at the end pressure domes and all shell penetrations, including the 312 thermocouple attachments. A gas management system, consisting of an externally mounted valve connected to the case, releases the cover gas after launch. Overall external dimensions of a single RTG are 15.7 inches in diameter by 22.9 inches in length, a volume of 359.5 cubic inches, and a total weight of 84 pounds.

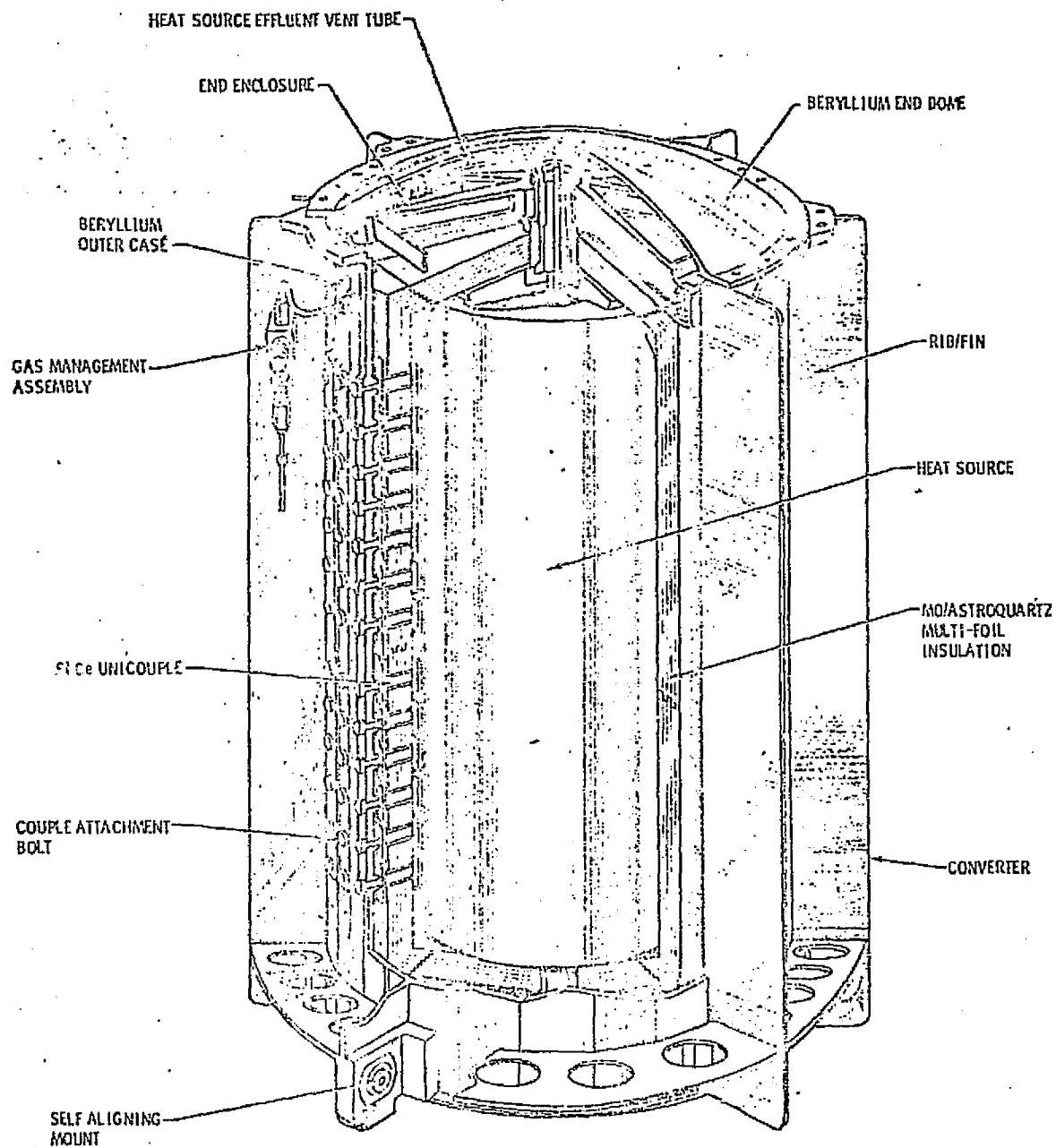


Figure A-6. RTG Cutaway View

The MHW heat source contains twenty-four spheres of plutonium dioxide to make up the 2400 watt (thermal) inventory (Figure A-7). Each sphere is encapsulated in an iridium post-impact containment shell and is provided with its own impact protection. This assembly is referred to as a fuel sphere assembly (FSA). The FSA's are arrayed in six planes along the length of the heat source, four FSA's to a plane, with each plane rotated 45 degrees with respect to the planes adjacent to it. For reentry protection, the FSA array is contained within a graphite aeroshell which is also the basic structure of the heat source. The aeroshell is enclosed by an iridium outer clad which provides the mechanical and thermal interface with the heat source, pneumatic isolation of the heat source from its environment, protection during the multiple skip class of reentries, and gas management for the helium generated by the fuel.

5.1.1 RTG Internal Impedance - Some effort has been expended to determine the internal impedance of a loaded RTG. Figure A-8 indicates the internal impedance with an inductance of a few microhenrys at a frequency of 1 Mega Hertz. Test data and analysis has indicated virtually no shunt capacitance. No specific effort has been made to map the RTG dynamic impedance over a range of frequencies.

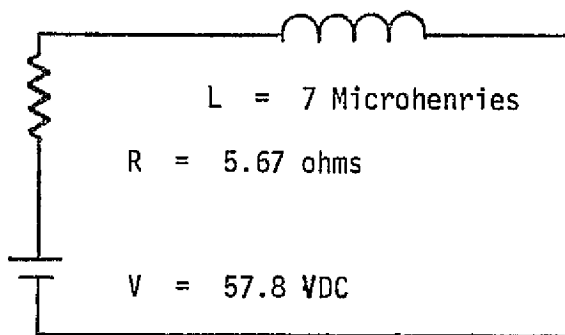
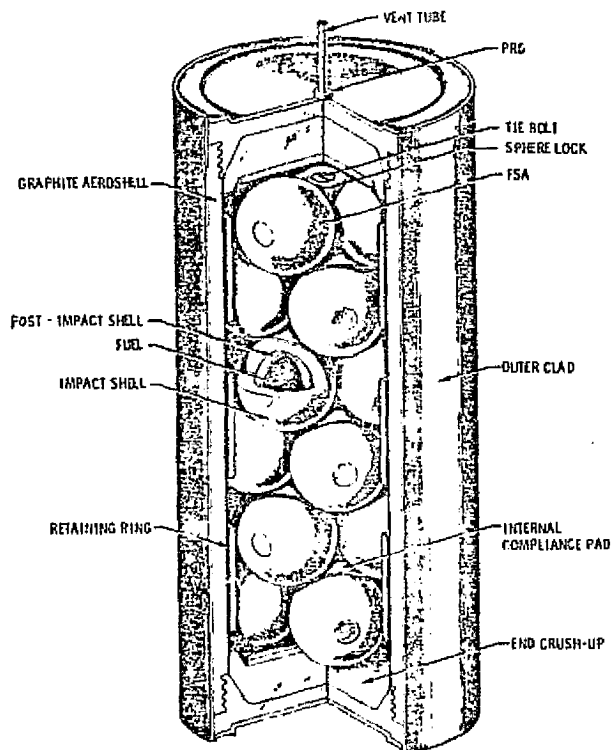


Figure A-8. Equivalent Circuit - RTG Internal Impedance



#### HEAT SOURCE (HS)

- THERMAL POWER  $2400 \pm 30$  WATTS
- LIFE
  - 1 YEAR STORAGE
  - 5 YEAR ORBIT OPERATION
- WEIGHT -20.3 KG (44.68 LB)
- DIAMETER 18.26 GAS (7.19 IN.)
- LENGTH -43.10 CM (16.97 IN.)
- VENTED TO SPACE

#### FUEL SPHERE ASSEMBLIES (FSA)

- $^{238}\text{PuO}_2$  CERAMIC COMPACT FUEL
- 24 FUEL SPHERES
- 100 WATTS, PER SPHERE
- 0.05 CM (0.02 IN) IR SHELL (PICS)
- 1.17 CM (0.46 IN) T-50 GRAPHITE

#### AEROSHELL

- POCO GRAPHITE
- THICKNESS -0.975 CM (0.384 IN)

#### IRIDIUM CLAD

- THICKNESS -0.025 CM (0.010 IN)
- GRAPHITE OXIDATION BARRIER
- MULTIPLE SKIP RE-ENTRY CAPABILITY

#### EMISSIVITY SLEEVE

- T-50 GRAPHITE
- THICKNESS -0.127 CM (0.05 IN)
- PROVIDES GOOD EMISSIVITY FOR NORMAL OPERATION

Figure A-7 RTG Heat Source Cutaway View

5.1.2 RTG Radiation - RTG radiation maps are presented in Figures A-9 and A-10 for the spacecraft configuration based on current design data for the MHW-RTG. The maps include gamma and neutron radiation flux based on calculations for three RTG units mounted in a single axis. The fuel age (10 years) is assumed to be a maximum expected for the mission including RTG fuel assembly and testing activities. Additional information is available in the Mariner Jupiter/Saturn 1977 Spacecraft Description, Jet Propulsion Laboratory, dated July 12, 1972.

5.1.3 RTG Life Characteristics - Available power as a function of fuel life is shown in Figure A-11.

## 5.2 Battery

Transient spacecraft power requirements which exceed the capability of the RTG power source will be met by the use of a rechargeable, hermetically sealed, nickel-cadmium battery. It has a capacity of approximately 3 ampere-hours, a weight of 5.0 pounds, and a volume of 178 cubic inches. It is capable of operating throughout the entire mission in a temperature range of zero to 25 degrees centigrade.



A-16

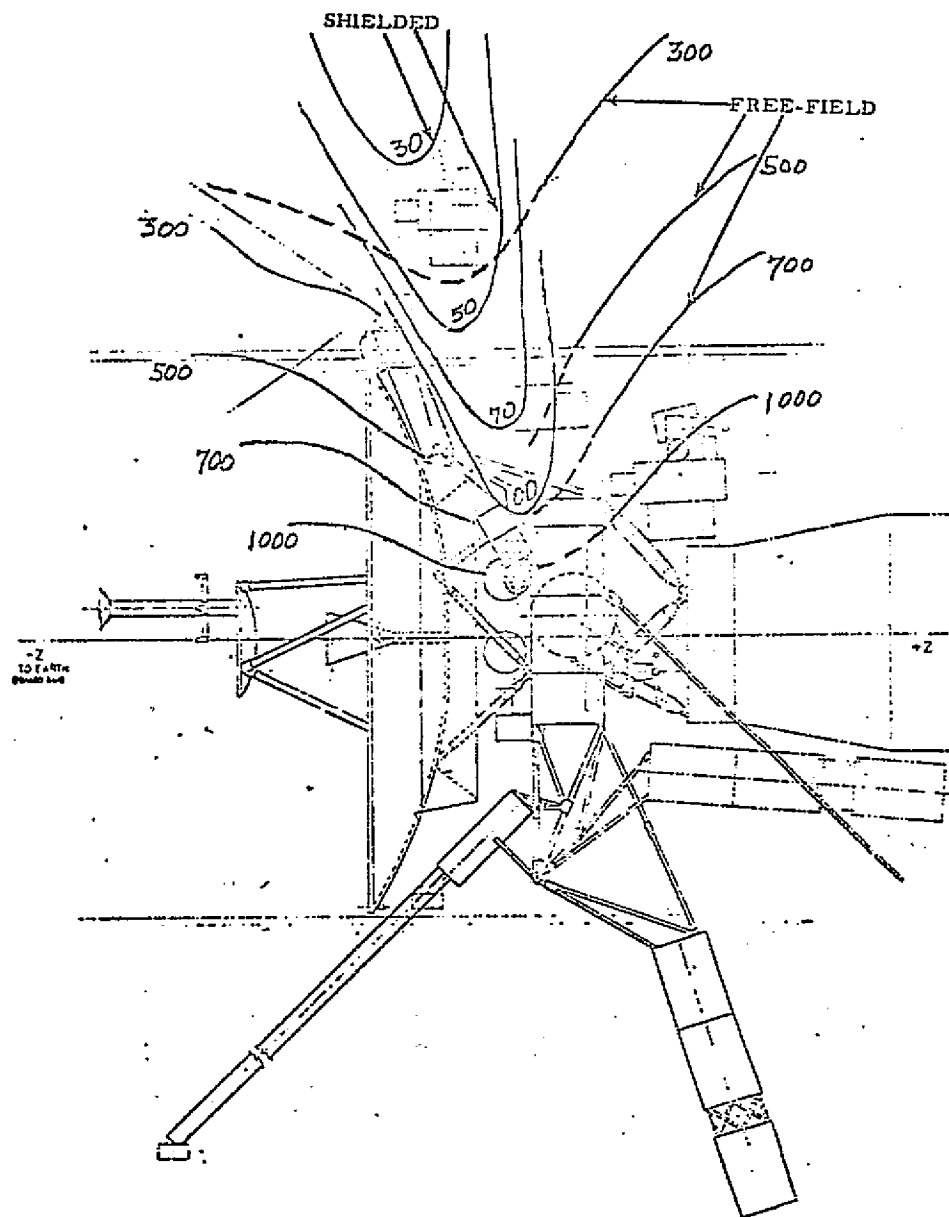


Figure A-9 Gamma Radiation Flux Map  
Units: Gammas per Square Centimeter-Second

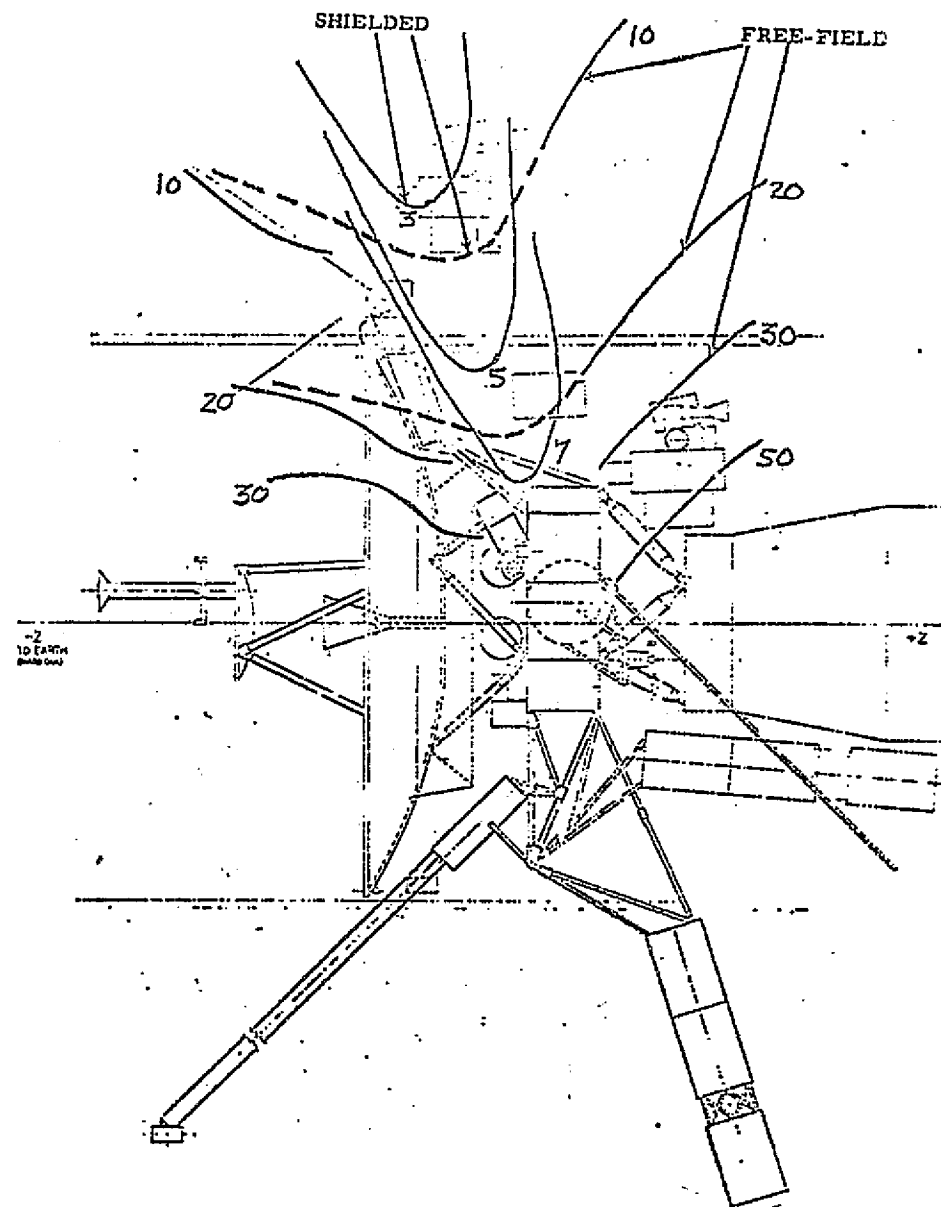


Figure A-10 Neutron Radiation Flux Map  
Units: Neutrons per Square Centimeter-Second

A-17

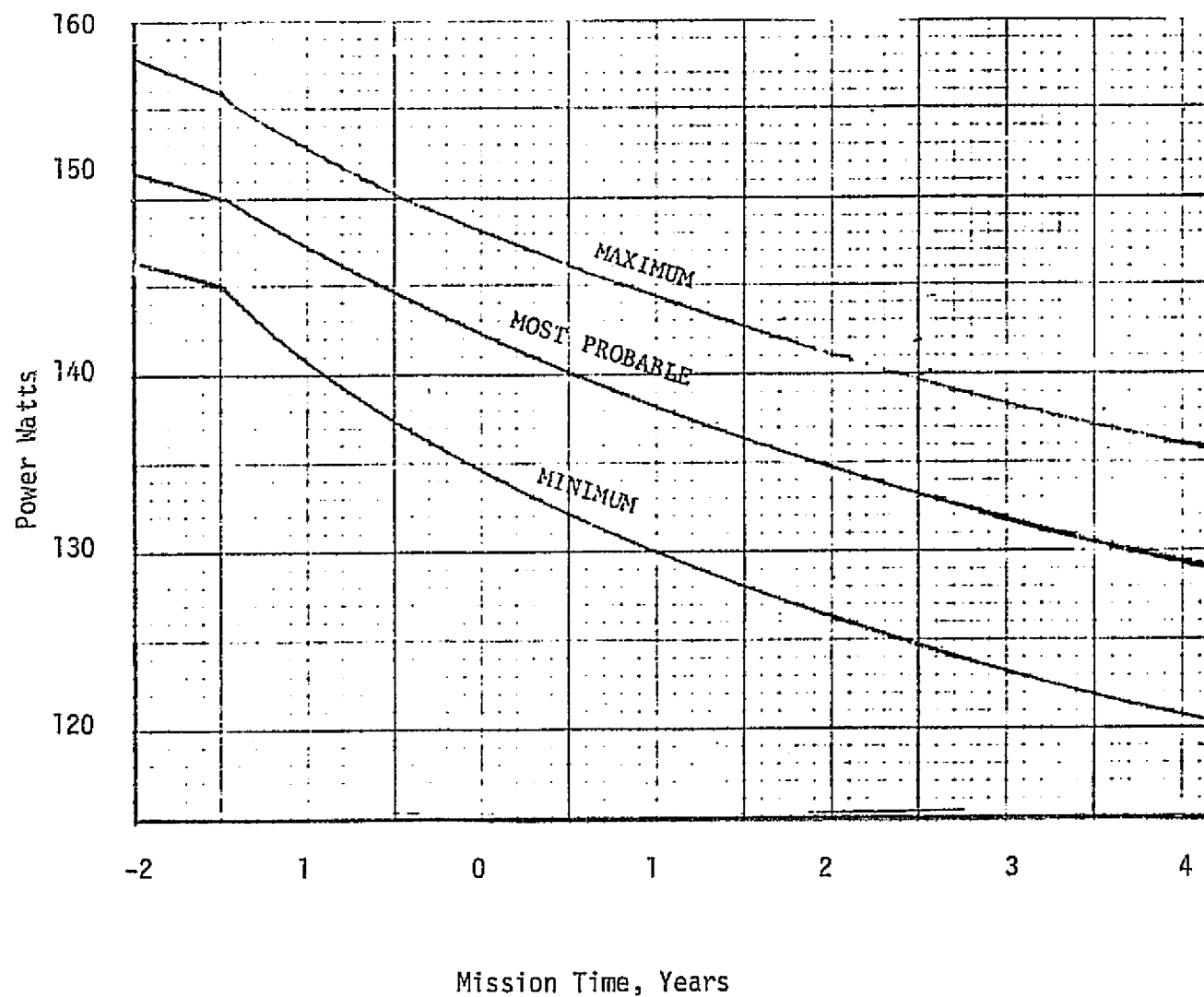


Figure A-11 RTG Performance in Vacuum

## 6.0 POWER PROCESSING EQUIPMENT

### 6.1 Main Inverter

The main inverter transforms the input voltage of 29 volts dc  $\pm 1$  percent, from the main bus to 50 volts rms, +3 percent and -4 percent, square-wave. The output power ranges from 145 watts minimum to 315 watts maximum. The rise and fall time of the output waveform is  $2 \pm 1$  microseconds. The inverter is designed either to run from a clock synchronized at 4800 Hz or to free run at 4750 Hz + 0 percent and -5 percent. The efficiency is to be at least 92 percent at full load. The output is short circuit protected for a period of 0.5 second with a source capability of 35 amperes. The inverter is to operate over a temperature range of  $-20^{\circ}\text{C}$  to  $+75^{\circ}\text{C}$ .

The inverter free run frequency is generated by an operational amplifier oscillator. The basic frequency of operation is determined by a resistor-capacitor time constant, R7 and C3 of Figure A-12. The actual frequency of operation, however, will be determined by the spacecraft central clock. Transistor Q1 synchronizes the oscillator to the clock frequency.

A buffer amplifier, Q2, amplifies and squares the oscillator output to drive the bistable multivibrator, Q3 and Q4. The state of the multivibrator is changed by the negative going edge of the square wave from the buffer amplifier. Therefore, the output of the multivibrator is a square wave whose frequency is one half the oscillator frequency.

The drive transformer, T1, converts the high voltage, low current square wave from the multivibrator to a low voltage, high current square wave to drive the power transistors, Q5 and Q6. Transformers T4 and T5 are volt-second devices which delay the turn on of the OFF transistor. This notch in the drive

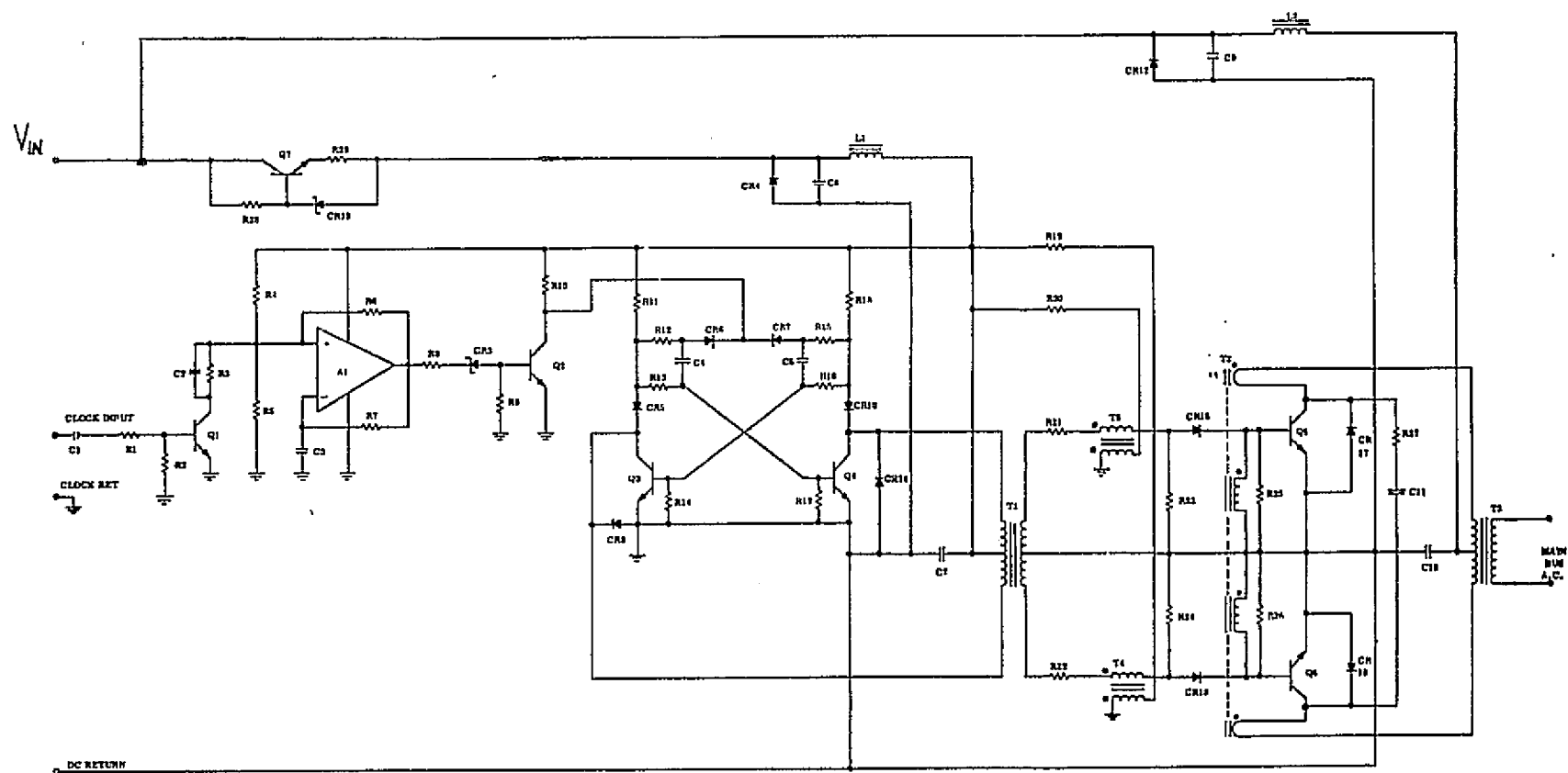


Figure A-12. Main Inverter Schematic

waveform allows the ON transistor to turn off before the OFF transistor turns on; preventing both Q5 and Q6 from being on at the same time. Resistors R23 and R24 are used to prevent the magnetizing current of the volt-second devices from turning on the output power transistors.

Transformer T2 is a current feedback transformer which increases the base drive as the collector current increases. This allows efficient inverter operation over a wide variation of the load. Resistors R25 and R26 assist in turning off the power transistors.

A short circuit on the inverter output will draw a maximum of 35 amperes, at zero volts, from the power source. With drive circuitry capable of deriving power from the dc bus and current feedback in the output power stage, the inverter can operate into an overload or short circuit.

Since a failure in the oscillator or multivibrator sections could pull the bus out of regulation, a current limiter was placed in series with the dc bus line. On the schematic of Figure A-12, the limiter is composed of circuit elements CR19, R28, and Q7. Two input filters (L1, L2, C7, and C10) reduce the amount of ac ripple current that will appear on the dc buses.

The main inverter weight is 5.0 pounds and occupies approximately 120 cubic inches. Measured efficiency as a function of output power is shown in Figure A-13.

## 6.2 Sequenced Shunt Regulator

The shunt regulator operates on a fail-safe philosophy which protects against faults that produce a continuous power drain and other faults that could reduce the required shunting capability of the regulator on the RTG's.

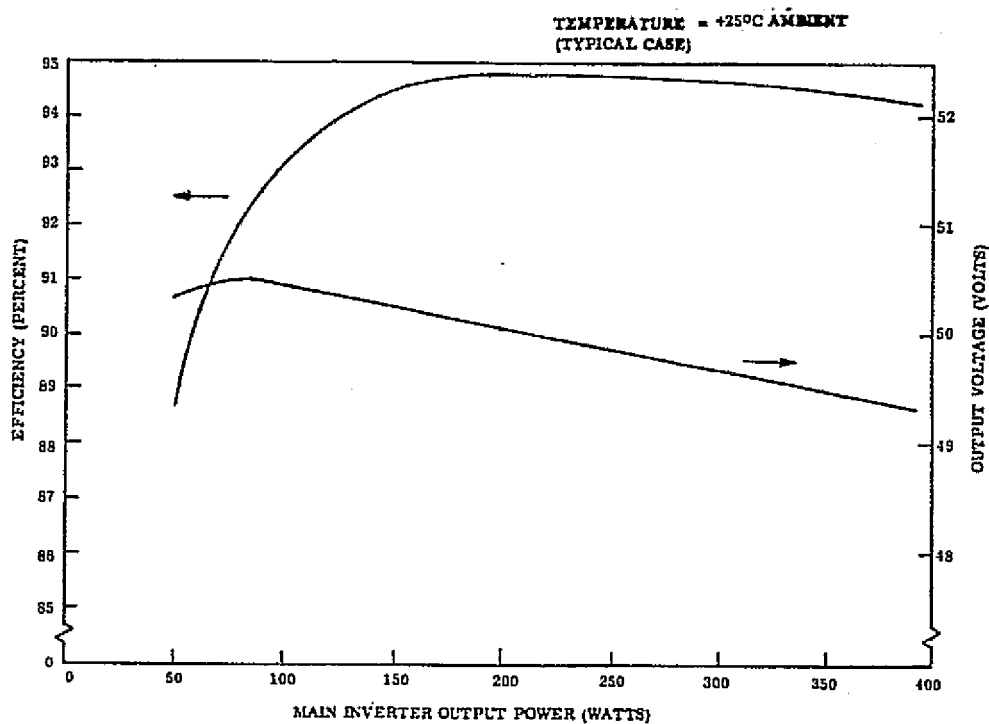


Figure A-13. Efficiency and Voltage Regulation

A block diagram of the sequencing shunt regulator is shown in Figure A-14 and may be used in the following description of the regulators' operation.

The three voltage error generators independently sample the regulated bus, compare this with their stable voltage reference and output the resultant error signal. It should be noted that the error generators sense points are randomly set within the small regulation band ( $29 \text{ VDC} \pm 0.3 \text{ volts}$ ) of the shunt regulator. The linear operation region of each error generator inherently will not overlap the others. Therefore, one of the error generators will be near the low limit of operation ( $28.7 \text{ VDC}$ ) while another will be near the upper limit ( $29.3 \text{ VDC}$ ) and the third somewhere in between.

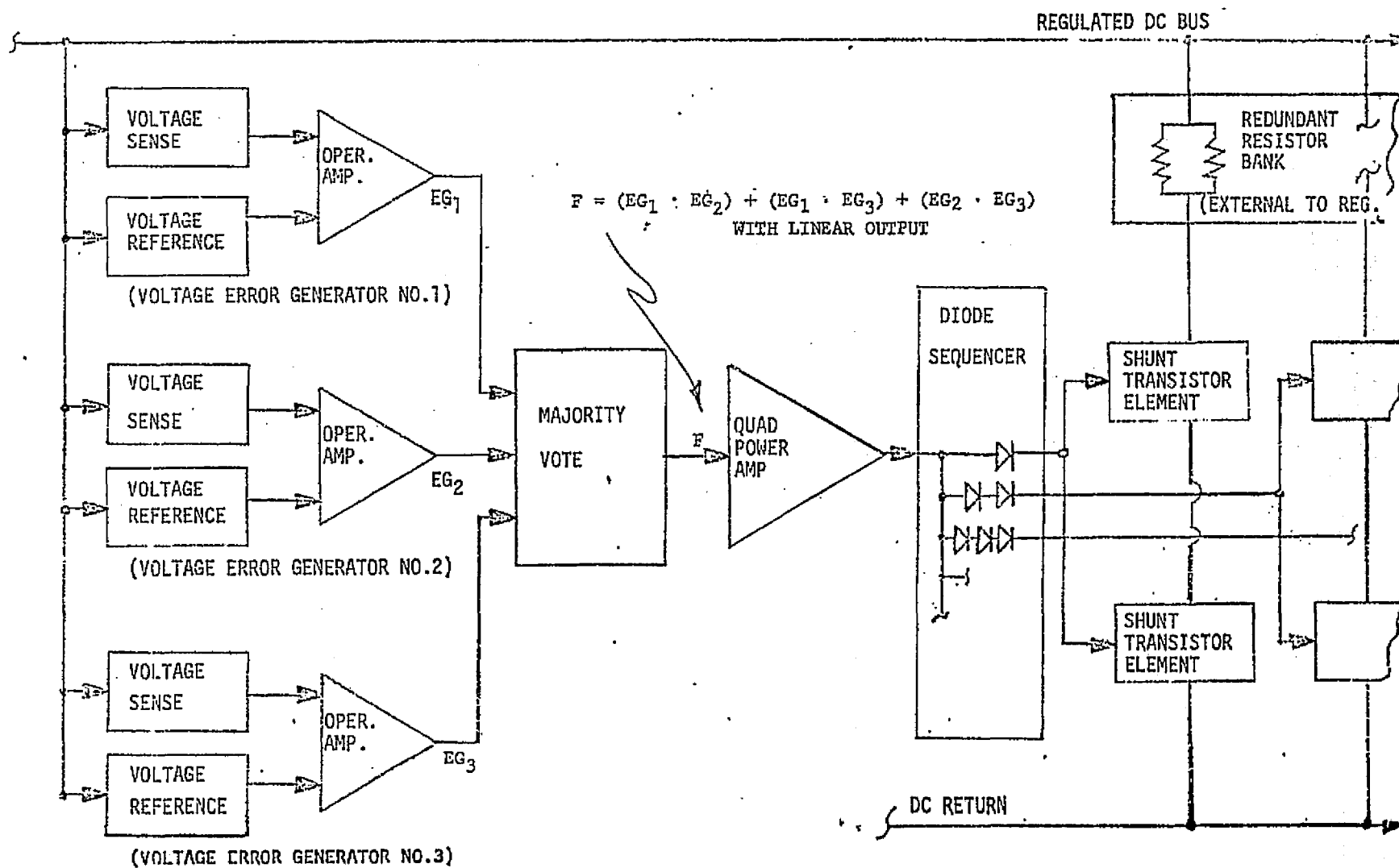


Figure A-14. Sequenced Shunt Regulator Block Diagram

In operation, assuming the bus voltage is  $\geq 28.7$  VDC, one error generator will always be full on, while a second will be operating in its linear region and a third generator will be off or it could have failed open or shorted - it doesn't matter, since only two of the three signals are required by the majority vote circuit.

The majority vote circuit is three sets of two serial transistor "AND" gates, with a wired "OR" operation to perform the Boolean functions indicated in the block diagram of Figure A-14. It should be noted that each transistor "AND" gate, if selected according to the Boolean function, will have one of its two series transistors in saturation while the other will operate in its linear region.

The majority vote stage provides an analog signal to the qual redundant power amplifier which by a simple diode sequencer stage, linearly turns on a series redundant transistor and associated in-line load redundant resistor. The number of load resistors that are switched in at any one time is totally dependent on the sensed line voltage and the resultant analog signal level from the power amplifier which causes the diodes in the sequencer to break down and conduct sequentially; thereby linearly operating one or more shunt transistor elements which effectively switches in one or more elements of the load bank. The load bank itself can be located external to the electronic package ring of the spacecraft to simplify the thermal design.

The shunt regulator has been designed, tested, evaluated and integrated with an RTG. The shunt regulator is well within the design requirements of Table A-1.



TABLE A-1

## DESIGN REQUIREMENTS

<u>FUNCTION</u>	<u>DESIGN VALUE</u>
DC Regulation	29.0 $\pm$ 0.3 VDC
Ripple	20 millivolts peak-to-peak
Power Dissipation Capability	450 Watts
Dynamic Impedance	100 milliohms from 100 Hz to 50 KHz
Transient Response	Return to DC regulation within 100 microseconds after termination of a 100 watt step load (less than 1 microsecond load rise/fall time).
Power Dissipation within the Electronics	50 watts maximum
Standby Power Loss	2 watts maximum
Operating Temperature	-20°C to +75°C
Transistor Power Dissipation	15 watts maximum. (Allows 45°C Junction temperature above control plate with a thermal resistance of 30°C/watt)
Piece Part Selection	From JPL approved parts List
Mission Life	3.5 years

The shunt resistor bank (or radiator) is estimated to weigh 6.5 pounds. The volume is not significant since it is mounted on an appendage to the spacecraft. The shunt regulator electronic equipment is estimated at 10.5 pounds and will occupy a volume of 338 cubic inches.

Empirical data has indicated that the shunt regulator will have a dynamic output impedance of less than 0.1 ohm over a frequency range of zero to 50 KHz and less than 0.3 ohms from 50 KHz to 1 MHz. The standby losses will be 400 milliwatts with a capability of handling 450 watts maximum. A Bode plot indicates positive gain out to 60 KHz with a phase margin of 20 degrees at this frequency.

### 6.3 Three Phase, 400 Hertz Inverter

The three phase 400 Hz inverter consists of four basic blocks as shown in Figure A-15. This package has a maximum weight of 3.4 lbs, requires a volume of 109 cubic inches, and has an efficiency slightly above 85% at 27.2 Vrms operating into a 12 watt load with a minimum lagging power factor of 0.5. The 400 Hertz output frequency stability is within  $\pm 0.01$  percent.

The inverter provides a quasi-square-wave output voltage virtually free of any third harmonic content. The three-phase output voltage powers the gyro motors in the Attitude Control Subsystem.

Output transistors in the three phase power amplifier drive each primary leg of the delta-connected output transformer. Each phase is driven by a push-pull stage through a coupling transformer. The drive signal for each push-pull pair is obtained from a divide-by-six counter circuit. The power converter is synchronized by the spacecraft 2.4 KHz, 50 Vrms, square wave through a coupling

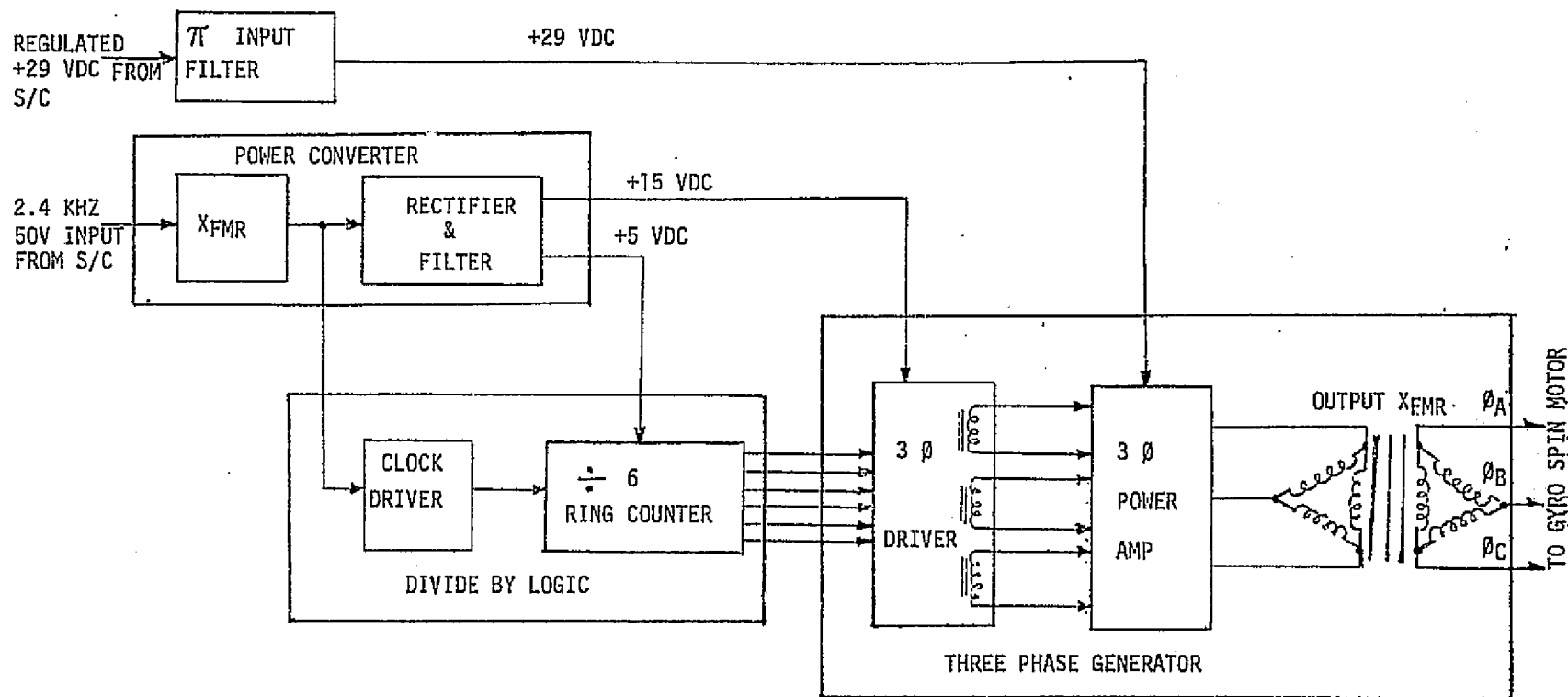


Figure A-15 Three Phase, 400 Hertz Inverter Block Diagram

transformer. This frequency is picked off to clock the ring counter, and is transformed, rectified, and filtered to +5 and +15 VDC for the ring counter and the three phase driver circuit. The counter logic consists of three J-K flip-flops and two "NAND" gates. The 2.4 KHz is divided by six by the counter to provide the three-phase, time displaced, square-wave drive signals to the driver of the three phase generator.

#### 6.4 Battery Charge Discharge Electronics

The battery charge circuitry provides the low level charging necessary to maintain the battery at full charge during inactive periods, and to provide recharge in the event of its use.

The battery discharge regulator provides control over the battery discharge and boosts the voltage of the battery to the level of the regulated bus.

A typical method of discharging a battery and providing that power to a higher voltage regulated bus would be the boost regulator. Although the component design is not completed, it is expected that the regulator will be required to boost about 200 watts. Its efficiency will be above 80 percent and its weight is estimated at 5 pounds, with a volume of 110 cubic inches. The output impedance is estimated at one ohm and the frequency response at 0.5 to 1.0 milliseconds. A conceptual design using an autotransformer pulse width modulation is shown in Figure A-15.

The battery charge circuitry will consist of a resistor for continuous trickle charge and a second resistor to provide a higher rate of charge via a commandable relay.

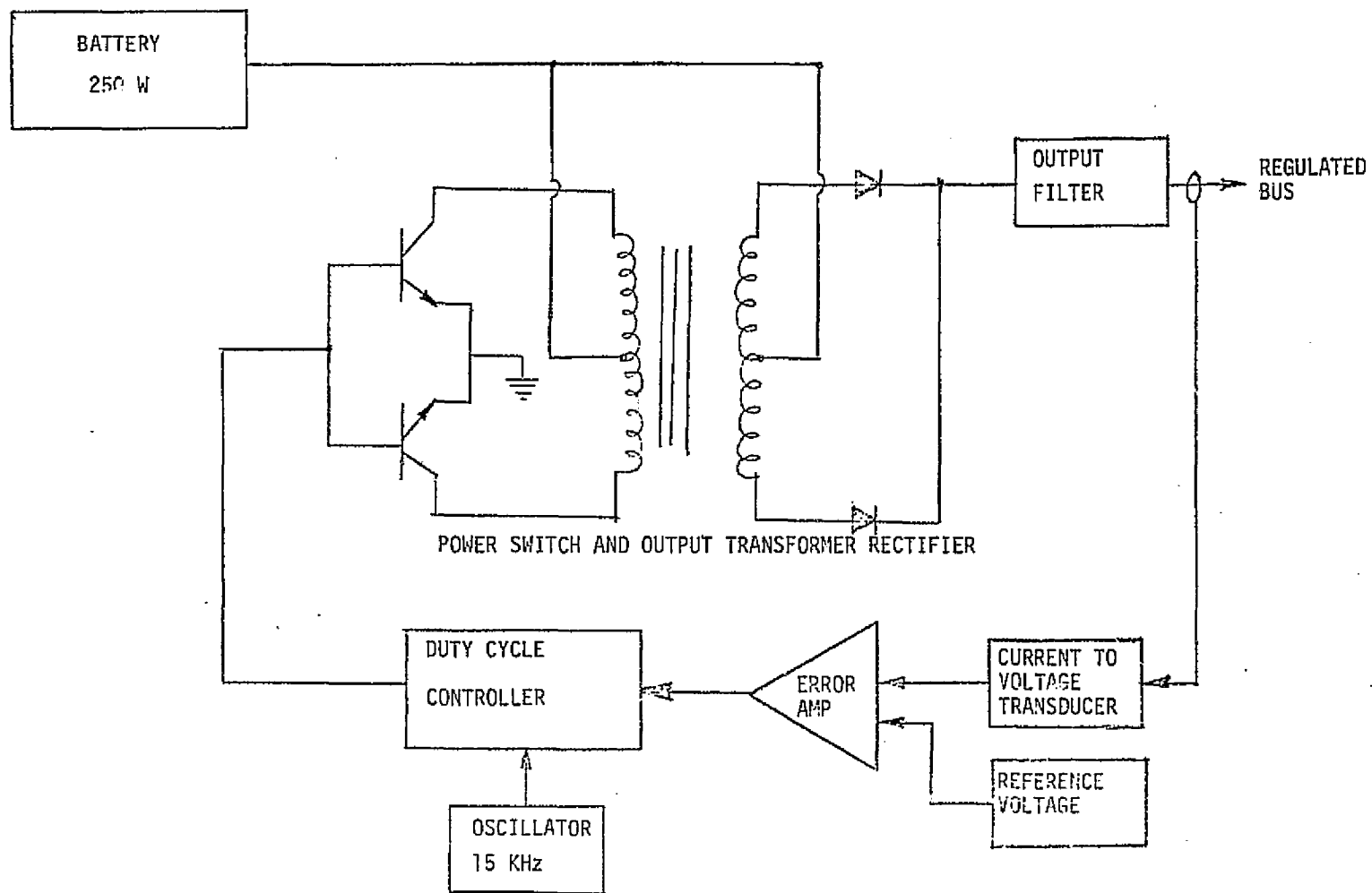


Figure A-16 Boost Regulator Block Diagram

## 6.5 Power Control

The power control unit contains the main inverter failure detector and switching circuitry for the 2.4KHz inverters, and the input/output telemetry functions for 2.4KHz inverters, 400 Hz, 3Ø inverter and DC distributed power. Here again, precise data is not available but it is expected that the component will weigh 7.0 pounds and require a volume of 110 cubic inches.

## 6.6 Power Distribution

The power distribution units contain the switches, drivers, and associated circuitry for commandable control of the spacecraft power distributed to the subsystems. It is expected that the total weight will be approximately 18 pounds and the volume about 330 cubic inches. Precise circuit details are not presently available.

## 7.0 POWER SYSTEM PERFORMANCE CHARACTERISTICS

### 7.1 Power Profile

The power profile shown in Figure A-17 is based on maximum steady state load values. Transient loads are generally assumed to be supplied from the RTG power margin or from the small battery included for this purpose. Sequencing of loads is expected in order to prevent excessive source drains. For example, the science scan platform will be slewed by operating the momentum wheels by time multiplexing power pulses to the three axes in sequence.

Representative science loads are expected to require approximately 67 watts at the instruments. Other spacecraft loads which must supply individual inverters with their inherent inefficiencies are also included in the total power profile of Figure A-17.

### 7.2 Electromagnetic Compatibility

The EMI requirement specified in Table A-1 for radiated noise in the 1 Hz to 40 MHz range is imposed to satisfy the requirements for the plasma wave and radio astronomy experiments. Conducted and radiated interference requirements are specified for science instruments and may not be appropriate for inherited spacecraft subsystems. The cost of modification of the inherited hardware from an EMI standpoint toward the new equipment requirements will be traded off against the expected improvement. EMC testing of flight hardware will be limited to these two environments.

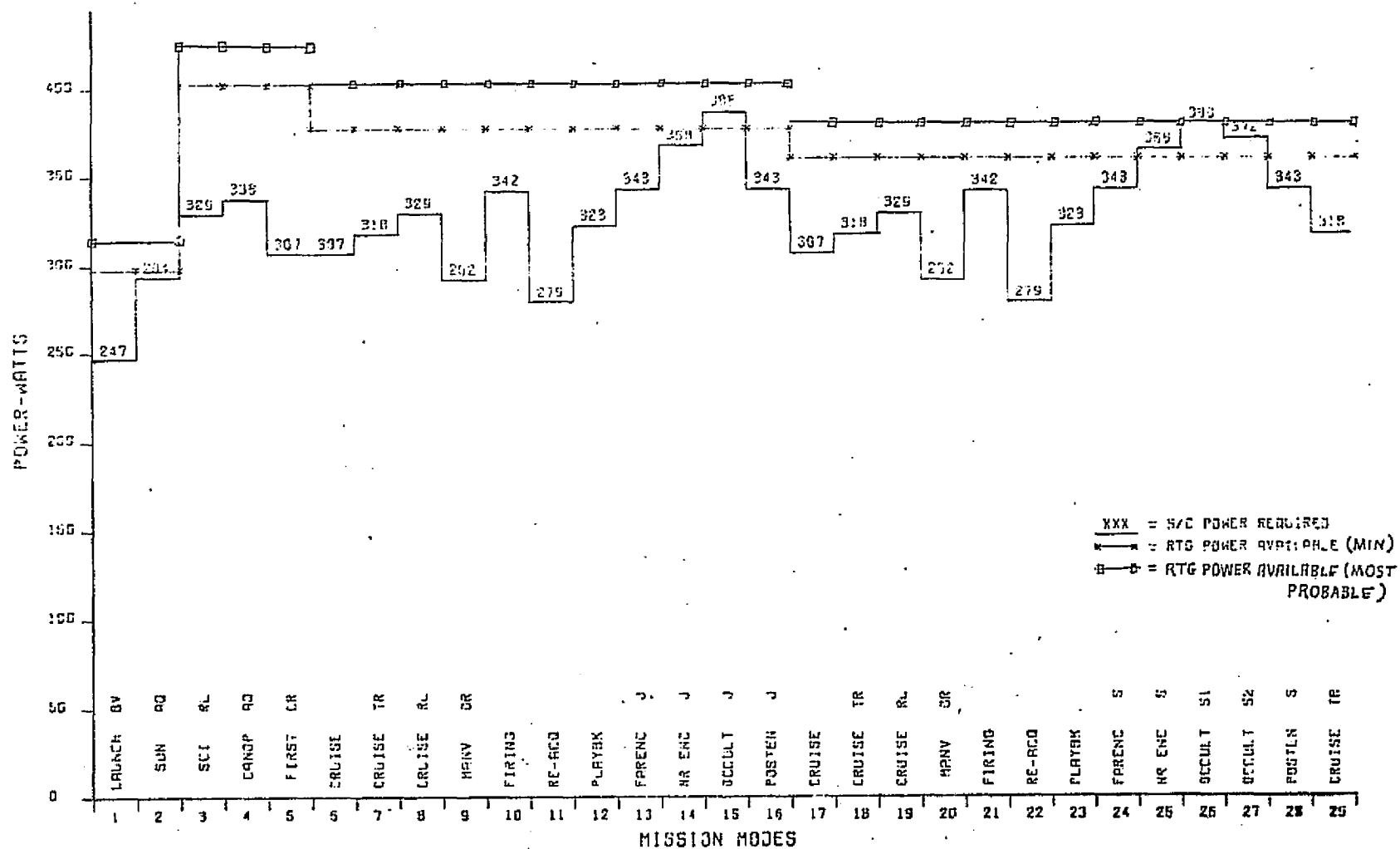


Figure A-17. Power Profile by Mission Mode



### 7.3 Radiation Effects

For the MJS mission the Jovian radiation environment will influence flyby closest approach and electronic piece-part selection on the basis of radiation susceptibilities. Susceptibility thresholds and radiation models have been selected.

APPENDIX B

APPLICATIONS TECHNOLOGY SATELLITE F

Appendix B  
Applications Technology Satellite F  
TABLE OF CONTENTS

<u>SECTION</u>		<u>PAGE</u>
1.0	INTRODUCTION . . . . .	B-1
2.0	SYSTEM OVERVIEW . . . . .	B-1
3.0	VEHICLE CONFIGURATION . . . . .	B-3
4.0	POWER SYSTEM FUNCTIONAL DESCRIPTION . . . . .	B-4
5.0	POWER SOURCE EQUIPMENT DESCRIPTION . . . . .	B-12
	5.1 Solar Array . . . . .	B-12
	5.1.1 Solar Array Operation . . . . .	B-13
	5.2 Battery . . . . .	B-16
6.0	POWER PROCESSING EQUIPMENT . . . . .	B-22
	6.1 Power Regulation Unit (PRU) . . . . .	B-22
	6.1.1 PRU - Boost Regulator . . . . .	B-25
	6.1.2 Boost Regulator Output Filter Capacitors . . . . .	B-27
	6.1.3 Boost Regulator Efficiency . . . . .	B-28
	6.1.4 PRU - Battery Charge Regulator . . . . .	B-29
	6.1.5 PRU - Shunt Regulator Control . . . . .	B-31
	6.1.6 PRU - Regulation Control Unit . . . . .	B-33
	6.1.7 PRU - Failure Detector and Low Voltage Cut-Off . . . . .	B-35
	6.1.8 PRU - Battery Over Temperature Control . . . . .	B-39
	6.1.9 PRU - Current Monitors . . . . .	B-40
	6.1.10 PRU - Command and Telemetry Interfaces . . . . .	B-42
	6.1.11 PRU - Parameters . . . . .	B-42
	6.2 Shunt Regulator . . . . .	B-45
	6.3 Power Controllers . . . . .	B-46

## Table of Contents (Continued)

<u>SECTION</u>		<u>PAGE</u>
	6.4 Electrical Performance of PIC and ECB . . . . .	B-46
	6.5 PIC Operation . . . . .	B-49
	6.6 Separation Controller . . . . .	B-51
7.0	POWER SYSTEM PERFORMANCE CHARACTERISTICS . . . . .	B-53
	7.1 Benefits of Central Power Regulation . . . . .	B-53
	7.2 Trade Studies . . . . .	B-55

## LIST OF TABLES

<u>TABLE</u>		<u>PAGE</u>
B-1	Defined Experiments . . . . .	B-7
B-2	Typical Battery Power Requirements . . . . .	B-17
B-3	PRU Commands . . . . .	B-43
B-4	PRU Telemetry Interface . . . . .	B-44
B-5	Subsystem Performance Matrix . . . . .	B-55

# LIST OF ILLUSTRATIONS

<u>FIGURE</u>		<u>PAGE</u>
B-1	Pre-launch Thru Acquisition - Power Requirements . . . . .	B-6
B-2	Payload Thermal Control Maneuver . . . . .	B-6
B-3	Spacecraft Configuration . . . . .	B-8
B-4	Power Subsystem Structural Interfaces . . . . .	B-9
B-5	Power Subsystem Functional Block Diagram . . . . .	B-10
B-6	Peak Power Capability . . . . .	B-11
B-7	Battery Depth of Discharge for 4-hour Peak Load . . . . .	B-11
B-8	Power Regulation Unit Efficiency . . . . .	B-11
B-9	Voltage Regulation . . . . .	B-11
B-10	Solar Array Power Output . . . . .	B-14
B-11	Arrangement of Solar Cell Modules . . . . .	B-15
B-12	Power Profile, Showing Battery Usage . . . . .	B-17
B-13	Discharge Characteristics (77°F) . . . . .	B-19
B-14	Discharge Characteristics (C/2 Rate) . . . . .	B-19
B-15	Prelaunch Power Capability . . . . .	B-20
B-16	Power Regulation Unit Functional Block Diagram . . . . .	B-24
B-17	Boost Regulator Schematic . . . . .	B-26
B-18	Boost Regulator Block Diagram . . . . .	B-27
B-19	Boost Regulator Efficiency Versus Power . . . . .	B-29
B-20	Battery Charge Regulator Schematic . . . . .	B-30
B-21	Block Diagram of Battery Charge Regulator . . . . .	B-31
B-22	Schematic of Shunt Regulator Control . . . . .	B-32
B-23	Regulator Control Unit Schematic . . . . .	B-33
B-24	Schematic Diagram of Current Limiter of Boost . . . . .	B-36

# List of Illustrations (Continued)

<u>FIGURE</u>		<u>PAGE</u>
B-25	Failure Detector Schematic . . . . .	B-37
B-26	Low Voltage Cutoff Block Diagram . . . . .	B-38
B-27	Battery over Temperature Control Schematic . . . . .	B-39
B-28	Current Monitor Basic Concept Diagram . . . . .	B-41
B-29	ECB and PIC Operating Modes . . . . .	B-48
B-30	PIC Schematic . . . . .	B-49
B-31	Separation Controller Functional Block Diagram . . . . .	B-52
B-32	Arm/Disarm Scheme . . . . .	B-52

## 1.0 INTRODUCTION

The Application Technology Satellite F&G, better known as ATS, was designed, breadboard tested and evaluated by General Electric Space Division, Valley Forge in cooperation with NASA, Goddard Space Flight Center, Maryland. The prime spacecraft was manufactured and tested for flight by Fairchild Space Division, Maryland, and was successfully launched on 30 May 1974.

## 2.0 SYSTEM OVERVIEW

ATS F, the sixth in a continuing series of Applications Technology Satellites was launched on a Titan III C vehicle for insertion into a synchronous orbit at 95 degrees West longitude. The power subsystem will supply the spacecraft nominal power requirements for the prelaunch through acquisition phase of the mission in accordance with the power profile shown in Figure B-1. Transfer to internal power may occur as much as 4-1/2 hours before liftoff, allowing a normal 2-hour prelaunch countdown plus up to a 2-1/2-hour hold.

During the launch phase of the mission, the solar array is folded into a box configuration around the equipment section of the spacecraft. At 289 seconds after liftoff, the shroud is jettisoned and the solar array is exposed in its folded configuration. The batteries support the spacecraft loads from transfer from ground power until after shroud separation when solar array output power is available to handle the load and for recharging the batteries.

The standard Titan III-C toast mode, "Rotisserie" maneuver, is utilized to maintain a low-array temperature (See Figure B-2). The thermal time constant for the solar array is approximately 20 minutes and the Titan maneuver is such



that it performs a 230 degree roll in 6 minutes, with a 1-minute dwell at each extreme position. In the toast mode with the sun vector normal to the roll axis, the maximum solar panel temperature will be about 95°F. Under these conditions, the average electrical power available is 250 watts. Power output will vary approximately as the cosine of the angle of incidence. Analyses of the launch and ascent trajectory indicate that the array will meet the load requirements and recharge the battery during transfer orbit injection.

The mission life has a minimum of two years with a design goal of five years. During the mission, the vehicle will be repositioned to 57 degrees West Longitude for air traffic control experiment on L-band; broadbeam coverage from Shannon, Ireland to New York.

Another repositioning event will be required for instructional television experiment (ITV) operation with India. Other on-board experiments are defined in Table B-1.

Some of the mission objectives are to demonstrate feasibility of a 30-foot deployable spacecraft antenna with good radio frequency performance up to ten gega Hertz; to provide spacecraft fine pointing (0.1 degrees) and slewing (17.5 degrees in 30 minutes); to demonstrate capability of forming hi-gain steerable antenna beams; to demonstrate capability of providing radio frequency links from ground, to ATS-F, and to other low orbiting spacecraft and return.

### 3.0 VEHICLE CONFIGURATION

The spacecraft launch weight is approximately 1957.5 pounds. This weight allows for an additional growth capacity of 25 percent. The power system weighs 396 pounds or about 20.2 percent of the launch weight. The power system weight is a summation of not only the electrical, but also the mechanical items necessary to its total support and operation. Briefly, these items are: the 160 square foot-fixed-solar array, including the solar cell modules, mounting panels, hinge tubes, booms and crossovers, deployment motors, and linkage. Other items included are the two 12 ampere hour storage batteries, electronics and power distribution components; as well as 110 pounds of distribution harness.

The entire spacecraft configuration from booster separation through array boom deployment and operation is shown in Figure B-3. Power subsystem components are located just above the Earth Viewing module and in bays 7 and 8 as shown in Figure B-4.

#### 4.0 POWER SYSTEM FUNCTIONAL DESCRIPTION

The power subsystem provides direct energy transfer from the solar array to the load for maximum efficiency. Energy storage is provided to support peak load demand and eclipse operation. Experiment interface circuit provides on-off and over-load control, noise suppression and isolation from the bus.

The power subsystem consists of two fixed solar array panels perpendicular to each other as shown in Figure B-3; two 19 cell batteries, a power regulation unit, 12 shunt regulators, two power controllers and a separation controller. This configuration of source power and power processors is functionally shown in the block diagram of Figure B-5.

Regulation is provided for three different modes. When the solar array output is sufficient to support the load, a direct transfer of energy to load occurs. As the load increases or the array output decreases, the batteries are used to support the load. When the load is less than the array capacity the batteries are recharged. If the array output exceeds both the load and battery charge requirement, the excess is dissipated in the shunt regulators. A bus voltage sensing circuit provides a reference to control the smooth transfer between modes.

Overload protection, common experiment interface, and isolation are provided by power interface controllers. These are switches which sense excessive power demands and ramp off the malfunctioning experiment. Each interface controller is set to a current level appropriate to the experiment with which it interfaces. Command resettable circuit breakers are also included to provide overload protection for the power subsystem from malfunctions in the spacecraft subsystem. A time

delay is provided to avoid tripping on transients. The separation controller provides for redundant actuation paths for all subsystems requiring release and deployment. Protection against premature actuation is assured by interlocking events and requiring both an enable and actuation command. Overrides are available for the interlock functions and an AGE bypass is provided for use during system test.

The power subsystem provides conversion of solar energy and regulation of the resultant power in two qualities,  $29.5V \pm 2$  percent,  $-3$  percent to all spacecraft subsystems and  $28V \pm 2$  percent to all experiment payloads. The solar array output varies between 612 and 395 watts initially decreasing to 565 and 350 watts in two years. The batteries in shallow charge/discharge cycles provide an average power available to the load of 483 to 436 watts. Peak power capability of the subsystem as a function of time, season and load magnitude and duration is shown in Figures B-6 and B-7.

Prelaunch and launch power requirements are supplied by two 12 ampere-hour batteries. Sufficient energy is stored to permit over four hours on internal power prior to launch and attainment of synchronous altitude, with fully charged batteries to support the deployment loads. Recharging is done by using the power available from the folded array during the transfer orbit. The spacecraft load of 230 watt-hours is supported by the batteries during the yearly eclipse periods. The nominal ripple has been measured at 10 mv pp with a maximum of 80 mv pp when the batteries are supporting a high load.

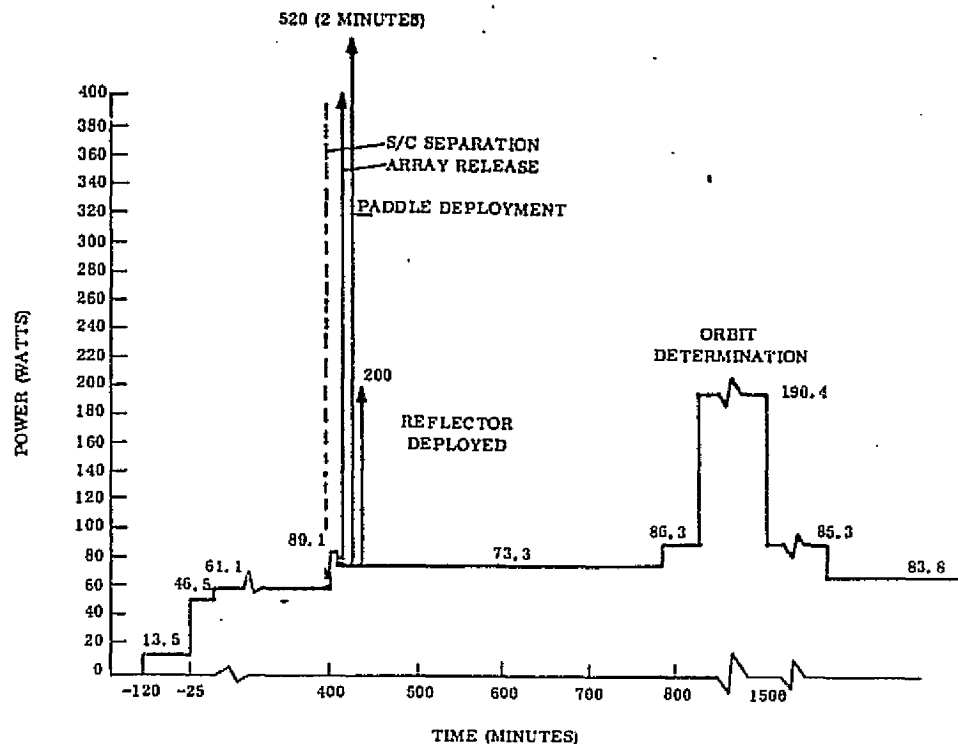


Figure B-1. Prelaunch Through Acquisition - Power Requirements

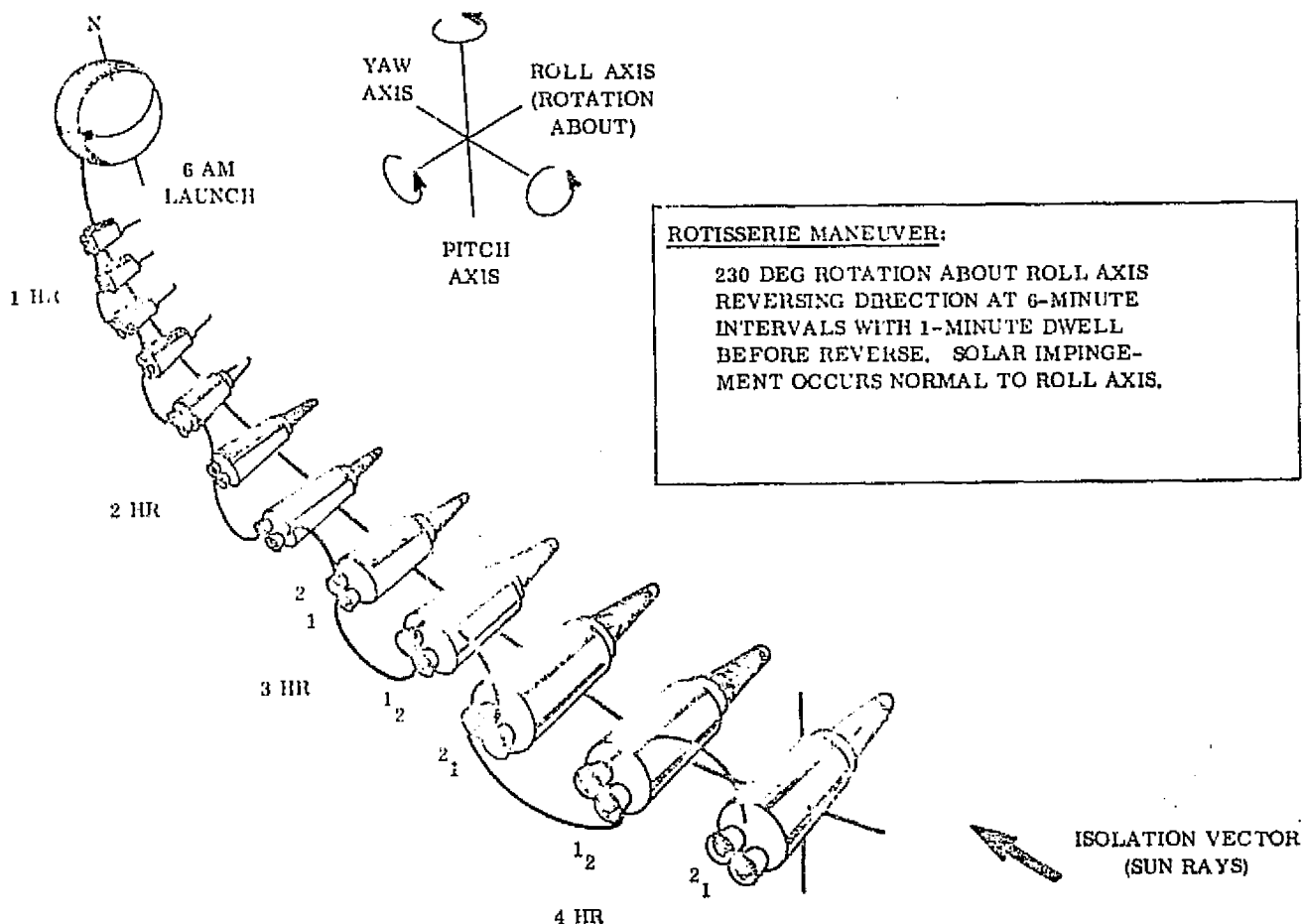


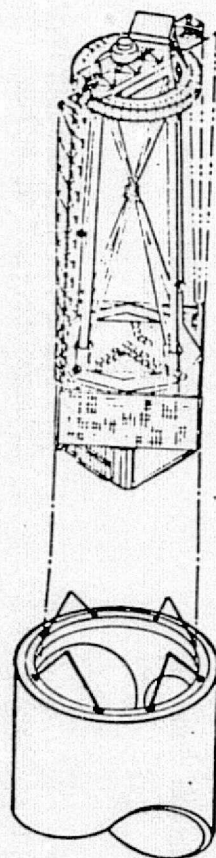
Figure B-2. Payload Thermal Control Maneuver (Rotisserie)

Table B-1  
Defined Experiments

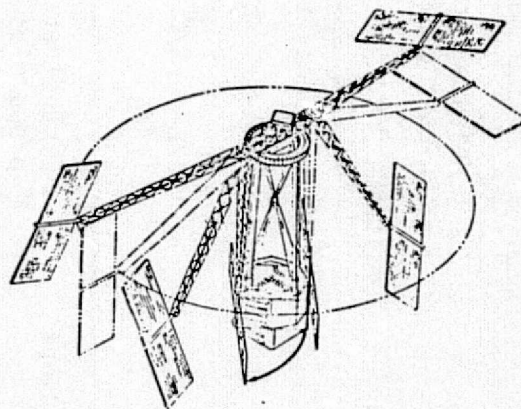
EXPERIMENT	PURPOSE
Data Relay (X and S-Bands)	Long duration, real-time communication with low-altitude satellites (Nimbus, Apollo)
PLACE (X and L-Bands)	Air traffic control
Instructional TV (TRUST)(ITV) (X-Band and 850 MHz)	Instructional TV distribution
Radio Frequency Interference (RFI)	Measure interference in COMSAT band
Time and Frequency Dispersion	Propagation experiment
Millimeter Wave	Measurement of atmospheric effects on K-band communications links
Radio Beacon	Measure ionospheric effects on radio frequency transmissions
Laser	Checkout of S/C-to-ground and S/C-to-S/C IR communication links
Commandable Gravity Gradient System (COGGS)	Demonstration of hybrid controls plus propulsion backup
Spacecraft Attitude Maneuvering Optimal Control, and Self-Adaptive Precision Pointing Attitude Control	Optimum control for attitude maneuvers; self-adaptive attitude control
High Resolution Camera	Meteorological mapping to 1 N. mile
Radiometer	IR and visible meteorological mapping to 5 N. miles
Integrated Scientific Experiment Package	Measure magnetic fields, particle densities & radiation-induced solar cell degradation

REPRODUCIBILITY OF THE  
ORIGINAL PAGE IS POOR

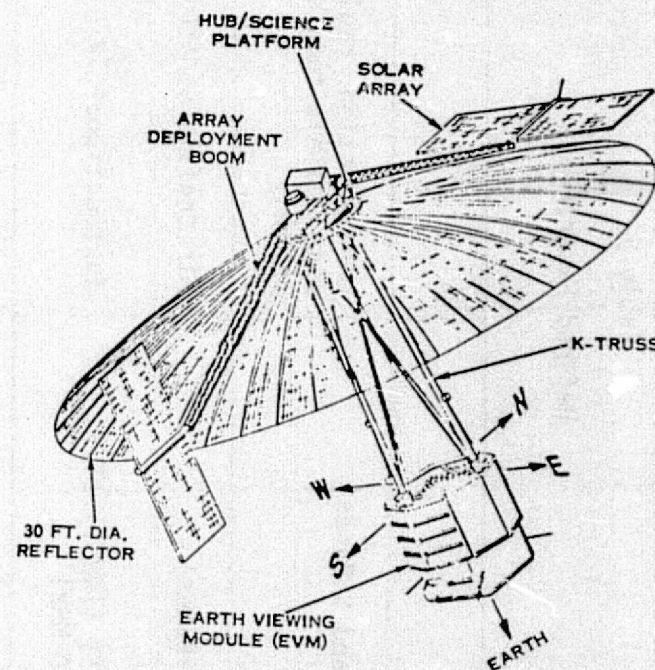
B-8



SEPARATION



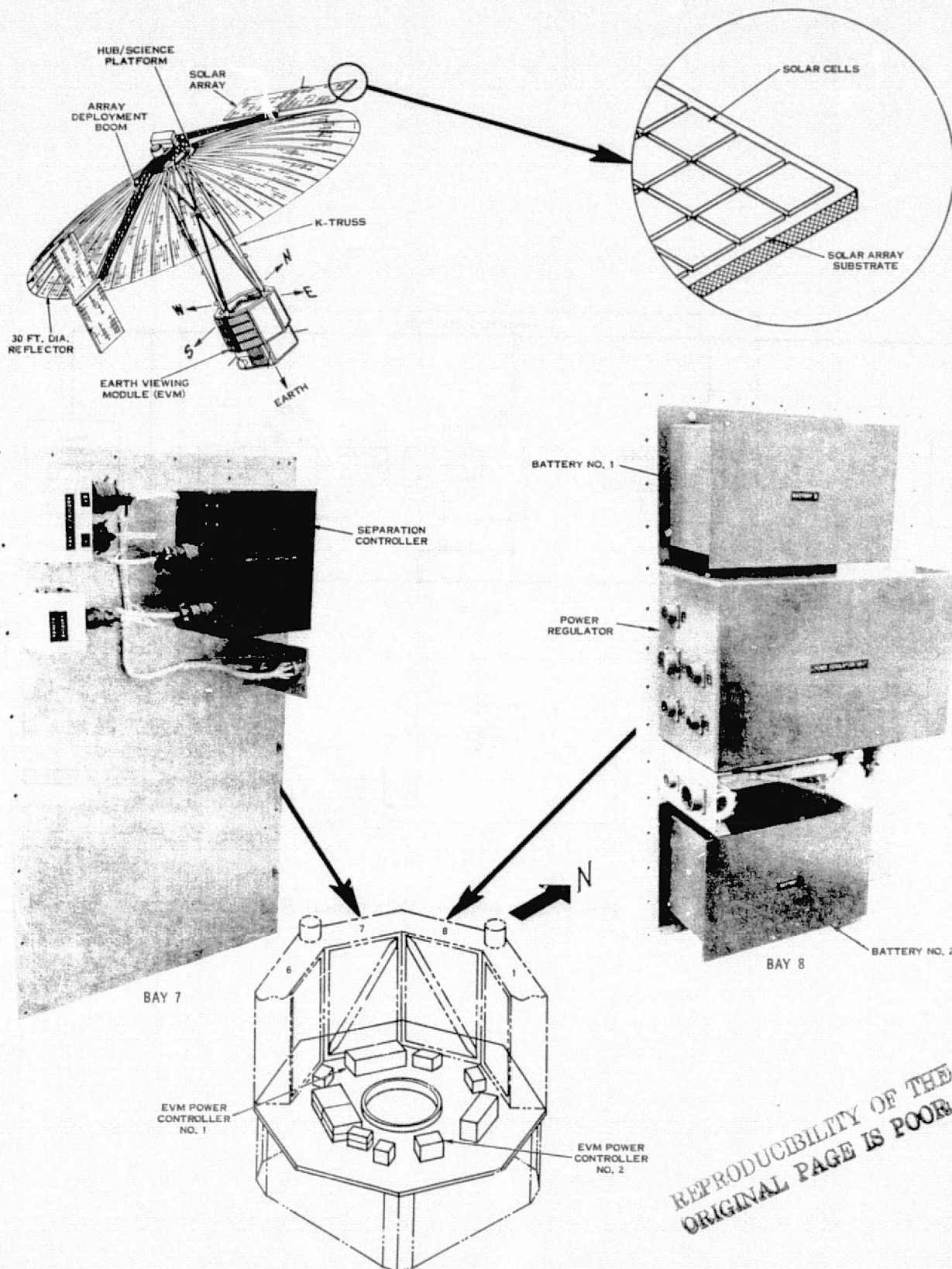
ARRAY AND BOOM DEPLOYMENT



OPERATIONAL CONFIGURATION

Figure B-3: Spacecraft Configuration





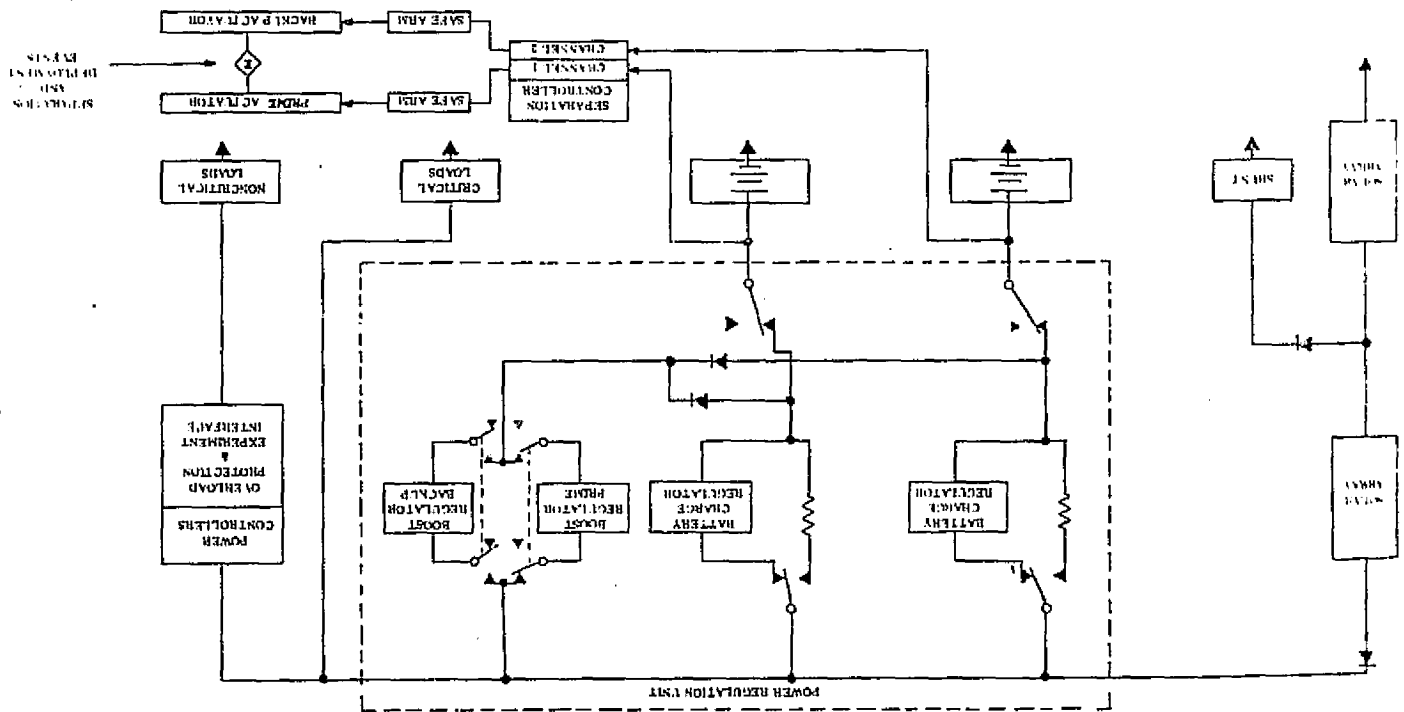
REPRODUCIBILITY OF THE  
ORIGINAL PAGE IS POOR

## POWER

Figure B-4 Power Subsystem Structural Interfaces



Figure B-5 Power Subsystem Functional Block Diagram



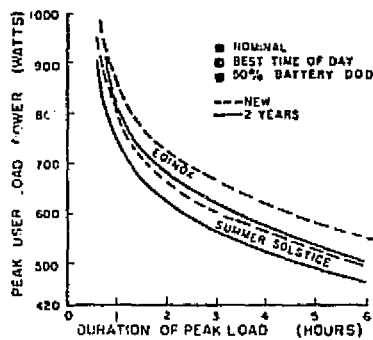


Figure B-6. Peak Power Capability

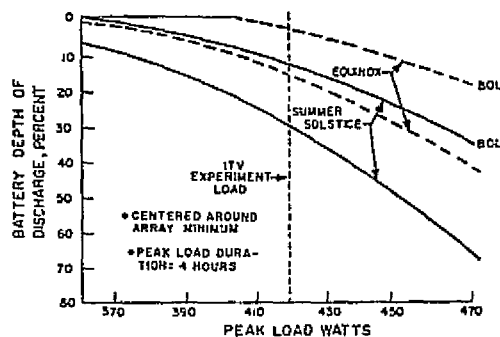


Figure B-7. Battery Depth of Discharge for 4-Hour Peakload.

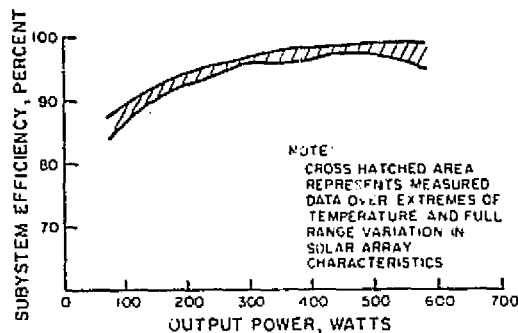


Figure B-8. Power Regulation Unit Efficiency

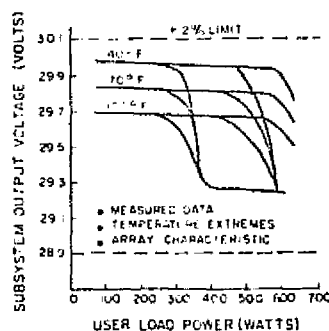


Figure B-9. Voltage Regulation

The curves at left illustrate the performance of the power subsystem. The upper curve shows the maximum capability of the subsystem to support peak loads as a function of the duration of the load. The differences between the equinox and solstice seasons of the year, as well as the beginning of life and two year design points, are also illustrated. Notice that the peak spacecraft load requirement (ITV experiment) which is drawn in at 420 Watts for four hours, lies well below the summer solstice condition at the two year design point.

The second curve again illustrates the peak load capability of the subsystem except this time the least favorable time of day was chosen. This curve illustrates the battery depth of discharge as a function of user load power drain with a four hour duration. Again the ITV experiment load requirement is drawn in to illustrate the margins in the power subsystem capability.

This curve illustrates the high degree of efficiency exhibited by the power subsystem electronics. The data was obtained from the Phase C subsystem breadboard testing and includes an internal component temperature range of 40°F to 100°F, and array characteristic extremes. Notice that the user load power region of 300 to 600 Watts, where load sharing takes place during various times of the mission, benefits from the highest efficiency (over 96 percent). This results in a smaller solar array, fewer battery cells in series (smaller, lighter battery) and improved battery charge to discharge efficiency.

This curve illustrates the bus voltage regulation characteristics where the Power Regulation Unit was stressed by temperature extremes (40°F to 100°F) and worst case solar array short circuit current and open circuit voltage. The curves were plotted from measured data from the Phase C breadboard test program.

Notice that the envelope of all voltage excursions lies well inside the  $\pm$  two percent specification limits shown as dotted horizontal lines.

## 5.0 POWER SOURCE EQUIPMENT DESCRIPTION

### 5.1 Solar Array

The prime electrical power source for the spacecraft is an array of photovoltaic cells arranged to provide adequate power at the required voltage and current. The array must be able to provide housekeeping power, experiment power, and battery charging power for spacecraft operation during eclipse periods. The array is sized to provide adequate power at 2 year design point, so that size compensates for various degradation factors. Excess power is therefore available for use during the early part of the mission.

Trade studies completed during earlier phases indicated that, although a motor driven sun-oriented solar panel system would be lighter, fixed solar panels would result in less program cost and the array would be simpler and more reliable.

The solar array must provide primary power to the spacecraft beginning no later than 90 minutes after launch, when the booster is placed into the "rotisserie mode", and continuing throughout the mission.

There are two flat solar panel assemblies, located on the + and - pitch axes (north and south axes), with solar cells on both sides of each panel assembly. Each panel assembly consists of two panels, one fixed and one free (hinged). By selecting the north panel to be horizontal (earth-facing), and canting the boom downward over the reflector, the field-of-view requirements of both the EME experiment and the Polaris tracker are satisfied. Furthermore, the time

of maximum array output is located in the evening (7 to 11 p.m.), which makes the greatest amount of power available for ITV during "prime time."

The maximum power output is available from the solar array during the equinox seasons, when the sun is closest to the orbit plane and the spacecraft axes are most nearly perpendicular to the sun. During the solstice seasons, the array output is less because the minimum angle of incidence on the solar panels is 23.5 degrees. The array output is least of all at summer solstice, since the earth's aphelion nearly coincides with the time of least favorable solar incidence angles. Therefore, the worst-case design point is selected to be at summer solstice.

#### 5.1.1 Solar Array Operation

Solar energy is converted to electrical power by 33,408 cells (2 X 2 cm) interconnected to form 12 strings of 72 cells in series. Each string has 8 or 10 cells in parallel on each of the four sides of the solar platforms. Cells are interconnected with silver mesh using a technique developed for controlling solder deposit thickness. The array has 144 square feet of solar cell area arranged on two platforms each consisting of two interchangeable panels with cells on both sides. The cells are N/P, 2 ohm-cm cells having an 11 percent conversion efficiency. 6 mil microsheet with blue filters provide radiation shielding. Taps are provided at the 42 cell point in each string to permit shunting excess array power during cold array or light load operating conditions.

The predicted power output of the solar array after 2 years in orbit is shown in Figure B-10. The "plus" flat panel configuration causes the 6-hour repeating cycle of power peaks. The variation for only the equinox and summer solstice conditions are shown. The winter solstice power output curve is similar and lies between the two curves given. When the solar array is new, the power output will be 10% greater than the values shown, which include the effect of radiation damage.

The arrangement of solar cell modules is shown in Figure B-11 with a summary of parameters given below.

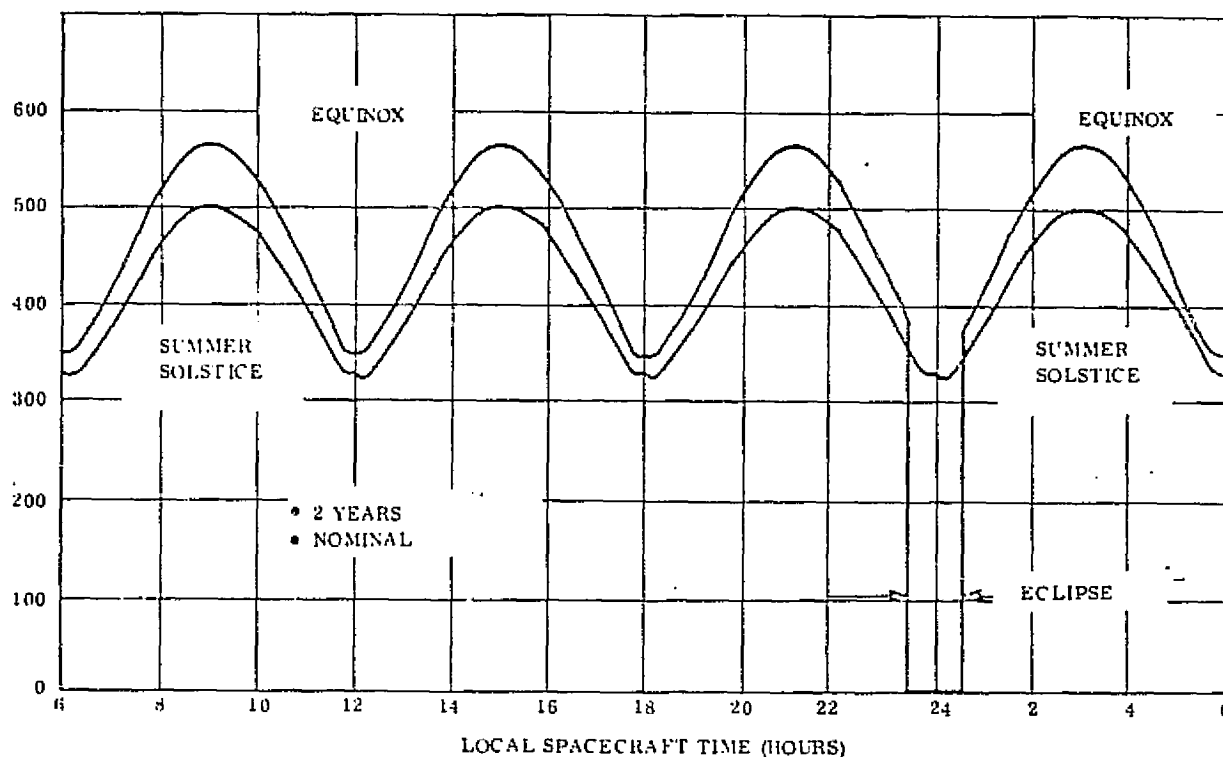


Figure B-10. Solar Array Power Output

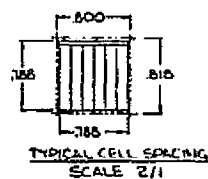
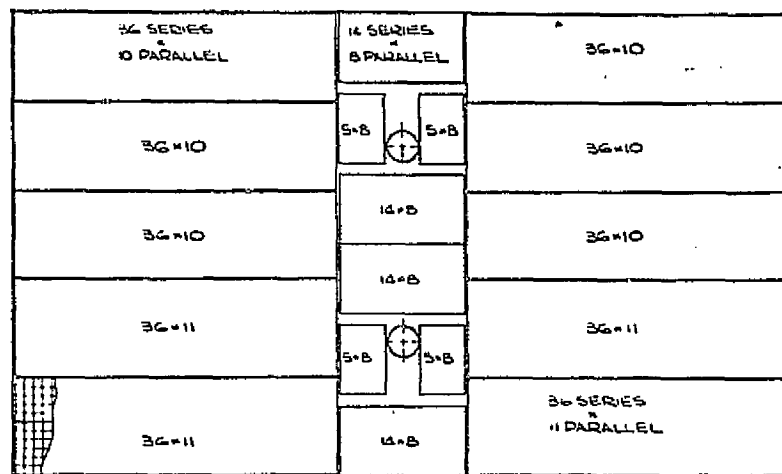


Figure B-11 Arrangement of Solar Cell Modules

A summary of solar array parameters is given below:

Series-connected cells:	72
Parallel cells, one side of panel:	58
Cells per side of panel:	4,176
Panels per vehicle:	4
Ce''s per vehicle	33,408
Gross solar array area:	163 ft <sup>2</sup>
Net active cell area (3.8 cm <sup>2</sup> /cell):	136.6 ft <sup>2</sup>

## 5.2 Battery

The energy storage system consists of two 19-cell hermetically sealed nickel-cadmium batteries of 12 ampere-hour capacity each. The type and size were selected on the basis of life and power requirements. The batteries are required to supply power to the spacecraft during the following phases:

1. Prelaunch
2. Powered flight
3. Deployment (EED and boom actuator)
4. Peak power loads when the demand exceeds the solar array capability
5. Eclipse

The power requirements during the entire cycle including prelaunch, powered flight and transfer orbit, acquisition, and the orbital life of the spacecraft are shown in the power profile (Figure B-12). The shaded portions indicate the power which must be supplied to the loads from the energy storage system. Using the measured efficiency (Figure B-19), the diode voltage drop, and a battery voltage of 23.5 volts, typical power which must be supplied by the batteries is shown in Table B-2.

The battery voltage is set by the number of series cells which in turn is determined by the voltage available for charging the battery. In this power subsystem configuration, the battery is charged from the regulated solar array bus of 29.5 volts. Allowing a 1-volt drop in the battery charge regulator and a maximum charge voltage of approximately 1.5 volts

per cell the battery is configured with 19 cells. On discharge the nominal voltage will be approximately 23.5 volts with a specified minimum of 21 volts, depending on the load. This minimum is approaching the lower limit specified by the booster regulator. In summary, the voltage requirements for the batteries are a maximum of 28.5 volts on charge and a minimum of 21 volts on discharge.

Figure: B-12 Power Profile, Showing Battery Usage

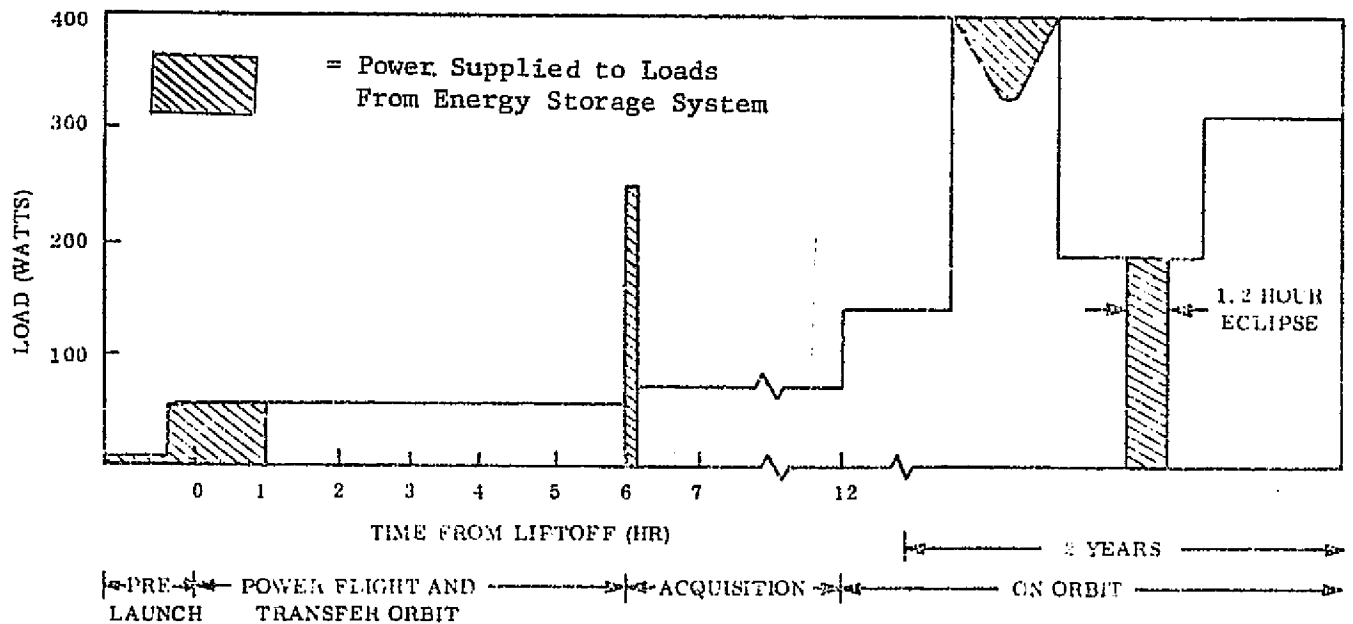


Table B-2 Typical Battery Power Requirements

	Total Bus (watts)	Total Battery (watts)	Total Battery (amps)	Total Battery (watt-hr)	Total Used Battery Capacity (amp-hr)	% Depth of Discharge
Prelaunch	13.5	16	0.67	32		
	55.5	65	2.7	32.5	2.7	11.2
Powered Flight	55.5	65	2.7	97.5	4	16.7
Deployment	660	690	33	23	1.1	4.6
Eclipse (Max)	190	224	10	268	12	50
Load Sharing (Typical)	420	105	4.3	181	7.3	30
Load Sharing (Typical Max)	420	142	6	290	12	50



The power subsystem is configured to charge the battery at a constant current of 1.2 amperes (C/10 charge rate) from a 29.5 volt bus. The charge rate selection is based on the time available to recharge the batteries between discharge periods and on a safe continuous overcharge rate. Provision is made for backup charge mode and over-temperature cut-out. The battery charge regulator takes power from the regulated bus and supplies a constant current of 1.2 amperes at a maximum of 28.5 volts to the battery. As the battery voltage approaches 28.5 volts, the charge rate will taper. In summary, the battery is required to become charged and accept a continuous overcharge at 1.2 amperes at a maximum of 28.5 volts.

Each battery, weighing 28 pounds and requiring 555 cubic inches is configured with 19 cells of 12 ampere-hour capacity and the number of cells is determined by the voltage of the solar array bus used to charge the battery. The cell size is selected on the basis of required power output and battery life. The most stringent power requirement is during eclipse which occurs at regular intervals over the 2-year orbital life. The capacity required from the battery during the maximum eclipse period is approximately 12 ampere hours. With two 12 ampere-hour batteries, this represents a depth of discharge of 50 percent which is a safe level, considering degradation over the 2-year orbital period due to load sharing cycles and memory effects.

The discharge currents associated with the loads and the expected electro-explosive device pulse loads are well within the capability of the nickel-cadmium system and will represent no voltage problem. The voltage variation

with a small load is shown in Figure B-13. For comparative purposes, the characteristics at a C and C/2 rate are shown. The voltage difference is less than 50 millivolts per cell for a 2 to 1 increase in current.

The effect of temperature on voltage at a constant C/2 rate is shown in Figure B-14. There is little variation in voltage except at high temperatures. The thermal design is configured to maintain the battery at a temperature of 50° F to 80° F except for small periods when the temperature may exceed 80 and approach 90° F. This is associated with the over charge period when the battery thermal dissipation is greatest. No voltage problem is anticipated due to temperature variation.

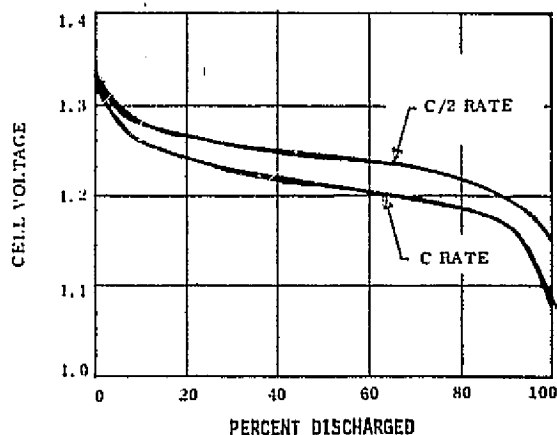


Figure B-13. Discharge Characteristics (77° F)

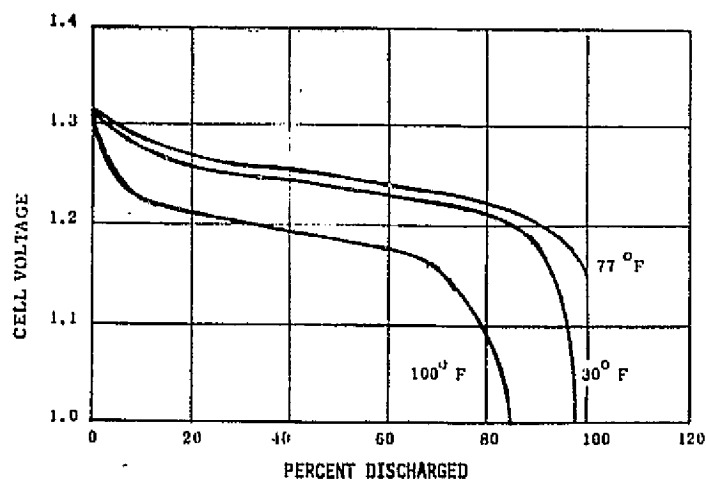


Figure B-14. Discharge Characteristics (C/2 Rate)

During prelaunch the battery supplies all the power used by the spacecraft. The length of time the battery can supply the necessary power is dependent

on the spacecraft load requirement. Figure B-15 shows the battery capability as a function of the power demand. This curve assumes approximately a 27-watt load during the ascent phase, sufficient array power to meet the load requirements no later than 60 minutes after launch, and a maximum depth of discharge of 50 percent on the two batteries.

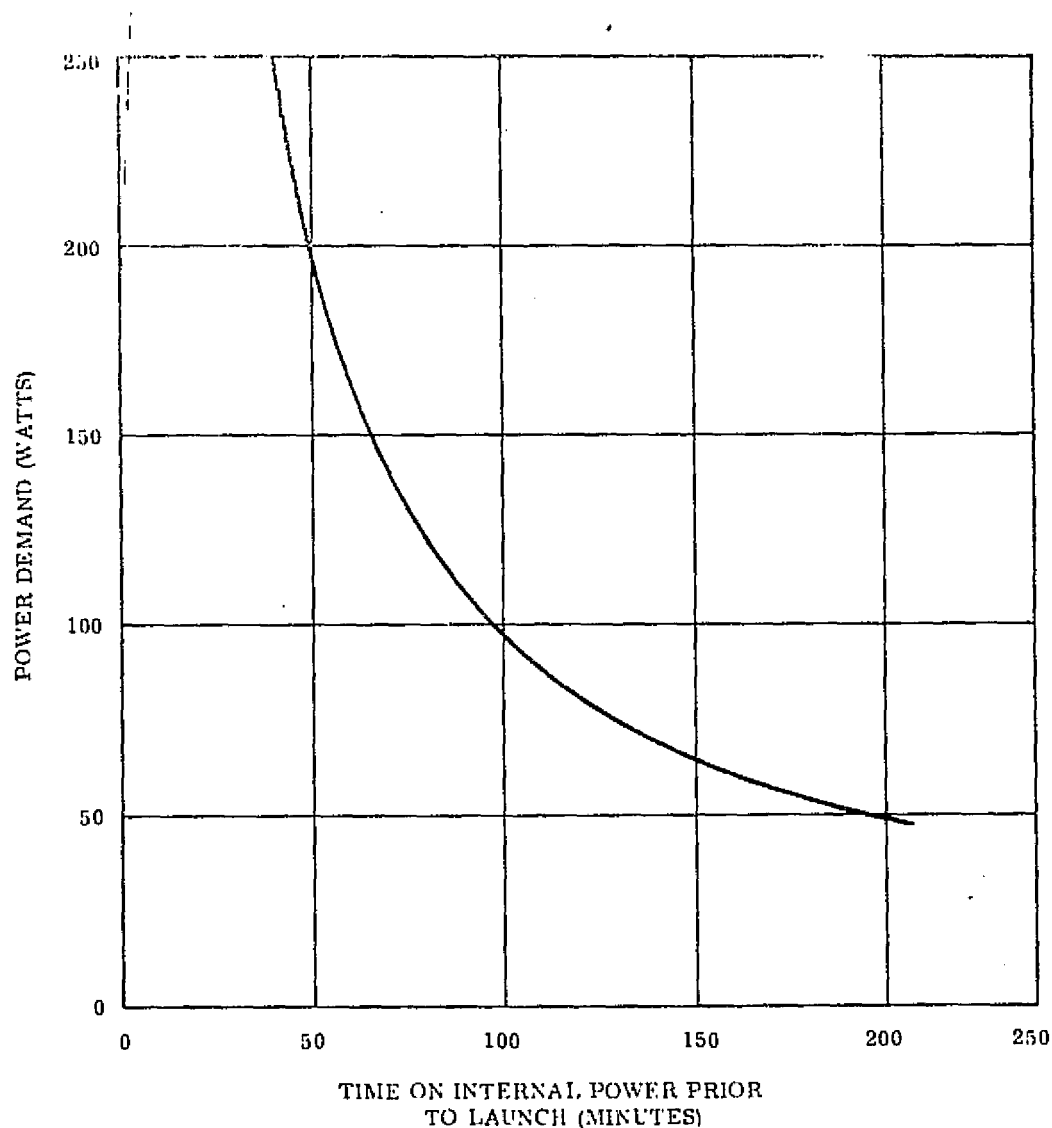


Figure B-15. Prelaunch Power Capability

Much has been written in the literature on the charge acceptance or charge efficiency of the nickel-cadmium system. The discussion and figures presented in this section were derived from a report prepared under Contract No. NAS5-9193 by the GE Research and Development Center, Schenectady, New York. Charge acceptance is a complex function of the previous history of the electrode, the temperature, the rate of charge, the concentration of electrolyte, the concentration and kind of impurities present in the electrodes and electrolyte, and the state of charge of the electrode.

## 6.1 Power Regulation Unit (PRU)

There are several modes of operation of the power subsystem, boosted battery, regulated solar array voltage, solar array plus battery load sharing. In order to make sure that the proper mode of operation is achieved at all times, the operating conditions must be sensed, and logically derived decisions must be made to determine which regulator will operate. This is the task of the Power Regulation Unit. This particular design incorporates the three-mode regulation concept.

The Power Regulation Unit maintains the vehicle electrical bus at a constant 29.5 volts direct current plus or minus two per cent with a variation in power demand from a minimum specified load of 13.5 watts to a maximum capability of 1000 watts. In addition, the Power Regulation Unit optimizes the electrical power subsystem performance by selecting the solar array, the batteries, or a combination of the two as the source of this power. It also controls recharge of the batteries when required if excess electrical power is available at the solar array. When the load demand is satisfied and the batteries are being charged at their design maximum rate, excess solar array power is dissipated in active transistorized shunt regulators to maintain the vehicle electrical bus within regulation limits.

To accomplish these functions, the Power Regulation Unit contains:

1. Redundant voltage regulation control circuit to sample the vehicle electrical bus, compare it with a voltage reference, and select and actively control the operation of the array shunt regulator, the battery charge regulator, and the boost regulator.

2. Redundant shunt regulator controls to furnish base drive current to the twelve shunt regulator modules located throughout the vehicle.
3. One battery charge regulator for each of the two nickel-cadmium batteries to furnish up to a C/10 constant current on demand of the battery when the solar array has available power in excess of that required by the load.
4. Redundant boost regulation to draw current from the batteries at the varying battery discharge voltage level; and by time ratio controlled voltage transformation, supply this power to the vehicle bus at a regulated voltage level.
5. A failure detector to monitor the vehicle electrical bus for an under-voltage or over-voltage condition, and switch from primary to stand-by units as required.

All of the required sensing, logic, active control, and switching functions are located in one component to minimize the complexity of the electrical and mechanical interface, to eliminate any potential need to supply matched sets of equipment in which interaction exists, to simplify logistics, and to eliminate the possibility of noise injection on sensitive signal lines. The single component provides a central, low impedance, electrical tie point for all loads and also allows closer voltage regulation, less common mode noise, and separate electrical wiring to each subsystem and each experiment.

The electronic equipment essential to electrical power subsystem performance is contained within the Power Regulation Unit, permitting subsystem testing at the component level and reducing the amount of test time in final assembly of the vehicle. Additionally, costs are reduced because of the necessity to develop, fabricate and test only one piece of equipment. The Power Regulation Unit is shown in the functional block diagram in Figure B-16. Each block of the Power Regulation Unit is functionally described in the following paragraphs:

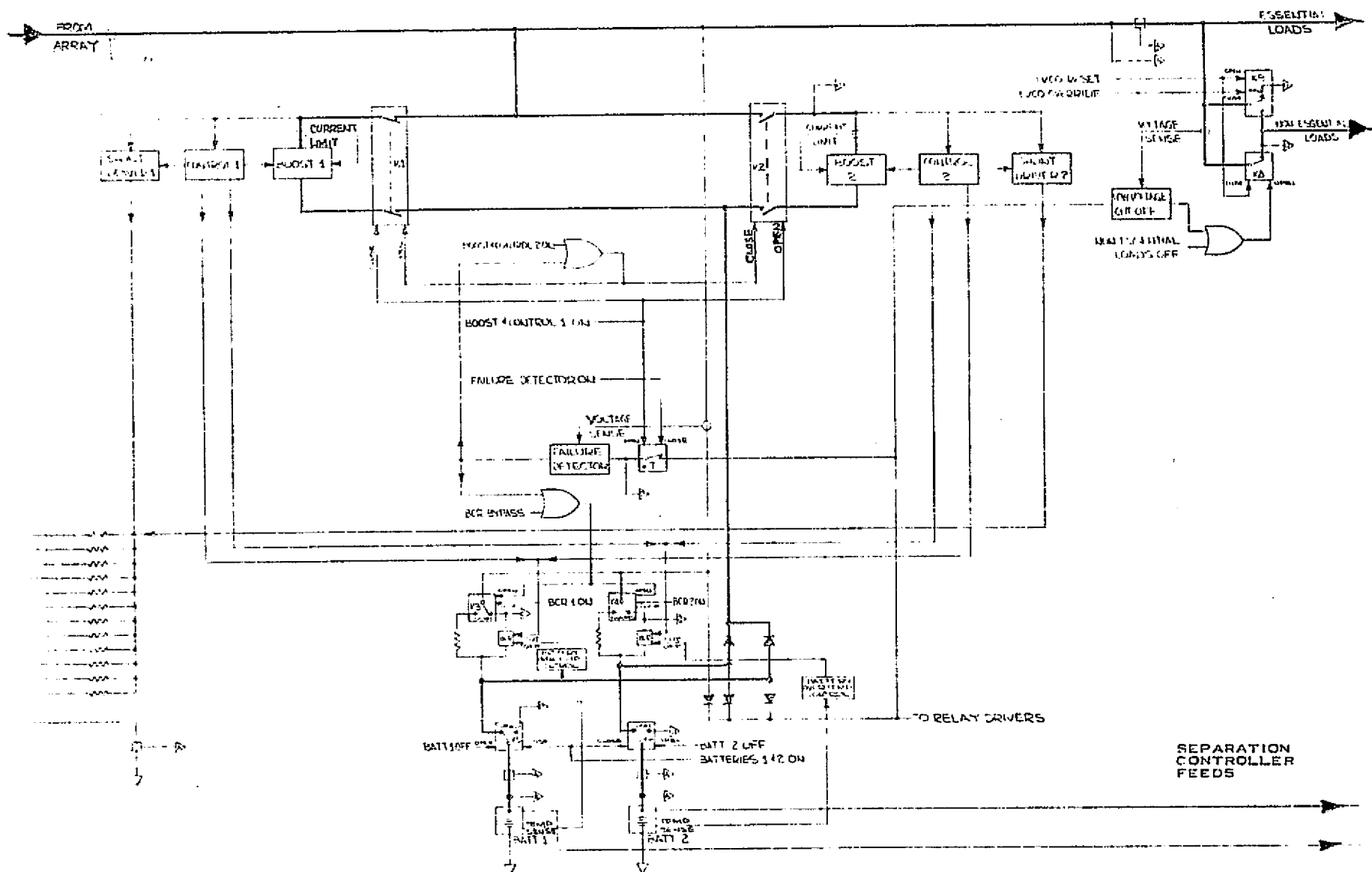


Figure B-16. Power Regulation Unit Functional Block Diagram

### 6.1.1 PRU - Boost Regulator

The Boost Regulator schematic is shown in Figure B-17. The Boost Regulator receives unregulated voltage and supplies regulated voltage to the user loads.

Unregulated voltage is applied to the center tap of both the primary and secondary winding of the output transformer T3. Therefore in the absence of any changing current in the primary, the secondary voltage will equal the unregulated input voltage (minus losses in copper and output rectifiers). Independent of this circuit function, a 10 KHz square wave voltage is produced by the saturable transformer T5. This square wave voltage is integrated by capacitor C14 and resistors R95 or R96, thus producing a constant amplitude triangular wave shape base drive into transistors Q39 and Q40. These wave forms are 180 degrees out of phase with one another. The emitters of these two transistors are connected to the collector of transistor Q45 which is driven by the regulation control unit. The error signal from the regulation control unit determines the collector voltage of Q45, thus determining the switching point of transistors Q39 and Q40. Thus, in this manner, the bias on the emitters of Q37 and Q38 is established at a level where the transistors turn on only when the triangular voltage has reached a sufficiently high voltage level ( $V_{BE(SAT)}$ ). Because the level of the triangular waveform is a function of the time from the beginning of the triangle, this circuit produces an output signal of variable pulse width. The actual width is a function of  $V_{CE}$  of Q45 which is actually a function of the error signal. This signal is stepped down in voltage by transformer T4 as a quasi square wave and used as base drive for the power transistors. The power transistors Q37 and Q38 amplify this quasi square wave, rectify it by CR 59 and CR 60 and add to the existing input voltage to



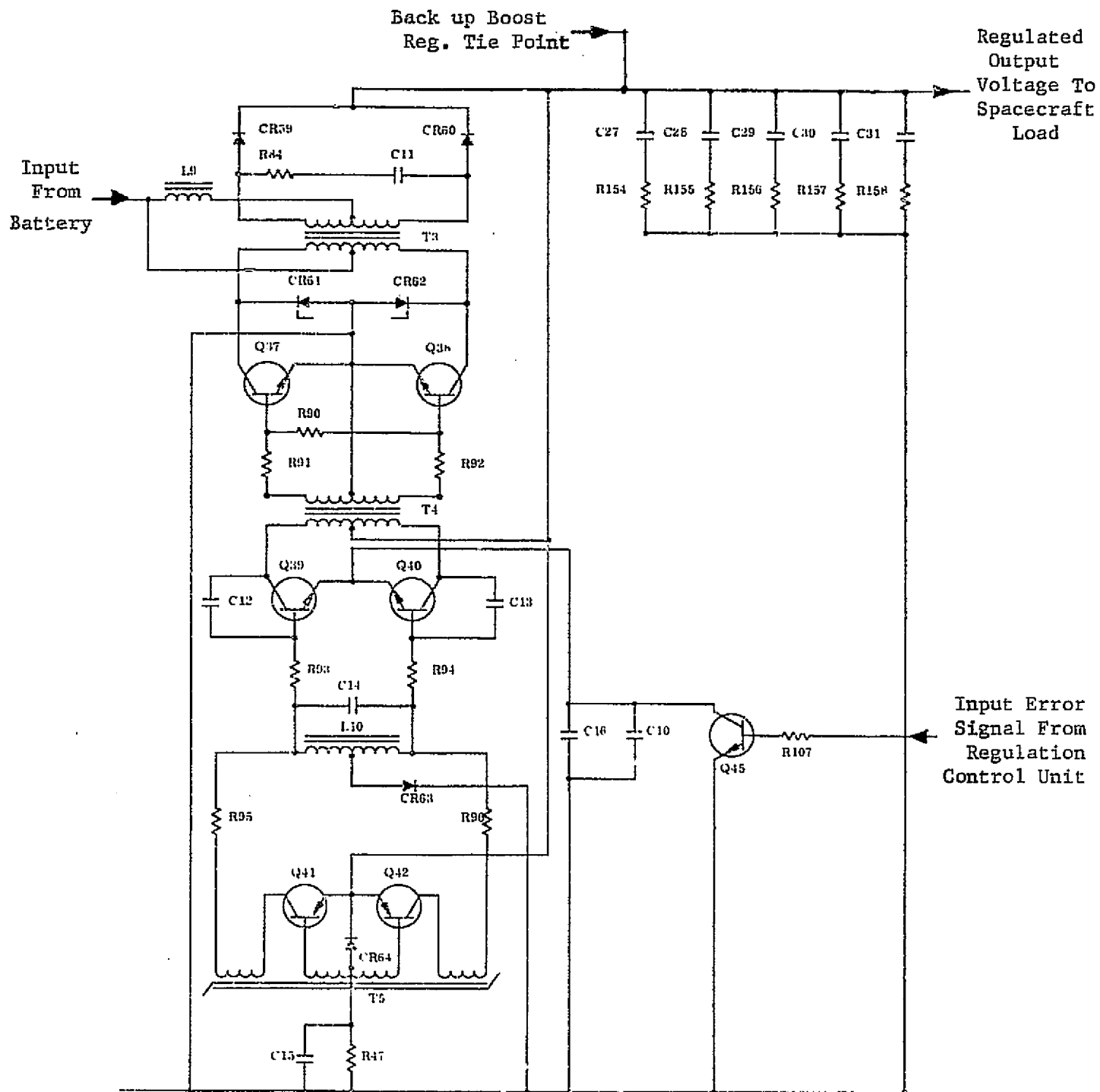


Figure B-17. Boost Regulator Schematic

provide a boosted regulated output voltage. The pulses produced are filtered by L9 and capacitors C27 through C31. The sum of unregulated input plus variable pulse width power constitutes the regulated output voltage. A block diagram of the boost regulator is shown in Figure B-16.

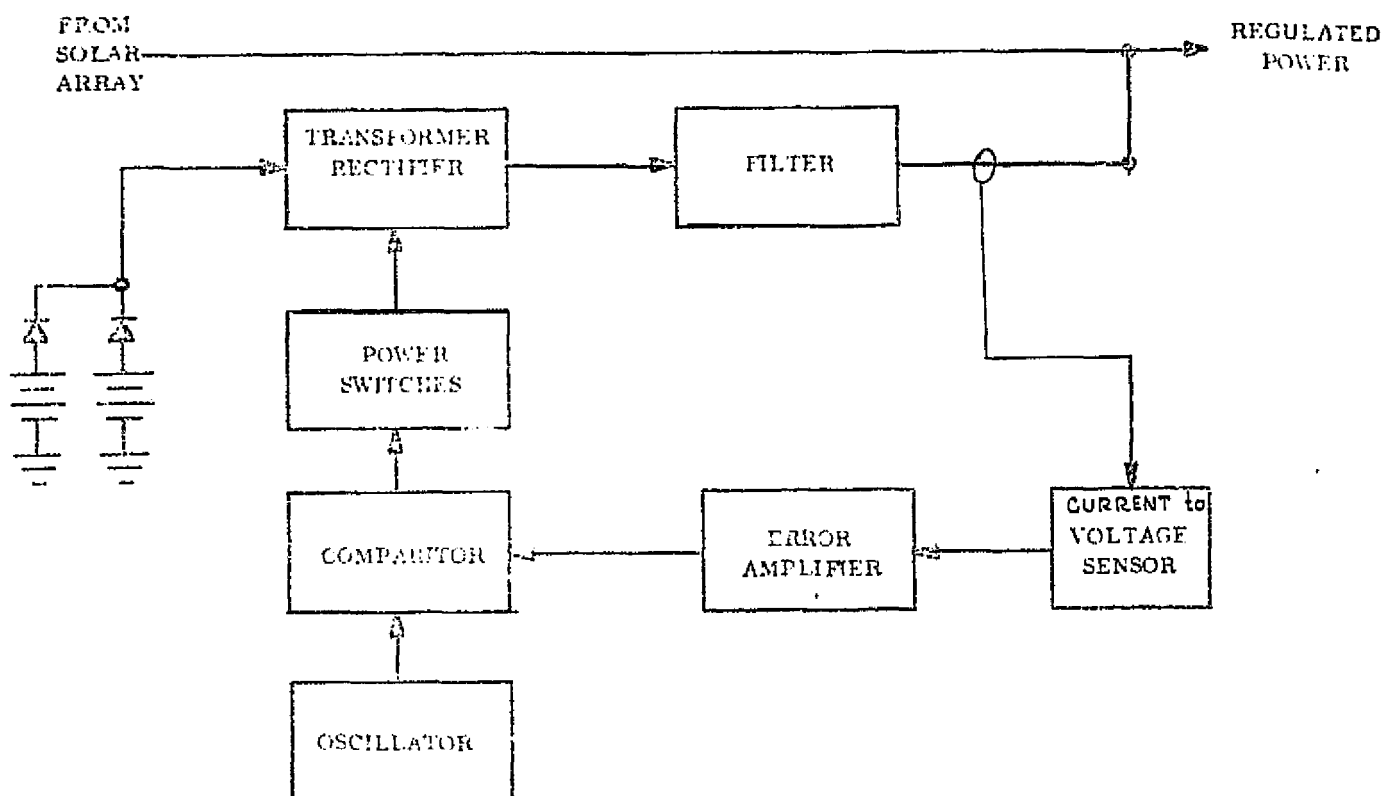


Figure B-18. Boost Regulator Block Diagram

#### 6.1.2 Boost Regulator Output Filter Capacitors

Five 400 microfarad tantalum foil capacitors (C27 through C31 Figure B-17) are used for filtering the output of the Power Regulation Unit. These capacitors are common to both redundant boost regulators for the following reasons:

1. Whenever a backup unit is turned on, the current through the relay contacts is just the load current of that particular unit at the time of switching. This eliminates any surge current to charge the capacitors if they were just being switched on to the bus line.
2. The capacitors maintain a constant bus voltage if there is a power interrupt of very short duration.

The five 400 microfarad capacitors in parallel are individually in series with low impedance, low power resistors which provide a fusing effect should one of the capacitors fail short to ground. Also, any failure of one of the capacitors will not in any way provide an output ripple in excess of the specified amplitude, or degrade the stability of the Power Regulation Unit.

#### 6.1.3 PRU - Boost Regulator - Efficiency vs. Output Power

The efficiency ranges from a minimum of 84% to a maximum of 95%. At the minimum load test point of 40 watts, the efficiency ranges from 84% to 88.5% over the full temperature and input range. At 250 watts, and the same environmental conditions, the efficiency ranges from 90% to 92.5%. The regulator was tested out to 440 watts with the efficiencies as indicated in Figure B-19. The general shape of the curves follows that of the typical regulator, i.e.,

1. Low efficiency at minimum load because of constant power losses.
2. Maximum efficiency at the design point.
3. Reduction in efficiency above the optimum load point because various parts are operating above their optimum point.

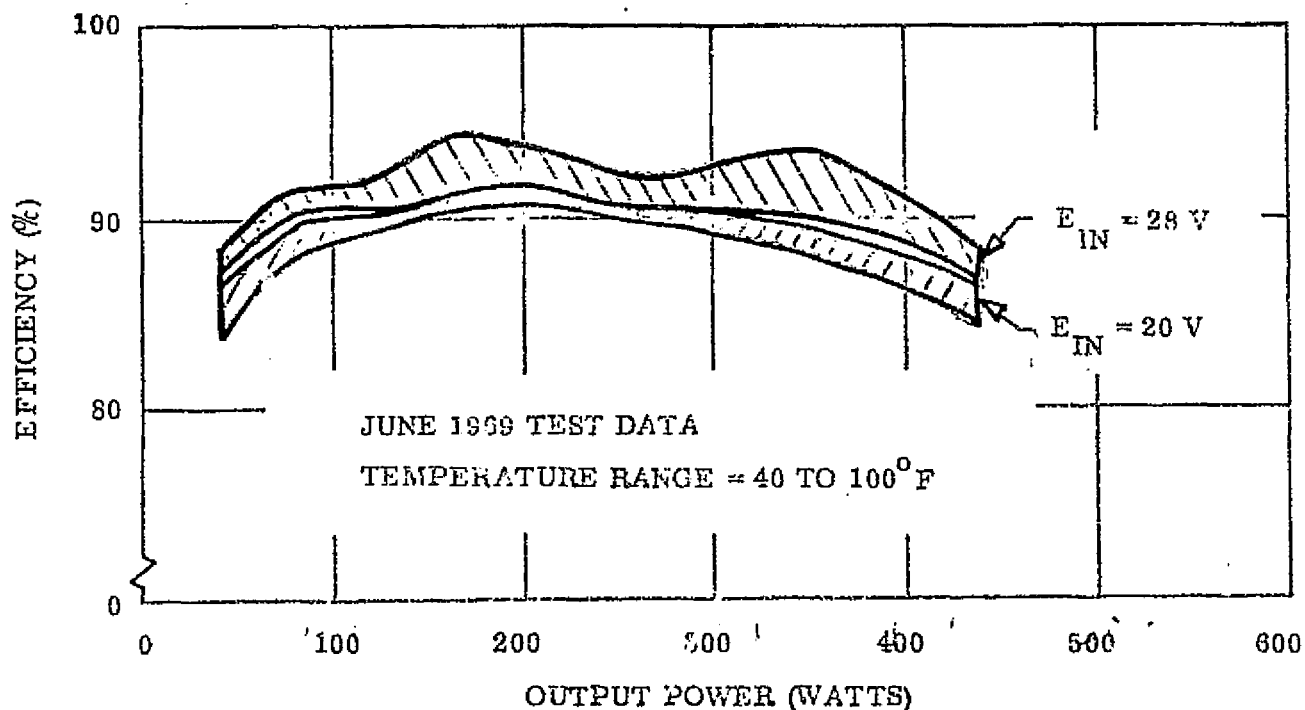


Figure B-19. Boost Regulator Efficiency versus Power

This type of characteristic is the normal one for regulators because usually low weight and high efficiency are incompatible. Therefore, the system is usually designed for a specified efficiency at a load level at which it will operate for the maximum time. The designer is willing to accept a lower efficiency at extremely high loads because these loads occur for only a short period of time, thus optimizing the weight/efficiency trade off.

#### 6.1.4 PRU - Battery Charge Regulator

The schematic diagram of the Battery Charge Regulator is shown in Figure B-20. There exists one Battery Charge Regulator for each battery and this is backed up with a resistor.

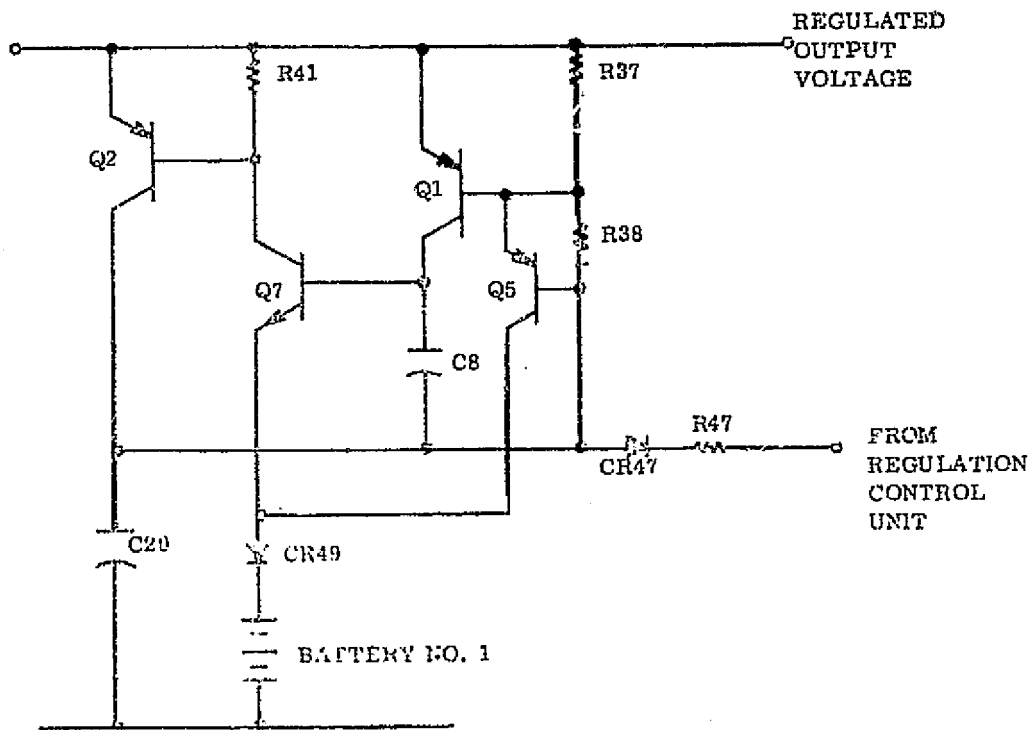


Figure B-20. Battery Charge Regulator Schematic

The regulation control unit introduces an error voltage to the battery charge regulator. If the line voltage is high enough the battery charge regulator is "enabled on" by lowering the potential of transistors Q5 and Q1. Transistor Q1 thus increases the base drive potential of Q7 providing charge current into the battery. As the array voltage tries to increase further, the battery current increases until a 1.2 ampere (C/10) level is reached. At 1.2 amperes, resistor R41 develops the voltage  $V_{BE}$  required to turn on transistor Q2. This limits the charge current by raising the voltage at the base of transistor Q5, thus turning it off.

The diode, CR49, is used to protect the transistors from a reverse voltage in case the bus voltage goes below the battery voltage during a failure or a transient. The block diagram for the battery charge regulator is shown in Figure B-21.

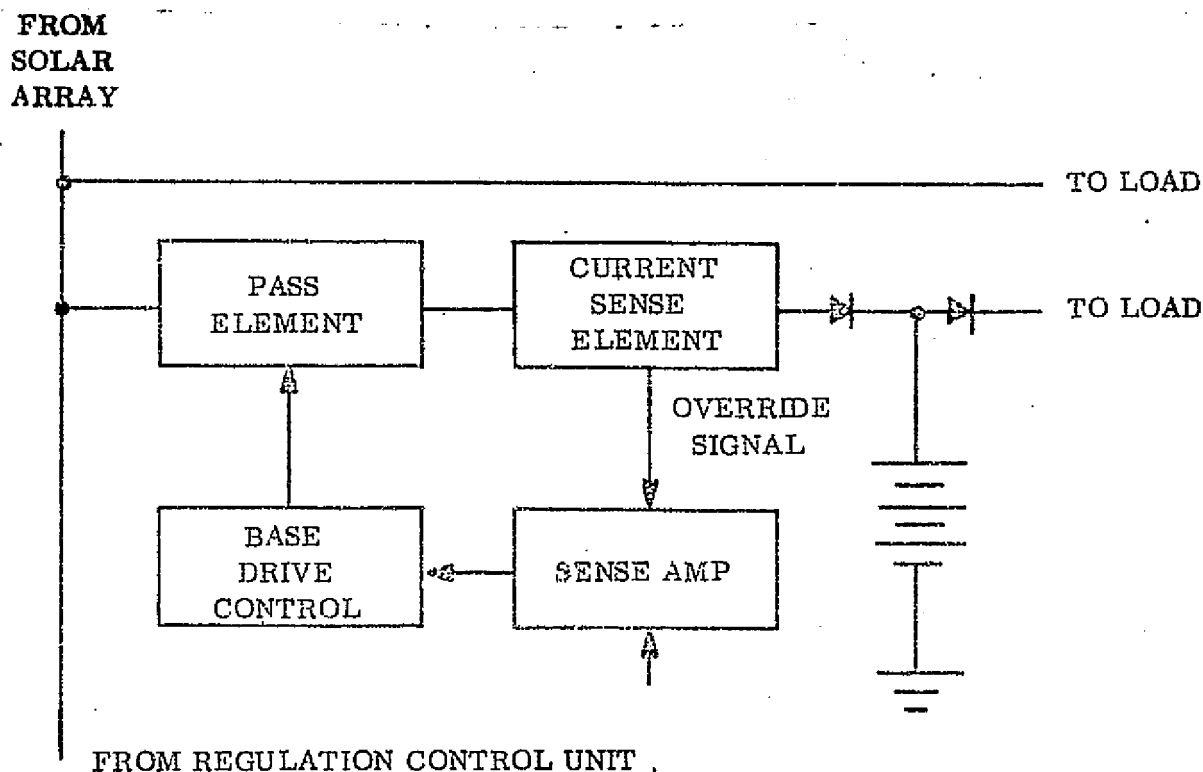


Figure B-21. Block Diagram of Battery Charge Regulator

#### 6.1.5 PRU - Shunt Regulator Control

The Shunt Regulator Control schematic is shown in Figure B-22. As the solar array voltage attempts to rise above that permitting the maximum battery charge rate,  $C/10$ , additional current is drawn from the lower half array in the shunt transistors. In order to operate the transistors at a lower voltage, and therefore a lower power point, only a part of the array is shunted.

### 3. SHUNT REGULATOR CONTROL

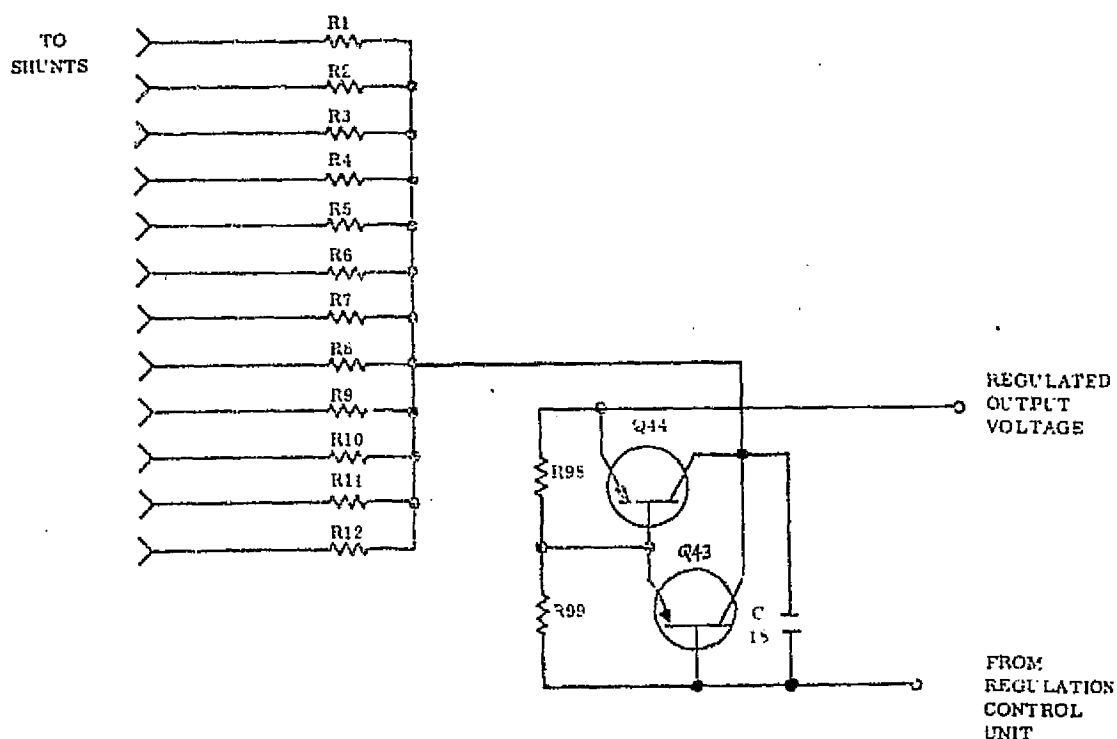


Figure B-22. Schematic of Shunt Regulator Control

The tap point on the solar array is selected considering the post-eclipse maximum case. This minimum temperature case will result in the highest array voltage characteristics, and the tap point must be selected so that the open circuit voltage on the unshunted portion of the array does not exceed the desired output voltage. A tap point 42 cells from the return bus in the series string was chosen, resulting in a calculated array section voltage of 27 v during the post-eclipse maximum. This yields a shunt voltage of 2.5 v allowing some margin for errors in estimating temperature.

The regulation control unit introduces an error control voltage to the shunt regulator control, thus biasing transistors Q43 and Q44. As the regulated

bus voltage increases the bias to those transistors also increases thus increasing the voltage at the resistors R1 through R12, and providing more drive to the shunts and drawing more current from the array. The result is that the main bus voltage is lowered into regulation.

#### 6.1.6 PRU - Regulation Control Unit

The schematic shown in Figure B-23 is that of the Regulation Control Unit. The output voltage is sensed by the regulation control unit and compared to a reference. An error voltage is produced that is proportional to the difference in actual output voltage and desired output voltage.

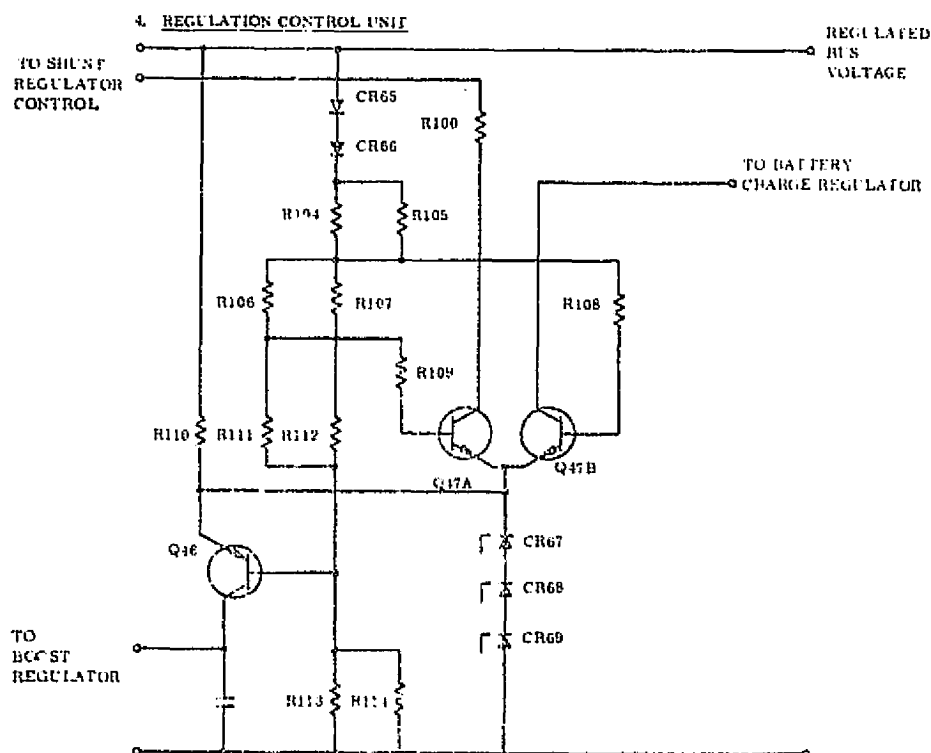


Figure B-23. Regulator Control Unit Schematic



The regulation control unit biases either the boost regulator when the bus voltage is low or the battery charge regulator when the boost regulator is off. There is more than adequate power available for the loads and the shunt regulator control when there is an excess power available and the batteries are being charged at a C/10 rate.

At a very low array voltage, when additional power is required, transistor Q46 turns on providing a bias to the boost regulator. In this condition the transistors Q47A and Q47B are off. The zener diodes CR67 through CR69 are used as a reference for the regulation control unit. As the bus voltage rises, transistor Q46 turns off and transistor Q47B turns on next, thus biasing the battery charge regulator.

Because transistor Q46 is used to turn on the boost regulator when the main bus voltage is low, a PNP transistor was used, and because transistor Q47A is used to turn on the battery charge regulator when the main bus voltage is high an NPN transistor was used. This combination of transistors aids in preventing both the boost regulator and the battery charge regulator being turned on simultaneously by their difference in bias polarity with the emitters being tied to the same zener reference CR67 through CR69.

When the battery charger is satisfied and the regulated bus voltage rises even further, transistor Q47A turns on thus providing bias voltage to the shunt regulator control. The transition through the three modes of operation has been demonstrated to be extremely smooth. (The only noticeable difference on the regulated bus voltage is a larger ripple when the boost regulator is in operation, compared to the other two modes of operation.) Diodes CR65 and

CR66 are used as a negative temperature compensation to improve the regulation with temperature. An additional function performed by the regulation control unit is current limiting of the boost regulator.

The circuit shown in Figure B-24 senses the output current of the boost regulator. If the current exceeds 15 amperes (at 450 watts from the boost regulator) the voltage across resistor R18 exceeds the breakdown voltage of the zener diode CR70, thus turning on transistor Q48. This will turn transistor Q45 off thus raising its collector voltage. Because the turning on of the boost regulator and the pulse width control depends on the collector voltage of Q45, the higher the voltage the more "off time" there is of the boost regulator. With Q45 off the boost regulator turns off.

#### 6.1.7 PRU - Failure Detector and Low Voltage Cutoff

The circuit shown in Figure B-25 senses the bus voltage for an over/under voltage condition. At over voltage, this device regulates at  $\pm 2\%$ , at low voltage ( $-10\%$ ) it disconnects the nonessential loads.

1. Failure Detector. The failure detector monitors the bus voltage for over-voltage and under-voltage conditions. If the regulated bus voltage exceeds  $+2\%$ , the output of A2 (referenced to the zener diode CR74) becomes low (A1 and A2 normally high). This turns off transistor Q29 which was charging capacitor C24 (providing a time delay to make sure that this condition does not occur during transients) until the zener breakdown voltage of CR75 is exceeded. This turns on transistors Q28A, Q20, Q28B and Q27, providing a current path through K1, K2, K3 and K4 relay coils thus switching to the backup components consisting of the boost regulator, shunt control, and regulation control unit. It also disconnects the two battery charge regulators and connects the trickle charge resistors R35 and R36.

Figure B-24. Schematic Diagram of Current Limiter of Boost

Figure B-25. Failure Detector Schematic

The same thing occurs when the bus voltage goes below -2%, except that now A1 becomes low. In order to determine the location of the fault, ground command can put each individual circuit back on the line until the improper load is identified. Override capability is included to bypass the failure detector by ground command.

2. Low Voltage Cutoff (LVCO). The low voltage cutoff disconnects the non-essential loads when the bus voltage goes below -10%. If an overload occurs such that the regulated bus voltage exceeds the -10% limit (referenced to the zener diode CR76), the output of A3 becomes low thus turning transistor Q35A off charging capacitor C26 (providing a time delay for transient rejection) until the zener breakdown voltage of CR77 is exceeded. This turns on transistors Q35B and Q32, energized K8 relay coil, and disconnects the nonessential loads. Ground command can override the low voltage cutoff by either resetting relay K9 (automatically opening relay K9) or closing relay K9 which is an override for the low voltage cutoff and a backup path for the nonessential loads. Figure B-26 shows the LVCO block diagram.

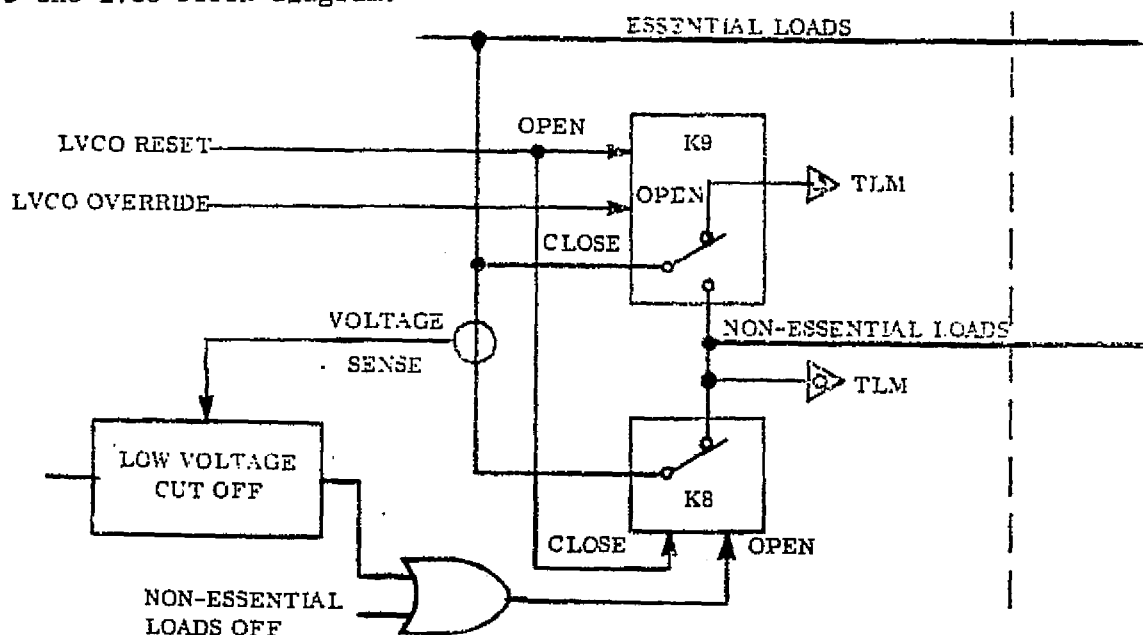


Figure B-26. Low Voltage Cutoff Block Diagram

### 6.1.8 PRU - Battery Over Temperature Control

The battery over temperature control circuit limits the battery temperature due to continuous overcharging by the charge regulator at the C/10 rate.

The schematic of the battery over temperature control is shown in Figure B-27.

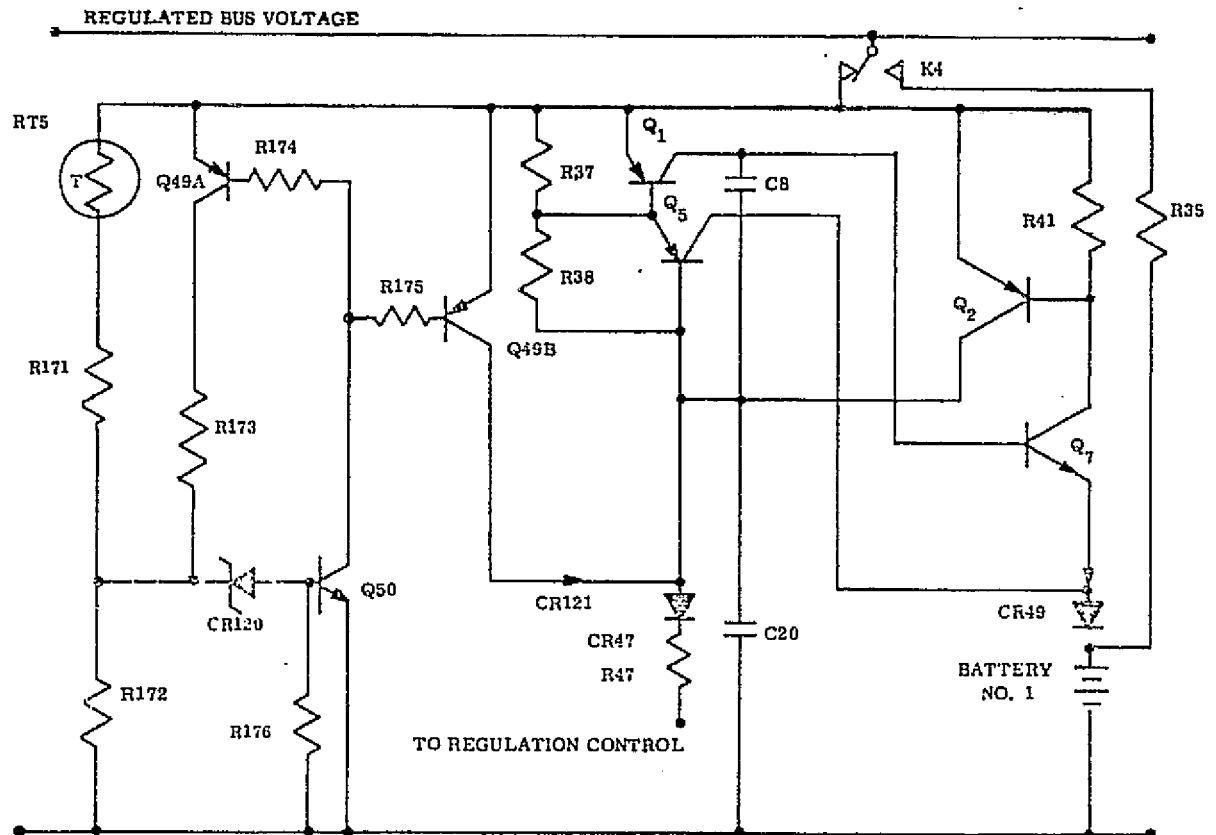


Figure B-27. Battery Over Temperature Control Schematic

As the battery temperature reaches 100°F, the voltage at the base of the transistor Q50 increases to a point where the transistor saturates.

As Q50 turns on, transistors Q49A and Q49B saturate. Transistor Q49B back biases transistor Q5 in the battery charge regulator, thus turning off transistors Q1 and Q7 (thus turning the battery charge regulator off).

Transistor Q49A closes the loop in the circuit and keeps the battery temperature control circuit turned on; that is, it keeps the battery charge regulator turned off even if the battery temperature returns to below 100°F.

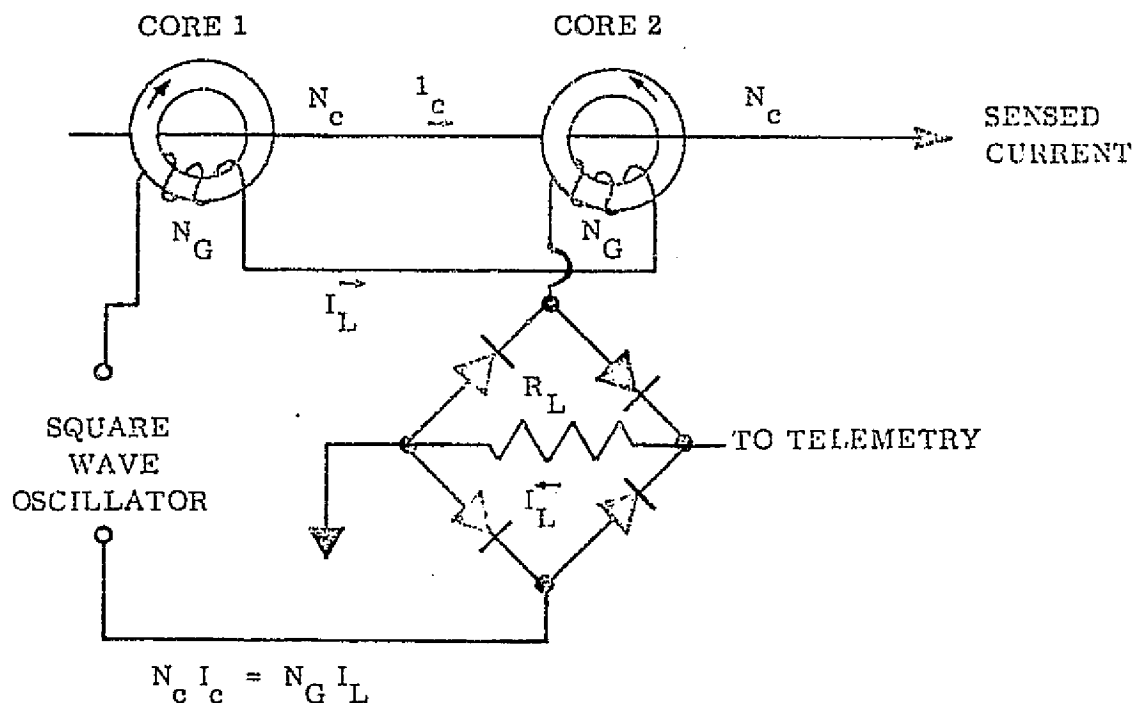
Ground command can override the battery over temperature control circuit by switching relay K4 into the trickle charge resistor R35. This will disconnect the battery charge regulator and deactivate the battery over temperature control circuit. If the battery charge regulator needs to be turned back on, relay K4 can be switched back to the battery charge regulator position and the battery over temperature control circuit will remain off (thus charging the battery) until the battery temperature reaches 100°F again.

The on and off switching of relay K4 in order to disconnect and then reconnect the battery charge regulator would not normally be done since the battery temperature of 100°F is an abnormal condition. The battery over temperature control circuit is only a safety device to protect the battery from over temperature until ground can react to the problem. This circuit would normally be turned off.

#### 6.1.9 PRU - Current Monitors

The seven current monitors used in the Power Regulation Unit were designed using the ac excited, direct current transformer method. The basic concept of the design is illustrated in Figure B-28. This current-to-voltage transducer consists of two coils stacked such that their flux polarities are opposing. The power lines (Nc) whose current is being sensed provides current which is designed to saturate both cores.

For the positive half-cycle of the square wave excitation, the gate winding of one core produces ampere turns to drive its core further into saturation. The other gate produces ampere turns to take its core out of saturation. Because the gate turns are large with respect to the one turn passing through the center, and the resistance  $R_L$  is properly sized, the law of equal ampere turns applies. Therefore, for each half cycle,  $N_c I_c = N_g I_L$ . Therefore,  $I_L$  is a function of the sensed current and the proper selection of  $R_L$  yields the required scaling for interfacing with the remote multiplexers of the telemetry system.



$I_L$  = AVERAGE VALUE OF RECTIFIED LOAD CURRENT

Figure B-28. Current Monitor Basic Concept Diagram



These devices provide 3% accuracy over a temperature range of 23 to 131<sup>o</sup>F as verified on over 100 space flight proven units. The major advantage of this technique is the complete isolation of the power line from the sensing circuit. Any failure in any of these current monitors can in no way jeopardize the power line.

#### 6.1.10 PRU - Command and Telemetry Interfaces

Command and Telemetry for the Power Regulation Unit is shown in Tables B-3 and B-4.

#### 6.1.11 PRU - Parameters

The Power Regulation Unit requires a volume of 1100 cubic inches and weighs approximately 25 pounds. The worse case minimum efficiency is 85.6 percent; best case maximum efficiency is 99.8 percent, based on nominal spacecraft conditions. An efficiency curve versus output power is shown in Figure B-8. A summary of breadboard data shows the source impedance to reach a minimum of 5 milliohms at 100 Hz. A maximum impedance of 300 milliohms will be reached at 300 Hz which is the resonant frequency of the Boost Regulator output filter. This value is reached only when the Boost Regulator is operating. The loads requiring a source impedance of 100 milliohms are connected to PIC's or ECB's (i.e. Power Interface Controllers or Electronic Circuit Breakers) which are located in the power controllers.

Voltage regulation between the extremes of minimum input voltage, maximum output current, and maximum input voltage, minimum output current, for a temperature variation of 60<sup>o</sup>F, is better than  $\pm 1.5$  percent. A voltage regulation curve versus user load power is shown in Figure B-9.

Table B-3. PRU Commands

No.	Name	Function
1	Boost & Control 1 Select	Connects Boost & Control 1, disconnects Boost & Control 2, disconnects failure detector
2	Boost & Control 2 Select	Connects Boost & Control 2, disconnects Boost & Control 1
3	Failure Detector ON	Connects failure detector
4	Battery 1 OFF	Disconnects Battery 1 from charge/discharge circuits
5	Battery 2 OFF	Disconnects Battery 2 from charge/discharge circuits
6	Batteries ON	Connects both batteries to charge/discharge circuits
7	Battery Charge Regulator 1 ON	Connects Battery 1 charge regulator and disconnects resistor
8	Battery Charge Regulator 2 ON	Connects Battery 2 charge regulator and disconnects resistor
9	Battery Charge Regulators Bypass	Disconnects both battery charge regulators and connects resistors
10	Low Voltage Cutoff Reset	Reconnects loads to bus which were disconnected by low voltage cutoff, and enables subsequent cutoff
11	Low Voltage Cutoff Override	Disconnected by LVCO, disables LVCO
12	LVCO Loads OFF	Disconnects loads which can be removed by LVCO until subsequent Reset or Override Command
13	Battery Over Temperature 1 OFF	Turns OFF the battery over Temperature 1.
14	Battery Over Temperature 2 OFF	Turns OFF the battery over Temperature 2.

Table B-4. PRU Telemetry Interface

No.	Name	Type	Description
1	Battery 1 Voltage	A	Battery 1 voltage
2	Battery 2 Voltage	A	Battery 2 voltage
3	Battery 1 Current	A	Battery 1 charge/discharge current
4	Battery 2 Current	A	Battery 2 charge/discharge current
5	Battery 1 Status	D	Battery 1 connected/disconnected to charge/discharge circuits
6	Battery 2 Status	D	Battery 2 connected/disconnected to charge/discharge circuits
7	Battery Charger 1 Status	D	Battery 1 BCR/resistor charge mode
8	Battery Charger 2 Status	D	Battery 2 BCR/resistor charge mode
9	Boost and Control Status	D	Boost and Control 1/boost and control 2 ON
10	Regulated Bus Voltage	A	Regulated bus voltage
11	Total Regulated Power Load Current	A	Total power subsystem output current
12	Solar Array Output Current	A	Total solar array output current
13	Total Shunt Current	A	Total shunt current
14	Nonessential Loads Bus Status	D	Nonessential load bus ON/OFF
15	LVCO Status	D	LVCO Overridden/Not Overridden
16	Failure Detector Status	D	Failure Detector ON/OFF
17	Battery 1 Temperature	A	Battery 1 temperature
18	Battery 2 Temperature	A	Battery 2 temperature
19	PRU Temperature 1	A	PRU Internal temperature
20	PRU Temperature 2	A	PRU Internal temperature

## 6.2 Shunt Regulator

The shunt regulator maintains the main bus voltage constant during the time that the solar array provides all of the spacecraft power. Output voltage is sensed and when it tends to change from its present value an error signal is provided. This error signal controls conduction of the shunt transistors which in turn draw current from a portion of the solar array and thereby dissipate the excess power. The additional current drawn represents a voltage drop; this voltage drop keeps the main bus voltage within the specification limits ( $29.5V \pm 2\%$ ).

The shunt consists of a Darlington amplifier in parallel with a portion of each solar array string. All of the Darlington amplifier inputs are controlled by the error signal generated in the power regulation unit. The physical position of the transistors is such that the mounting surfaces are kept close to an isothermal temperature.

The maximum voltage appearing across the Darlington amplifier is 15 volts.

The maximum power is 20 watts at 10 volts, on a per-shunt element basis.

There are 12 shunt elements in the spacecraft. Each shunt weighs approximately 0.5 pounds and consumes a volume of 9.4 cubic inches.

### 6.3 Power Controllers

Two Power Controllers will be required to distribute bus power to the various electronic components within each subsystem. Individual Power Interface Controllers (PIC) located within each Power Controller will supply individually regulated power,  $+28\text{vdc} \pm 1\%$  to each of the experiments. Individual Electronic Circuit Breakers (ECB) located within Power Controller No. 1 will supply bus power to each vended electronic component in the Control Subsystem.

The required redundant on and off commands from the Remote Command Decoders will be accepted by each PIC or ECB to apply power to nonessential loads. A telemetry signal will be supplied by each PIC and ECB to indicate when power is being applied. The digital type signal, +5.0 volts in the on condition and 0.0 volts in the 'off' condition will be routed to the Telemetry Subsystem.

Power Controller No. 1 weighs 7 pounds and requires a volume of 403 cubic inches. Power Controller No. 2 has a weight of 6 pounds and a volume of 200 cubic inches.

### 6.4 Electrical Performance PIC and ECB

Protection of the power source from damage due to malfunction in any load is provided by either an electronic circuit breaker or a power interface circuit. It provides for turn-on and turn-off by command. These circuits provide an automatic cutoff for a current overload which is resettable by ground command. Turn-on and turn-off rate of current change is limited to minimize conducted interference. It also provides filtering of each

individual load. In addition, the power interface controller also provides a  $\pm 1\%$  regulated line to experiment loads. The operation of the two circuits is discussed below.

The Power Interface Controller (PIC) and Electronic Circuit Breaker (ECB) circuits will be identical except for current loads and the regulation requirement of 28 vdc  $\pm 1\%$  for the PIC. Each ECB and PIC will ramp-on or-off by command at a peak rate of 100,000 amperes per second or less. Each circuit will ramp-off due to a current overload with a delay of approximately one second (See Figure B-29).

The load requirements will be standardized into various groupings to limit the number of different individual circuits and thereby increase reliability. This will allow for changes in power requirements during the design cycle by selecting the proper internal components when the final design power requirements are established.

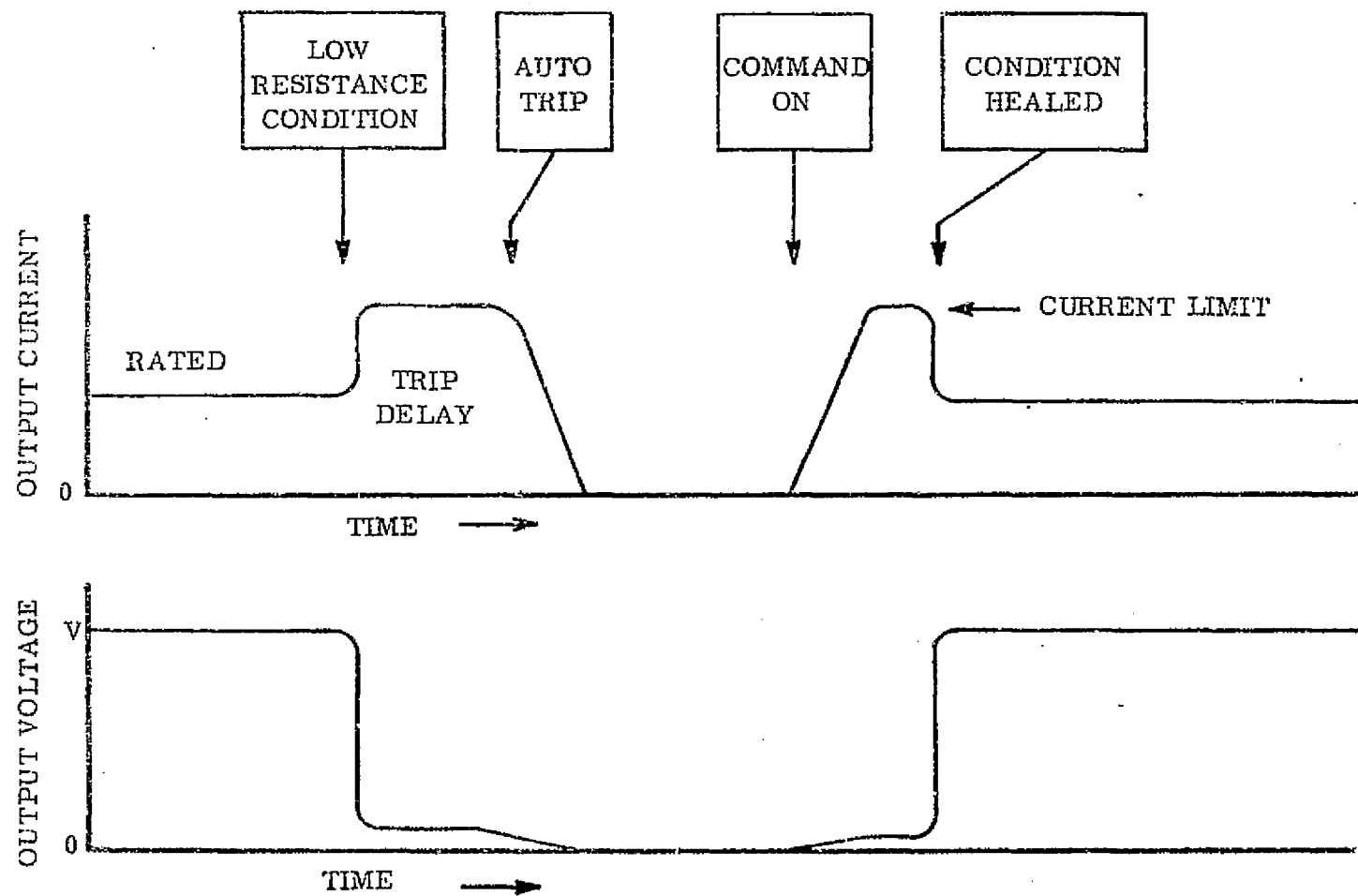
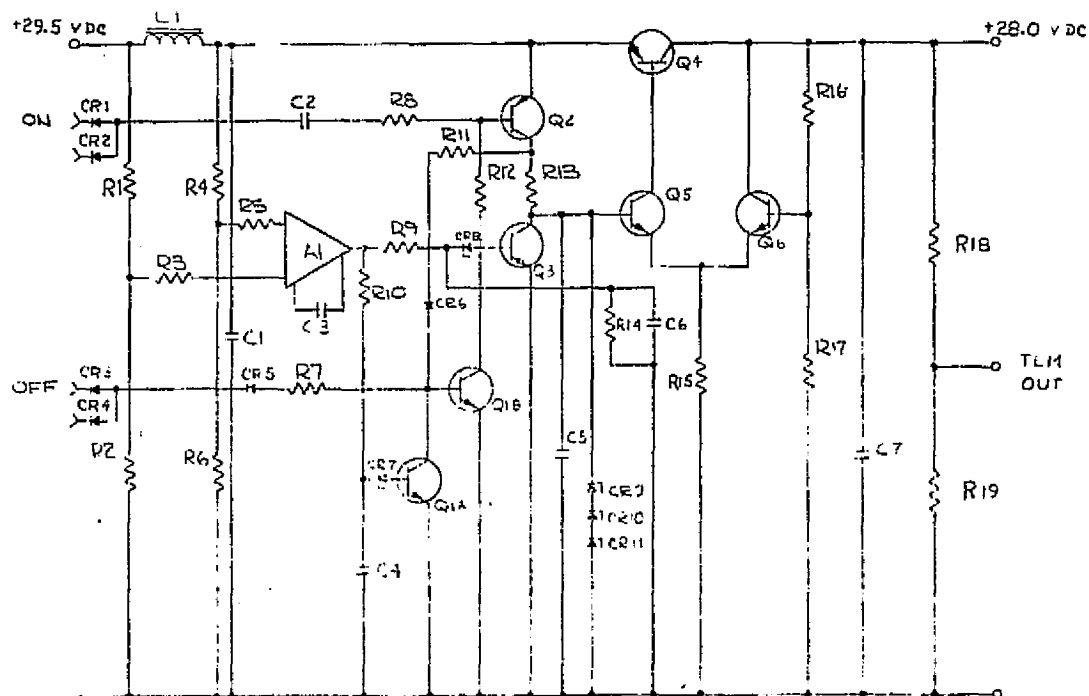


Figure B-29. ECB and PIC Operating Modes

The PIC is an electronic circuit breaker with series regulation. This is accomplished by controlling the base current for other than turn-on, turn-off conditions, by an error signal. This error signal is generated by the differential amplifier, Q6, Q5, R15, the voltage sense resistors, R16, R17, and the reference zener diodes, CR9, CR10, and CR11. Additional regulation and noise immunity is thereby provided for those loads requiring it.



B-49



The design limit for the output impedance of the PIC is 0.1 ohms over the frequency range of dc to 15 kilohertz. This requirement is easily satisfied using the circuit defined by the schematic of Figure B-30. The output impedance will remain below 0.1 ohms over a wide frequency range because of the nature of the active, high gain voltage regulator. For any real value of load current, the output terminal voltage is sensed with a resistor sampling network (R16 and R17), and compared with a zener reference voltage. The error signal developed is a function of the difference between the actual output terminal voltage and 28 volts established by the zener diode string (CR9, CR10, CR11). This error signal is then amplified and used to control the effective resistance of the pass transistor (Q4). When the load current changes, the voltage drop across the pass transistor is adjusted by the high gain feedback loop in order to maintain the output voltage constant. The output impedance is defined as the change in output voltage for a change in output current and therefore becomes the open loop impedance divided by the gain of the error amplifier which includes the pass element and all drive stages. The error amplifier open loop gain is sufficiently high to maintain the impedance to a level well below the specified 0.1 ohms. In order to ensure stable circuit operation, sufficient phase and gain margins are provided by rolling off the error amplifier response at the proper frequency. Low source impedance is maintained above the roll-off frequency by shunting the output terminals of the PIC with a capacitor. The capacitor, by exhibiting a decreasing impedance with an increasing frequency, maintains the PIC source impedance below the specified level.

## 6.6 Separation Controller

The application of power to actuation devices to accomplish the backup separation and deployment functions is controlled by ground command via the separation controller. Separate redundant firing circuits are provided for each function. Each function is interlocked to the completion of the previous function. Both enable and actuate commands are required. Command override is provided for all interlock functions. An AGE interface is provided to permit test sequencing of the separation and deployment functions. In addition to the initial deployment reference, the controller also contains the actuation circuits associated with COGGS and the enabling of the back-up cold gas attitude control thruster.

The separation controller connects the electro-explosive devices (EED) and actuators to the battery. This is controlled by command, sequence interlocks, and internal logic. The component contains arm/disarm switches for EED safety. It also provides event status telemetry and an AGE test interface for final EED circuit tests. The separation controller functional block diagram is shown in Figure B-31 and the arm/disarm scheme in Figure B-32.

The separation controller has a net weight of 8 pounds and consumes a volume of 269 cubic inches.

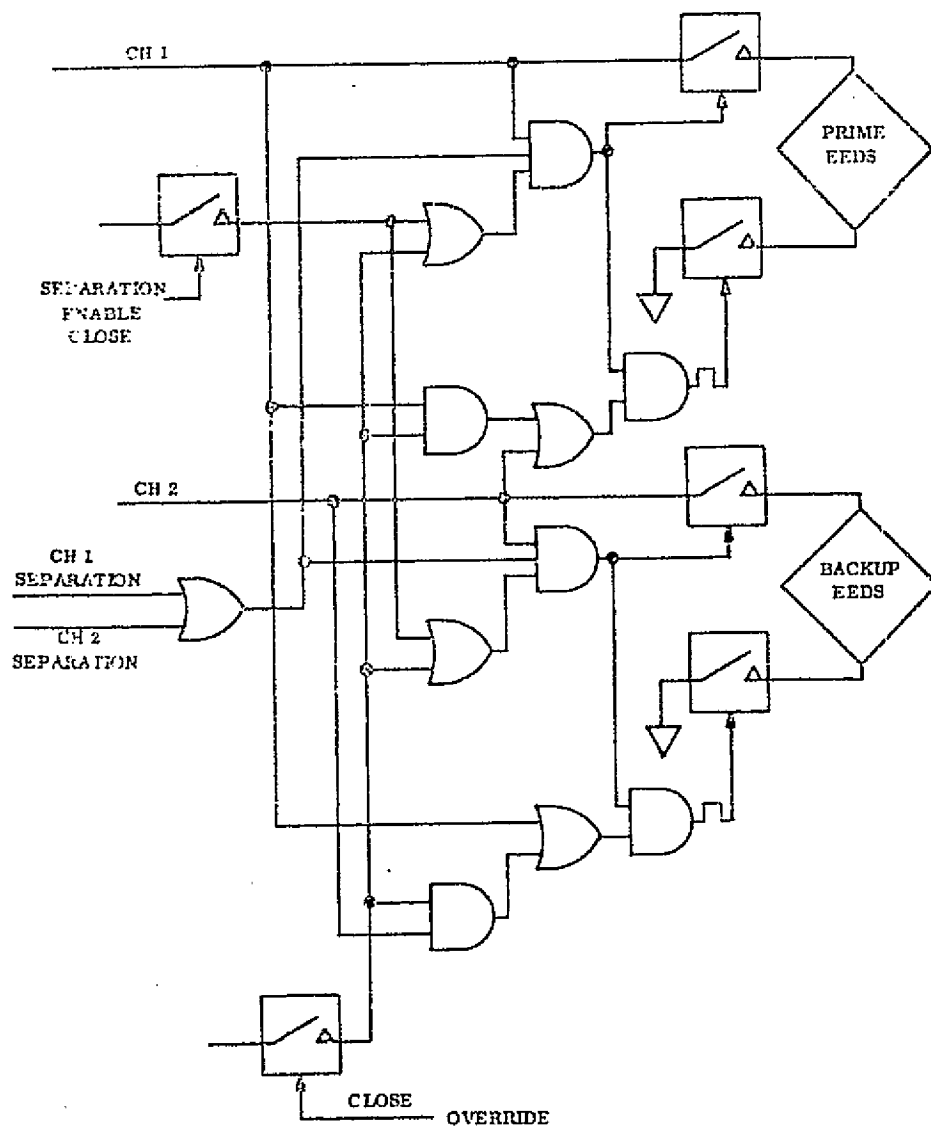


Figure B-31. Separation Controller Functional Block Diagram

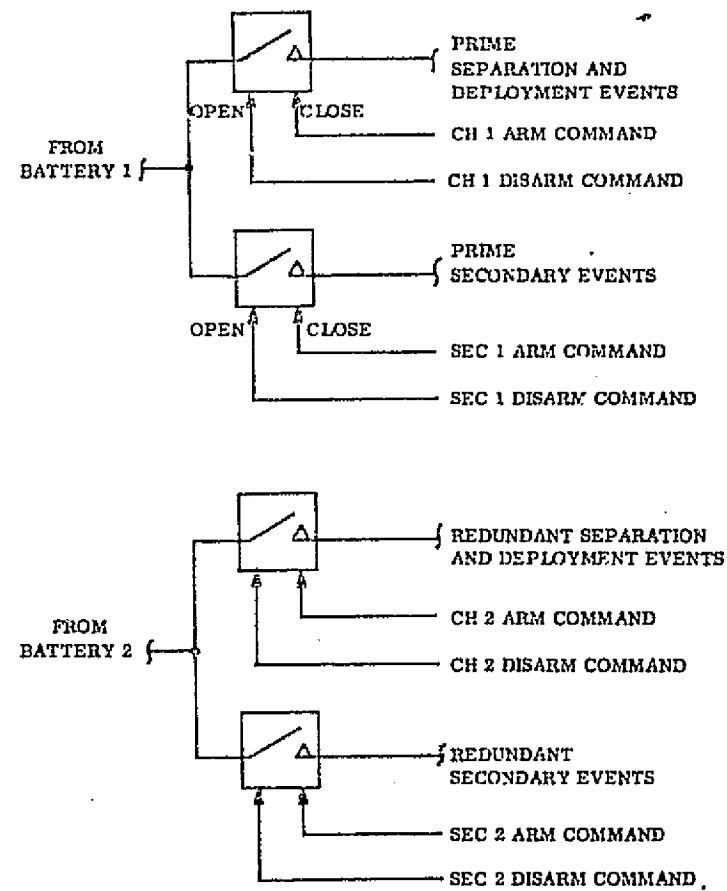


Figure B-32. Arm/Disarm Scheme

## 7.0 POWER SYSTEM PERFORMANCE CHARACTERISTICS

### 7.1 Benefits of Central Power Regulation

Beneficial side effects are available when a regulated bus system is selected over the distributed regulation system. The first is lower source impedance over the full range of array current. The unregulated solar array has a voltage change with current demand of approximately 1/2 volt per ampere, or an impedance of 0.5 ohms. The battery will have a lower inherent resistance than the solar array, but it too will show a decreasing voltage with increasing load current. In the shunt boost system, when the shunt regulator is operating in parallel with the solar array, the load can change over the full range of array current capability of approximately 18 amperes. The boost regulator will provide a characteristic impedance less than half that of the battery, and the bus will remain at 29.5 volts  $\pm$  2% or less than 1/2 volt per 18 amperes. This is a 10 to 1 improvement in source impedance when the loads are drawn from the solar array, and a 2 to 1 improvement over the battery.

A second advantage of a regulated bus system is constant voltage operation for all loads. Electronic piece part failure rates are a function of operating voltage, and typically increase with increasing applied voltage expressed as a percent of rated value. A piece part will operate more reliably at constant voltage than it will over a voltage range, provided that the part is applied at the same percent of rated voltage in both systems. An additional advantage of constant voltage is that devices such as solenoids and relays can be applied more easily. A common problem is assuring that the solenoid device will operate at a minimum voltage and

still be capable of dissipating power applied at the maximum voltage, since the dissipation increases with the square of the applied voltage. When a part is selected for minimum voltage and the voltage varies, the excess voltage causes wasted power, thermal degradation, and an increase in failure rates.

The third advantage is a weight and power saving outside the power subsystem. There is a saving in secondary power conditioning equipment since these devices will require less drive capability when they are designed to operate at constant voltage than if they are designed to operate over a range of input voltage. Savings occur from the power difference and the weight of heat sinks and thermal conductive paths.

An overall view of the vehicle electrical system indicates that significant advantages will accrue from selection of a regulated bus voltage approach. A single-point voltage is sufficient for analysis and test, rather than a continuous range. More reliable performance and fewer system test constraints are required for such devices as power converters, solenoids, relays, and heaters. The experiments, when turned on, will operate at a constant thermal condition. Power conditioning circuits with a constant input voltage are simplified in that they operate with increased efficiency and with a lower total weight than those designed to accept a wide range of input voltage.

## 7.2 Trade Studies

Trade studies were performed to make a selection among three alternate photovoltaic/battery power subsystems as indicated in the first column of Table B-5.

The studies considered weight, power capability, reliability, efficiency and ease of implementation. The results of the studies (Table B-6) indicated the selection of shunt-boost approached as the best to meet ATS F & G mission requirements. Additional details are available in GE proposal (SD proposal N-21630) for Applications Technology Satellite F & G, Phase D, Book 1, Technical Volume IE, Power, Date 17 Sept. 1969.

TABLE B-5. Subsystem Performance Matrix

Alternative	Average Power Available at 2 Year Design Point (Watts)	Reliability Figure of Merit
Shunt-boost	410	0.9668
Shunt-series	$410 \pm 1\%$ *	0.9635
Distributed Regulation	385	0.9658
* Detailed analysis not performed. Performance estimate based on known component efficiencies, in comparison to shunt-boost approach.		

APPENDIX C

THREE-PHASE, 400 HERTZ AIRCRAFT ELECTRICAL SYSTEMS

## APPENDIX C

### Three-Phase, 400 Hertz Aircraft Electrical Systems

#### TABLE OF CONTENTS

<u>SECTION</u>		<u>PAGE</u>
1.0	INTRODUCTION	C-1
2.0	ALTERNATE GENERATING SYSTEMS	C-2
3.0	AC TO DC CONVERTERS	C-3



# LIST OF TABLES

<u>TABLE</u>		<u>PAGE</u>
C-1	Characteristics of Ideal Rectifiers with Infinite Inductance Choke-Input Filters	C-4
C-2	Transformer Secondary Utilization for Multiple-Phase Rectifiers	C-5

## LIST OF ILLUSTRATIONS

<u>FIGURE</u>		<u>PAGE</u>
C-1	Three-Phase Half-Wave Rectifier Circuit	C-5
C-2	Three-Phase Half-Wave Voltage Waveform	C-6
C-3	Three-Phase Full-Wave (Bridge) Rectifier Circuit	C-7
C-4	Three-Phase Full-Wave Rectifier Voltage Waveform	C-7
C-5	Three-Phase Full-Wave Rectified Voltage Waveform	C-8
C-6	Three-Phase Double-Wye with Interphase Rectifier Circuit	C-8
C-7	Three-Phase Double-Wye with Interphase Voltage Waveforms	C-9

## 1.0 INTRODUCTION

Unless there is an unexpected breakthrough in the technology of exotic energy sources or dense energy storage devices, the electromechanical process will continue to be used for aircraft electronic power generation in the future, and in the space shuttle during the atmospheric transition.

Present aircraft use the constant speed, constant frequency system, in which a gearbox is installed with each engine. A drive shaft and a power disconnect coupling connect the gearbox to the engine power takeoff pad. The gearbox provides mounting pads for installation of an air turbine for engine start, a generator or a generator constant speed drive combination for the electrical system, one or two hydraulic pumps for the hydraulic system, and an air compressor for the pneumatic system. The gearbox usually incorporates a cooling system that includes a gear-driven air blower and an oil-to-air heat exchanger for cooling the gearbox and the accessories.

Various configurations have been developed to accommodate the conflicting requirements of variable engine speed and a constant frequency electrical system.

In the variable speed constant frequency system, the alternator operates at a relatively high and variable frequency. The alternator feeds an electronic cycloconverter that converts the high variable frequency to a low and constant frequency.

A second method is to use a DC link, either by a static rectifier and electronic inverter, or by a motor and generator set of rotating equipment. A modification of the conventional motor and generator set with its slip-rings and brushes is the line commutated rotating inverter that uses solid state commutation.

A third system uses a mechanical differential interposed between the variable speed engine and the constant speed alternator. An induction machine, running from the main AC line, adds or subtracts the engine speed in the differential drive to maintain a constant output speed to the alternator.

A wild frequency system controls the voltage but does not modify the alternator frequency. Frequency sensitive equipment is supplied with a rectifier and inverter.

Additional data is reported in "Study of Aircraft Electrical Power Systems," NASA CR-120939, June, 1972.

### 3.0 DC to DC CONVERTERS

AC power is converted to low voltage DC power by a circuit consisting of a step-down transformer, a rectifier, and a filter. When more than a fractional kilowatt of d-c power is required from an a-c source, a multiple-phase rectifier circuit is used typical of those shown on Table C-1. As the lowest harmonic frequency on the output ripple is increased, the rectifier conduction interval is decreased and the harmonic current content in the transformer secondary windings increases without an increase in d-c output power. This increases the required transformer rating, where the utilization factor (U.F.) of the transformer is defined as the ratio of the amount of d-c power delivered to the volt-amperes of transformer secondary rating required.

The total secondary volt amperes are  $mV/\sqrt{2}$  times the rms current, or

$$\text{volt-amperes} = m \frac{V}{2} \frac{V}{R} \sqrt{\frac{1}{2\pi} (\beta + \sin \beta + \cos \beta)}$$

and the d-c power delivered is

$$P_{d-c} = \frac{V^2}{R} (\sin \beta / \beta)^2$$

where  $\beta = \pi/m$  and  $m$  is the lowest harmonic frequency from Table C-1.

The utilization factor for an  $m$ -phase rectifier transformer is

$$\text{U.F.} = \frac{P_{d-c}}{\text{volt-amperes}} = \frac{2 \sin^2 \beta}{\beta \sqrt{\pi (\beta + \sin \beta + \cos \beta)}}$$

Values of the utilization factor have been determined and tabulated in Table C-2 for useful rectifier circuits. The maximum value occurs

TABLE C-1 CHARACTERISTICS OF IDEAL RECTIFIERS WITH INFINITE INDUCTANCE CHOKE-INPUT FILTERS

	SINGLE-PHASE FULL-WAVE SINGLE WAY	SINGLE-PHASE FULL-WAVE BRIDGE	TWO-PHASE FULL-WAVE STAR	THREE-PHASE STAR SINGLE WAY	THREE-PHASE BRIDGE	SIX-PHASE STAR SINGLE WAY	SIX-PHASE DOUBLE-WYE INTERPHASE
Tabulated Data based on Zero Rectifier and Transformer Resistance and Zero Transformer Leakage Inductance							
DC Load Current, $I_{d-c}$	1.00	1.00	1.00	1.00	1.00	1.00	1.00
Rectifier Average Current	$0.500 I_{d-c}$	$0.500 I_{d-c}$	$0.250 I_{d-c}$	$0.333 I_{d-c}$	$0.333 I_{d-c}$	$0.167 I_{d-c}$	$0.167 I_{d-c}$
Rectifier RMS Current	$0.707 I_{d-c}$	$0.707 I_{d-c}$	$0.500 I_{d-c}$	$0.577 I_{d-c}$	$0.577 I_{d-c}$	$0.408 I_{d-c}$	$0.289 I_{d-c}$
Secondary RMS Current	$0.707 I_{d-c}$	$I_{d-c}$	$0.500 I_{d-c}$	$0.577 I_{d-c}$	$0.816 I_{d-c}$	$0.408 I_{d-c}$	$0.289 I_{d-c}$
Peak Rectifier to Load Current Ratio	1.00	1.00	1.00	1.00	1.00	1.00	0.500
Secondary VA Rating	$1.57 I_{d-c} V_{d-c}$	$1.11 I_{d-c} V_{d-c}$	$1.57 I_{d-c} V_{d-c}$	$1.48 I_{d-c} V_{d-c}$	$1.047 I_{d-c} V_{d-c}$	$1.813 I_{d-c} V_{d-c}$	$1.49 I_{d-c} V_{d-c}$
Primary RMS Rating	$I_{d-c} V_s/V_L$	$I_{d-c} V_s/V_L$	$0.707 I_{d-c} V_s/V_L$	$0.577 I_{d-c} V_s/V_L$	$0.816 I_{d-c} V_s/V_L$	$0.577 I_{d-c} V_s/V_L$	$0.408 I_{d-c} V_s/V_L$
Primary VA Rating	$1.11 I_{d-c} V_{d-c}$	$1.11 I_{d-c} V_{d-c}$	$1.11 I_{d-c} V_{d-c}$	$1.48 I_{d-c} V_{d-c}$	$1.047 I_{d-c} V_{d-c}$	$1.282 I_{d-c} V_{d-c}$	$1.047 I_{d-c} V_{d-c}$
Total VA Rating	$2.68 I_{d-c} V_{d-c}$	$2.22 I_{d-c} V_{d-c}$	$2.68 I_{d-c} V_{d-c}$	$2.96 I_{d-c} V_{d-c}$	$2.094 I_{d-c} V_{d-c}$	$3.095 I_{d-c} V_{d-c}$	$2.537 I_{d-c} V_{d-c}$
DC Load Voltage, $V_{d-c}$	1.00	1.00	1.00	1.00	1.00	1.00	1.00
Output Voltage, $V_{d-c}$	$0.9 V_s$	$0.9 V_s$	$1.27 V_s$	$1.17 V_s$	$2.34 V_s$	$1.35 V_s$	$1.17 V_s$
DC Output Watts	$I_{d-c} V_{d-c}$	$I_{d-c} V_{d-c}$	$I_{d-c} V_{d-c}$	$I_{d-c} V_{d-c}$	$I_{d-c} V_{d-c}$	$I_{d-c} V_{d-c}$	$I_{d-c} V_{d-c}$
Rectifier Peak Inverse Voltage	$3.14 V_{d-c}$	$1.57 V_{d-c}$	$2.23 V_{d-c}$	$2.09 V_{d-c}$	$1.047 V_{d-c}$	$2.09 V_{d-c}$	$2.09 V_{d-c}$
Ripple Factor, m	2f	2f	4f	3f	6f	6f	6f
Peak to Peak Ripple Voltage	$1.57 V_{d-c}$	$1.57 V_{d-c}$	$0.326 V_{d-c}$	$0.604 V_{d-c}$	$0.140 V_{d-c}$	$0.140 V_{d-c}$	$0.140 V_{d-c}$
Rms Voltage, Lowest Harmonic	$0.471 V_{d-c}$	$0.471 V_{d-c}$	$0.250 V_{d-c}$	$0.177 V_{d-c}$	$0.0405 V_{d-c}$	$0.0405 V_{d-c}$	$0.0405 V_{d-c}$
Rms Voltage, Second Lowest Harmonic	$0.0944 V_{d-c}$	$0.0944 V_{d-c}$	$0.0224 V_{d-c}$	$0.041 V_{d-c}$	$0.0099 V_{d-c}$	$0.0099 V_{d-c}$	$0.0099 V_{d-c}$
Rms Voltage, Third Lowest Harmonic	$0.0405 V_{d-c}$	$0.0405 V_{d-c}$	$0.0099 V_{d-c}$	$0.018 V_{d-c}$	$0.0043 V_{d-c}$	$0.0043 V_{d-c}$	$0.0043 V_{d-c}$

Table C-2

## TRANSFORMER SECONDARY UTILIZATION FOR MULTIPLE-PHASE RECTIFIERS

NUMBER OF PHASES	UTILIZATION FACTOR
2	0.448
3	0.520
4	0.484
6	0.392
8	0.323
12	0.237
16	0.187
24	0.131

at  $m = 3$ , which implies that the most economic conduction angle from a transformer utilization standpoint is  $120^\circ$ .

A simple three-phase half-wave rectifier circuit is shown in Figure C-1 where the load resistance  $R$  is connected between the diode common

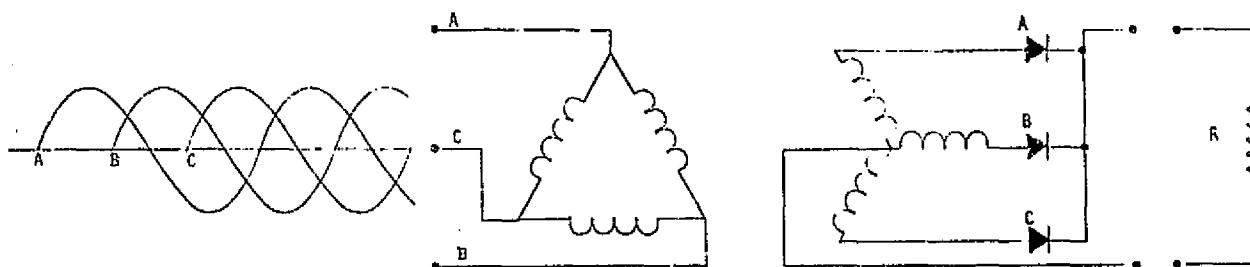


Figure C-1 Three-Phase Half-Wave Rectifier Circuit

cathode and the transformer secondary neutral. The rectified output voltage waveform is shown in Figure C-2 with the most positive anode diode

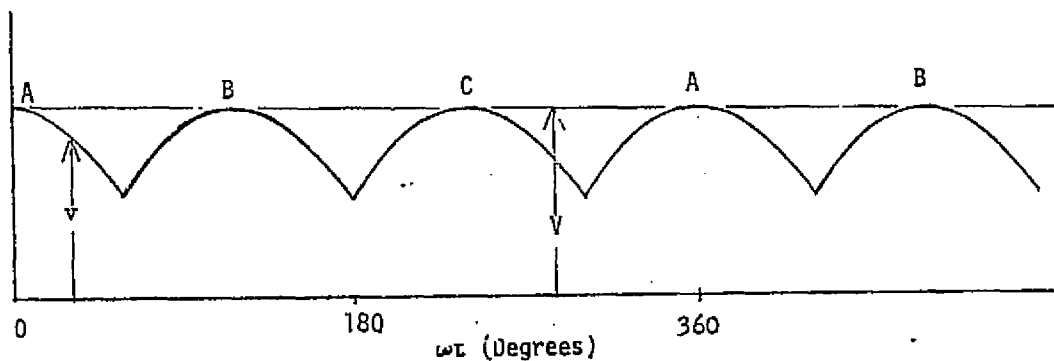


Figure C-2 Three-Phase Half-Wave Rectifier Voltage Waveform

conducting for  $120^\circ$  of each cycle. The anode current of a diode can be written as

$$i = \frac{V \cos \omega t}{R} \quad -\pi/3 \leq \omega t \leq \pi/3$$

The total load current is the sum of the three diode currents displaced in time, or

$$I_{d-c} = \frac{3}{2\pi} \int_{-\pi/3}^{\pi/3} \frac{V \cos \omega t}{R} d(\omega t) = \frac{0.827 V}{R}$$

and the d-c output voltage and the transformer secondary voltage to produce it may be obtained from

$$V_{d-c} = I_{d-c} R = 0.827 V = 1.17 V_{rms}$$

the rms current is

$$I_{rms} = \sqrt{\frac{3}{2\pi} \int_{-\pi/3}^{\pi/3} \frac{V^2 \cos^2 \omega t}{R^2} d(\omega t)} = \frac{0.838 V}{R}$$

and the percent ripple is

$$\text{Ripple} = 100\% \sqrt{\left(\frac{I_{rms}}{I_{d-c}}\right)^2 - 1} = 100\% \sqrt{\left(\frac{0.838}{0.827}\right)^2 - 1} = 17\%$$



These relationships hold for ideal transformers and rectifiers. In an actual transformer, the voltage drop associated with the d-c current flow and the transformer winding resistance results in a d-c component that causes the operating B-H loop to move toward saturation. For this reason, the simple three-phase half-wave rectifier circuit is seldom used.

The advantage of  $120^\circ$  conduction on transformer economy and a lowest harmonic ripple frequency of six times the a-c source make the three-phase full-wave (bridge) circuit of Figure C-3 of great practical value. Voltage waveforms are shown on Figure C-4 where the dotted lines are the

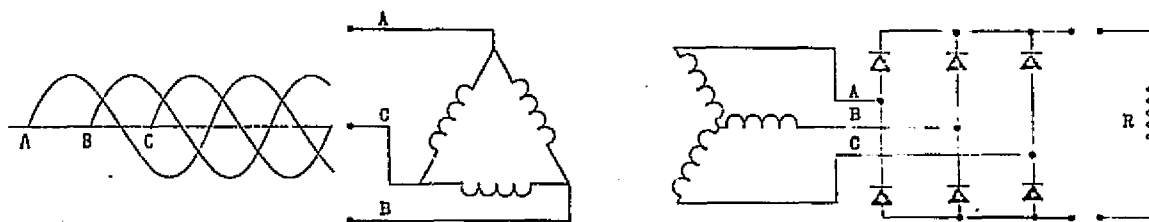


Figure C-3 Three-Phase Full-Wave (Bridge) Rectifier Circuit

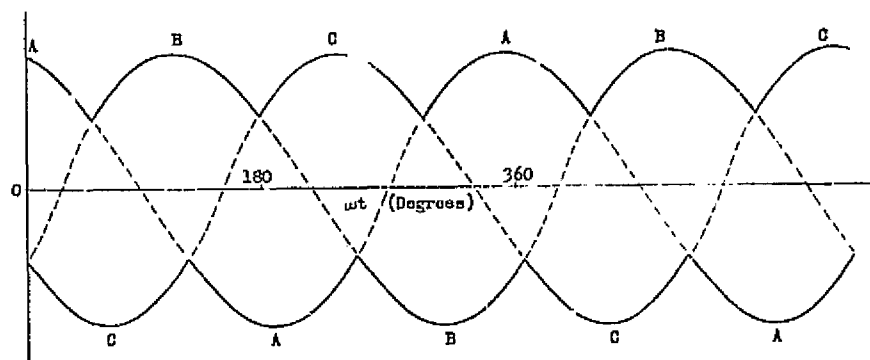


Figure C-4 Three-Phase Full-Wave Rectifier Voltage Waveforms

three phase a-c voltages at the transformer secondary with respect to neutral, the solid line envelope at the top represents the common cathode, and the solid line envelope at the bottom represents the common anode. Each diode conducts for  $120^\circ$ , and current flows alternately in both directions in each transformer secondary. The peak to peak voltage appears across the load resistance as six-phase ripple with respect to the negative terminal as shown in Figure C-5.

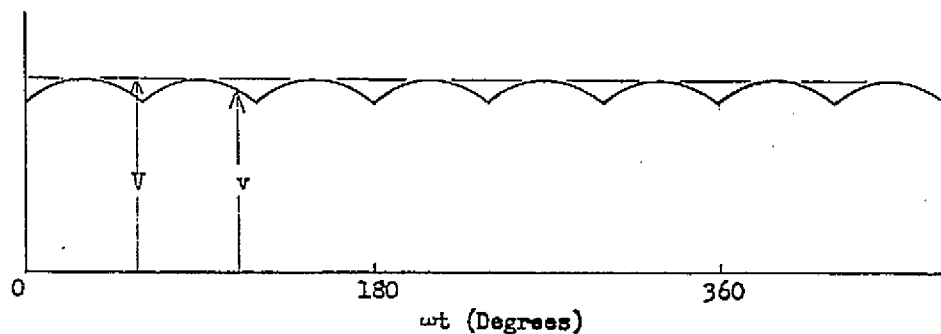


Figure C-5 Three-Phase Full-Wave Rectified Voltage Waveform

The load current flows thru two transformer secondary windings and two diodes at any instant, making it unattractive for low-voltage high-current output power.

The circuit of Figure C-6 utilizes a double wye secondary with windings in opposition on each core leg. An interphase transformer is

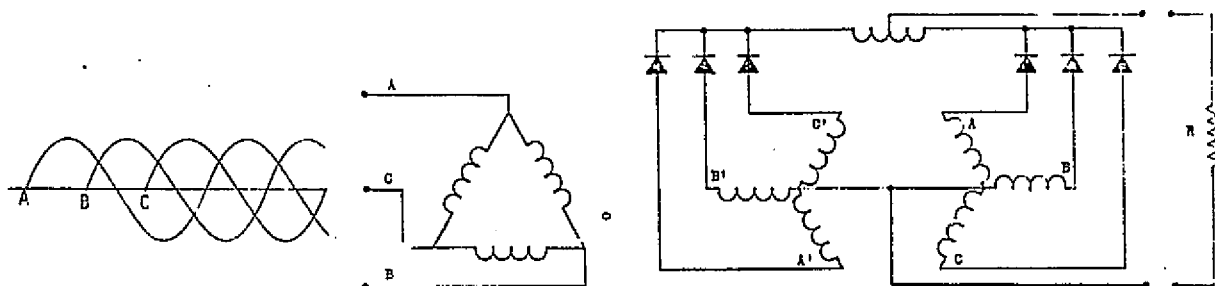


Figure C-6 Three-Phase Double-wye with Interphase Rectifier Circuit

connected between the two, forcing conduction in both wye circuits at all times. This configuration provides  $120^\circ$  conduction, double-way transformer current to eliminate d-c saturation, one rectifier and winding in series with load current flow, and six phase output ripple. Voltage waveforms are shown in Figure C-7 where the dotted lines are the two three-phase

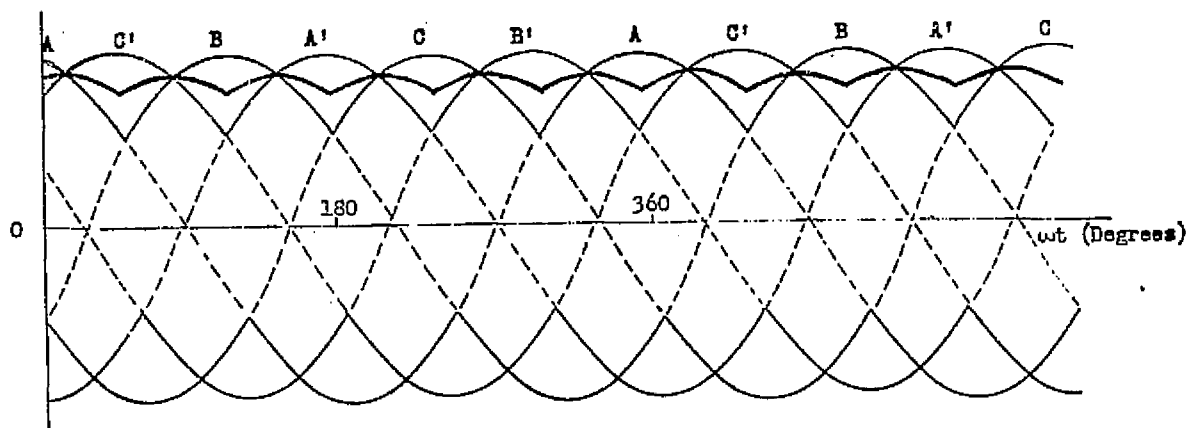


Figure C-7 Three-Phase Double-wye with Interphase Voltage Waveforms

a-c voltages at the transformer secondary terminals with respect to neutral, the light solid lines show the two common cathodes, and the heavy solid line the voltage that appears across the load resistance. It can be seen that the potential across the interphase transformer changes three times per cycle of the a-c source. A small third harmonic current is necessary to excite the interphase transformer, and when the load current falls below a critical value, the circuit reverts to operation as a six-phase star, the interphase transformer behaves as a short circuit, and the output voltage rises by about 10% as shown on Table C-1.

APPENDIX D  
FUEL CELL OR PRIMARY BATTERY SYSTEMS

APPENDIX D  
FUELL CELL OR PRIMARY BATTERY SYSTEMS

TABLE OF CONTENTS

<u>SECTION</u>	<u>PAGE</u>
1.0 INTRODUCTION	D-1
2.0 SYSTEM OVERVIEW	D-2
3.0 VEHICLE CONFIGURATION	D-4
4.0 POWER SYSTEM FUNCTIONAL DESCRIPTION	D-8
4.1 Primary Power	D-8
4.2 Reentry Power	D-8
4.3 Deorbit Power	D-9
4.4 Power Control and Distribution	D-9
5.0 POWER SOURCE EQUIPMENT DESCRIPTION	D-10
5.1 Fuel Cell	D-10
5.2 Orbital Battery	D-15
5.3 Fuel Cell Controller	D-16
5.4 Bus Current Telemetry	D-19
5.5 Battery Ampere Hour Telemetry	D-19
5.6 Deorbit Batteries	D-21
5.7 Capsule Heater Battery/Reentry Battery	D-22
5.8 Recovery Battery	D-22
6.0 POWER PROCESSING EQUIPMENT	D-23
6.1 Reentry Vehicle Inverter Power Supply	D-23
6.2 Adapter Inverter Power Supply	D-28
7.0 POWER SYSTEM PERFORMANCE CHARACTERISTICS	D-35
7.1 System Volt-Ampere Characteristic	D-35
7.2 Load Sharing	D-36
7.3 Orbital Fuel Cell Power Requirements	D-39
7.4 Orbital Battery Energy Requirements	D-39
7.5 Electromagnetic Compatibility	D-41

## LIST OF TABLES

<u>TABLE</u>		<u>PAGE</u>
D-1	Re-entry Vehicle Inverter DC Outputs	D-24
D-2	Re-entry Vehicle Inverter AC Outputs	D-24
D-3	Adapter Inverter DC Outputs	D-29
D-4	Adapter Inverter AC Outputs	D-29
D-5	Adapter Inverter Combined Loads	D-30
D-6	Adapter Inverter Losses	D-30
D-7	Orbital Fuel Cell Power Requirements	D-40
D-8	Orbital Battery Energy Requirements	D-40

# LIST OF ILLUSTRATIONS

<u>FIGURE</u>	<u>PAGE</u>
D-1 Biosatellite Physical Configuration	D-5
D-2 Biosatellite Spacecraft - Exploded Isometric View	D-6
D-3 Biosatellite Electrical Power and Distribution Flow Diagram	D-7
D-4 Fuel Cell Stack Assembly	D-10
D-5 Fuel Cell Equivalent Circuit	D-11
D-6 Typical Fuel Cell Operating Characteristic	D-12
D-7 Fuel Cell Interfaces	D-12
D-8 Simplified Fuel Cell System Schematic	D-13
D-9 Orbital Battery Performance Characteristic	D-15
D-10 Fuel Cell Bus Back-Up Circuitry	D-18
D-11 Ampere-Hour Circuitry	D-20
D-12 Re-entry Vehicle Inverter Block Diagram	D-26
D-13 Adapter Inverter Block Diagram	D-32
D-14 System Load Distribution	D-37
D-15 Power Source Operating Region	D-37
D-16 Electrical System Characteristics	D-38
D-17 Voltage Versus Time Characteristics	D-38
D-18 Vehicle Grounding Diagram	D-42

## 1.0 INTRODUCTION

The 30 Day Biosatellite was designed, manufactured, tested, and launched by the General Electric Company, for and in cooperation with NASA, Ames Research Center, California.

The spacecraft was launched successfully from Cape Kennedy on June 29, 1969 carrying a live, instrumented primate. Its mission was to determine the effects of prolonged weightlessness on the cardiovascular and central nervous system, and to study metabolism and behavior.

Mission objectives and significant system design parameters which affect the power processing system were considered and are reviewed here briefly.



## 2.0 SYSTEM OVERVIEW

The primary spacecraft requirement was to maintain a near-zero gravity condition not to exceed  $1 \times 10^{-4}$  gravity units and to maintain less than  $1 \times 10^{-5}$  gravity units for 95 percent of the orbital mission time.

Shirt-sleeve conditions were maintained in the experiment capsule throughout the mission. Temperature variation within the primate static envelope was limited to 68 to 81°F and relative humidity was maintained between 42 percent and 56 percent. The two gas standard atmosphere system supplied a laboratory environment for the primate. The capsule total pressure was maintained between 13.2 and 16.2 pounds per square inch absolute, with partial oxygen pressures of 135 to 165 millimeters of mercury. Toxic gas levels such as carbon dioxide concentrates were maintained in the range of 0.2 to 7.6 millimeters of mercury. Food pellets and fuel cell by-product water were accurately measured, telemetered, and dispensed to the primate under the control of the psychomotor programmer. Primate waste products were removed, measured, analyzed, and stored during the orbit; and accumulated data was transmitted in real time.

The primate's light level was maintained between 6 and 20 foot candles during the day, and the night level occurred as programmed at a light intensity less than 1/30 of the day. Photography was maintained under these light conditions in both single frame and cine-modes.

The combined fuel cell and orbital battery provided prime spacecraft power. A 20 percent margin above the mission power demand was demonstrated, and this exceeded the 6 percent margin requirement. The fuel cell operated for a total period of 38 days.

Management of nitrogen, hydrogen and oxygen expendables for fuel cell operation and environmental control was maintained over the 30 day flight with sufficient margin of quantity.

Recovery of the capsule was accomplished via helicopter pickup following a water impact.

This overview indicates a high quantity of electromechanical devices such as pumps, motors, and solenoids; as well as sophisticated switching logic were required for spacecraft operation. The interaction of the pulse power requirements of the electromagnetic equipment with the low noise threshold solid state devices provides an opportunity to evaluate the power processing equipment designed to make these two classes of equipment electrically compatible.

### 3.0 VEHICLE CONFIGURATION

A second area of interest to the power processing system description is the vehicle configuration and its launch, orbital and recovery sequences which affected packaging density and weight.

The orbiting vehicle shown in Figure D-1 consists of the mated adapter, the satellite re-entry vehicle, and the recovery capsule as shown in Figure D-2. The airborne subsystems are distributed between these three basic vehicle sections on the basis of equipment use in the mission.

The adapter houses those functions required during orbit but not needed for the deorbit sequence or required to be recovered. At the end of the orbital phase, the vehicle aligns itself for the deorbit phase and the adapter is separated from the satellite re-entry vehicle and remains in orbit. Only the satellite re-entry vehicle begins a controlled re-entry.

The satellite re-entry vehicle consists of the re-entry vehicle and the thrust cone. The re-entry vehicle consists of a forebody, a recovery capsule, and an aft thermal cover.

After adapter separation, a retro-rocket is fired under controller conditions and re-entry into the atmosphere begins. When the deorbit mechanism has completed its function, the thrust cone is separated from the re-entry vehicle. The re-entry vehicle continues its ballistic trajectory protected by the ablative forebody. The forebody is jettisoned when the re-entry vehicle enters an atmosphere sufficient to support parachute operation. The Electrical Power and Distribution System is divided across the three basic vehicle sections as indicated in the block diagram of Figure D-3.

D-5

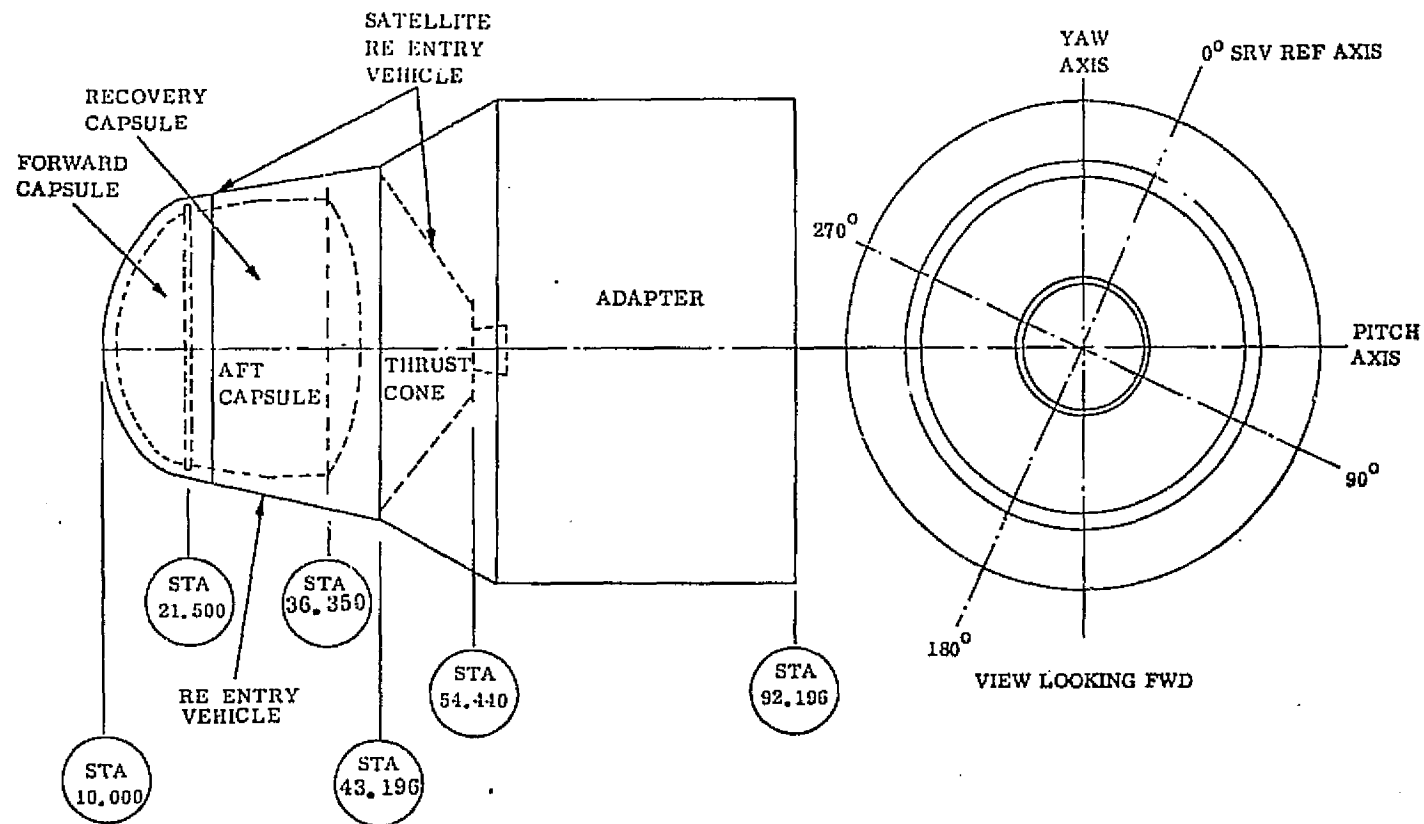


Figure D-1. Biosatellite Physical Configuration

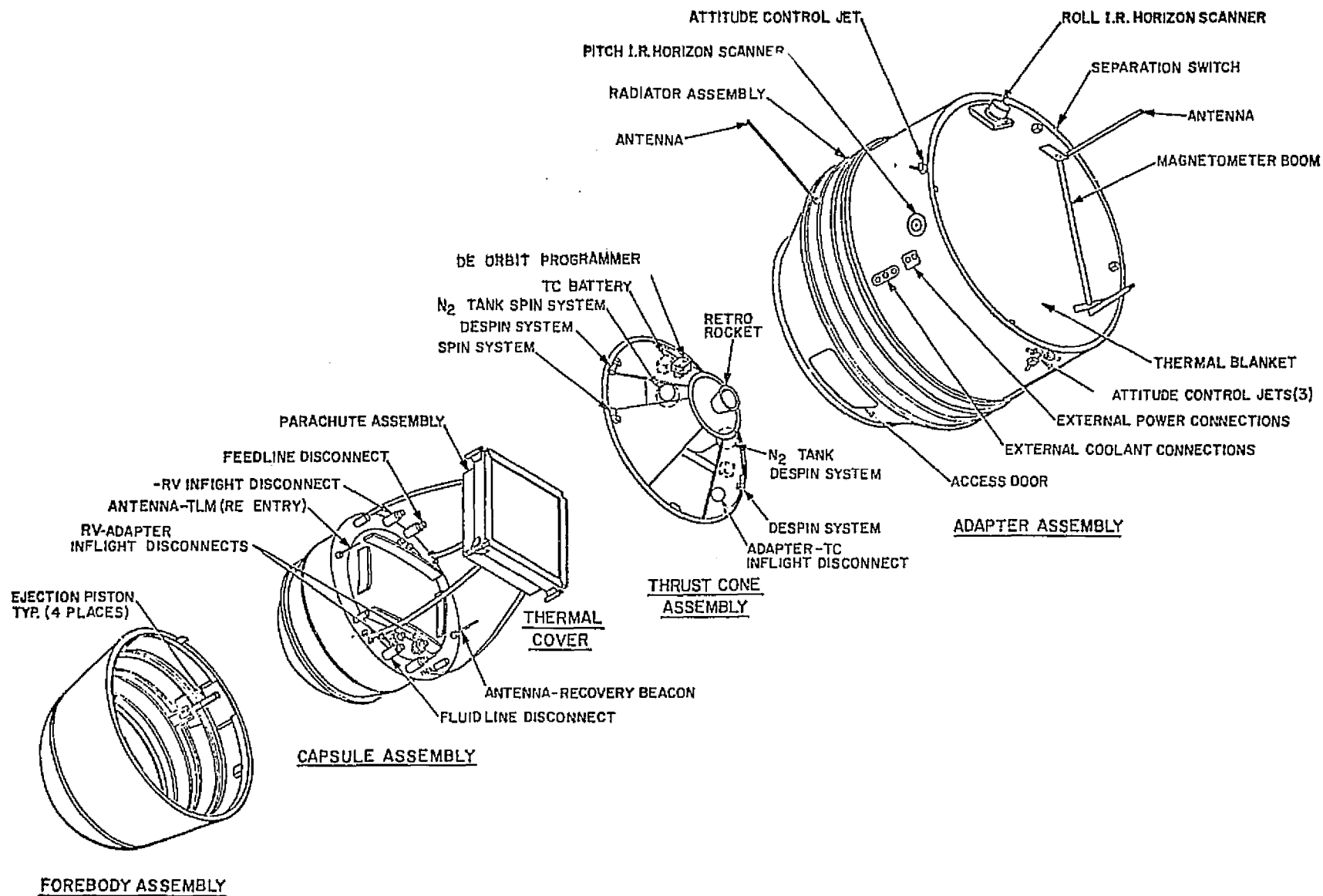


Figure D-2. Biosatellite Spacecraft - Exploded Isometric View

D-7

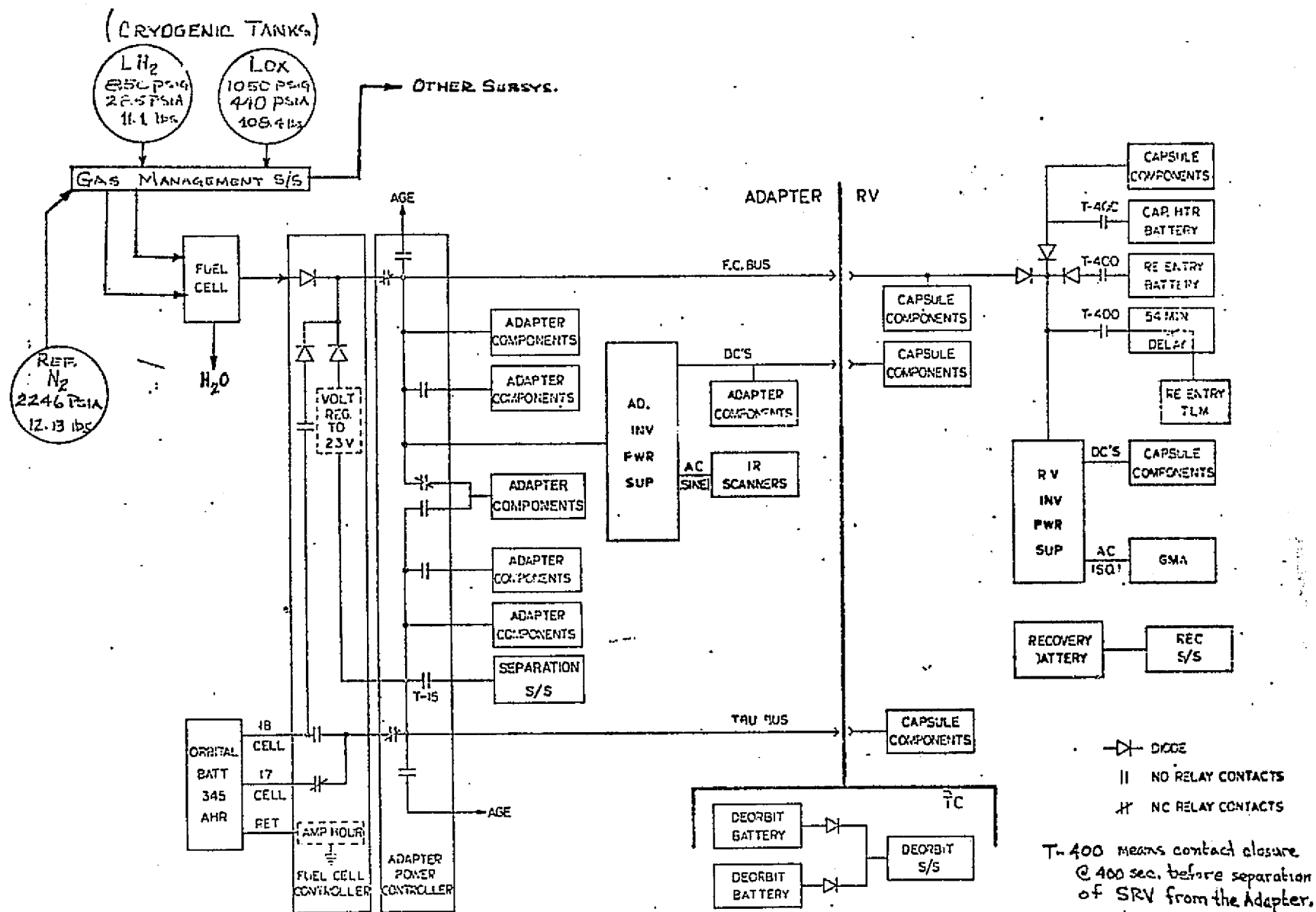


Figure D-3. Electrical Power and Distribution Flow Diagram

## 4.0 POWER SYSTEM FUNCTIONAL DESCRIPTION

### 4.1 Primary Power

Primary power was supplied by a hydrogen-oxygen, ionic membrane, solid electrolyte fuel cell, with a back-up orbital battery. The fuel cell was activated on the launch pad prior to transfer to internal power, and supplied power from the time of transfer during prelaunch until separation of the reentry vehicle and the adapter during reentry. The fuel cell and its cryogenically stored fuels were located in the adapter. The fuel cell also provided water for the primate.

A primary, silver-zinc, manually activated, electro-chemical battery was provided to supplement the fuel cell by carrying transient and short-time loads, and, in addition, was capable of carrying the entire electrical system for approximately 18 orbits in the event of a fuel cell failure. The electrical system could have been transferred from the fuel cell to the orbital battery either automatically or by real time command. Nominal capacity of the battery was 345 ampere hours at 27 volts DC. Power for the separation subsystem was provided by the orbital battery.

### 4.2 Reentry Power

During reentry, primary power for the experiment, life support, reentry telemetry, and data recording was supplied by two paralleled primary, silver-zinc, electro-chemical batteries from a time after the spacecraft had been oriented for retrofire, during reentry, and until landing. Power could have continued to be supplied for the experiment and for life support for six hours after landing. These batteries were located in the reentry vehicle

and had a combined nominal capacity of 16 ampere hours at 27 volts DC. Diode isolation was provided in any power distribution circuits common to the orbital power source. Battery power was applied to the bus by activation of an explosive switch assembly.

#### 4.3 Deorbit Power

Primary power for the deorbit subsystem; including reentry vehicle spin-up, retrorocket firing, vehicle despin, and separation of the thrust cone from the reentry vehicle; was supplied by two redundant, special, high-duty batteries located in the thrust cone. These batteries were activated by a voltage applied to pyrotechnic initiators within the batteries.

#### 4.4 Power Control and Distribution

In general, power control was centralized in power controllers which respond to commands from the command subsystem, signals from the programmer timer, internal timers, or hardwire commands on-pad. As appropriate, the controllers contained auxiliary functions such as diagnostic signal conditioning and circuit protection.

The buses were designed for each system voltage to distribute power as required by components, to provide for switching as required by commands and the mission event sequence, to comply with voltage regulation requirements, to permit assembly and disassembly of the major parts of the vehicle, and to permit testing as required by the various subsystems and experiments.



## 5.0 POWER SOURCE EQUIPMENT DESCRIPTION

### 5.1 Fuel Cell

The fuel cell module consists of a 32-cell stack mounted inside a fabricated titanium container. The 32 cells comprising the stack are mechanically loaded between end plates and electrically connected in series. Details of the internal fuel cell assembly are shown in Figure D-4.

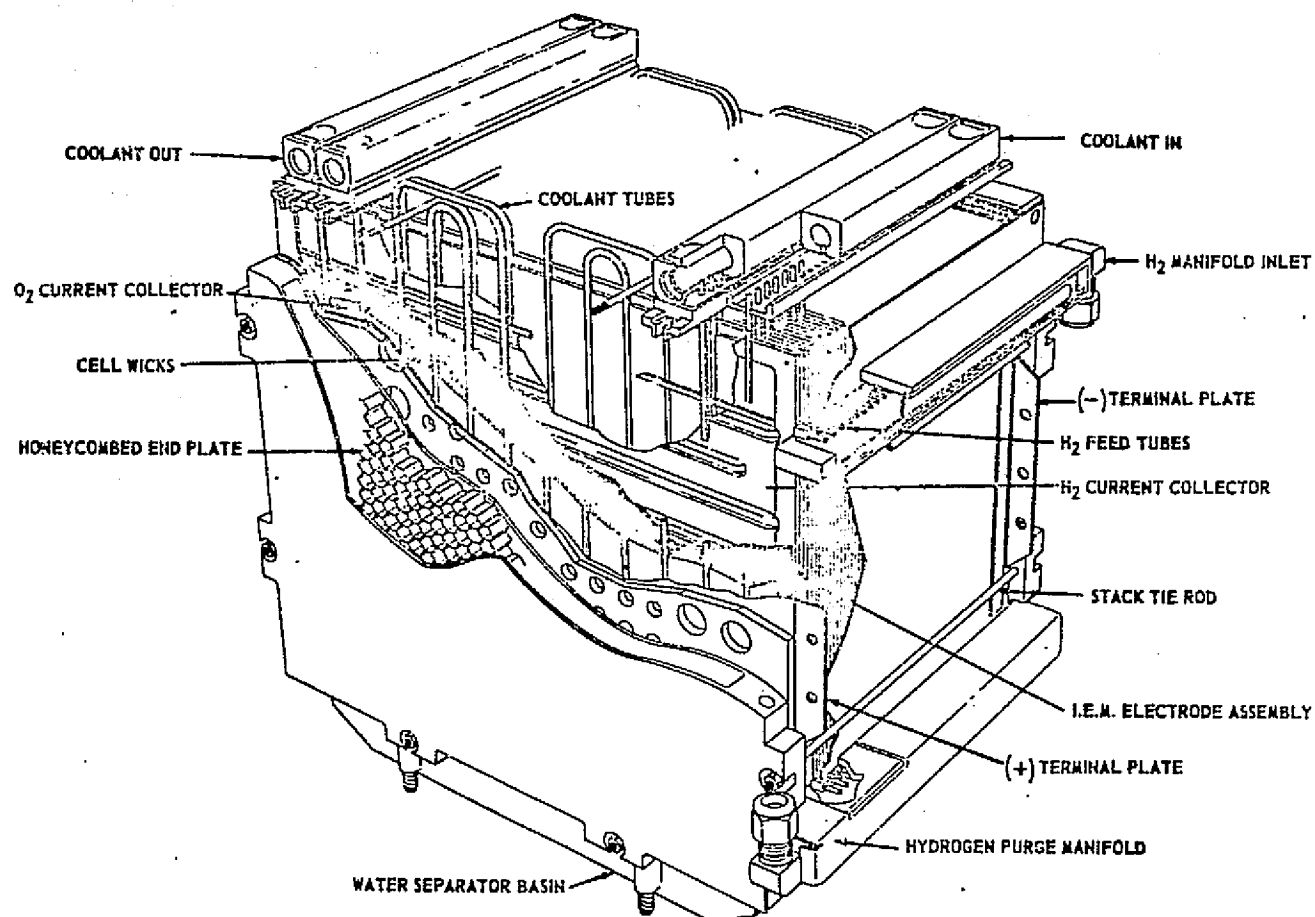


Figure D-4. Fuel Cell Stack Assembly

The 32 cell stack is mounted in a 14 inch diameter cylinder approximately 17 inches long requiring a volume of 238 cubic inches with a gross weight of 35 pounds.

The stack was designed to deliver a terminal voltage of 31 to 23 VDC with an output of 113 to 187 watts for the 30 day mission. The fuel cell efficiency is typically 2.1 times the stack voltage, or 65 to 48% efficient.

The internal impedance of the stack is shown in the equivalent circuit of Figure D-5, where  $R_1 = 0.21$  ohms and represents the polarization effect at fuel cell start-up and  $R_2$  is the ohmic effect which varies with current demand and fuel cell life. For a new fuel cell  $R_2 = 0.17$  ohms and will approach 0.7 ohms as the 1000 hour design life is reached. The value of  $C = 1.09$  farads and is fixed.

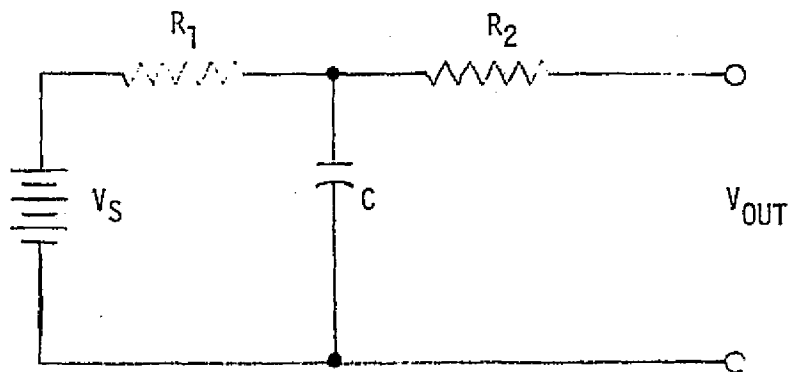


Figure D-5. Fuel Cell Equivalent Circuit

The current and voltage characteristics of the hydrogen-oxygen, ionic membrane, solid electrolyte fuel cell are shown in Figure D-6.

The fuel cell module incorporates four operating systems: hydrogen; oxygen; product water; and coolant as shown in Figure D-7.

Interfacing and operation of the fuel cell is defined in a simplified block diagram of Figure D-8.

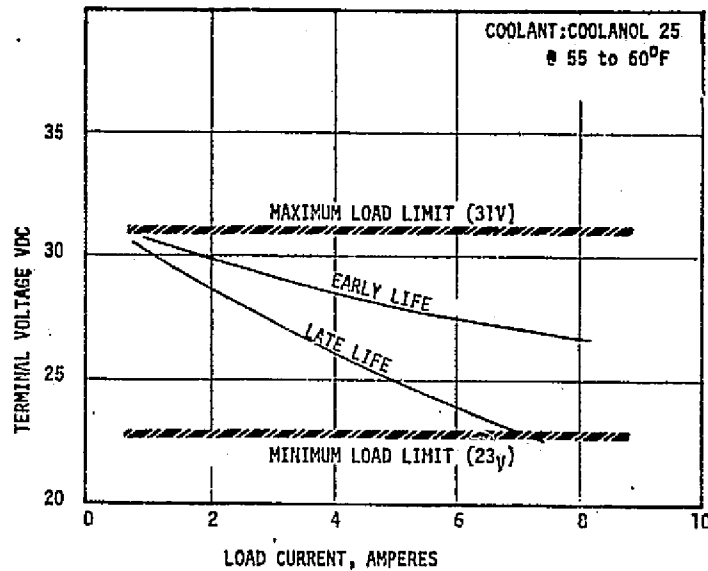


Figure D-6. Typical Fuel Cell Operating Characteristics.

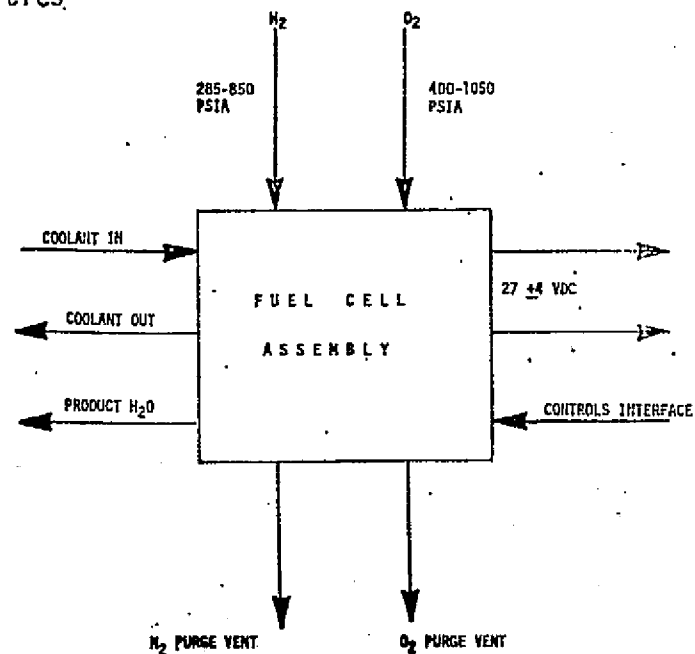


Figure D-7. Fuel Cell Interfaces

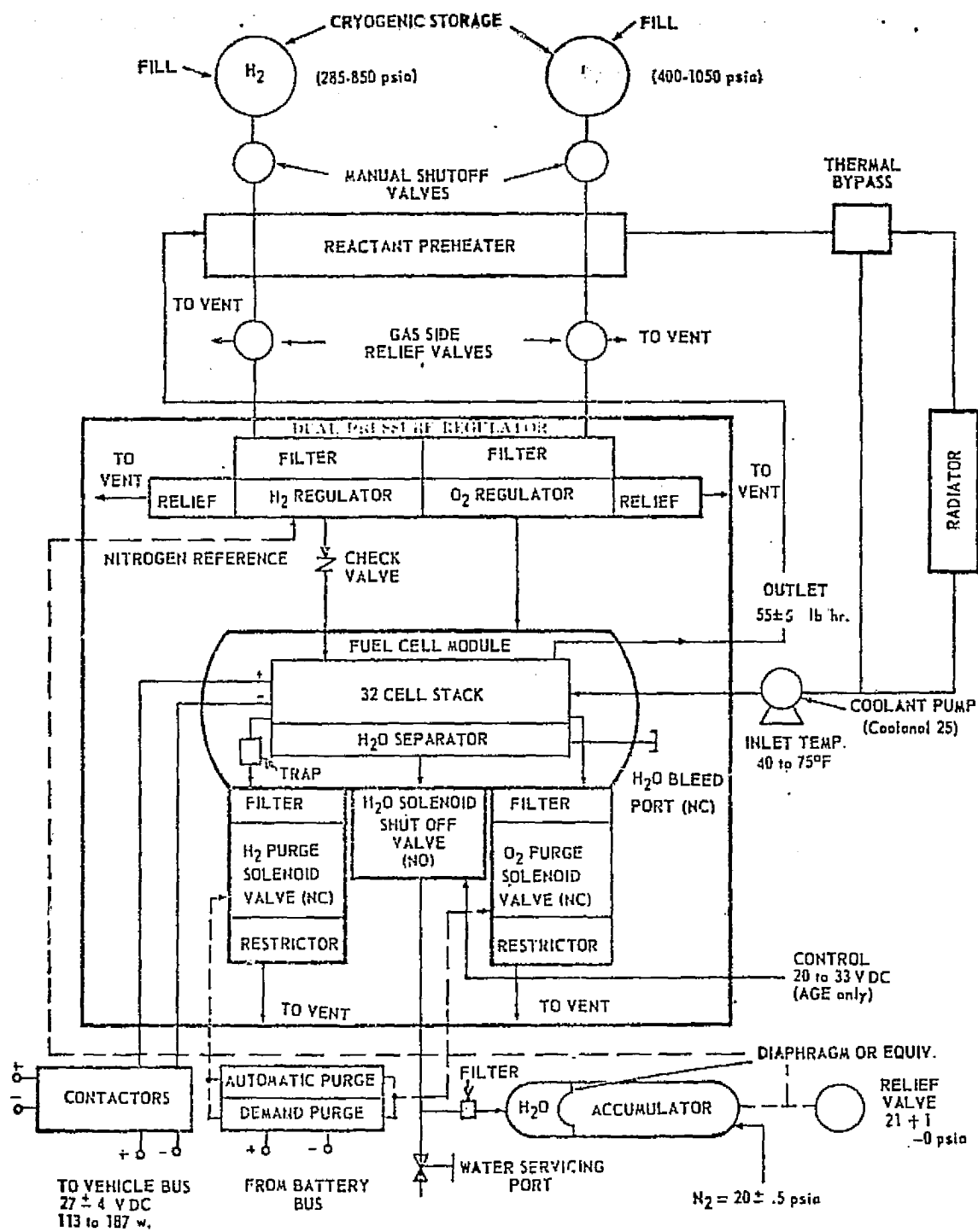


Figure D-8. Simplified Fuel Cell System Schematic

Hydrogen gas is used as the fuel and oxygen gas is the oxidizing agent. In the fuel cell, the hydrogen-oxygen gases are reacted in the presence of a catalyst and produce electrical energy and product water. Waste heat is removed from the fuel cell stack by coolant fluid which is pumped across the cells continuously through small diameter tubes. After passing across the stack, the coolant fluid is cooled by the spacecraft heat exchanger.

Thermal dissipation of the fuel cell in BTU/hr may be derived from equation:

$$Q = 3.413 \times P \left( \frac{47.5}{V} - 1 \right) \\ = 3.413 \times I (47.5 - V)$$

where I is current drawn by the load and V is the terminal voltage of the fuel cell.

Reactant consumption by the fuel cell may be derived from the following equations:

$$O_2 \text{ rate in lbs/hr} = 2.653 \times 10^{-3} (I) \\ \text{plus purging @ 0.275 lb/hr for 12 sec/6 hr}$$

$$H_2 \text{ rate in lbs/hr} = 21.216 \times 10^{-3} (I) \\ \text{plus purging @ 0.437 lb/hr for 120 sec/6 hr}$$

Water generation may be derived from the following equation

$$H_2O \text{ rate in lbs/hr} = 23.86 \times 10^{-3} (I)$$

The ratio of total fuel in pounds consumed (the sum of  $H_2$  and  $O_2$  not including purge) to the electrical energy in kilowatt hours generated is a useful relationship. It is a function of fuel cell characteristics, electrical load level and electrical load mix. It is of the order of 0.88 pounds per kilowatt hour and can vary 2 to 3% over the range in interest.

## 5.2 Orbital Battery

The silver-zinc, manually activated, electro-chemical battery has a 345 ampere hour capacity over a sixty day activated stand. The 124 pound, 18 cell battery is housed in a cast magnesium case. A 17 cell tap is provided in order to meet the maximum voltage requirement of 31 VDC without preloading. The 18th cell is commanded on during orbit mode when the bus is near 28 VDC.

The actual flight battery curve for voltage over orbit time is shown in Figure D-9.

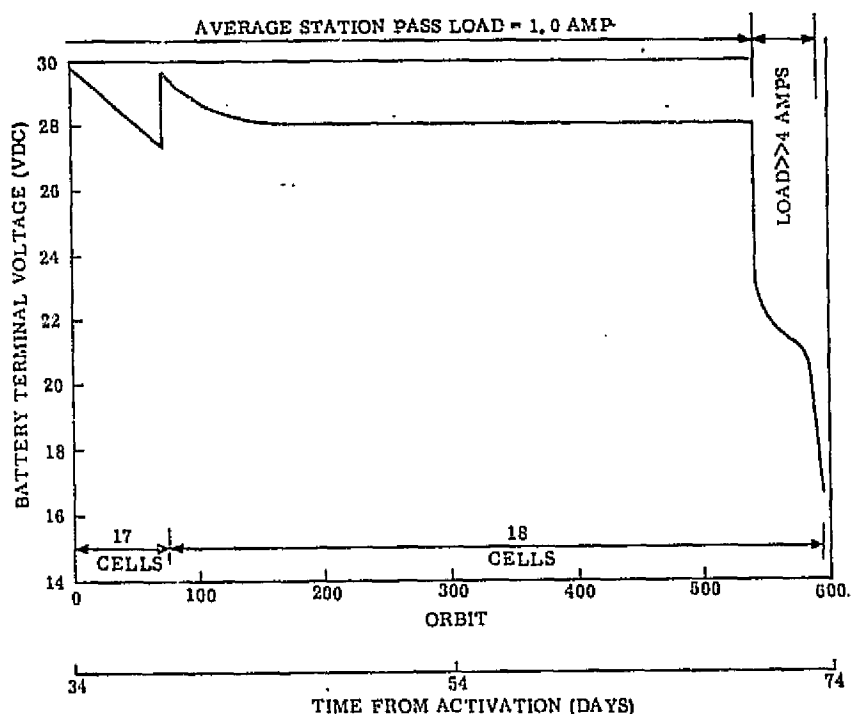


Figure D-9. Orbital Battery Performance Characteristic

### 5.3 Fuel Cell Controller

A fuel cell controller provides six basic functions as follows:

1. Oxygen and hydrogen purging for several seconds every six hours.
2. Current sharing with the orbital battery to hold the fuel cell bus at 23 VDC.
3. Full orbital battery power to the fuel cell bus should the fuel cell fall below 20 VDC.
4. Switch-on capability of the orbital battery's 18th cell.
5. Orbital battery/fuel cell current monitor.
6. Orbital battery ampere-hour monitoring and store last reading in event of power drop out.

A fuel cell controller counts the ten minute timing pulses. When the total input pulses reach 36 (6 hours) a purge is initiated. This purge consists of activating the oxygen solenoid for  $120 \pm 10$  seconds and during the last  $12 \pm 1$  seconds activating the hydrogen solenoid.

A purge can be initiated by real time command. A real time command can initiate an oxygen solenoid actuation for  $108 \pm 5$  seconds or a hydrogen purge for  $12 \pm 1$  second. Telemetry is generated to indicate:

- (1) Energization of hydrogen solenoid
- (2) Energization of oxygen solenoid
- (3) Completion of a purge cycle.

Facilities exist for AGE to:

- (1) Hold the counter to stop responding to the 10 minute timing pulses.
- (2) Accelerate the time by sending fast pulses into the fuel cell controller. (It is anticipated that the maximum pulse rate will be ten pulses per second.)

Circuits are provided as a back-up to the fuel cell to current share loads in order to hold the fuel cell bus at 23 volts. If this should fail, the orbital battery will be switched directly to the fuel cell bus if the bus voltage falls below 20 volts. Diode coupling is incorporated to prevent reverse current flow into either the fuel cell or the orbital battery, as shown on Figure D-10.

The fuel cell bus assist regulator is a series regulator circuit using the bus from the power controller as a source to maintain the fuel cell bus at 23 volts or more. If the fuel cell voltage decreases under load, the regulator will current share with the fuel cell to maintain the bus at 23 volts. The regulator circuit uses a differential comparator circuit with a temperature compensated zener for a voltage standard. The circuit is capable of maintaining  $23.3 \pm .3$  volts from 0 to 10 amperes output with an input voltage of 26.5 to 31 volts.

An automatic regulator bypass circuit is provided which will switch the orbital battery directly to the fuel cell bus upon command or if the fuel cell bus drops to 20 volts or below for approximately 100 milliseconds. The switching element is a two pole, double throw, motor driven switch with make-before-break, 15 ampere contacts. The sensing element is a differential comparator circuit similar to the one used in the regulator. It drives dual unijunction firing circuits which activate a relay to drive the switch. The unijunction circuit was chosen to reduce the susceptibility to transients and two firing circuits are used for redundancy. Either circuit will actuate the relay. When the switch bypasses the regulator, the supply to the regulator and the automatic switching circuit is removed to conserve power.



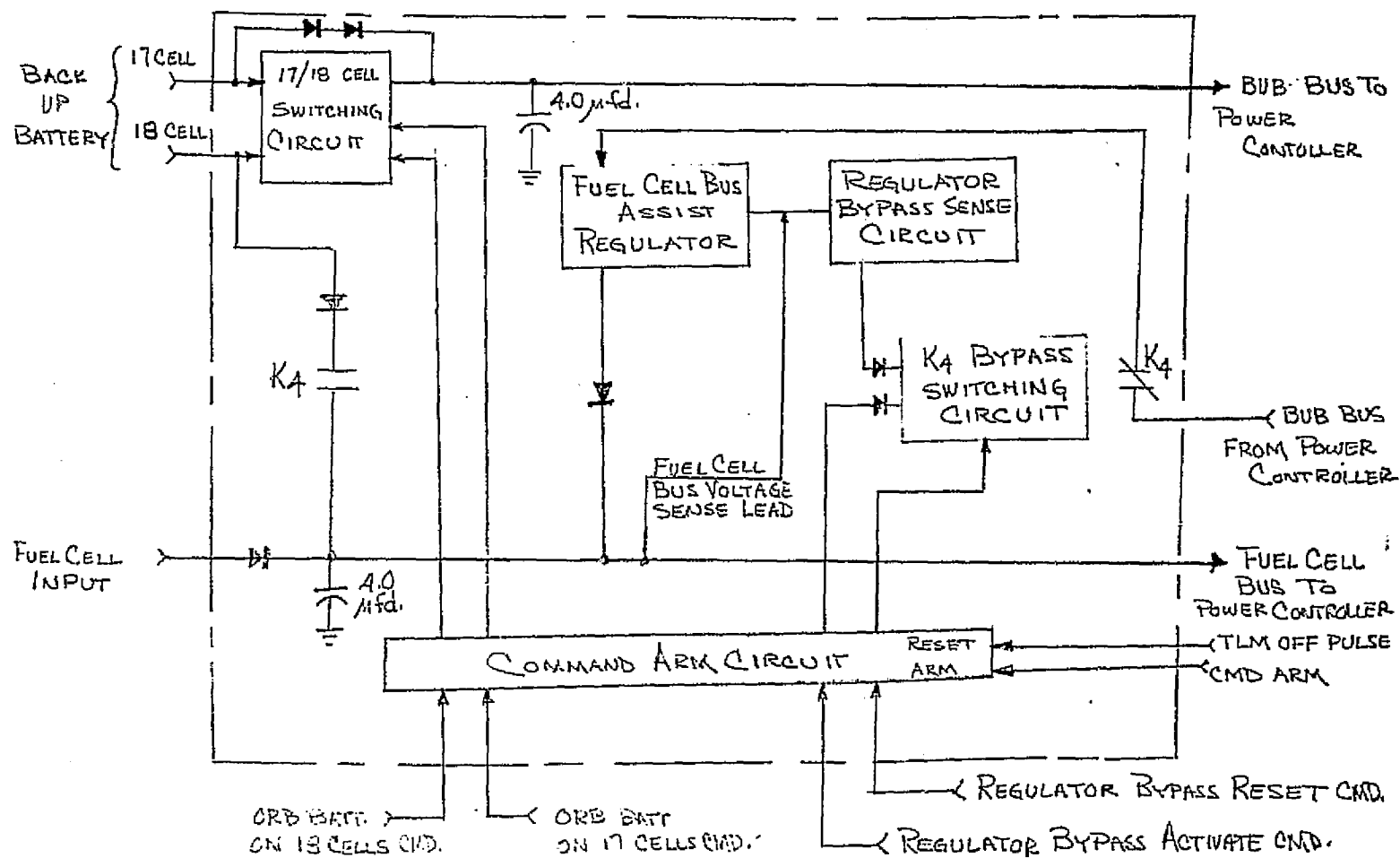


Figure D-10. Fuel Cell Bus Back-up Circuitry

The orbital battery has two output connections to this component, one at 17 cells and one at 18 cells. A switching circuit is provided to transfer to either the 17 cell or 18 cell tap of the battery. A "Command Arm" command is required to enable the 17/18 cell switching commands and the regulator bypass and reset commands. This arming function is automatically reset by a telemetry "Off" pulse from the power controller each time telemetry is switched off.

#### 5.4 Bus Current Telemetry

The component monitors 0 - 10 amperes on the fuel cell bus and the orbital battery bus, using differential comparator circuits. The telemetry output is 0 - 5 volts with an accuracy of  $\pm 1\%$  or 15 millivolts, whichever is greater. The input can be 14 amperes continuous or 30 ampere, 50 millisecond pulses without degradation to the circuit.

#### 5.5 Battery Ampere-Hour Telemetry

The component is capable of monitoring ampere-hours with inputs from 0 - 10 amperes. The output is from 0 -5 volts in 32 steps. The logic stores the last output step in the event of voltage dropout.

The ampere-hour telemetry has an inherent threshold of not more than 50 milliamperes.

The ampere-hour circuitry is shown in the block diagram of Figure D-11.

The x10 amplifier senses the voltage across a resistor and develops a voltage across an emitter resistor of the integrating current source. If this voltage exceeds a pre-determined value (equivalent to 50 milliamperes of current) the

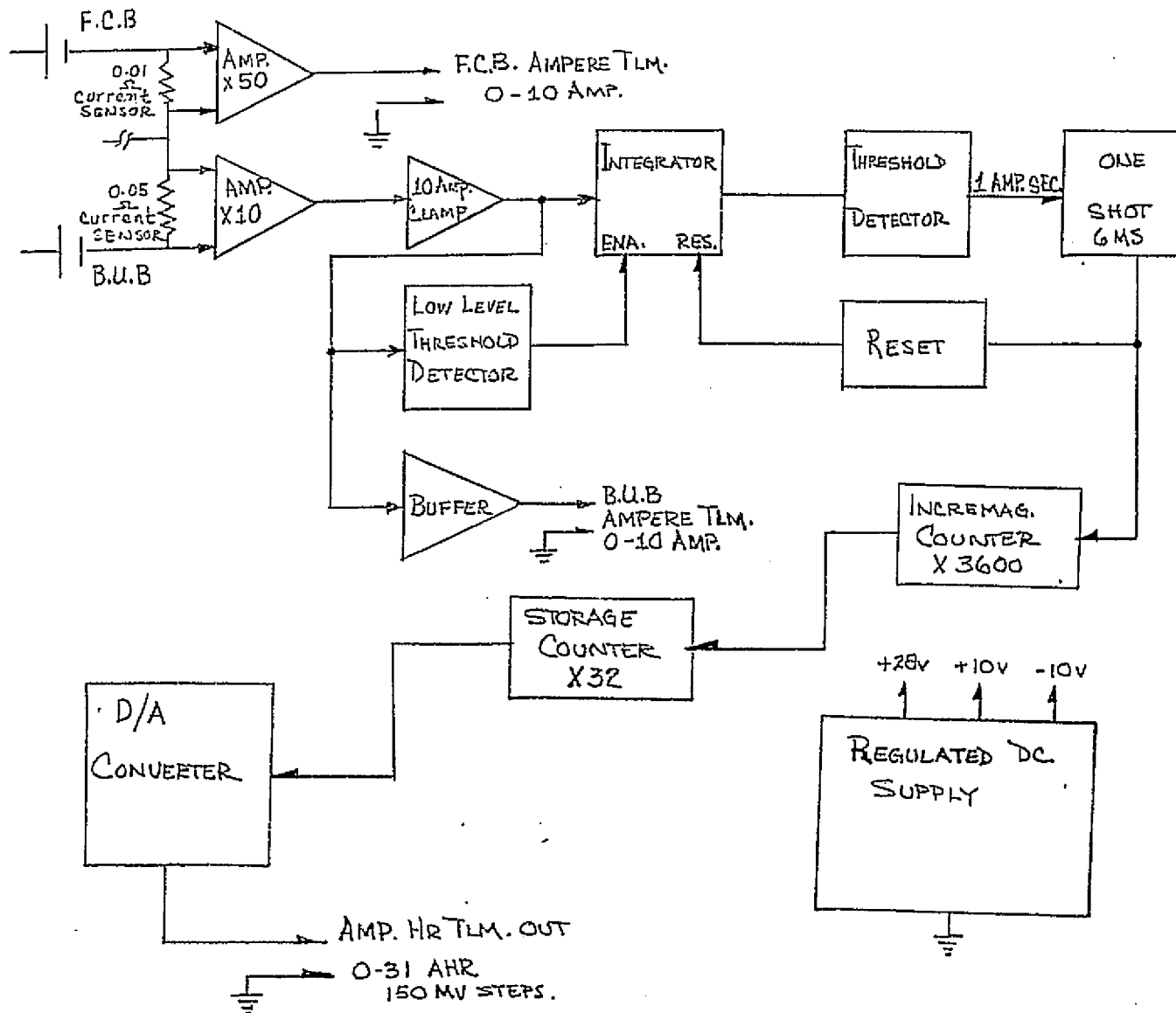


Figure D-11. Ampere-Hour Circuitry

low level threshold enables the integrating capacitor allowing it to charge at a rate proportional to the input current. The circuitry at this point has converted the orbital battery current-time integral to a voltage appearing across the integrating capacitor. The circuit parameters have been adjusted such that when this voltage reaches a value equivalent to 1 ampere-second the high level threshold detector triggers and generates a pulse which turns on a reset transistor and discharges the capacitor to its initial state through a current limiting resistor. Simultaneously, the pulse enters one count in the increasing chain. When 3600 discrete counts have been completed, one count is entered into the storage counter whose output is monitored through a digital to analog ladder by the vehicle telemetry. Each discrete telemetry step is equivalent to one ampere-hour of orbital battery energy. When a total of 32 ampere-hours have been accumulated, the counter resets and starts a new series of counts.

It should be noted that the  $\times 10$  amplifier is fed back from the emitter resistor of the integrating current source to close the sensing loop. The current source is initially biased up by a stable reference source to insure that the integrating transistor is out of the low-current non-linear operating range. Its base is clamped to the input 10 ampere current level to enable the metering to continue, although at a reduced rate, to indicate an excessive current drain on this telemetry channel due to possible system failure modes. Therefore, pulse currents in excess of 10 amperes are reduced to 10 amperes automatically by this section.

### 5.6 Deorbit Batteries

The deorbit battery is a fuse-salt electrolyte battery. Two deorbit batteries are connected in parallel, with either battery capable of carrying the entire load during spin, retrofire, despin and separation, at a voltage of  $32 \pm 5$  VDC. The batteries supply a continuous current of 1 ampere with three pulse loads of 12 amperes for a minimum of 0.5 seconds and a 35 ampere pulse for about 40 milliseconds. All events are completed in approximately 20 seconds.

### 5.7 Capsule Heater Battery/Reentry Battery

These two batteries share the capsule electrical load 400 seconds prior to separation of the satellite recovery vehicle from the orbiting adapter until 6 hours after water impact. Since the capsule heater battery has one more cell, and thus higher terminal voltage than the reentry battery, it will discharge first. Both batteries have silver-zinc couples. The reentry battery has an 11 ampere-hour capacity and the capsule heater battery is rated 5 ampere-hours. Note that certain capsule loads, such as the reentry vehicle inverter power supply, are supplied by the fuel cell during the orbital phase and by the reentry batteries at T-400 seconds (T = time of adapter separation).

### 5.8 Recovery Battery

A recovery power source consists of two parallel batteries to power the recovery subsystem by initiating the parachute cover ejection and supplying power to the recovery beacon for 12 hours after satellite recovery vehicle separation.

## 6.0 POWER PROCESSING EQUIPMENT

### 6.1 Reentry Vehicle Inverter Power Supply

The reentry vehicle inverter power supply was designed to convert the prime 26 volt or the secondary 28 volt direct current into 400 Hertz AC and six other regulated DC voltages as shown in Table D-1 and D-2.

The regulated AC and DC voltages are supplied from the time of on pad check-out to the end of mission.

The inverter was designed to handle both the 21 and 30 day missions. The 3 day mission required less than 50% of the 21/30 day regulated power and therefore it was separately designed and housed.

For comparative purposes, the 3 day inverter was designed for a maximum input power of 20 watts at 31 VDC with its output fully loaded at 12.0 watts maximum. This would indicated an efficiency of 60%. The 3 day inverter also required a volume of 40 cubic inches (4 x 5 x 2 inches) and had a maximum weight of 3.8 pounds.

The 21/30 day inverter was designed to accept the wide input voltage range of 21 to 31 VDC with a maximum input of 44 watts when fully loaded at 28 watts. This would indicate an efficiency of 64%. The 30 day inverter consumed a volume of 108 cubic inches (6 x 6 x 3 inches) and had a maximum weight of 5.3 pounds.

Table D-1

## Reentry Vehicle Inverter DC Outputs

OUTPUT VOLTS DC	LOAD, AMPS	(WATTS)	REGULATION ALL CAUSES*	RIPPLE PK-PK	OUTPUT IMPEDANCE
	MIN	MAX.			
-5.0	.003, (.015)	.025, (0.13)	<u>+0.3%</u>	0.2%	Less than 1 ohm, DC to 150 KHz
-2.5	.020, (.05)	.100, (0.25)	<u>+10%</u>	2.0%	
+4.25	.250, (1.06)	.500, (2.12)	<u>+6%</u>	0.1%	
+5.0	.045, (.225)	.420, (0.6)	+1%, -.5%	0.4%	
+8.0	.410, (3.3)	.510, (4.0)	<u>+15%</u>	0.5%	
10.0	.001, (0.01)	.020, (0.2)	<u>+0.3%</u>	0.1%	
*steady state regulation: Total excursion due to load, temperature and input voltage variations.					
NOTE: All values apply to a temperature range 40°F to 105°F.					

Table D-2

## Reentry Vehicle Inverter AC Outputs

OUTPUT VOLTAGE	SQUARE WAVE FREQUENCY	LOAD		REGULATION ALL CAUSES*	OUTPUT IMPEDANCE
		MIN	MAX		
26 VAC	400 Hz	0.26W	0.26W	$\pm 5\%$	Less than 10% of Load Impedance
115 VAC	400 Hz	10VA	20.7 VA	$\pm 3\%$	

\*Steady state regulation includes excursion due to load, temperature and voltage input variation.

The Reentry Vehicle Inverter has three basic sections which are best described with the use of Figure D-12.

The first section is a series pre-regulator, with Pulse Width Modulation control operating into a LC integrator which feeds two post regulators.

The DC post regulator is driven by a 10 KHz Jensen oscillator, power amplified, transformer isolated, rectified and filtered to supply six, operational amplifier type - series regulators feeding the spacecraft loads. Each series output regulator is current limited to protect against a continuous short.

The AC post regulator is driven by a common 400 Hz Flip-Flop which drives a push-pull power amplifier stage that is operating into an isolation transformer to supply the spacecraft load with 400 Hz square wave, at 115 VAC and 26 VAC. Overload protection is provided by sensing the current at the power amplifier and driving a one-shot to remove the Flip-Flop drive for one millisecond, then allowing recovery of power; again sensing and removing the power if the overload remains.

Voltage regulation is maintained by sensing the current in the return leg of the AC post regulator output transformer and performing a current to voltage transformation followed by rectification and filtering. This voltage signal is then summed with a second voltage signal that is sensed at the input of the DC post regulator.



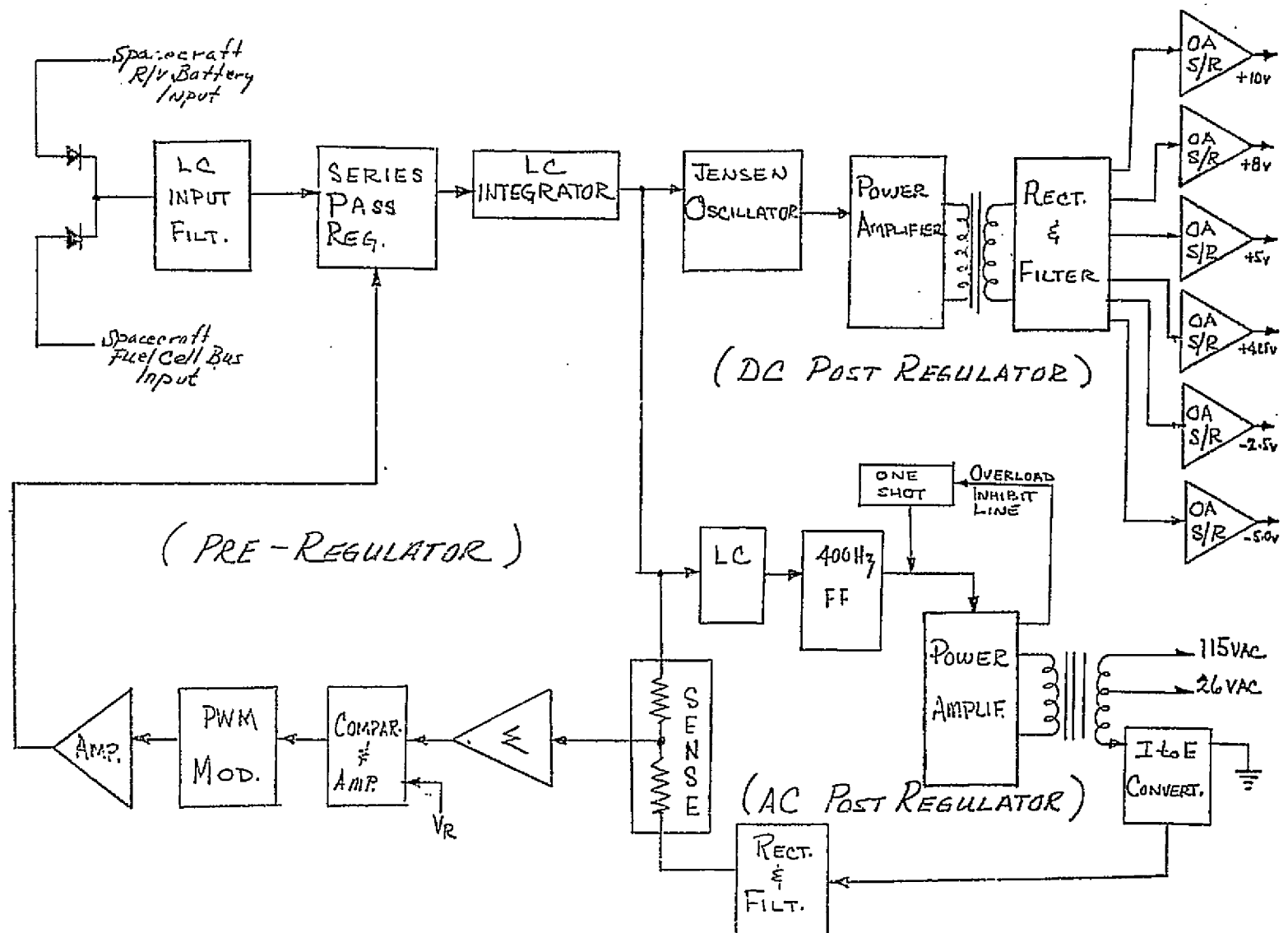


Figure D-12. Reentry Vehicle Inverter Block Diagram

The summed signal is then compared with a temperature compensated, zener reference voltage. The resultant error signal is amplified and used to modulate a simple constant current, RC relaxation oscillator, operating at a basic frequency of 20 KHz. The net output of the oscillator is a pulse width modulated signal which is then amplified and buffered to modulate the base-emitter junction of the series pass transistor within the pre-regulator.

Telemetry voltage monitors (0 to 5V, voltage dividers) are provided at the output of each DC series regulator. The fuel cell bus input to the Inverter is zenered to 5V for telemetry. The 115 VAC is monitored via a step-down transformer followed by full wave rectification. This DC signal then drives an operational amplifier, with feedback, generating a zero to five volt level for the telemetry subsystem.

EMI effects were reduced by a compartment packaging concept at module and board levels. Extensive use of EMI feed-thru filters provided board interconnections between compartments. Additional protection was provided by the use of RF gaskets at the housing/cover interfaces. The design approach of isolation transformers provided the signal to power ground isolation.

## 6.2 Adapter Inverter Power Supply

The Adapter Inverter Power Supply was designed to convert the 26 volt DC into 400 cycle AC and eight other regulated DC voltages as shown in Table D-3 and D-4.

The regulated AC and DC voltages are supplied from the time of on pad checkout until satellite recovery vehicle separation.

It should be noted that this inverter was designed to handle several Bio-satellite missions; 3 day, 21 day and the 30 day. Table D-5 shows the maximum expected wattage dissipation for each Inverter output and for each mission as compared to the maximum design value.

The inverter was designed to except the wide range of 21 to 31 VDC. The input power dissipation was limited to 220 watts with the unit fully loaded by any mission power profile.

The maximum design load configuration was limited to 139 watts for any one mission. The internal inverter losses may be calculated with the use of Table D-6 and by inserting assumed loads on each voltage line, but not exceeding the design load of 139 watts. For example, if nominal loads are extracted from Table D-5 (30 day mission) and calculated based on Table D-6, then the inverter losses would approach 26 watts with an external load of approximately 56 watts. This would indicate an efficiency of near 70%.

Table D-3  
Adapter Inverter DC Outputs

OUTPUT VOLTS DC	MIN.	MAX.	REGULATION ALL CAUSES (*)	RIPPLE PK-PK(**)	OUTPUT IMPEDANCE
-28	0.0, (0.0)	0.18, (5.0)	+2, -1	2%	Less than 1 ohm, DC to 150 KHz
+10	0.0, (0.0)	1.0, (10)	+2, -1%	2%	
-10	0.0, (0.0)	0.5, (5.0)	+2, -1%	2%	
+ 6	0.0, (0.0)	2.17, (13)	+3, -0%	2%	
+ 5	0.0, (0.0)	0.15, (0.75)	+1, -0.5%	2%	
-6	0.0, (0.0)	1.5, (9.0)	+2, -1%	2%	
+28	0.5, (14)	2.2, (61.6)	+2, -1	2%	Less than 2 ohms DC to 20 KC.
+31	0.226, (7)	0.97 (30)	+3%	10%	

\* Steady state regulation: Total excursion due to load, temperature and input voltage variations.

\*\* Switching transients shall be less than 1.5V peak-to-peak at double the chopping rate.

Table D-4  
Adapter Inverter AC Outputs

OUTPUT VOLTAGE	FREQUENCY	LOAD		REGULATION(*)	TOTAL HARMONIC DISTORTION
		MIN.	MAX.		
26 VRMS	400 cps <u>+2%</u>	0.0W	10W 0.9 P.F.	<u>+2%</u>	Less than 5%
115 VRMS	400 cps <u>+2%</u>	0.0W	10W 0.9 P.F.	<u>+2%</u>	Less than 5%

\* Steady State Regulation includes total excursion due to load, temperature and input voltage variations

Table D-5

## Adapter Inverter Combined Loads

OUTPUT VOLTS DC	MISSION DAYS						MAXIMUM DESIGN WATTS
	MINIMUM WATTS			MAXIMUM WATTS (*)			
	3	21	30	3	21	30	
-28	0.1	0.1	0.1	4.4	4.4	4.4	5.0
+10	0.1	4	1	1	10	3	10
-10	0.1	0.2	0.2	0.6	0.8	0.8	5.0
+ 6	0.1	3	0.1	7.2	12	7.2	13
+ 5	0.1	0.1	0.2	0.2	0.2	0.3	0.75
- 6	0.1	3.6	0.1	1	8.2	1.2	9.0
+28	18	22	25	53	60	61	61.6
+31	7	26	24	8	30	27	30
115	None	None	None	8	8	8	10.0
26	5	None	None	6	None	None	10.0
*Total combined loads shall not exceed 139 watts for any load configuration							

Table D-6

## Adapter Inverter Losses

OUTPUT VOLTS DC	CONSTANT TERM WATTS	VARIABLE TERM COEFFICIENT TIMES LOAD WATTS	TOTAL LOSS IN WATTS
-28	0.70	+.056 (load)	
+10	0.80	+.248 (load)	
-10	0.35	+.150 (load)	
+ 6	0.60	+.470 (load)	
+ 5	0.80	+.600 (load)	
- 6	0.40	+.415 (load)	
+28	3.00	+.069 (load)	
+31	4.80	+.082 (load)	
115 VAC	4.80	+.480 (load)	
TOTAL	16.25		
TOTAL LOSS = 16.25 WATTS + VARIABLE TERMS			

The low efficiency might be caused by the tight regulation requirement under all loads and temperatures for three different missions of 3 to 30 days, or the input voltage excursion of 10 VDC. The inverter was required to supply regulated voltages to many thermal controllers, sensors, heaters, pump controls, and other equipments which are physically too small for self contained voltage/current regulators. These loads are variable, complicating efforts toward efficient design.

The inverter requires a volume of approximately 300 cubic inches and has a maximum weight of 10 pounds. It was designed to operate over a temperature range of 0°F to 160°F and endure vibration levels of 8.0 g's (peak) over a frequency range from 65 Hertz to 2 KHz sinusoidal and  $0.13 \text{ g}^2/\text{Hz}$  random over a 50 hertz to 1 KHz range.

A functional description of the inverter may be best understood with the use of the block diagram in Figure D-13. The inverter accepts +21 to +31 VDC at the input connector. The input is redundantly wired to feed-thru EMI suppression filters to the main series-input, LC Filter, and a zener voltage clamp. It drives a 10 KHz Royer oscillator and feeds the primary and secondary of power converter No. 1 (a saturable toroid). The toroid output is rectified and filtered to 31 VDC and fed to the differential comparator circuit with a temperature compensated zener for the voltage reference. The comparator's error signal is fed to a magnetic amplifier which increases or decreases the voltage coupling from the Royers' output thru power converter No. 1. It should be noted that a decrease of input voltage from 31 to 21 VDC will be sensed by the comparator and magnetically amplified to boost the voltage coupling. The pre-regulated 31 VDC is then used by four other loads.



The post regulator consists of power converter No. 2 which is essentially two power switching transistors with their bases phase driven by the Royer oscillator. Their collectors are tied to the pre-regulated +31 VDC with their emitters driving the primary of a center-tapped grounded power transformer. The secondary windings provide the required voltages which are rectified and filtered. These voltages are then series regulated, current limited and fed to the spacecraft.

One other major section in the inverter is the AC generator. The fundamental of the 400 Hz sine wave is generated by a common 400 Hz flip-flop. One side drives the base of a single stage input amplifier. The collector of this amplifier is controlled by a series regulator in the multistage feedback loop. The output of this single stage drives into a 0.5 cubic inch, double quadradic, passive, 400 Hz bandpass filter. The filtered output is sinusoidal with less than 1% harmonic distortion and 5% dissymmetry, and drives an operational amplifier with a self-feedback loop. The output of this drives a second operational amplifier. The outputs of these two operational amplifiers are coherent but 180° out of phase. These two signals then drive the push-pull power amplifier. The output stage drives the primary of the power transformer. The secondary is tapped to supply the spacecraft with 115 VAC and 26 VAC.

The multistage feedback is sensed at the 26 VAC tap, rectified, series regulated, and fed to the collector of the single input stage. Overload protection is provided by current sensing at the power amplifier and using this signal to control turn-off of the feedback series regulator. This removes drive until the overload fault is removed.



Signal conditioning and telemetry monitoring of each voltage line, including the 115 VAC line, is accomplished within the adapter power controller, the point of central power distribution.

## 7.0 POWER SYSTEM PERFORMANCE CHARACTERISTICS

### 7.1 System Volt-Ampere Characteristic

The fuel cell has an internal impedance which degrades with life and complicates predicting fuel consumption, heat dissipation, coolant flow control and water generation.

An analytical and graphical method for determining the actual power source terminal conditions as a function of power source characteristics has been developed.

Basically, the spacecraft load is considered as three elements; constant power, constant current, and constant resistance, all operating at a nominal voltage of 26 VDC.

The system load data of each element is accumulated and summed to generate one system V-I curve. This curve is then superimposed with the early and late life curves of the power source. The net result yields the operating region of the power source over system loads.

In Biosatellite, the system load is approximately 50% constant power, 30% constant current and 20% constant resistance. Initially the system was 67%, 27% and 6% respectively.

The initial system load (V-I) characteristics and the total element makeup is shown in Figure D-14.

The effect of superimposing the fuel cell early and late life characteristics on Figure D-14 is shown in Figure D-15.

Here the operating region for the actual power source voltage varies from 28 to 24 volts, the actual current from 5.5 to 6.0 amperes and the actual power from 154 to 144 watts, all during the power source life.

This graphic approach is also developed analytically in terms of  $V$  and  $I$  for any given point in the life of the fuel cell. These  $V$ - $I$  equations can be used to correct nominal data processed by power management computer programs.

## 7.2 Load Sharing

The essential system characteristics are shown in Figure D-16. These curves were extracted from the Biosatellite flight data. It can be seen that the characteristic at launch was better than at initial activation. After approximately the first day of orbital operation, the performance improved, then remained constant at the "orbital mode" curve. Figure D-16 also shows typical non-station pass, station pass, and the powered flight system load lines, as well as the load sharing level as seen by the fuel cell upstream of the blocking diodes.

Voltage versus time characteristics of the fuel cell at station pass load levels are shown in Figure D-17. Included in the figure are corresponding curves of the performance of the qualification unit (3001) and of the unit used in the primate compatibility test (3004). The 3005 unit stabilized after a few hours at a level slightly lower than previously tested units. It then improved gradually until it reached nominal performance.

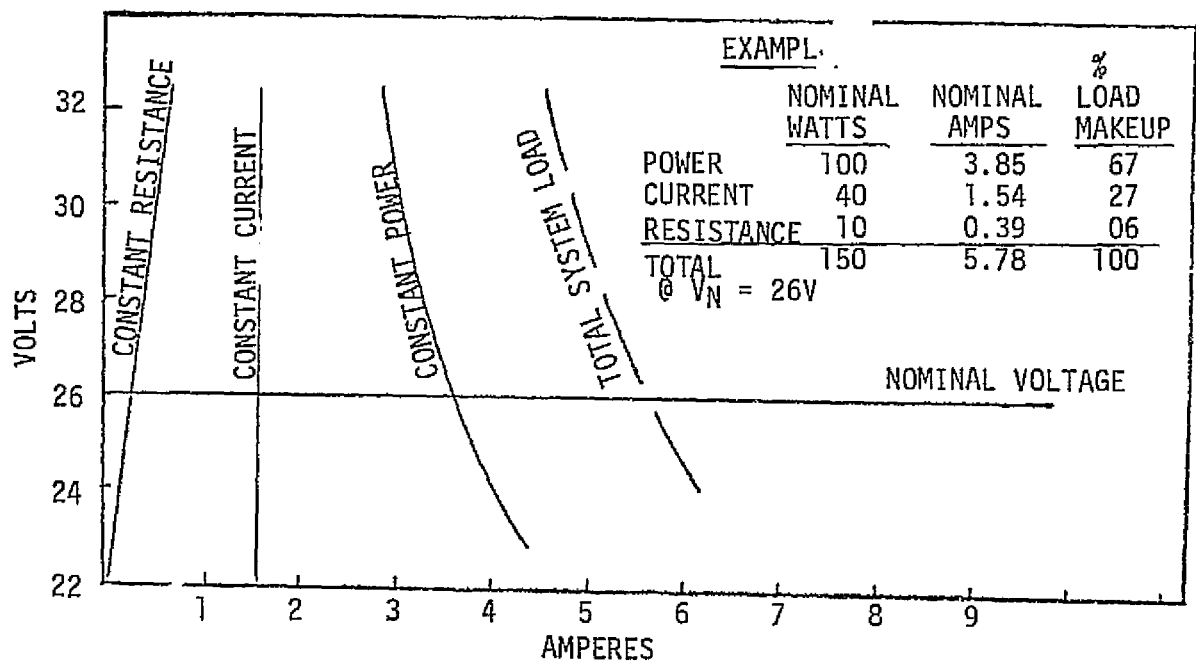


Figure D-14. System Load Distribution

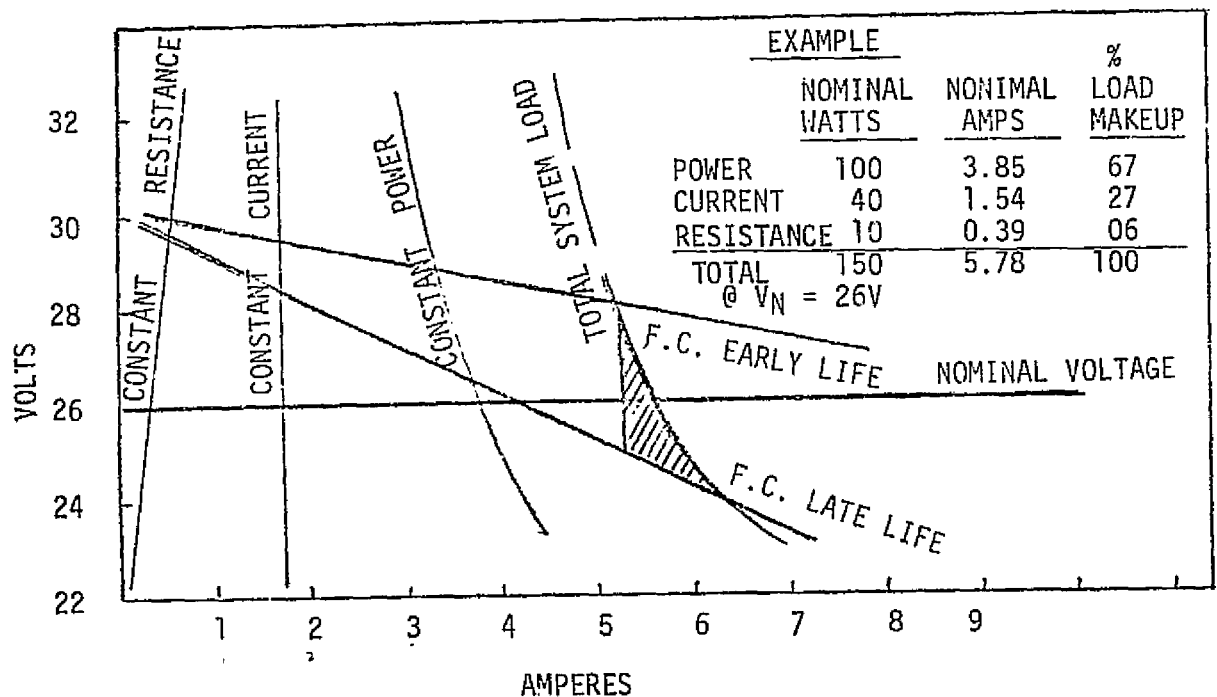


Figure D-15. Power Source Operating Region

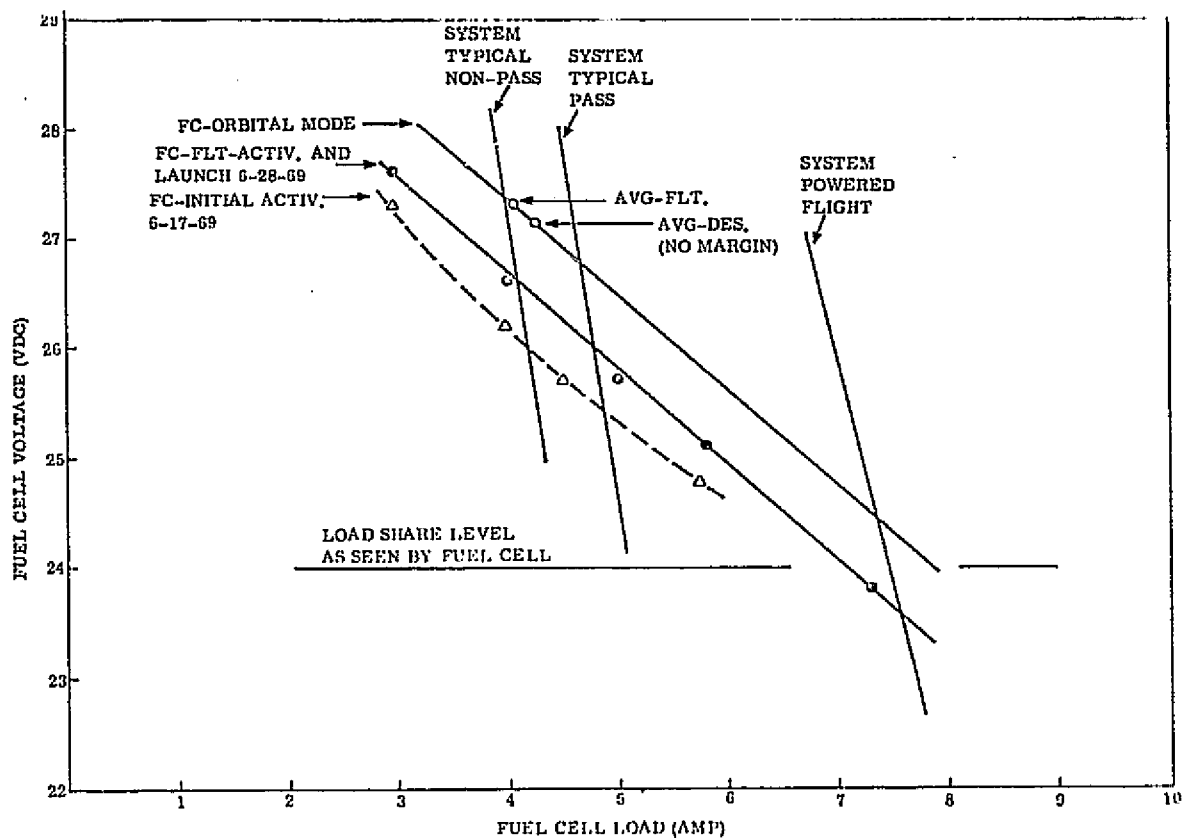


Figure D-16. Electrical System Characteristics

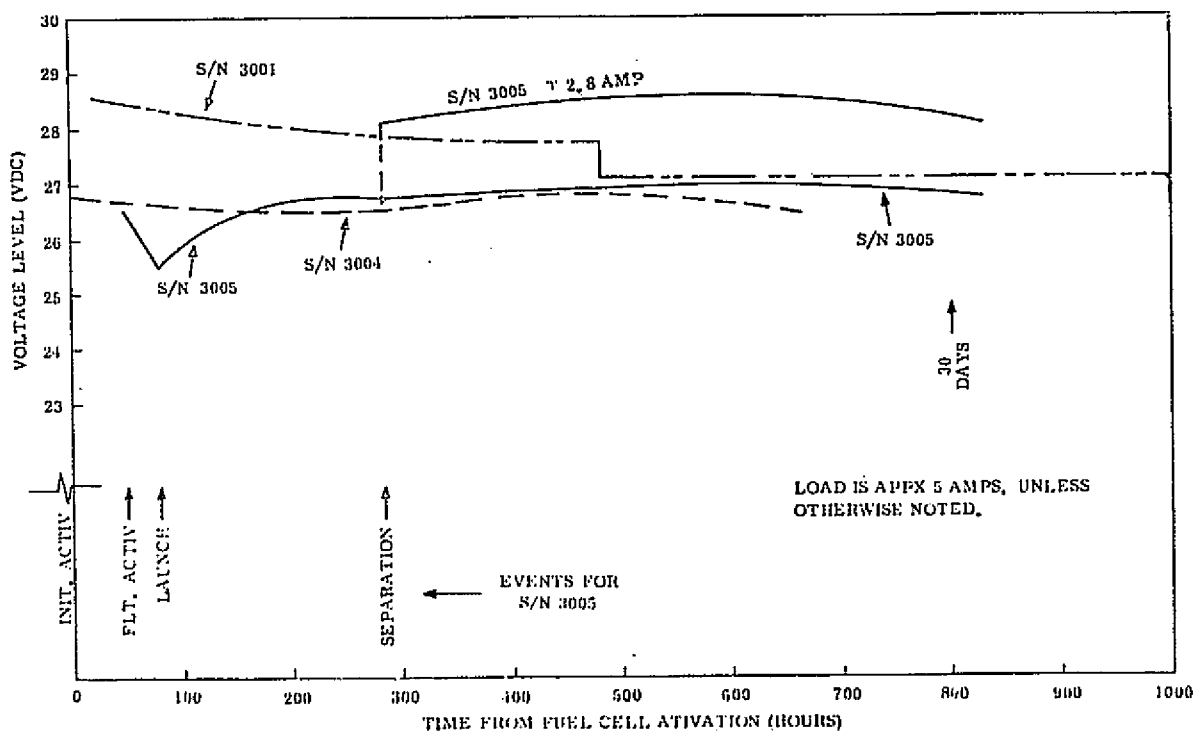


Figure D-17 Voltage Versus Time Characteristics

### 7.3 Orbital Fuel Cell Power Requirements

Vehicle subsystem and experiment power requirements are shown in Table D-7.

Average watts for the 30-day period are shown at the nominal level. Additional factors include a correction based on actual voltage levels, a prelaunch provision and a 6% margin. The fuel cell is required to carry those loads which are essentially constant and of high energy content.

### 7.4 Orbital Battery Energy Requirements

The requirements on the battery are summarized in Table D-8. The various subsystems and experiments require a total of 136.4 ampere-hours for mission functions for the 30-day period. The provision for 24 hours of emergency operation is 173.6 ampere-hours. Other provisions for instrumentation and telemetry errors, as well as a 6% margin are shown. The orbital battery is required to carry loads which are of short time duration and of low energy content, except, of course, for the emergency condition.

Table D-7

## Orbital Fuel Cell Power Requirements

Subsystem	Average Power - Watts
Attitude Control	12.72
Electrical	39.44
Life Support	26.07
Environmental Control	20.65
Experiment USC + UCLA	6.90
Pace/Rho	6.45
Telemetry, Tracking, Command	4.21
Separation and Gas Storage	<u>0.13</u>
SUBTOTAL at 26 VDC	116.57
Correction to Actual Volts	<u>2.13</u>
SUBTOTAL at actual volts	118.70
Prelaunch equivalent	2.70
6% Margin	<u>7.28</u>
TOTAL - WATTS	128.68
TOTAL - Kilowatt Hours	92.65

Table D-8

## Orbital Battery Energy Requirements

ORBITAL LOADS	AMPERE-HOURS
Prelaunch	1.5
Orbital Period (480 Orbits)	<u>134.9</u>
	136.4
Emergency (24 Hours)	173.6
Instrumentation Errors	8.1
6% Margin	20.0
Unassigned	<u>6.9</u>
TOTAL	345.0

## 7.5 Electromagnetic Compatibility

EMC is implemented by maintaining tight control at the component level. Interference generation is limited and susceptible circuits are isolated. Further isolation is maintained by proper twisting and shielding in the harness. On the 30 day vehicle the grounding system and EMC control concentrated on maintaining clean data from the primate. This is the most critical parameter in the vehicle. The grounding diagram is shown in Figure D-18.

System generated transients were measured on power lines and selected control and signal lines. The amplitudes were measured using detectors with a 50 nano-second response time. Detection points are selected to test all power lines, returns, control and signal lines test for susceptibility.



C-4

D-42

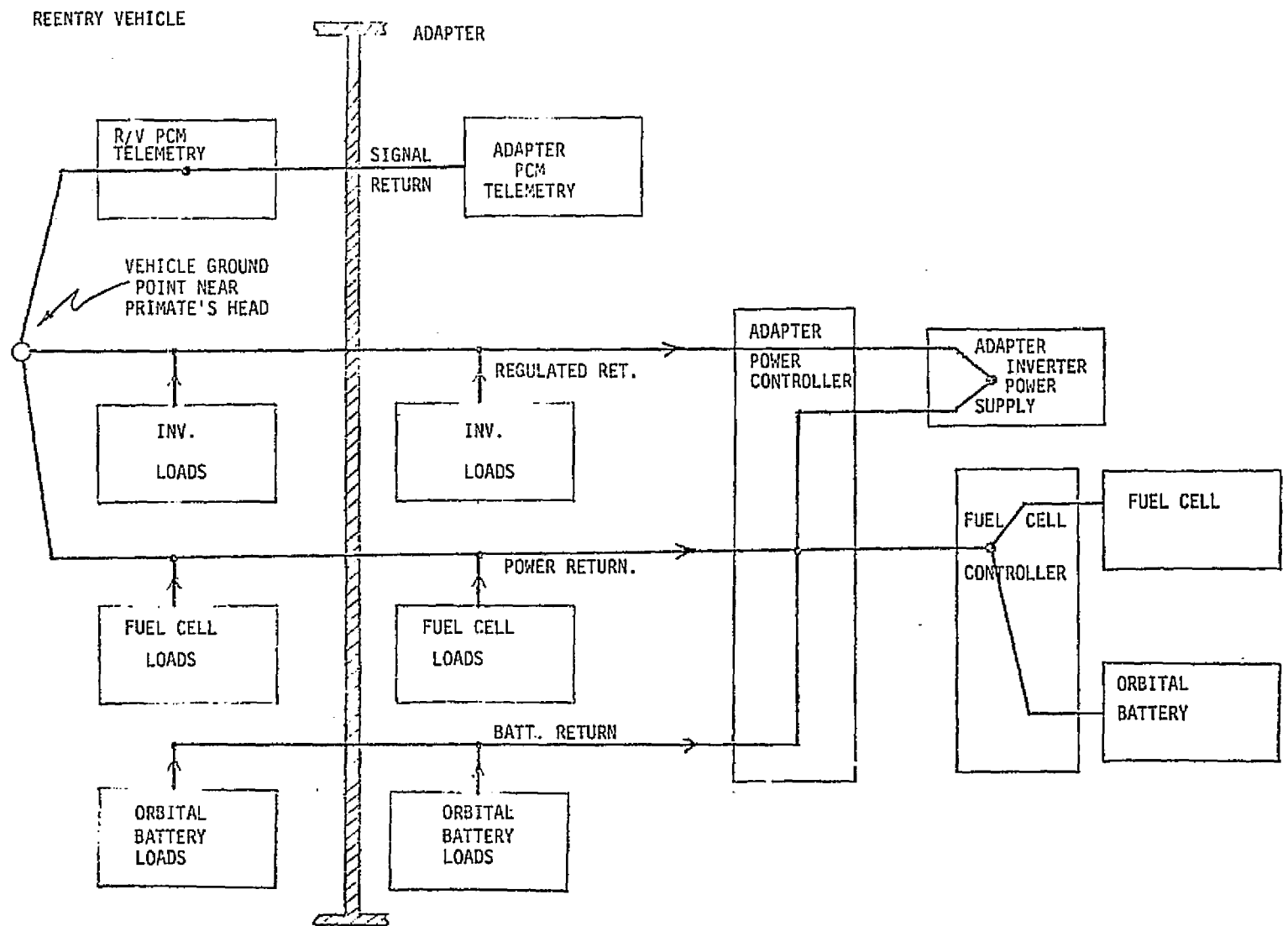


Figure D-18. Vehicle Grounding Diagram

APPENDIX E  
SOLAR ARRAY AND SECONDARY BATTERY SYSTEMS

# APPENDIX E

## SOLAR ARRAY AND SECONDARY BATTERY SYSTEMS

### TABLE OF CONTENTS

<u>SECTION</u>	<u>PAGE</u>
1.0 INTRODUCTION .....	E-1
2.0 SYSTEM OVERVIEW .....	E-2
3.0 VEHICLE CONFIGURATION .....	E-5
4.0 POWER SYSTEM FUNCTIONAL DESCRIPTION .....	E-7
4.1 Solar Array .....	E-14
4.1.1 Solar Array Volt-Ampere Characteristic .....	E-14
4.1.2 Solar Array Physical Characteristics .....	E-15
4.1.3 Solar Array Operation .....	E-16
4.2 Storage Modules .....	E-17
4.2.1 Battery Charge Control .....	E-20
4.2.1.1 Region I Operation .....	E-22
4.2.1.2 Region II Operation .....	E-23
4.2.1.3 Region III Operation .....	E-25
4.2.1.4 Region Transitions .....	E-27
4.2.1.5 Ground Commands .....	E-29
4.3 Power Control Module .....	E-30
4.3.1 Series Pulse Width Modulator Circuit Description .....	E-30
4.3.2 Series Pulse Width Modulator Circuit Operation .....	E-33
4.3.3 Series Pulse Width Modulator System Considerations .....	E-36
4.4 Payload Regulator Module .....	E-43
4.5 Parameter Descriptions .....	E-43
4.6 Shunt Dissipator .....	E-45
4.7 Auxiliary Regulator .....	E-51
4.8 Auxiliary Load Controller and Load Panels .....	E-55

APPENDIX E  
SOLAR ARRAY AND SECONDARY BATTERY SYSTEMS  
TABLE OF CONTENTS

<u>SECTION</u>	<u>PAGE</u>
4.9 Power Switching Module .....	E-55
4.10 Power Subsystem Telemetry Summary .....	E-55
4.10.1 Battery Voltage Telemetry .....	E-58
4.10.2 Regulated Bus and Solar Array Current Telemetry .....	E-60
4.11 Power Management .....	E-62

# LIST OF TABLES

<u>TABLE</u>		<u>PAGE</u>
E-1	Subsystem Power Demands .....	E-4
E-2	Operational Mode Power Demands .....	E-11
E-3	Payload On-Time Capability .....	E-13
E-4	Battery Charger Parameters .....	E-28
E-5	PCM and PRM Series PWM Regulator Characteristics .....	E-44
E-6	Shunt Dissipator Characteristics .....	E-50
E-7	Auxiliary Regulator Characteristics .....	E-54
E-8	Telemetry Characteristics .....	E-57

# LIST OF ILLUSTRATIONS

<u>FIGURE</u>		<u>PAGE</u>
E-1	Observatory Configuration .....	E-6
E-2	Power System Simplified Block Diagram .....	E-8
E-3	Power System Functional Block Diagram .....	E-9
E-4	Orbital Load Profile .....	E-12
E-5	Solar Array Characteristic .....	E-14
E-6	Battery Charger Functional Block Diagram .....	E-19
E-7	Region of Normal Charge Control Operation .....	E-21
E-8	Current Regulator Block Diagram .....	E-22
E-9	Maximum Battery Voltage as a Function of Temperature .....	E-23
E-10	Charge Control Operation in Region II .....	E-24
E-11	Charge Current Operation in Region III .....	E-26
E-12	Pulse Width Modulator Block Diagram .....	E-31
E-13	Pulse Width Modulator Voltage Regulation Mode .....	E-34
E-14	Pulse Width Modulator Current Limit Mode .....	E-37
E-15	Failure Detector and Switchover Block Diagram .....	E-40
E-16	Failure Detector Response Time .....	E-42
E-17	Switching Regulator Efficiency .....	E-42
E-18	Simplified Input/Output Filters .....	E-43
E-19	Simplified Shunt Dissipator Circuit .....	E-47
E-20	Power Dissipation of Shunt Limiter .....	E-48
E-21	Shunt Dissipator Dynamic Impedance .....	E-49
E-22	Shunt Dissipator Loop Stability .....	E-49
E-23	Simplified Auxiliary Regulator Schematic .....	E-52
E-24	Auxiliary Regulator Loop Gain and Phase Angle .....	E-53

## LIST OF ILLUSTRATIONS

<u>FIGURE</u>		<u>PAGE</u>
E-25	Auxiliary Regulator Dynamic Impedance .....	E-53
E-26	Battery Voltage Telemetry Circuit .....	E-59
E-27	Typical Voltage Calibration Curve .....	E-59
E-28	Current Telemetry Circuit .....	E-60
E-29	Typical Current Calibration Curve .....	E-61
E-30	Power Management Flow Diagram .....	E-63

## 1.0 INTRODUCTION

The initial spacecraft of the Earth Resources Technology Satellite Program, ERTS-1, was designed by General Electric Space Division, Valley Forge, in co-operation with NASA, Goddard Space Flight Center, Maryland, and was launched on July 23, 1972.

The ERTS observatory design is based upon highly successful Nimbus satellites that have regularly returned meteorological data and pictures of the Earth's weather and surface since 1964.

The ERTS-1 spacecraft power processing system is similar to Nimbus with modifications introduced to provide increases in average and peak power capability from its polar-orbit, sun-tracking solar array.



## 2.0 SYSTEM OVERVIEW

The 2100 pound Earth Resources Technology Satellite was launch into a 500 mile, polar orbit from Vandenberg Air Force Base and Missile Test Center, California, aboard a two-stage Delta 900 launch vehicle.

The spacecraft has been designated as a research and development tool to demonstrate that remote sensing from space is a feasible and practical approach to efficient management of earth resources.

Specific requirements of the ERTS system are to provide multispectral photographic and digital data of large scene (100x100 nautical mile) in user-oriented quantities, repetitive land and costal observations at the same local time, image overlap in direction of flight, image sidelap from adjacent orbits, image location to better than 2 nautical miles, world coverage in less than three weeks, and a spacecraft life of one year. It should be noted that the ERTS spacecraft has been operating since July 1972 and is continuing to produce over 100,000 images.

The ERTS observatory carries two television-type camera subsystems; Return Beam Vidicon(RBV) and Multispectral Scanner (MSS) which furnish independent views of the Earth (900 kilometers) directly beneath the satellite to data acquisition stations on the ground. Two wideband video tape recorders store up to 30 minutes of picture information for delayed readout. The observatory also carries a Data

Collection Subsystem (DCS) which serves as a relay for collecting data from remotely located ground platforms.

An active attitude control subsystem maintains the spacecraft within  $\pm 0.7$  degree of local vertical and  $\pm 0.7$  degree in the orbit plane (YAW).

Electrical power (520 watts) is generated by two independently driven solar arrays, with energy storage provided by 8 nickel-cadmium batteries for eclipse periods, launch, and pulsed loads. Independent power processors are used to supply payloads and spacecraft subsystems.

Communication links between the spacecraft and ground stations are provided via wideband (2.2GHz) and narrow band (2.1GHz to 137.8MHz) subsystems. The Wideband Telemetry Subsystem accepts and processes data from the RBV, the MSS, and both wideband video tape recorders. It consists of two 20-watt FM transmitters and associated filter, antennas, and signal conditioning equipment. The subsystem permits transmission of any two data sources simultaneously, either real time or recorded.

Commandable power-level traveling-wave-tube (TWT) amplifiers and shaped beam antennas provide maximum data fidelity at minimum power.

The communication links are mentioned here since they and the three experiments (RVB, MSS, and DCS) are the larger power consumers as indicated in Table E-1.

Table E-1  
Subsystem Power Demands

<u>Service Subsystems</u>	<u>Watts</u>
Attitude Control-----	35.7
Command and Data Handling-----	76.2
Telemetry-----	9.3
	<hr/> 121.2
<u>Payload Support Subsystems</u>	
Wideband Communications-----	144
Wideband Tape Recorders	
Record-----	172
Playback-----	175
<u>Payloads</u>	
Multispectral Scanner-----	52.3
Return Beam Vidicon-----	174.1
Data Collection System-----	1.3

### 3.0 VEHICLE CONFIGURATION

The spacecraft launch weight is approximately 2073.1 pounds including 107 pounds for the adapter. The power system weighs 540.1 pounds or about 26 percent of the launch weight. The power system weight is a summation of not only the electrical but also the mechanical items necessary to its total support and operation. Briefly some of these items are the solar array panels, servo drive and transition section, latch mechanisms, and slip rings. Other items included are the batteries, power regulators, timers, electronics, power controllers, and 183 pounds of harnessing and installation hardware.

The major identifying features of this ERTS/Nimbus class of vehicle as show in Figure E-1 are its 5 foot diameter sensory ring containing 18 bays for mounting various types of equipment; the attitude control module supported by a truss tube structure from hard points on the sensory ring; and the two solar array paddles driven from separate drive mechanisms contained in the attitude control module. The payload sensors are mounted mainly on the underside of the sensory ring to afford unobstructed view of the earth's surface. An orbit adjust subsystem is mounted in the region just above the sensory ring to assure the orbital period is within the prescribed limits.

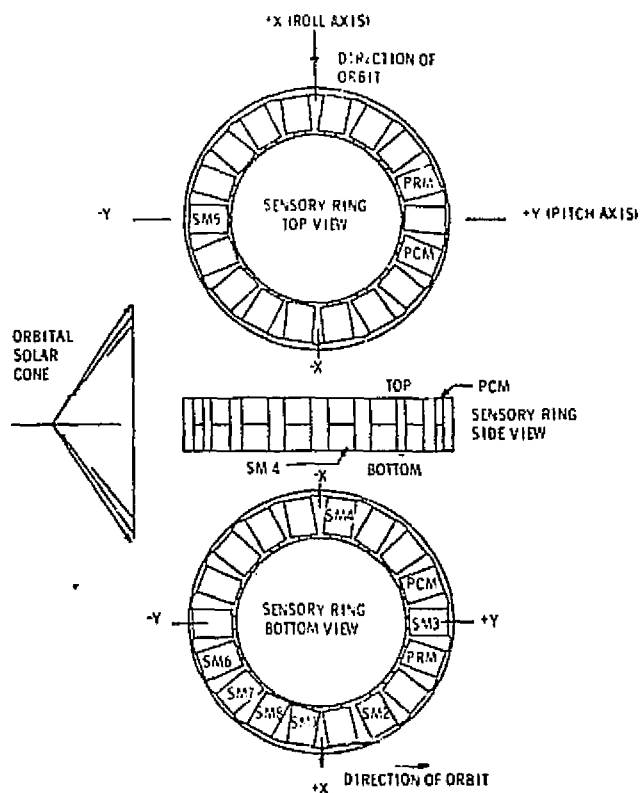
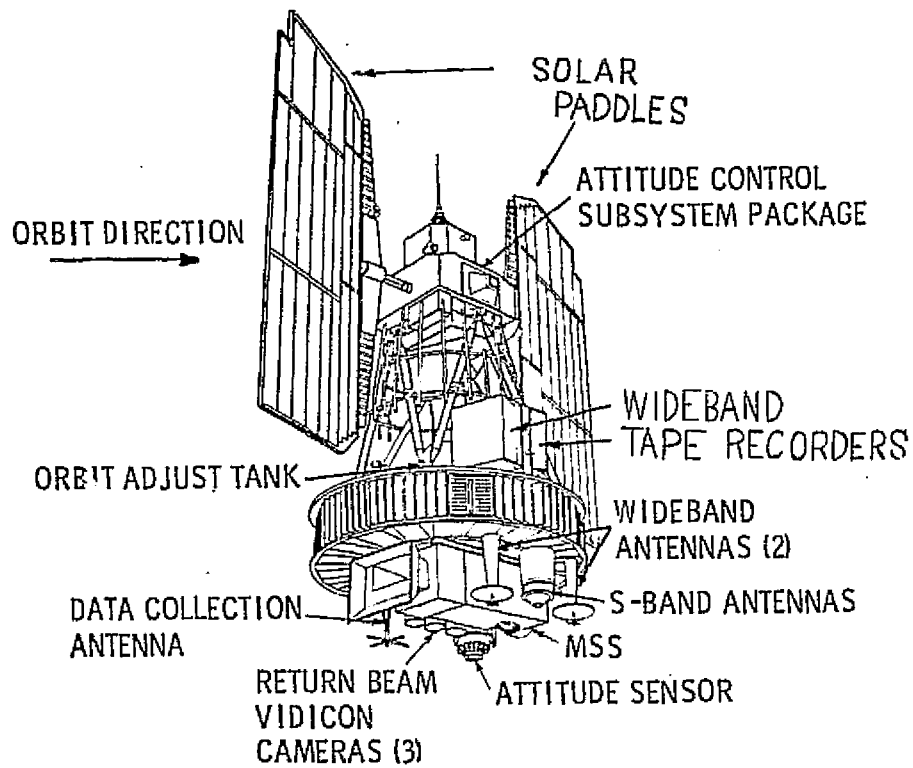


Figure E-1 Observatory Configuration

#### 4.0 POWER SUBSYSTEM FUNCTIONAL DESCRIPTION

The power subsystem is designed to process solar array energy at -38 vdc to regulated power at  $-24.5 \pm 0.5$  vdc to the bulk of the spacecraft loads. Unregulated power is also available for certain pulsed loads, mainly associated with pyrotechnic events, and a small amount of power is provided at  $-23.5 \pm 0.5$  vdc from auxiliary regulators for back up purposes in the event of failure in the main power system. Figure E-2 shows a simplified block diagram of this power subsystem.

As shown on the functional block diagram of Figure E-3 the power system consists of: (1) two solar array platform assemblies with a combined BOL output capability of roughly 520 watts; (2) a separate solar array drive and slip ring assembly for each platform; (3) 8 storage modules, each containing a 23-cell, 4.5 ampere-hour battery and charge electronics; (4) a power control module (PCM) having the main function of voltage regulating the array and battery power to the service subsystems with a rating of 20 amperes; (5) a payload regulator module (PRM) which specifically voltage regulates the power to the main imaging payloads with a rating of 26 amperes; (6) a power switching module (PSM); (7) and (8) auxiliary loads and controller for absorbing excess array power; and (9) an unfold timer for deploying the solar array after injection into orbit.

Under normal spacecraft day conditions the solar array supplies power at a voltage of about -38 vdc. Power from the array is transferred to the loads through in-line diodes to the PCM and PRM buck regulators, which regulate the power to an output at  $-24.5 \pm 0.5$  vdc. The PCM and PRM regulators establish separate regulated buses, the PCM bus being devoted to the service subsystems and the PRM bus to the major payload sensing systems. The PCM and PRM designs are essentially identical. Besides taking advantage of the Nimbus developed PCM, the separation into service and payload buses has resulted in excellent

E-8

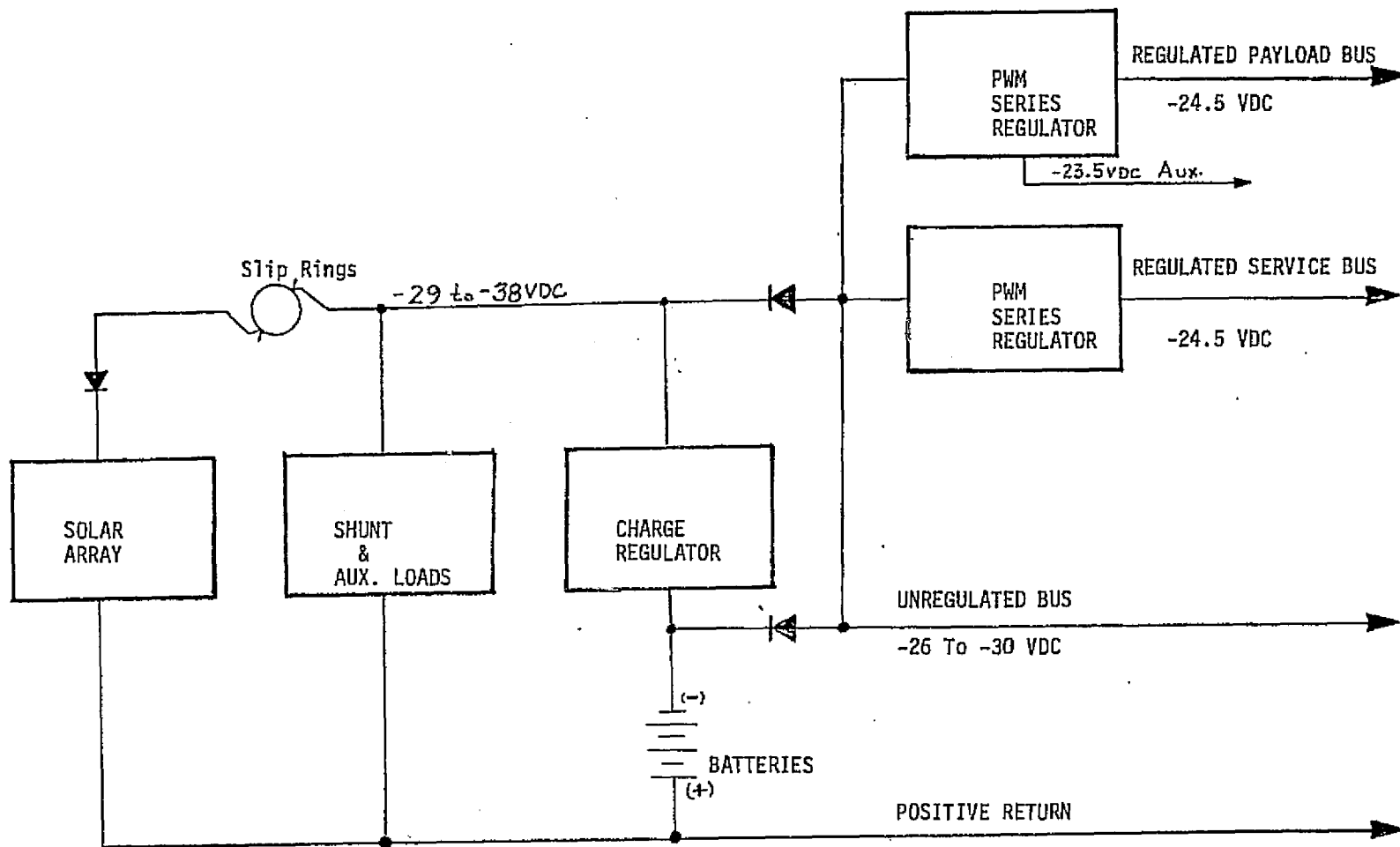


Figure E-2 Power System Simplified Block Diagram

REPRODUCIBILITY OF THE  
ORIGINAL PAGE IS POOR

٩٤

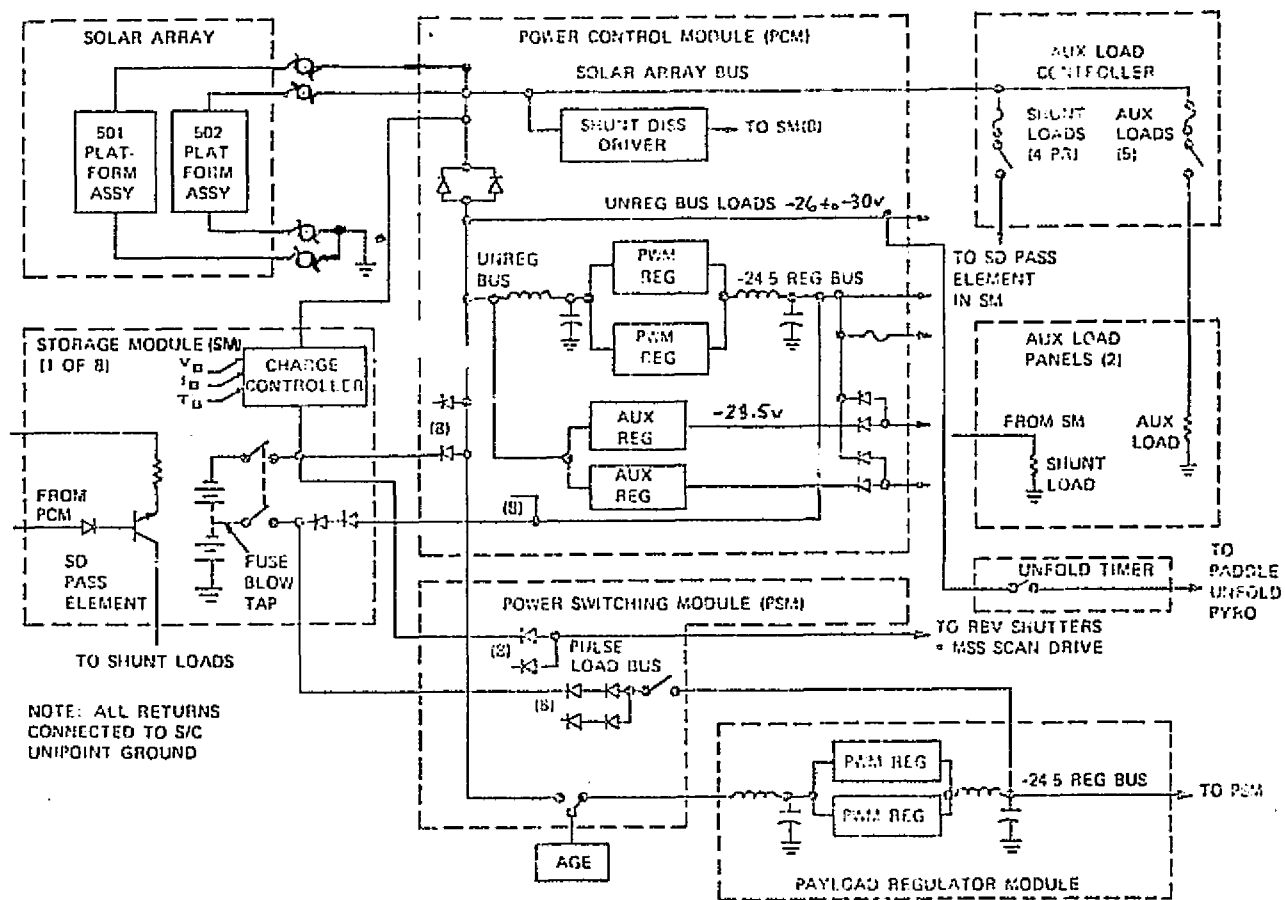


Figure E-3 Power System Functional Block Diagram



buffering against the effects of turn-on transients and noise.

Power from the array for battery charging is transferred through each of the eight chargers to the batteries with charge voltages roughly in the range of -29 to -33 vdc. Each battery is individually controlled in accordance with current and combined temperature/voltage limit criteria. Since the array voltage is higher (more negative) than the charge voltage, each battery is prevented from discharging by means of blocking diodes in the discharge leg of each battery.

During spacecraft night the batteries supply power through their discharge diodes at voltages in the range of -26 to -30 vdc. This is still above the lower limit of the buck regulator for producing regulated power at  $-24.5 \pm 0.5$  vdc.

During spacecraft day when the loads exceed the array output, the array voltage drops, allowing the batteries to supply current through their discharge diodes. In this case, both the array and batteries share the burden of current supplied to the PCM and PRM buck regulators.

Under certain circumstances, with small load and battery charge demands, the array voltage can become abnormally high. This condition can be avoided by absorbing the excess array power with shunting loads. Automatic shunts are incorporated in the system in the form of eight transistor-resistor circuits which are activated in response to array voltages more negative than -38 vdc. These circuits can be enabled or disabled by ground command. Fixed auxiliary loads

can also be used, which are likewise enabled or disabled by ground command. These loads have been used to control charge to the batteries by adjusting control of the current limit at lower levels than that achievable by the internal charge controls of each battery.

The in-line diodes between the array and the series PWM regulators are used to prevent the auxiliary loads from absorbing battery energy during spacecraft night operation.

Fault clearing capability for the system is provided by means of a fuse blow tap located at the 15th cell (negative from the positive return) of each battery. These are joined to the main bus through diodes and are normally inactive. If a severe fault depresses the regulated voltage, sufficient current may be drawn directly from the batteries through the fuse blow taps to clear the fault.

Table E-2 indicates demand levels during launch, minimum satellite and orbital modes. The minimum satellite mode pertains to the demand required during emergency conditions when it might be necessary to conserve energy to the greatest extent possible.

Table E-2  
Operational Mode Power Demands

	<u>Watts</u>
Launch Mode	146
Minimum Satellite Mode	97
Orbital Mode (without payloads)	121
Orbital Mode (with payloads)	521

Figure E-4 shows a typical orbital load profile as reflected at the regulated bus. Continuous loads associated with basic service subsystems account for about 121 watts. The major load peak results from payloads with a maximum demand of 521 watts. These high power demand payloads are the Multi-spectral Scanner (MSS) and the Return Beam Vidicon (RBV), both associated with imaging aspects of the mission. The on-time duration per orbit of these payloads was not specified as a hard requirement but is rather tailored to the capability of the power system.

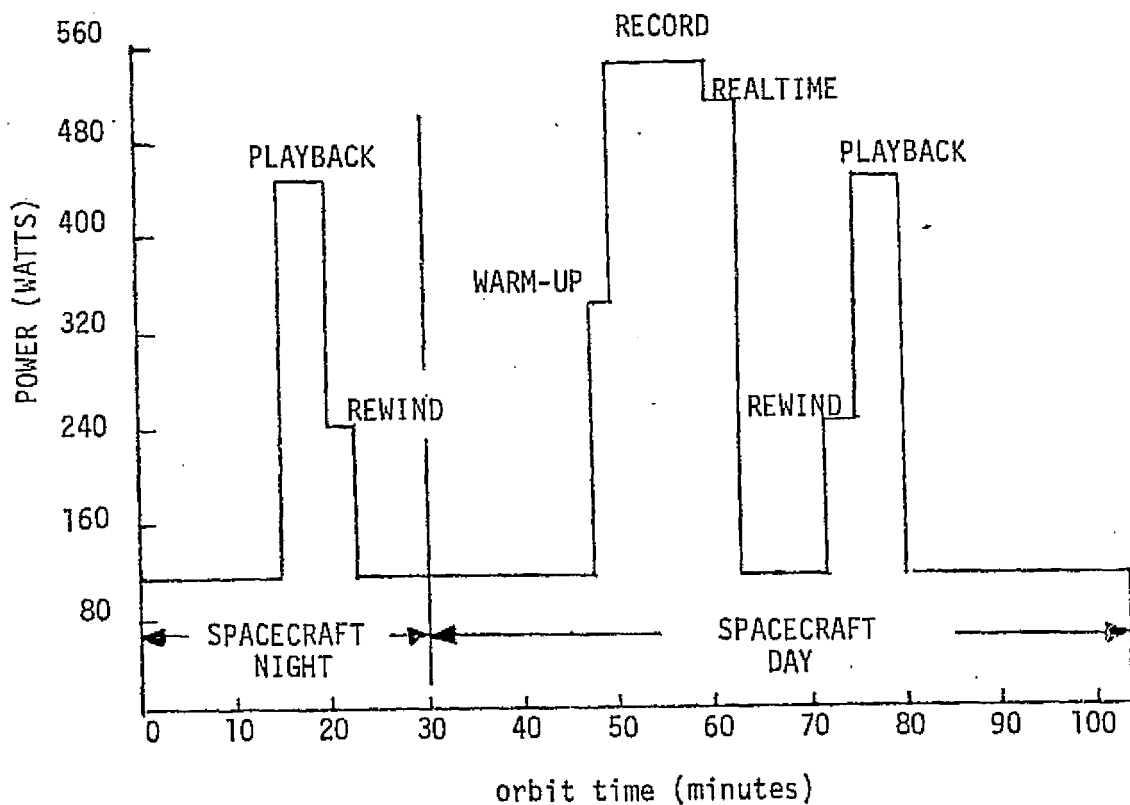


Figure E-4 Orbital Load Profile

Table E-3 indicates the estimated on-times as a function of specific mission durations and are based on the predicted power system output degradation principally due to ionizing radiation.

The other load peaks of significance are associated with playback (PB) of recorded data during passes over receiving ground stations in line-of-sight.

with the spacecraft. Such passes occur about equally during satellite night and day accounting for the equal allocation of playback shown. Rewind of the tape recorder pertains to repositioning of the tape for use in its next mode of operation.

Table E-3 Payload On-time Capability

Elapsed Time in Orbit	Payload On-time Per Orbit
Initial Orbit	16 minutes
6 months	13 minutes
12 months	9 minutes

Basis:

1. Both the Return Beam Vidicon and the Multispectral Scanner in operation concurrently
2. Record for 75% of Payload on time
3. Transmit on realtime for 25% of Payload on time
4. Payload playback occurs: 50% in Satellite Day, 50% in Satellite Night

## 4.1 Solar Array

### 4.1.1 Solar Array Volt-Ampere Characteristic

The solar array volt-ampere characteristic is shown in Figure E-5. Unique to the normal solar array characteristic is its post eclipse character where the solar cells have experienced a cold soak period in the Earth's shadow, zero array power output, followed by a post eclipse or sun-soak period. Here the array voltage is almost twice its normal value as indicated by the upper curve in Figure E-5. The thermal time constant or the time for the array voltage to return to its nominal voltage level is dependant on many factors, but is in the neighborhood of 20 minutes.

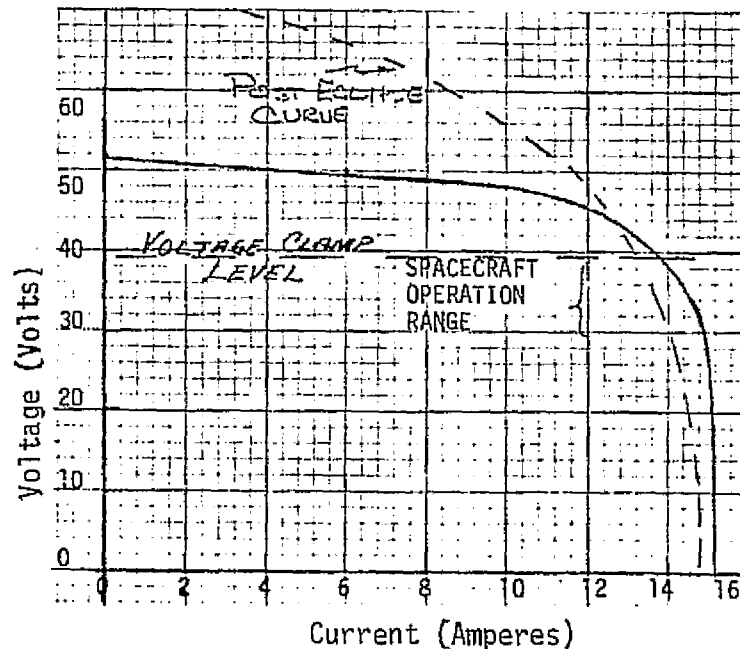


Figure E-5 Solar Array Characteristic

This post eclipse, overvoltage condition for a relatively long period is unacceptable to most subsystem components and/or regulators, and essentially dictates the need for a voltage clamp as indicated by the horizontal dotted line in Figure E-5. A clamping device takes the form of a transistor/resistor shunting element (located in the storage modules), with control provided by spacecraft bus voltage level sensing and comparator circuit amplifiers to provide the drive control. The net affect of the clamp is to hold the spacecraft bus to a preselected upper voltage level that is acceptable for power regulation.

One other unique solar array characteristic must be considered. That is the eclipse period itself. Here the power from the array drops to zero. This characteristic dictates the need for the 8 energy storage devices, (batteries), that must provide the required power for a maximum eclipse period. Additional power management functions are carried out by the commandable Auxiliary Load Controller which causes power to be drained from the solar array bus to the Auxiliary Load Panels. These auxiliary loads are generally required when it is desired to reduce the power dissipated in the Storage Modules.

#### 4.1.2 Solar Array Physical Characteristics

The two solar array paddles, aluminum honeycomb (3X8 feet each), and two transitions sections (1X7 feet each), weighing 75.1 pounds are configured with nineteen diode isolated solar cell circuits. Each circuit contains an average of 9 parallel and 93 series connected cells for a total of 10,888

2 by 2 centimeter solar cells. These are N on P type with a base resistivity of 1 to 3 ohm-centimeters with titanium-silver contacts and are nominally rated at 132 milliamperes and 0.46 volt when measured at 28°C under equivalent

air mass zero illumination. Six-mil microsheet (Corning 0211) coverslides bonded to the solar cells are used for radiation protection. Silver expanded metal Z-bar strips are used to interconnect the solar cells.

#### 4.1.3 Solar Array Operation

During the launch sequence, the solar array is in the stowed position and the batteries must supply the required loads. Upon separation of the spacecraft from the adapter, relays are energized in the Unfold Timer which cause the paddle unfold pyros to fire at predetermined intervals. When the cables are cut, the unfold motor is started, deploying the solar array. In approximately 16 minutes, the array begins to slew to acquire the sun and with its acquisition the solar array assumes the power generating function for the spacecraft.

During sunlight periods, the solar array delivers power to the solar array bus in the power control module at a voltage of about -30 to -39 volts. The lower limit is set by the battery discharge voltage. As -30 volts is approached, load sharing occurs and the batteries begin to carry the spacecraft load.

## 4.2 Storage Modules

There are eight essentially identical storage or battery modules on the ERTS spacecraft. Each storage module contains 23 series connected, 4.5-ampere-hour, hermetically sealed, nickel-cadmium cells; weighing approximately 15.4 pounds and requiring 312 cubic inches.

In addition, each module contains the closed-loop charge controller associated with each battery as shown in Figure E-6. This controller limits the charge current to a preset value (1.1 amperes per module) and also reduces this when either the battery voltage or temperature reaches a predetermined limit. A ground commandable override circuit in the Power Control Module inhibits the voltage-temperature control loop in the charge controller, permitting battery charge rates based on the battery/solar array voltage relationship.

In the negative leg of each battery is a battery disconnect latching relay which can be actuated by ground command for the purpose of removing a degraded battery. This relay also disconnects the battery fuse blow tap line. The battery tap is used to supply the necessary current to clear faults on the fused power lines.

The battery module also contains one of the dissipating legs for the spacecraft shunt limiter. Although this circuit bears no direct relationship to battery operation, the battery module provides a convenient location in the spacecraft from which the heat dissipated by the shunt limiter may be rejected.



A functional block diagram of the battery charge controller is shown in Figure E-6. The controller electronics represents a significant area of power processing and therefore the subsequent paragraphs will attempt to describe the functional operation. It should be recalled that this system is a mid-1960 design and therefore does not contain integrated circuits.

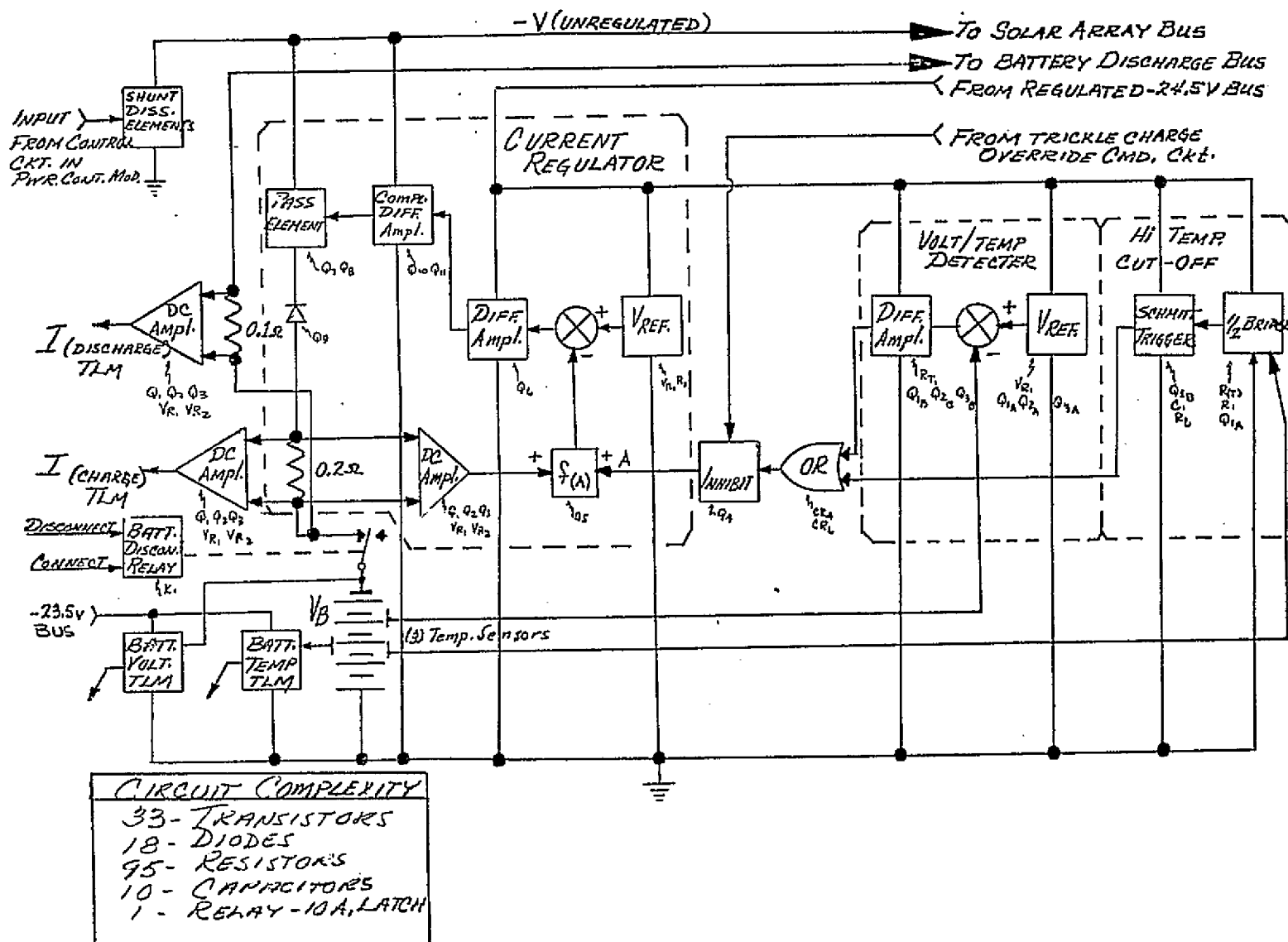


Figure E-6 Battery Charge Functional Block Diagram

#### 4.2.1 Battery Charge Control

The purpose of the charge controller is to protect the battery from over-current, over-voltage, and over-temperature conditions while it is being charged.

The circuit performs this function by monitoring and operating upon the following parameters:

1. Battery charge current
2. Battery temperature
3. Battery terminal voltage

The control circuitry was designed to accept signal inputs corresponding to each of the above parameters and to compare these inputs with built-in references. Deviations or error signals are amplified and ultimately adjust battery charging current in such a manner as to decrease the error.

There are three normal modes in which the charge controller might operate. These modes or regions of operation are indicated in Figure E-7.

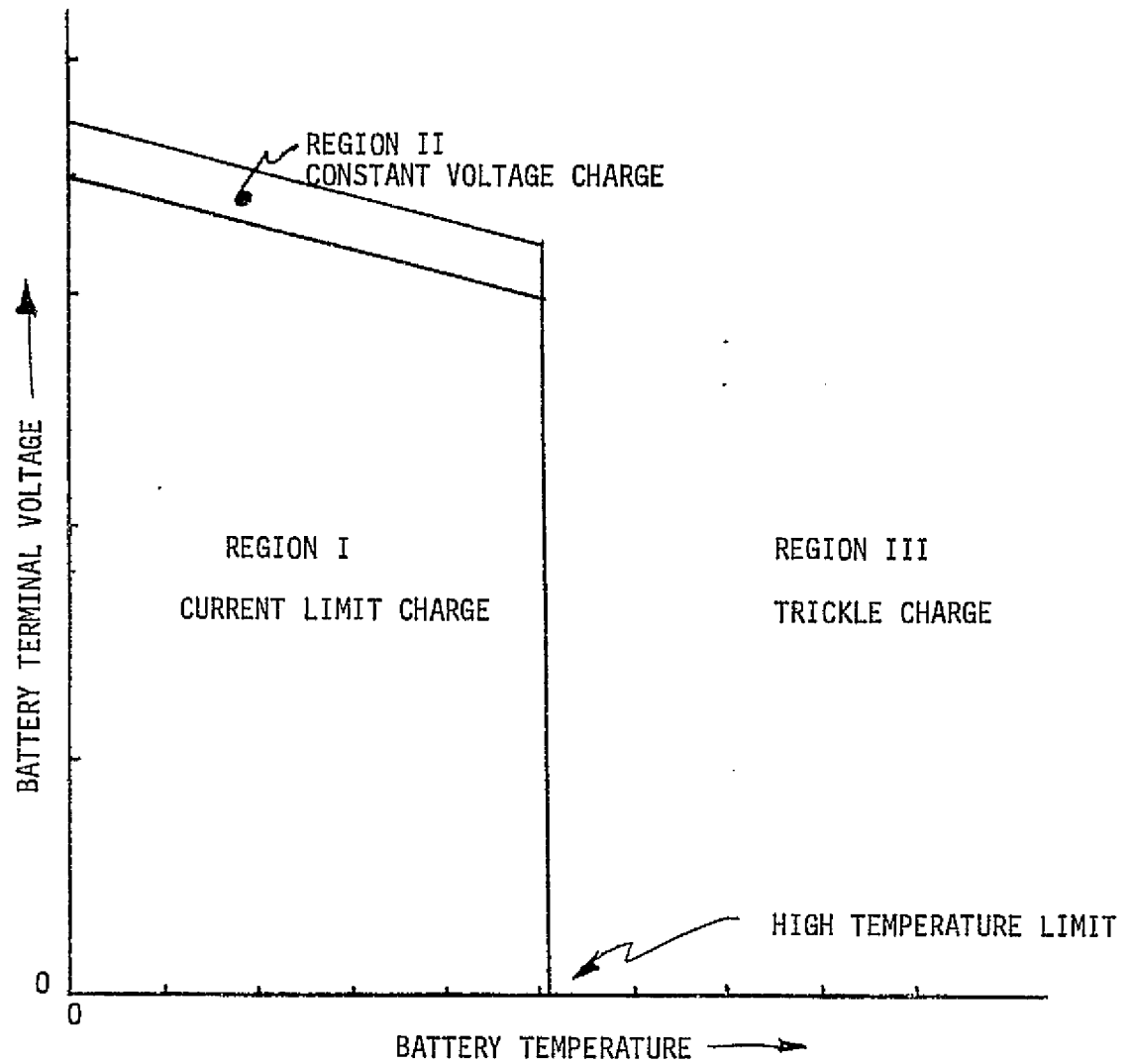
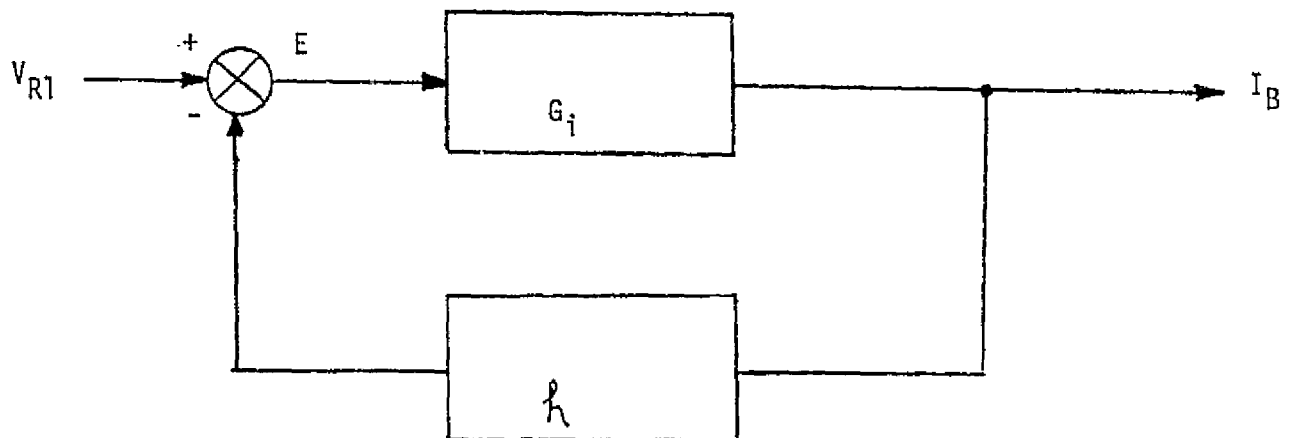


Figure E-7 Region of Normal Charge Control Operation

4.2.1.1 Region I Operation. In Region I, it is desired to maintain charging current as close as possible to the maximum allowable current. In addition, any current less than that required to maintain energy balance could result in a degraded mission through insufficient charging. The tolerance requirements on the charge current have dictated a closed loop or feedback type of current regulating circuit.

Figure E-8 presents a block diagram of the current regulator. In Figure E-8 the symbol,  $V_{R1}$ , represents a reference voltage derived from a temperature compensating zener diode and a voltage divider. " $G_i$ " represents the forward gain or transconductance of the transistor circuitry; " $h$ " represents the feed back element which senses battery current,  $I_B$ , and transforms the current level to a voltage level which is compared with  $V_{R1}$ . The difference between  $V_{R1}$  and the converted current level is the error,  $E$ , which activates the forward gain to control the charge current.



$$\text{TRANSFER FUNCTION: } I_B = V_{R1} \left[ \frac{G_i}{1 + h G_i} \right]$$

Figure E-8 Current Regulator Block Diagram

4.2.1.2 Region II Operation. In Region II it is desired to limit the voltage to which the battery may charge. It is also desired to adjust this limiting voltage with battery temperature as shown in Figure E-9.

Normally, at the beginning of charge, the battery will cause the charge controller to operate in Region I, the current limited mode. As the battery

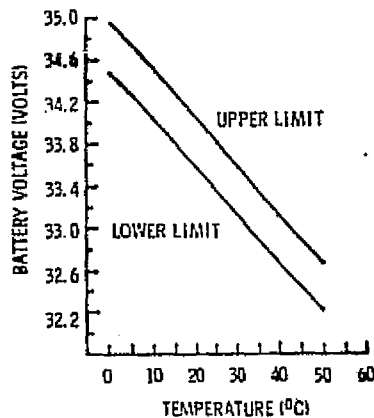


Figure E-9 Maximum Battery Voltage as a Function of Temperature

is charged, its terminal voltage and/or temperature will increase. Should the voltage/temperature combination enter Region II, the charge controller will sense this condition and act in such a manner as to maintain the operating condition of the battery within this region. Since the charge controller may operate directly on charge current and on other parameters only as a function of charge current, the circuitry was designed to vary the current in order to maintain operation in Region II.

Within Region II, the charge controller becomes essentially a voltage regulator with an output voltage related to temperature. Figure E-10 illustrates this mode of operation.

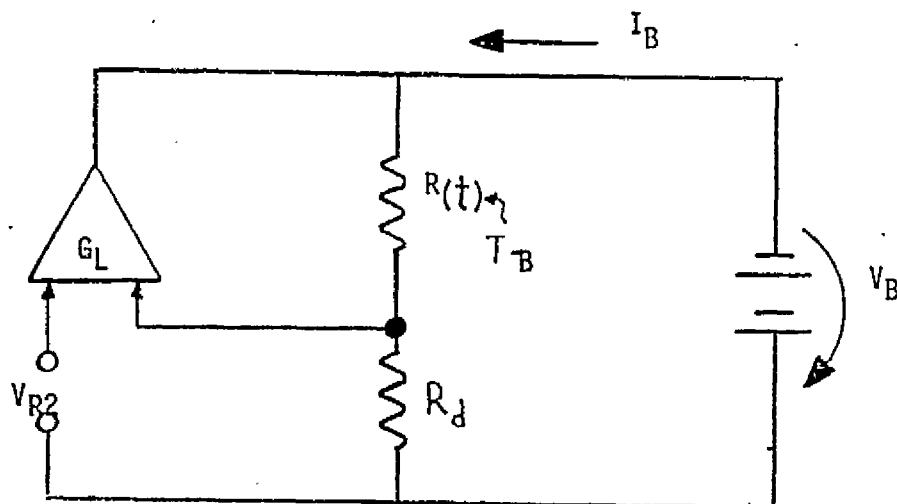


Figure E-10 Charge Control Operation in Region II

If the gain,  $G_L$ , is high, then it may be shown that

$$V_B = V_{R2} \left( 1 + \frac{R_t}{R_d} \right)$$

Where:

$G_L$  = Effective transconductance of transistor circuitry  
in Region II.

$V_B$  = Battery voltage.

$V_{R2}$  = Reference voltage for V/T circuit

$R_d$  = Constant resistance

$R_t$  = Temperature sensitive resistor with a negative  
temperature coefficient.

As the battery temperature increases,  $R_t$  decreases thereby reducing the value of  $V_B$  at which the circuit will regulate.

4.2.1.3 Region III Operation. In Region III, the charge controller operates as a constant current regulator in essentially the same manner as in Region I with the exception that the regulated current is the trickle charge current. There are two conditions which could lead to operation in Region III.

The first condition would occur in Region II operation if battery voltage and temperature conditions forced the voltage/temperature circuit to reduce charging current to the trickle charge limit.

The second condition would occur should the battery temperature rise to the high temperature limit indicated in Figure E-7. In this case, the circuitry designed to detect this high temperature condition would immediately reduce or cut-out charge current to the trickle rate. Should the temperature decrease by a small, predictable amount, the charge current will be returned or cut-in to a level determined by the current regulator and the voltage/temperature sensing circuits. If, after the higher charge current level is restored, battery dissipation could be high enough to cause the high temperature limit to be reached, a cyclical condition might be established. Essentially, in this mode of operation, the charge controller acts as a temperature regulator and controls battery power dissipation in order to regulate battery temperature.

Charge controller operation in this mode is described in Figure E-11. In



Figure E-11 the battery temperature is sensed by thermistor,  $T_B$ , and resistor,  $R_S$ , which act as half-bridge.

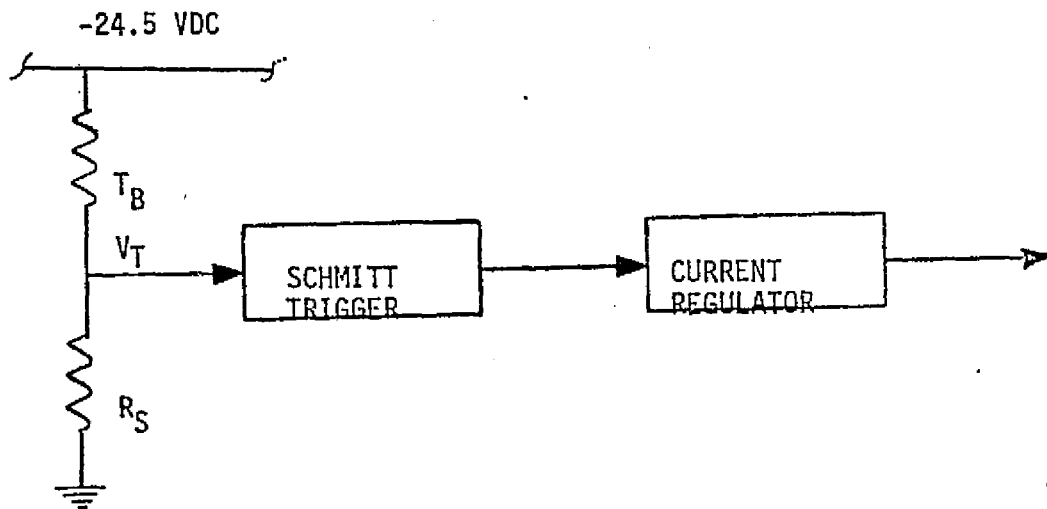


Figure E-11 Charge Current Operation in Region III

The voltage,  $V_T$ , reaches the trip level of the Schmitt Trigger at the high battery temperature due to the negative temperature coefficient of the thermistor. At the trip level, the Schmitt Trigger delivers a step current to the current regulator which causes the battery current,  $I_B$ , to be reduced to the trickle charge level. As the battery temperature decreases,  $V_T$  will decrease by an amount equal to the hysteresis of the Schmitt Trigger.

Upon reaching the lower trip level, the Trigger will change state and allow the current regulator to charge the battery at the normal rate.

4.2.1.4 Regional Transitions. As has been established in the foregoing discussion, the transition from one operating region to another is afforded by changes in the operating mode of the charge controller system. The basic operating mode is regulation of charge current. All transitions are accomplished by causing a reduction in the level of regulated current as a function of signal inputs to the current regulator from the high temperature sensing circuits and/or the voltage/temperature sensing circuits. The nature of these signals is a voltage level shift from a high impedance point which is "OR' gated into the appropriate current regulator input and which is derived from each of the sensing circuits. Figure E-6 presents an operational diagram of the entire charge controller. As indicated, the sensing signal inputs modify the feedback ratio of the current regulator in order to affect a change in the battery current.

The major parameters of the battery charge controller as well as the telemetered parameters are indicated in Table E-4.

Table E-4  
Battery Charger Parameters

Parameter	Range
Normal Charge Current	1.1±0.1 amperes
Trickle Charge Current	0.15± .05 amperes
High Temperature Limit	51.7±28°C
Hi-Temp Detection Circuit Hysteresis	2.6±2.4°C
Battery Voltage/Temp Detection Band	See figure E-9

Analog Signals for Telemetry Subsystem		
Parameter	Parameter Range	Nominal TLM Range
Battery Voltage	-20 to -40v	0 to -6 volts
Battery Temperature	-10 to +70°C	-1 to -6 volts
Battery Charge Current	0 to 1.2 amps	-0.5 to -6 volts
Battery Discharge Current	0 to 2.4 amps	-0.5 to -6 volts

4.2.1.5 Ground Commands. For the purpose of protection against various failure modes and for the flexibility of load programming, two ground commands are included as indicated in Figure E-6. One command protects against failure in the temperature and voltage circuits by providing a trickle charge override. Here, the trickle charge override disables the temperature and voltage sensing circuits at their connection to the current regulator loop by merely blocking their outputs until command off.

The function of the second ground command is to disconnect a battery from the subsystem. There are sixteen commands available for this purpose (2 for each battery ) so that individual batteries may be removed and reconnected as required.

### 4.3 Power Control Module (PCM)

The Power Control Module contains the spacecraft's main and standby PWM series (bucking) regulator, a voltage sensing and switchover circuit, redundant auxiliary regulators, a bus-voltage sensing circuit and driver circuit for the 8 shunt dissipator circuits located in the storage modules and auxiliary load panels, and a number of telemetry and diode circuits.

The entire module weighs approximately 22 lbs, requires a volume of 624 cubic inches, and has an orbital average thermal dissipation of 27 watts. The main and standby regulators weigh approximately 6 pounds and about 80% of this weight is attributed to the common input LC filter and the common output energy storage network.

Each of the functional areas within the Power Control Module will be described with major emphasis placed on the main and standby pulse width modulated regulator.

4.3.1 Series Pulse Width Modulator Circuit Description. The current limited pulse width modulated (PWM) voltage regulator is shown in block diagram form in Figure E-12. This regulator in simplest form is composed of the following sections.

- (1) Input Filter
- (2) Power Switching Network
- (3) Output Filter
- (4) Constant Current Drive Amplifier
- (5) Pulse Width Modulator and Sawtooth Oscillator
- (6) Over Current Sensing Amplifier
- (7) Voltage Sensing Amplifier

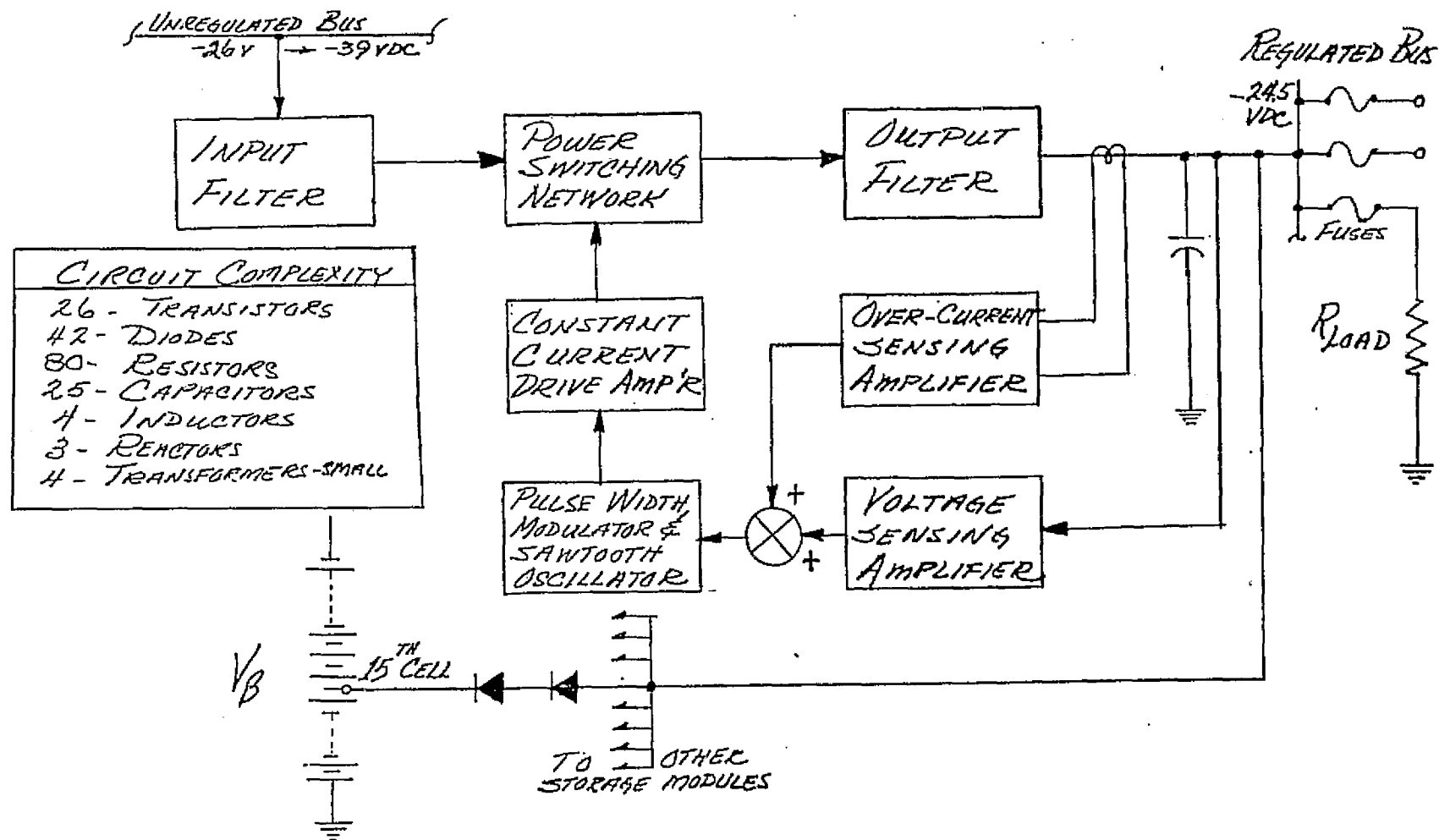


Figure E-12 Pulse Width Modulator Block Diagram

The input filter is placed between the unregulated bus and the power switching network to eliminate large ripple currents which would otherwise flow. The power switching network is used to alternately connect and disconnect the unregulated bus and the output filter. The voltage sensing amplifier senses the output voltage; compares it with a stable reference voltage; amplifies the error between the two voltages and transmits the amplified error signal to the pulse width modulator and sawtooth oscillator. The pulse width modulator transmits a rectangular pulse train; and the sawtooth oscillator determines the frequency of the pulse train. The duty cycle of the square wave pulse train is determined by the signal level transmitted from the voltage sensing amplifier. The constant current drive amplifier accepts the pulse train as an input and transmits a constant current amplitude pulse to the power switching network at a duty cycle determined by the pulse width modulator circuit. The system employs a negative feedback voltage loop (composed of the voltage sensing amplifier, pulse width modulator, and the constant current drive amplifier) to vary the duty cycle of the power switch network and establish a well regulated output voltage level which is essentially independent of input voltage and load current variations.

An excessive current is also translated to a proportional voltage which is compared with a stable reference voltage. The difference between the two voltages is amplified and transmitted to the pulse width modulator and sawtooth oscillator. This system employs a negative feedback current loop (composed of the over current sensing amplifier, pulse width modulator, and constant current drive amplifier) to vary the duty cycle of the power switch network to reduce the output voltage, thereby limiting the output current.

4.3.2 Series Pulse Width Modulator Circuit Operation. For purposes of simplification, operation of the regulator in the voltage regulation mode and current limit mode will be discussed separately.

(A) Voltage Regulation Mode

Operation of the voltage regulation mode may be explained on the basis of the functional block diagram in Figure E-13. The DC input voltage is modulated by the switch to produce a rectangular pulse train at the averaging filter input. The average or DC value of the pulse train is the duty cycle of the switch times the input voltage. The averaging filter is a low pass type which greatly attenuates the AC component and passes the DC component of the pulse train with little or no attenuation. The output voltage is given as

$$V_o = \alpha V_{in}$$

$$\text{where } \alpha = \text{duty cycle}$$

$$V_{in} = \text{input voltage}$$

The switch is driven from the modulator with a constant frequency, variable duty-cycle current pulse. The modulator has a transfer function.

$$\text{Modulator Transfer Function} = \int = \frac{\%}{\text{ampere}}$$

where "%" refers to percent "on time"

and "ampere" refers to the modulator signal input current

The signal current to the modulator is derived from the differential amplifier which has a transconductance,  $G_d$ . The output current of the differential amplifier is

$$I = G_d E$$

where  $G_d$  = diff. amplifier transconductance

$E$  = error voltage



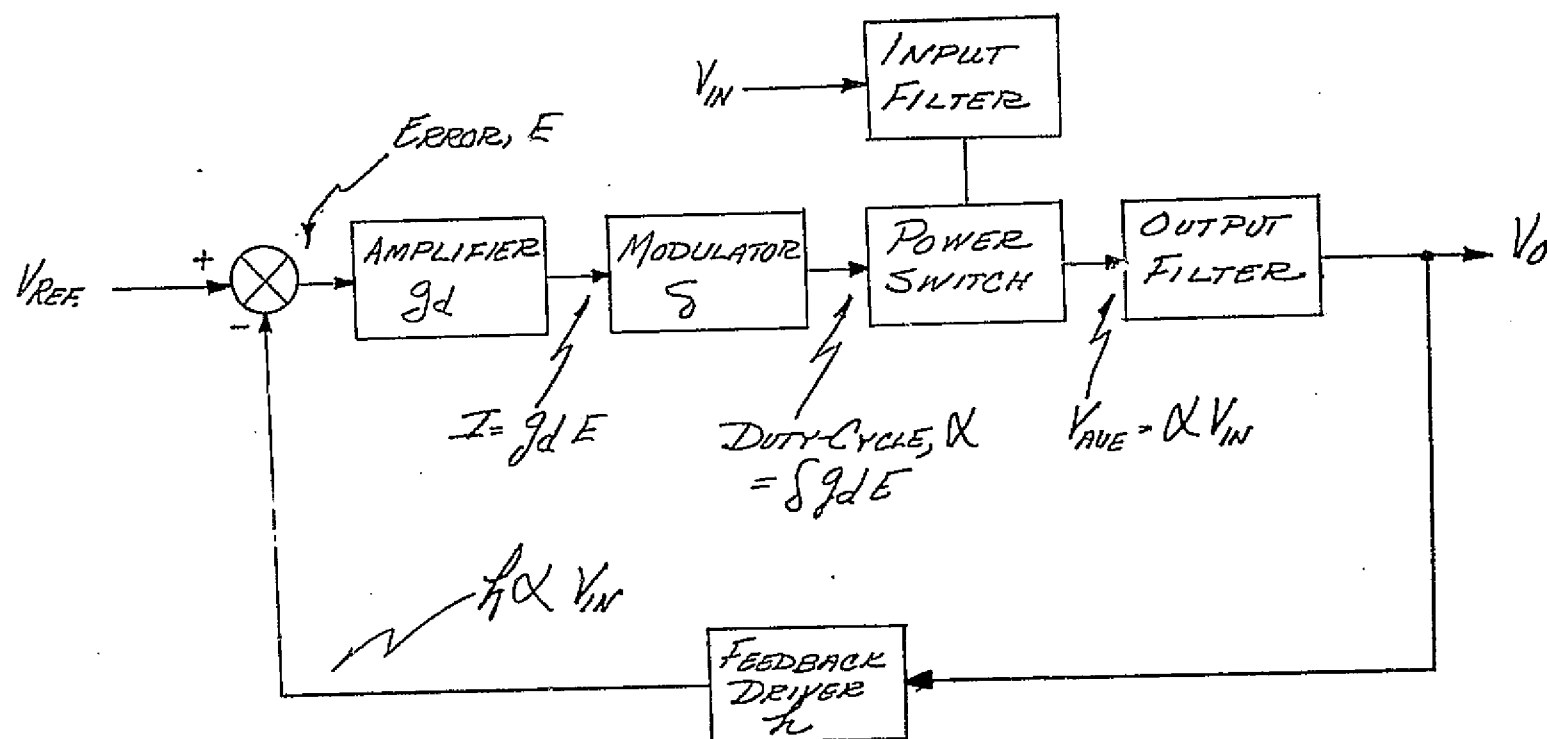


Figure E-13 Pulse Width Modulator Voltage Regulation Mode

and

$$E = V_R = h\alpha \tilde{V}_{in}$$

All the expressions thus far mentioned may be combined to express the output in terms of the reference and the individual transfer functions shown in Figure II-3, and, it may be shown that

$$V_o = \left[ \frac{V_{in} G_d}{1 + h V_{in} G_d} \right] \times V_R$$

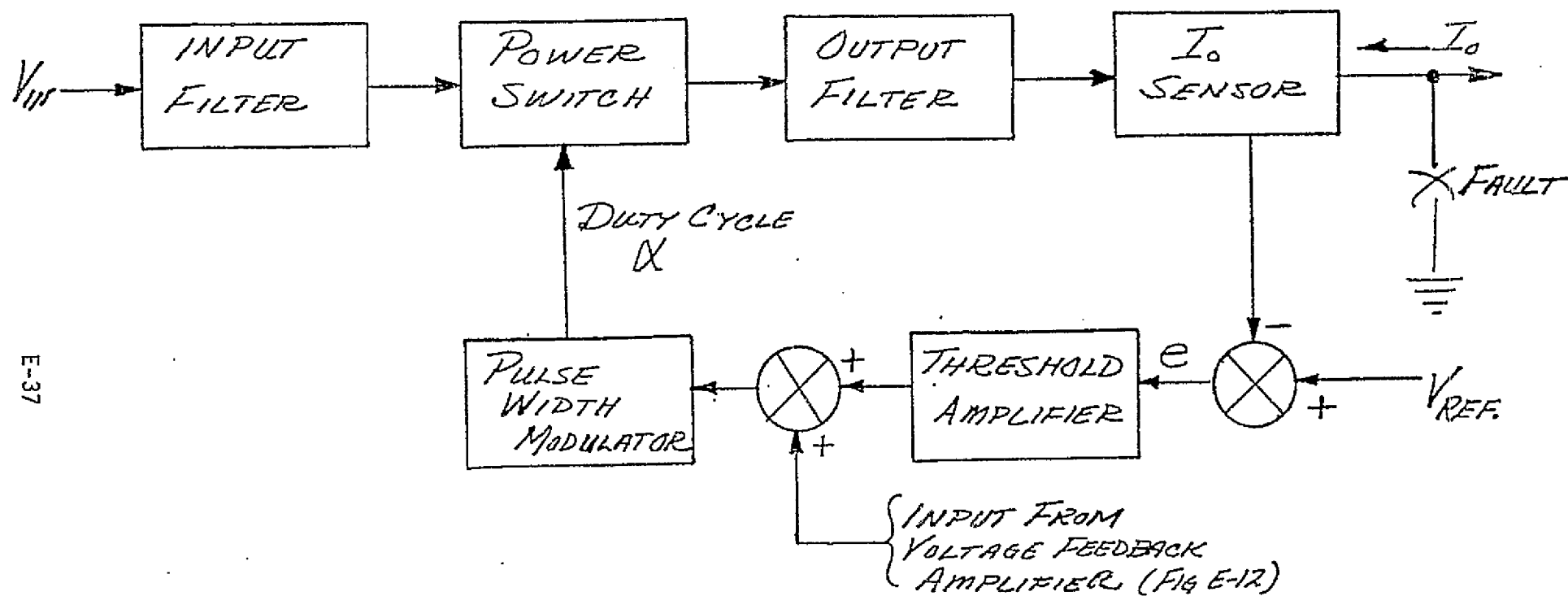
(B) Current Regulation Mode

A functional diagram of the pulse width modulator in the current limit mode is shown in Figure E-14. The current sensor produces an output voltage proportional to the peak value of output current. The sensor is a series connected saturable reactor driven by a square wave (2.4 KHz) inverter. Its output is rectified, filter and delivered via an impedance transformation stage to the indicated differential amplifier.

The difference "e" is sensed by an amplifier with a threshold which allows no amplifier output unless "e", as indicated, becomes negative. At this point, a signal is issued to the modulator which causes a reduction in power switch duty cycle. The resulting duty cycle is proportional to the magnitude of "e". The output voltage then falls as the duty cycle is reduced.

4.3.3 Series Pulse Width Modulator System Considerations. In formulating a method for modeling and analyzing power processing systems some consideration should be given to total system requirements in the area of protection and redundancy. Toward this end, three considerations are highlighted here; A, current limit protection of the PWM regulator; B, redundant PWM regulator and switch-over methodology; C, the need for an auxiliary regulator.

(A). Of prime importance is the possibility that one or more of the spacecraft loads could sustain a low impedance fault; drawing excessive current and pulling the main bus out of regulation.



E-37

Figure E-14 Pulse Width Modulator Current Limit Mode

Under this consideration the regulator must be current limited until the fault is removed or cured. If the regulator in this system were a dissipative type current limiting could be achieved merely by limiting drive to the control element wherein the regulator is transformed from a constant voltage device to a constant current device until fault removed.

In the case of a switching regulator, the output current is sensed and transformed to a proportional voltage to regulate the duty cycle of the regulator's control element. The net effect is reduced output voltage for excessive currents. This method protects the regulator from overloads including a short-circuit.

Now, considering the system as a total and under a fault condition; the system bus voltage level will drop with excessive currents, until the fault is removed or cured. Hence, the battery tap and fuse protection system is employed as shown in Figure E-12. This system operates to clear any sustained fault. If a fault develops, the regulator attempts to supply the current, but the regulator goes into its current limit mode and the spacecraft bus voltage drops to the battery tap voltage for a period of time necessary to open the fuse, clear the fault, and allow the regulator to maintain bus voltage control. Bus voltage perturbation during emergency operation must be carefully reviewed with this type of protection.

(B). Although the main regulator is current limited, protecting itself against external faults, it is usually required, from a reliability stand-point, to provide redundancy for any in-line system throttling device.

Redundancy may be approached from a piece-part stand-point, but this often becomes too complex for an in-line regulator and generally requires block redundancy, where an entire second regulator is paralleled to the main regulator and placed in a stand-by mode of operation.

Once block redundancy is accepted, a method of sensing a failure in the main regulator and switching over to the redundant regulator is required. Further, the switch-over method should minimize perturbations on the regulated spacecraft bus voltage. For this reason it is generally accepted to design the input filter and the output energy storage network of the regulator to be common to both regulators.

Internal failure detection of the main regulator is achieved as shown on Figure E-15 by sensing and comparing the bus voltage with a stable voltage reference and detecting the error signal (under or over voltage) via a schmitt trigger. The output of this device drives into a flip-flop which further drives a relay opening the failed regulator path and closing the path of the redundant regulator to the common output energy storage network. To prevent arcing of relay contacts, associated EMI effects and feedback into a failed regulator, a second flip-flop is employed to inhibit current

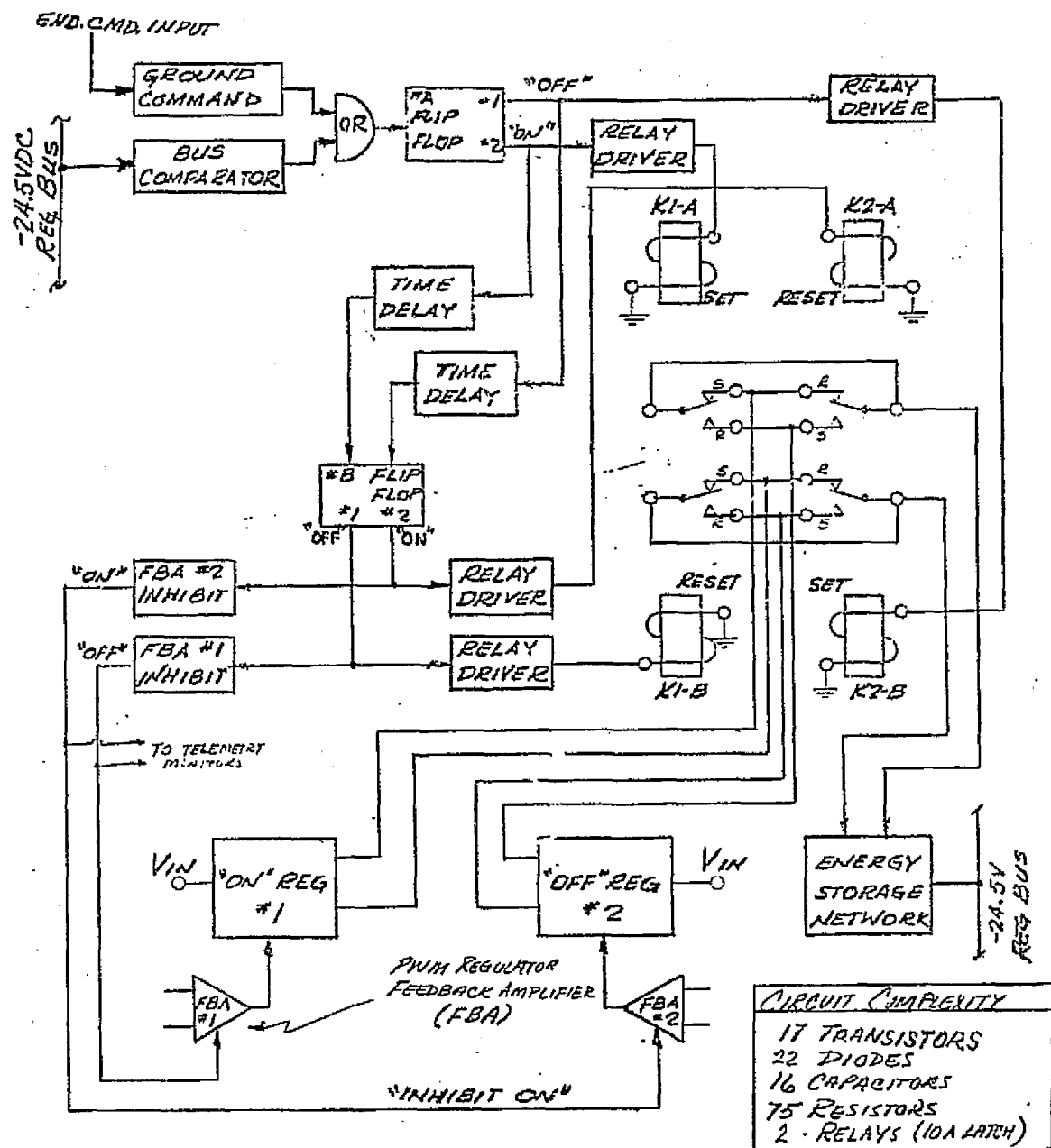


Figure E-15 Failure Detector and Switchover Block Diagram

flow from the redundant regulator until the relay contacts are firmly in place. A typical time response curve is shown in figure E-16.

Since the current limit mode of the regulator has the effect of reducing the bus voltage for a finite time, it is necessary for the current detector circuit to provide an inhibit signal to the under/overvoltage detector to prevent switchover to the redundant regulator during system fault clearing operations.

(C). In order to implement internal regulator failure detection, external over-current protection and certain control circuits, it is necessary to provide a separate regulated supply which is independent of the main regulated bus. This is achieved via an auxiliary regulator, operating one volt below the main spacecraft bus. The auxiliary regulator is a simple series dissipative type with linear base control of the pass element. The maximum current flow through the regulator is in the order of 1 ampere. A second auxiliary regulator is paralleled and diode or'd with the first as indicated in Figure E-12. Both regulators are diode gated to the regulated bus to provide power to the spacecraft command receivers so that unencoded commands can be received during temporary loss of regulated bus voltage.



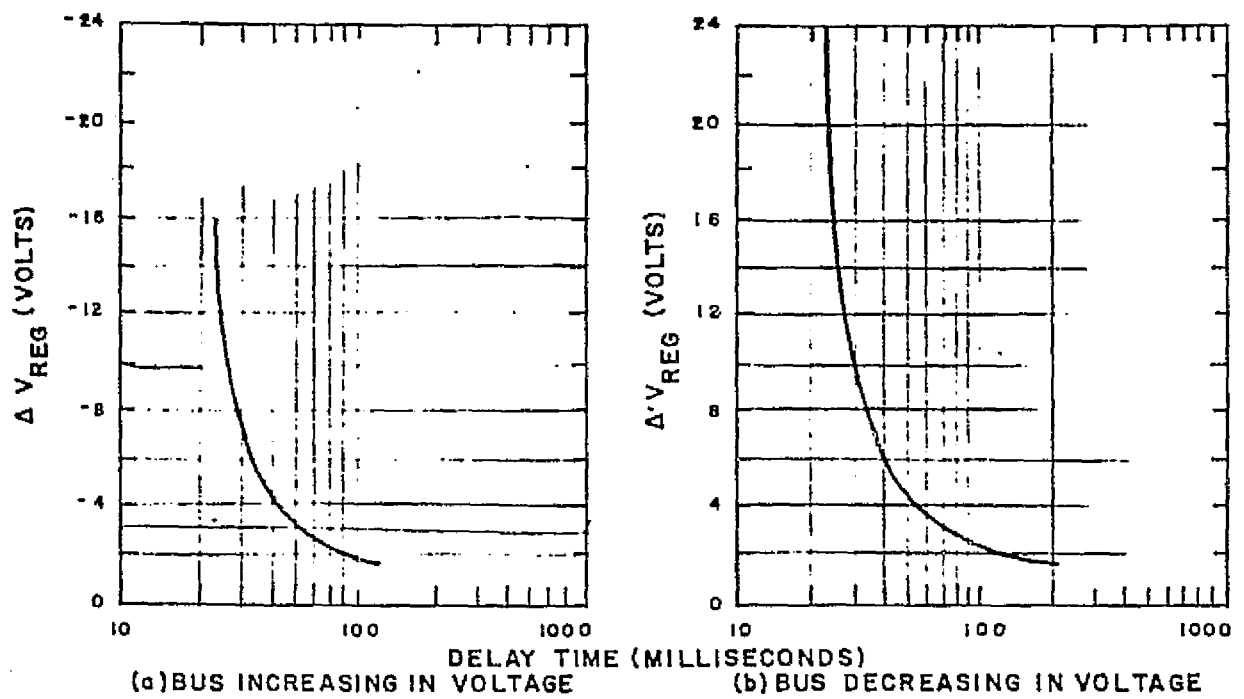


Figure E-16 Failure Detection Response Time at 25°C Centigrade

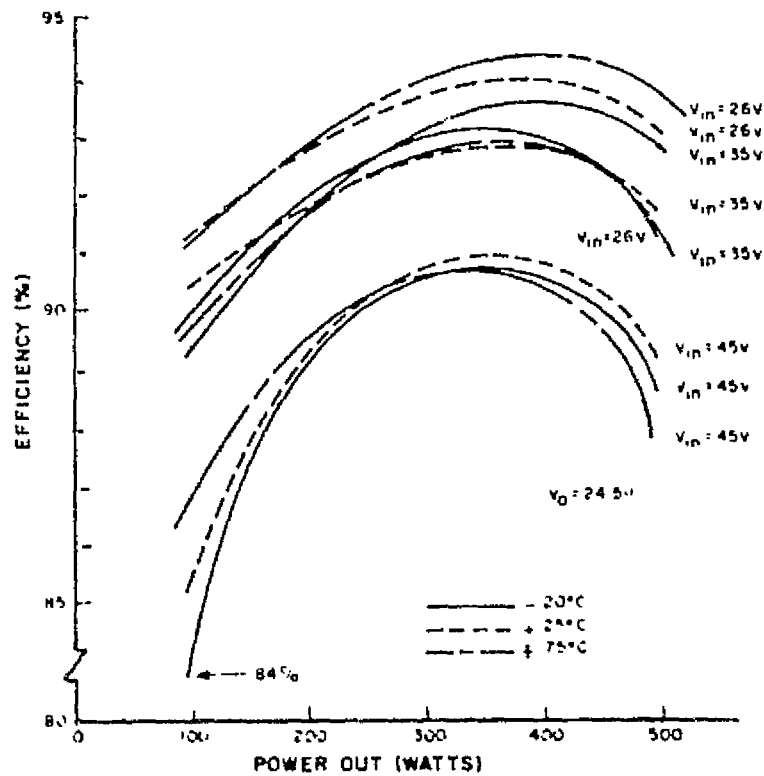


Figure E-17 Switching Regulator Efficiency

#### 4.4 Payload Regulator Module

This unit is identical to the Power Control Module except that the current limit of the series regulator is increased from 20 to 26 amperes to accommodate turn-on transients associated with payloads.

#### 4.5 Parameter Descriptions

Table E-5 summarizes the major parameters of both regulators. Figure E-18 shows a simplified circuit of the input and output filter networks.

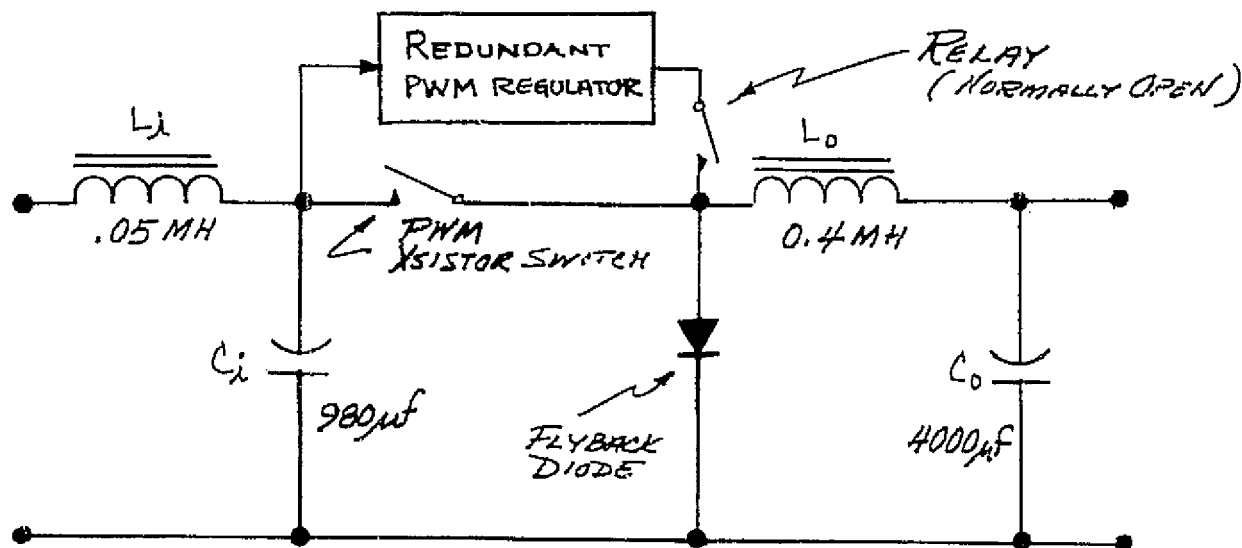


Figure E-18 Simplified Input/Output Filters

Table E-5

Power Control Module & Payload Regulator Module  
Series PWM Regulator Characteristics

PARAMETER	RANGE
Input Voltage Range	-26 to -40vdc
Output Voltage Range	-24.5±0.5vdc
Output Current	2 to 20 amperes*
Regulation**	0.5%
Ripple Voltage	50 mv p-p max.
Efficiency	see figure E-17
Output Impedance	< 0.1 ohms 10hz to 10khz
Standby Power Dissipation	7 watts
Transient Response	Return to Regulation 24.5±0.5 vdc within 4 ms after a 4 amp step load.
Operating Frequency	7.0 KHz

\* 26 amperes(max.)for Payload Regulator Module

\*\* Regulation for line, load and temperature combined.

#### 4.6 Shunt Dissipator

The shunt dissipator limits the maximum voltage that may appear on the solar-array bus. During low spacecraft power demand conditions, the power subsystem operating point will attempt to move along the solar array V-I curve (fig E-5) in a direction toward the array open-circuit voltage. For a current demand of five amperes, the operating point could be at array voltages exceeding -68 volts at cold array temperatures. This voltage is unacceptable to most regulators and must be limited.

Two important parameters govern the design of the shunt dissipator: (1) the threshold voltage and (2) the amount of power to be dissipated. In determining the threshold voltage and power to be dissipated the upper design limit (-40vdc) of the PWM series regulator is used together with the maximum solar array current of 15 amperes. These two parameters must include maximum array current on the first day of orbit, and system losses such as isolation diodes, harness, and slip rings. Also, the design must provide the minimum voltage between the battery and solar array bus that will allow the maximum charge current to enter the battery. The shunt dissipator as designed has a cut-in point of  $-38.0 \pm .3\text{vdc}$  and can handle 549 watts with a no-load dissipation of 0.6 watts.

The shunt dissipator circuitry (Figure E-19) is essentially a bus voltage error amplifier; (Differential amplifier with zener voltage reference); the output is delivered to a two-stage current amplifier to provide the linear base drive to each of the eight transistor/resistor shunting elements located in each of the eight storage modules. Current telemetry is provided for each shunting element via a voltage divider. Failure protection is provided via ground command operations of 8 relays which remove each shunting transistor/resistor element on an individual basis.

Power dissipation as a function of shunted current is shown in Figure E-20.

The dynamic output impedance of the shunt dissipator as a function of frequency under the conditions of 7 ampere load and  $+70^{\circ}\text{C}$  is shown in figure E-21.

The loop stability characteristics of the shunt dissipator are shown in Figure E-22. The circuit exhibits a maximum loop gain of 41 db at low frequencies when operating from a source having a resistance of 1 ohm, and rolls off to 0db at 3.8 KHz with a phase margin of 80 degrees.

Table E-6 summarizes the major parameters of the shunt dissipator.

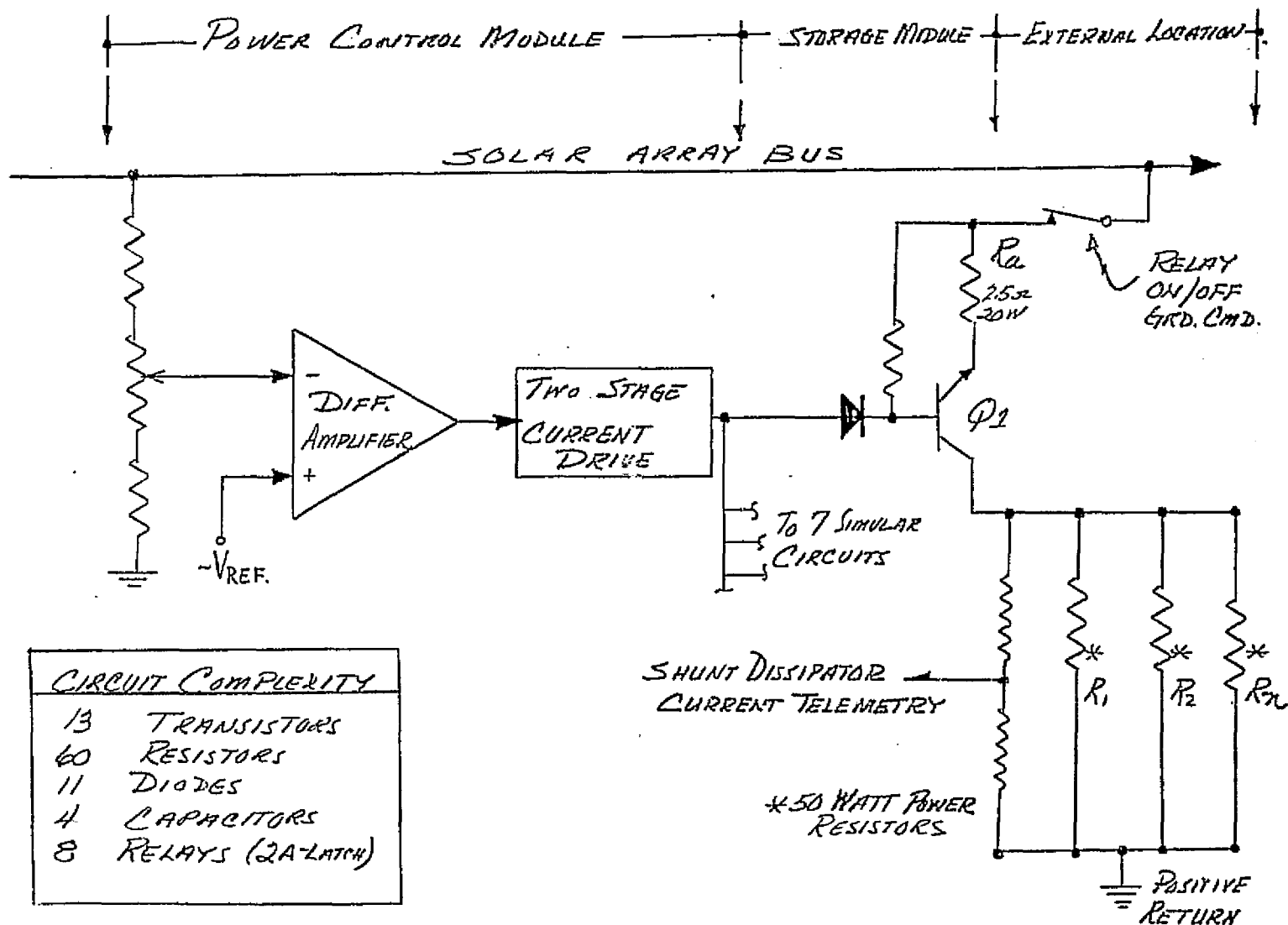


Figure E-19 Simplified Shunt Dissipator Circuit

E-48

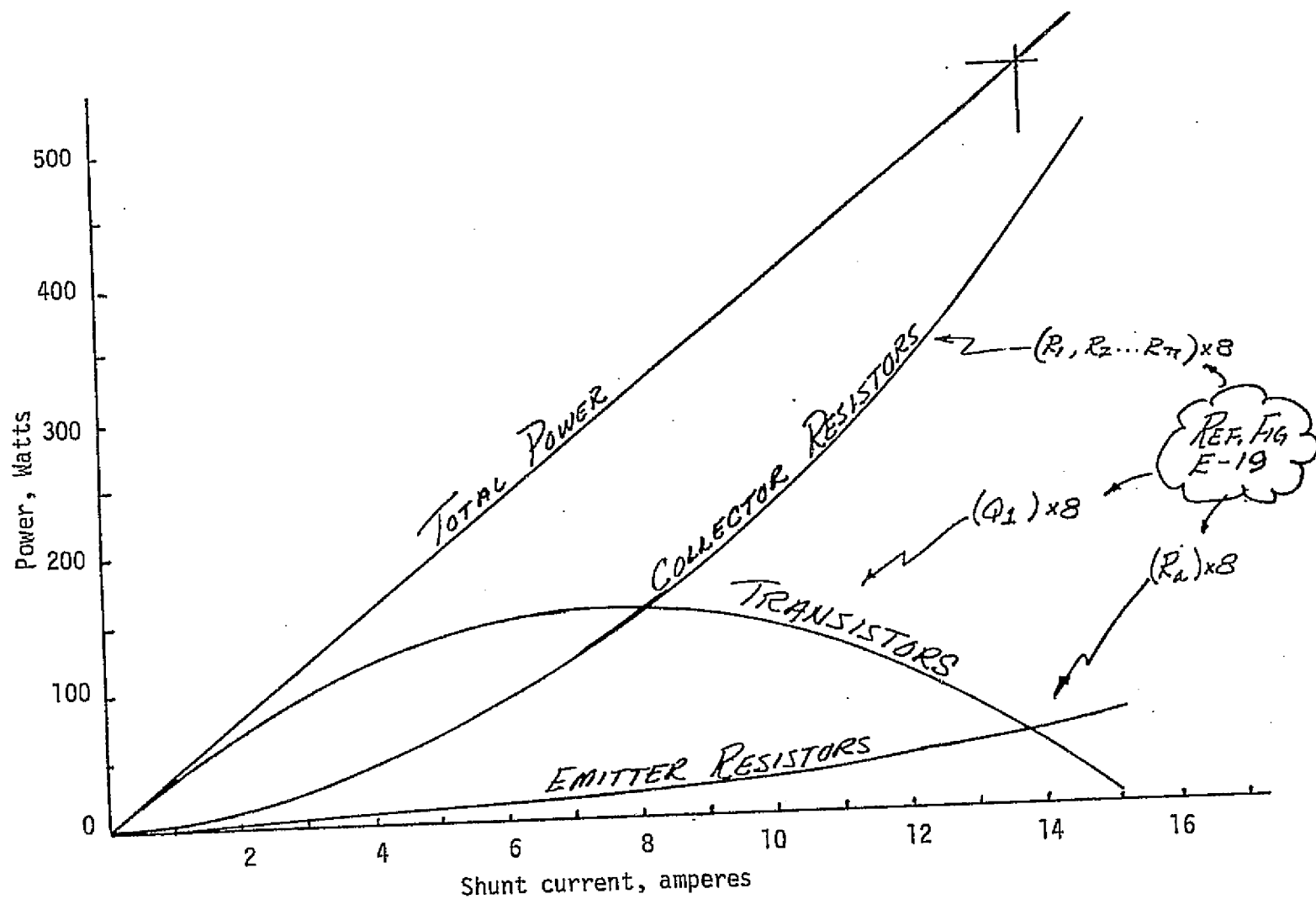


Figure E-20 Power Dissipation of Shunt Limiter

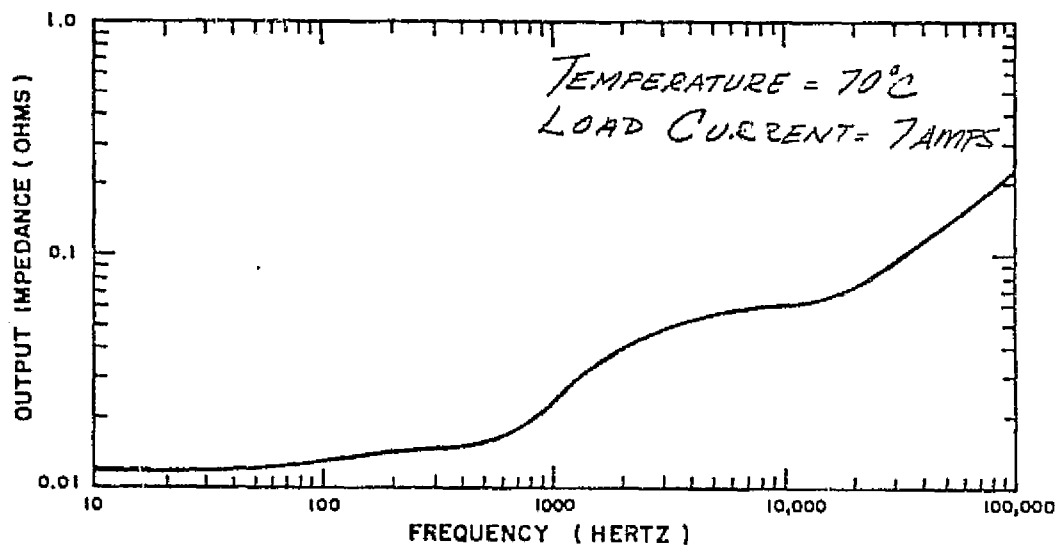


Figure E-21 Shunt Dissipator Dynamic Impedance

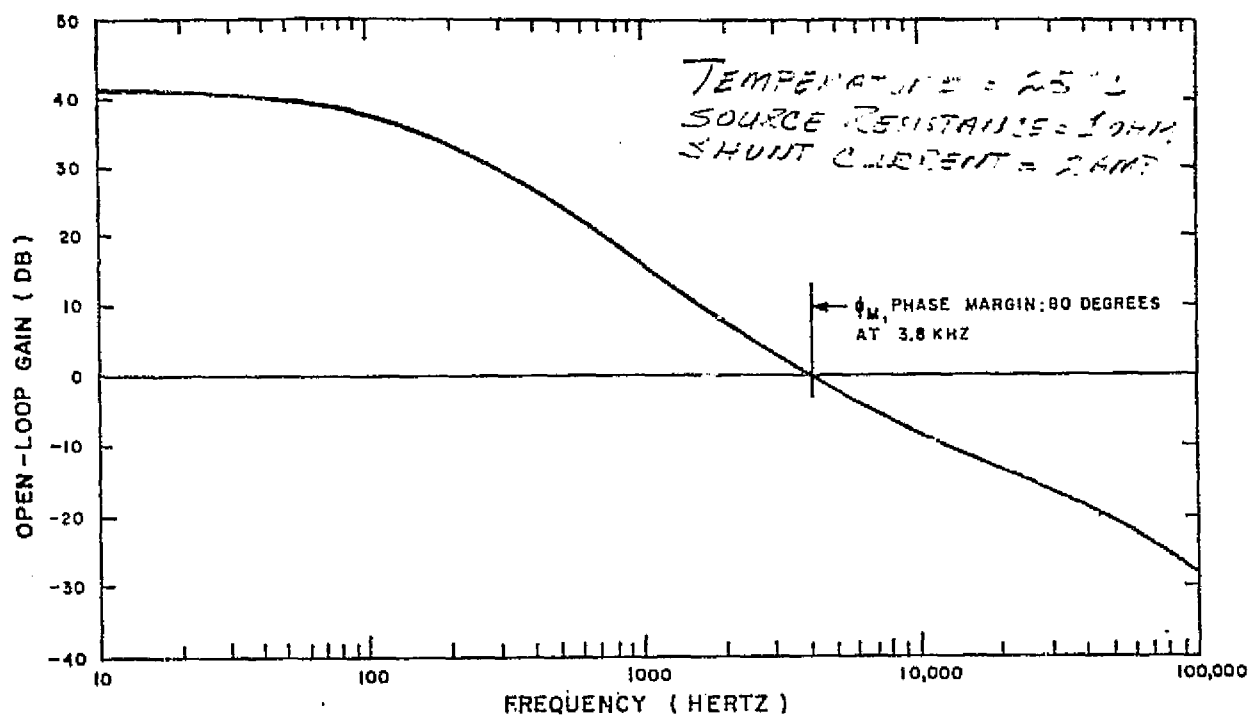


Figure E-22 Shunt Dissipator Loop Stability



Table E-6

## Shunt Dissipator Characteristics

Parameter	Range
Output Voltage	-37.7v to -38.8v <sup>(2)</sup>
Cut-In Regulation	-38±0.3vdc <sup>(2)</sup>
Load Regulation	0.5vdc <sup>(2)</sup>
Temperature Regulation	See note 1
Adjustability/Resolution	±.025vdc <sup>(3)</sup>
Shunt Loss	18 ma <sup>(4)</sup>
Max. Pass Transistor Dissipation @ Base Plate Temp. =55°C	21.7 watts/shunt elem. <sup>(5)</sup>
Load Sharing/Shunt	±20% average <sup>(6)</sup>
Output Impedance	See Figure E-21
Stability Criteria	See Figure E-22

## Notes:

1. All parameters subjected to -10 to +70°C
2.  $I_{Load} = 0.1A$  to 14A
3.  $I_{Load} = 0.1A$ ,  $T = 25^{\circ}C$
4.  $V_{in} = 37vdc$
5.  $I_{Load} = 9A$ ,  $V_{in} = -38.8vdc$
6.  $I_{Load} = 2A$  to 14A

#### 4.7 Auxiliary Regulator

The Auxiliary Regulator provides a separate source of voltage (isolated from the main regulated spacecraft bus) to the main and redundant PWM series regulators for failure detection circuits. Other lower-level system requirements have been defined under the system considerations section.

The Auxiliary Regulator is a simple voltage sensing, linear controlled, dissipative type 25 watt regulator with a regulated voltage ( $23.5 \pm 0.05$  VDC) output.

In operation, as shown in Figure E-23, a change in load voltage, due to fluctuations in either load resistance or input voltage, is applied to one input of the differential amplifier by the voltage dividing network R1/R2. This sampling of the load voltage change appears as an amplifier error-voltage when compared to the stable voltage reference. The error-voltage drives a push-pull type current gain stage to provide sufficient drive to the pass-transistor element; increasing or decreasing its voltage drop and maintaining the regulated output. A phase-lag network has been incorporated into the current drive stage to start the gain roll-off at a low frequency and with a controlled rate of decrease. The output capacitor provides a low output impedance at frequencies beyond the point where the normal regulator impedance increases because of loop-gain reductions.

The loop-gain and phase angle relationships of the Auxiliary Regulator are shown in Figure E-24.

The dynamic impedance is shown in Figure E-25 for a given input voltage and load current with temperature as a parameter.

The major parameters of the Auxiliary Regulator are listed in Table E-7.

E-52

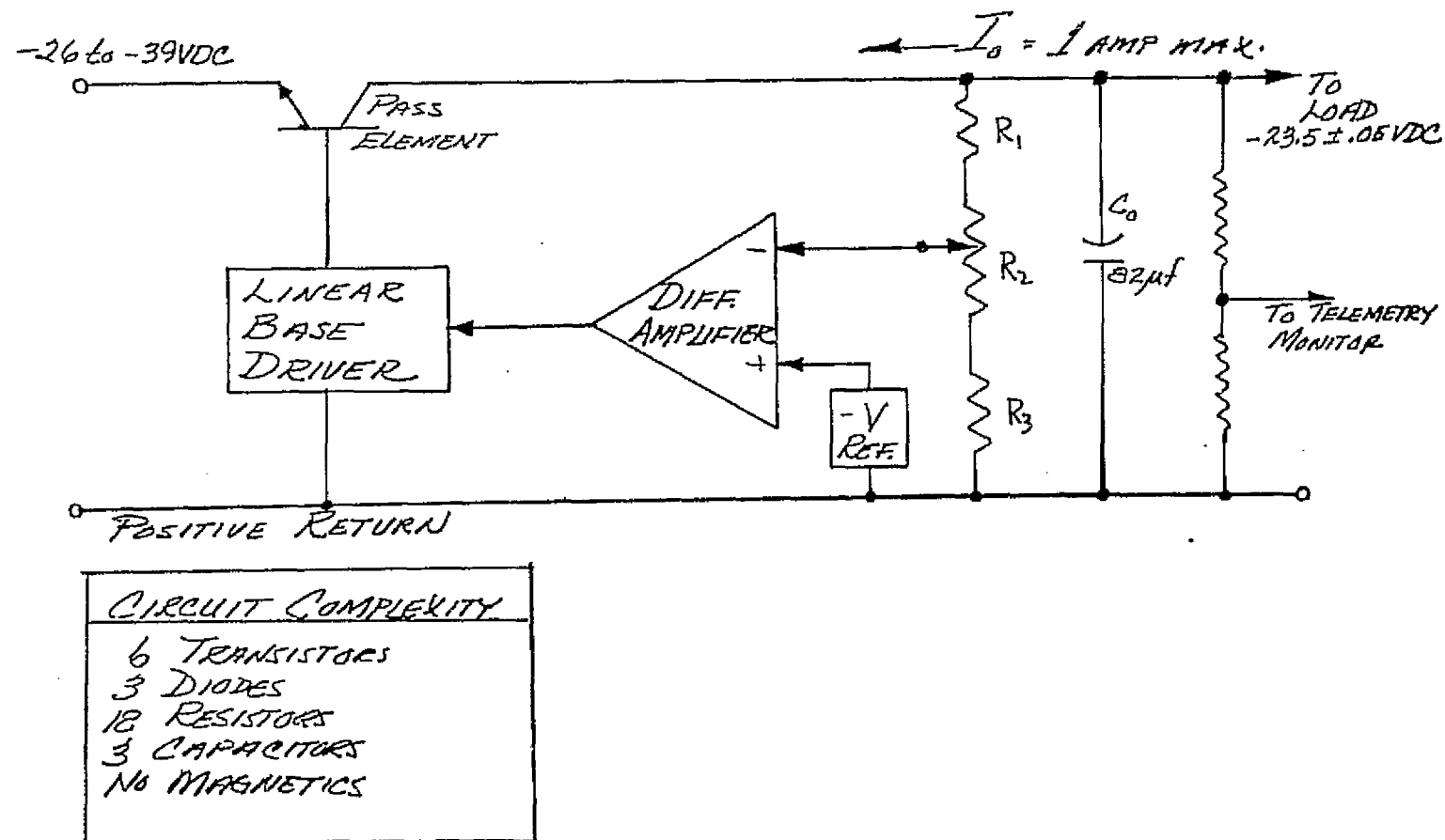


Figure E-23 Simplified Auxiliary Regulator Schematic

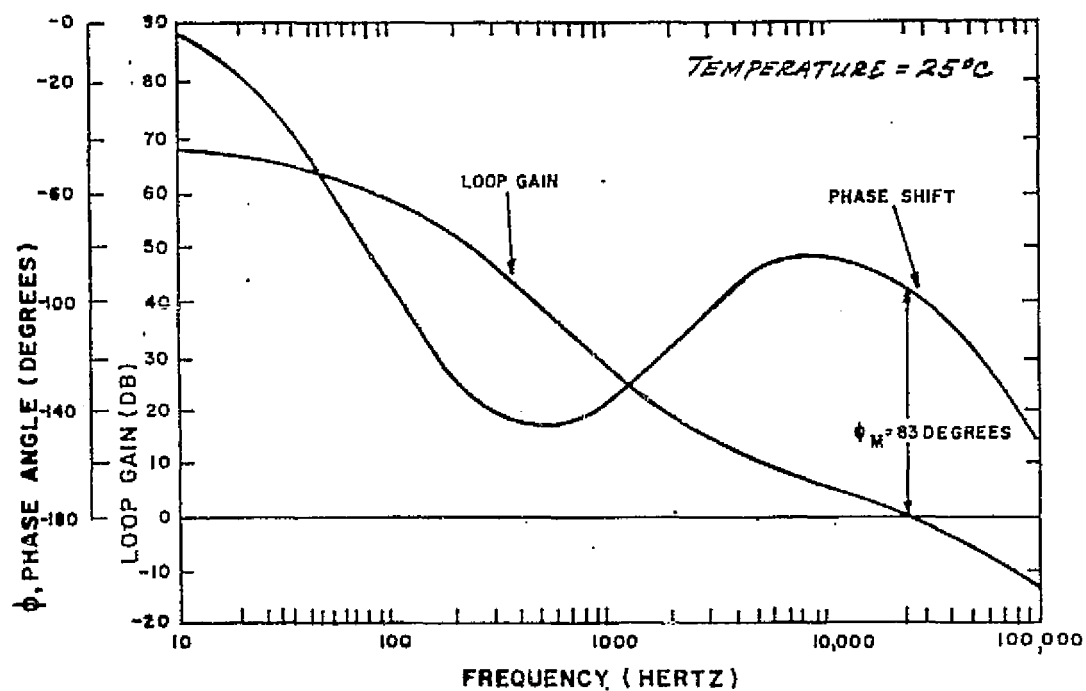


Figure E-24 Auxiliary Regulator Loop Gain and Phase Angle

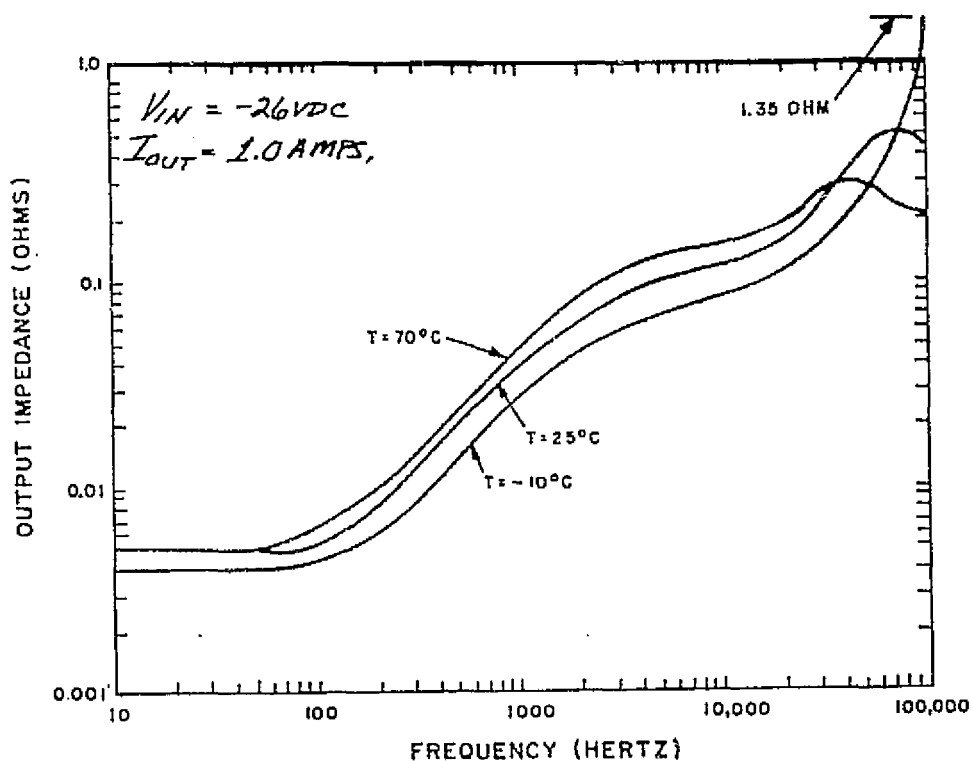


Figure E-25 Auxiliary Regulator Dynamic Impedance

# Auxiliary Regulator Characteristics

PARAMETER <sup>1</sup>	RANGE
Output Voltage	$-23.5 \pm 0.05 \text{ VDC}^2$
Line Regulation	$0.002 \text{ VDC}^3$
Load Regulation	$0.005 \text{ VDC}^4$
Temperature Regulation	$0.05 \text{ VDC}^5$
Adjustability/Resolution	$\pm 0.04 \text{ VDC}^5$
Min./Max. Allowable $V_{IN}$	$-26\text{V to } -39\text{V}^6$
Shunt Loss, No Load and Full Load	26 and 29 milliamperes <sup>7</sup>
Output Impedance	See Figure E-25
Stability Criteria	See Figure E-24

NOTES:

<sup>1</sup>All Parameter subjected to  $-10^{\circ}\text{C}$  to  $+70^{\circ}\text{C}$

<sup>2</sup> $I_{LOAD} = 0$  to 1 amp.,  $V_{IN} = -26\text{V to } -39\text{V}$

<sup>3</sup> $I_{LOAD} = 1$  amp.,  $V_{IN} = -26\text{V to } -39\text{V}$

<sup>4</sup> $I_{LOAD} = 0$  to 1 amp.,  $V_{IN} = -26\text{V}$

<sup>5</sup> $I_{LOAD} = 1$  amp.,  $V_{IN} = -26\text{V}$

<sup>6</sup> $I_{LOAD} = 1$  amp.

<sup>7</sup> $I_{LOAD} = 0$  amp.,  $V_{IN} = -26\text{V}$

#### 4.8 Auxiliary Load Controller and Load Panels

The auxiliary load controller contains the circuitry for switching the auxiliary and shunt loads onto the solar array bus. In addition, this module provides isolation for the various signals monitored and functions controlled by the ground test equipment through the spacecraft umbilical. Telemetry functions derived in this module include auxiliary, shunt and compensation load ON/OFF status and shunt load current monitors.

There are five basic auxiliary loads, each capable of dissipating 20, 50, 50, 140, and 140 watts respectively. The loads can be commanded onto the solar array bus to consume excess array power. In flight operation, the auxiliary loads are generally programmed according to the power management profile, discussion to follow. These loads can act as a fine trim on battery charge control and under power management, will supercede the automatic shunt dissipator control.

The auxiliary load resistors are mounted on a thermally isolated panel, external to the main spacecraft electronics ring. This configuration permits radiation directly to space, reducing additional vehicle thermal balance control.

#### 4.9 Power Switching Module

The power switching module provides the necessary regulated and unregulated power distribution (at command discretion) to the spacecraft subsystem loads. This type of component or module is generally tailored to a specific spacecraft design and will have little bearing on this study; therefore, no additional description is provided.

#### 4.10 Power Subsystem Telemetry Summary

Various subsystem functions are telemetered in order to provide a means of analyzing the performance of the subsystem in meeting the spacecraft power requirements and to provide information in the event of power subsystem or spacecraft failure. These telemetry functions are useful during the spacecraft test phases as well as during orbital flight. In order to provide a more detailed insight into the functional significance of the telemetered parameters, two typical circuits are herein discussed. A summary of the characteristics of the telemetry circuits is shown in Table E-8.

The following quantities of telemetry circuits are provided.

<u>Telemetry Circuit</u>	<u>Number of Circuits in System</u>
Battery Voltage Telemetry	8
Battery Temperature Telemetry	8
Battery Charge Current Telemetry	8
Battery Discharge Current Telemetry	8
Regulated Bus Voltage Telemetry	1
Unregulated Bus Voltage Telemetry	1
Auxiliary Regulator Voltage Telemetry	2
Regulated Bus Current Telemetry	1
Solar Array Current Telemetry	1
PWM Regulator ON-OFF Telemetry	2
Shunt Dissipator Current Telemetry	8
Solar Array Voltage Telemetry	4
Solar Array Temperature Telemetry	2
Solar Panel Position Telemetry (Proposed)	2





#### 4.10.1 Battery Voltage Telemetry

Simple resistor dividers heretofore employed to measure voltages throughout the power supply subsystem are considered inadequate for this application. The inadequacy is brought about by grounding limitations within the spacecraft. Spurious voltage drops in ground returns add to or subtract from the simple divider output resulting in measurement inaccuracy.

The battery voltage telemetry circuit shown in Figure E-26 provides an isolated signal output return which may be connected to the encoder signal ground at any point without interference from power ground currents. Zero suppression has been included for greater telemetry accuracy and better resolution.

This circuit was designed to accommodate a range of from -20 to -40 volts within the specified telemetry range from 0 to -6.4 volts. Circuit operation is as follows: No output appears across resistor R4 until the voltage to be telemetered exceeds the reference voltage of the base (approximately 20 volts). The voltage across resistor R3 establishes an emitter current in transistor Q1B which for large values of current gain equals the collector current. Since the collector current is essentially independent of collector voltage, the output voltage across resistor R4 will be independent of voltages between the power ground and the telemetry encoder grounds. The capacitor across resistor R4 reduces any high frequency noise which might appear in the output. Transistor Q1A is connected in such a manner as to cancel temperature variations in  $V_{BE}$  of transistor Q1B. Circuit operation can be summarized by the calibration curve shown in Figure E-27.

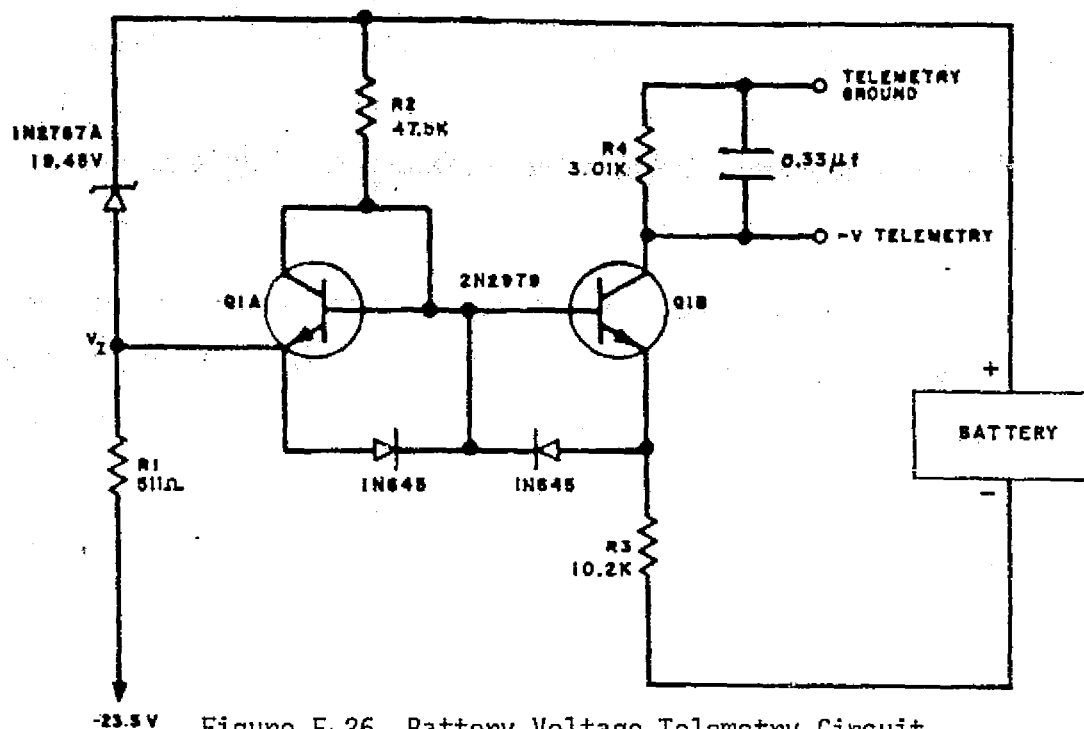


Figure E-26 Battery Voltage Telemetry Circuit

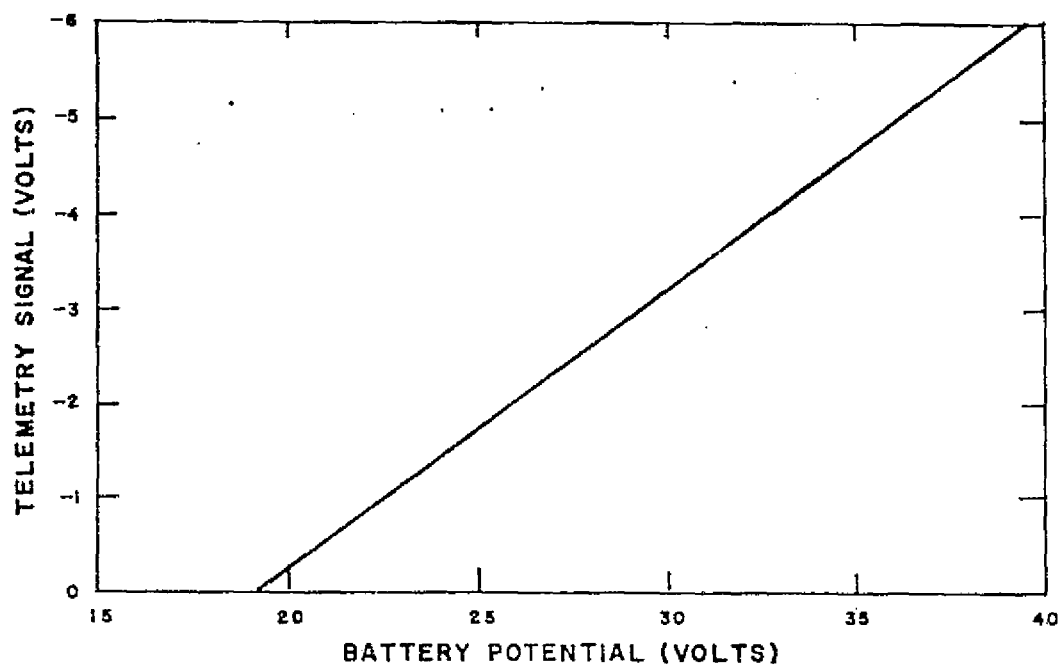


Figure E-27 Typical Voltage Calibration Curve

#### 4.10.2 Regulated Bus and Solar Array Current Telemetry

The regulated bus current and the solar array current requirements are functionally identical. The circuit, shown in Figure E-28, consists of a series-connected saturable reactor (L) transformer coupled to a full wave bridge (CR1, CR2, CR3, CR4) terminated with an accurate wirewound resistor (R2), and a low pass filter (R1, R3, C1). The current telemetry transducers are excited by a 3.5 to 4.0 kilohertz inverter.

The series connected saturable reactor consists of two identical toroidal reactors stacked one on top of the other, and electrically connected in series opposition with respect to a common control winding,  $N_C$ . With a high control circuit impedance as seen from the gate winding  $N_g$ , the reactor acts as a current inverter, whereby the D-C control current,  $I_C$ , is converted to a square wave current whose peak-to-peak value is  $2 (N_C/N_g) I_C$ . This D-C voltage and a small amount of ripple appears across capacitor C1. The two diodes across the output capacitor provide overvoltage protection of the telemetry system. The calibration curve for this type telemetry circuit is shown in Figure E-29.

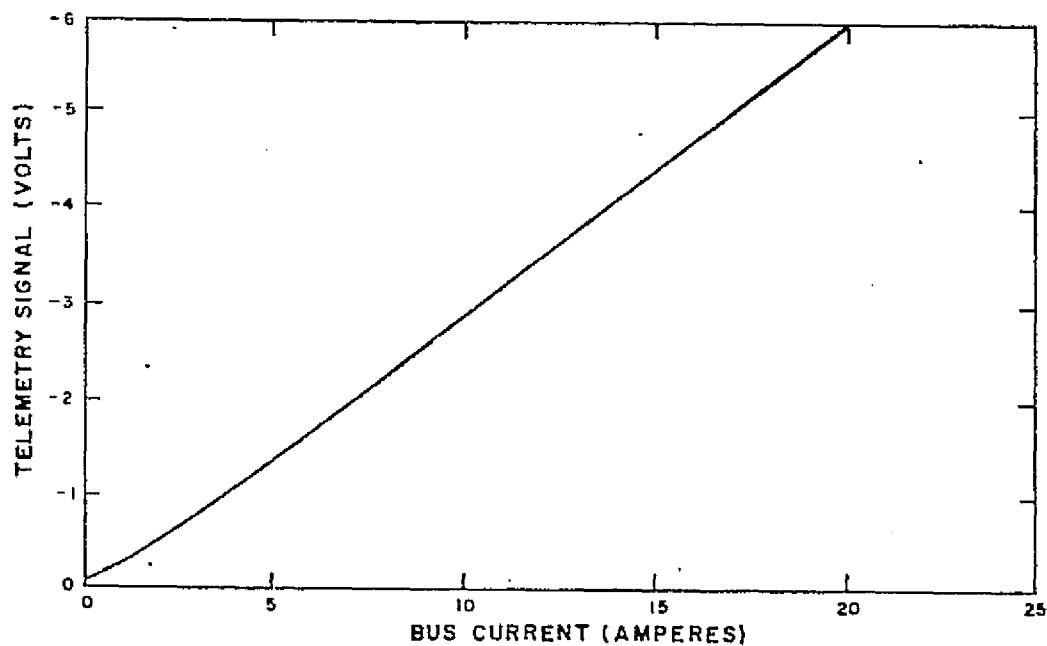
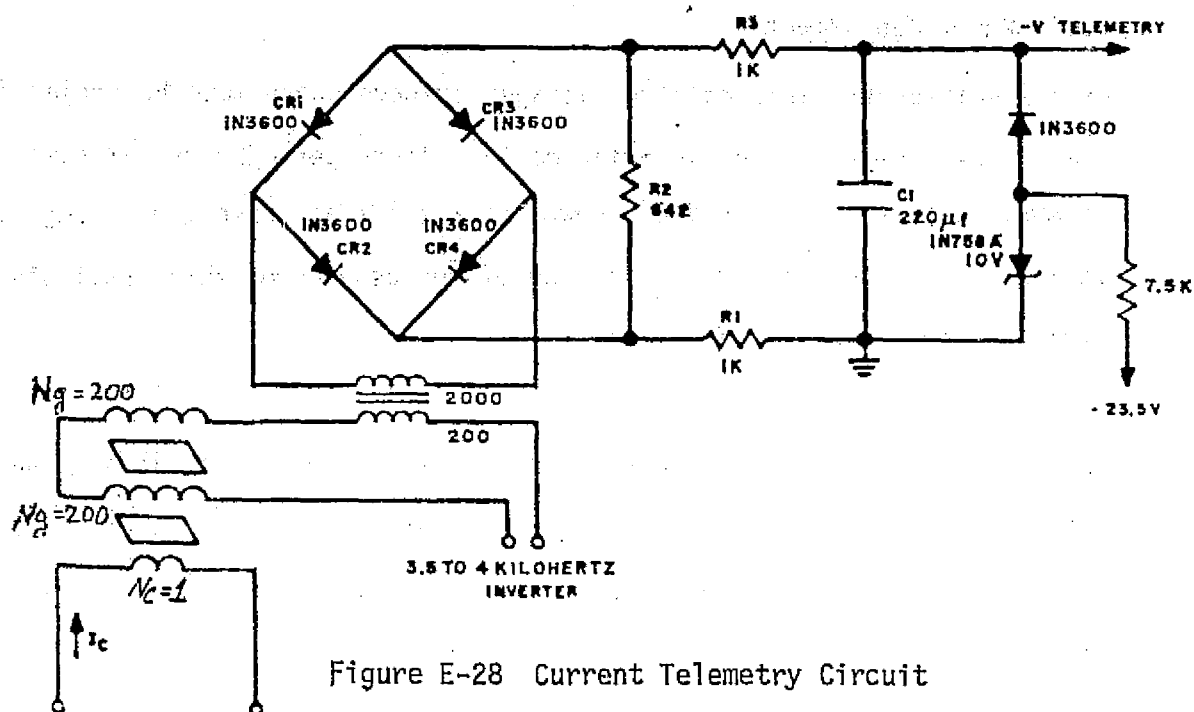


Figure E-29 Typical Current Calibration Curve

#### 4.11 Power Management

With a spacecraft carrying high wattage payloads which must be cycled and a solar array power source receiving daily eclipse periods; proper power management is essential. In fact, power management as performed through ground monitoring and command control can be viewed as another functional block within a power processing system.

The objective of power management for the ERTS-1 spacecraft is to assure that planned load profiles are adequately satisfied by the power system. The major criterion for determining this adequacy is that the batteries be properly recharged on an orbit-to-orbit basis.

Conceptually, as long as load, battery recharge, and power system loss demands are less than the power produced by the solar array, the power system should be fully capable of handling recharge and disposing of any excess power. Because of uncertainties in battery performance, charge control is exercised as an aspect of power management as described below.

The basic strategy is shown in Figure E-30. Essentially, it involves assessing the energy demands associated with planned mission sequences and battery recharge and comparing these demands with the capability of the solar array. Any excess is handled by programming auxiliary loads of sufficient magnitude.

The procedures for performing these steps have been worked out in fairly elaborate detail. Plans for the spacecraft activities are provided daily by mission operations. Each day the mission scheduler, after receiving his

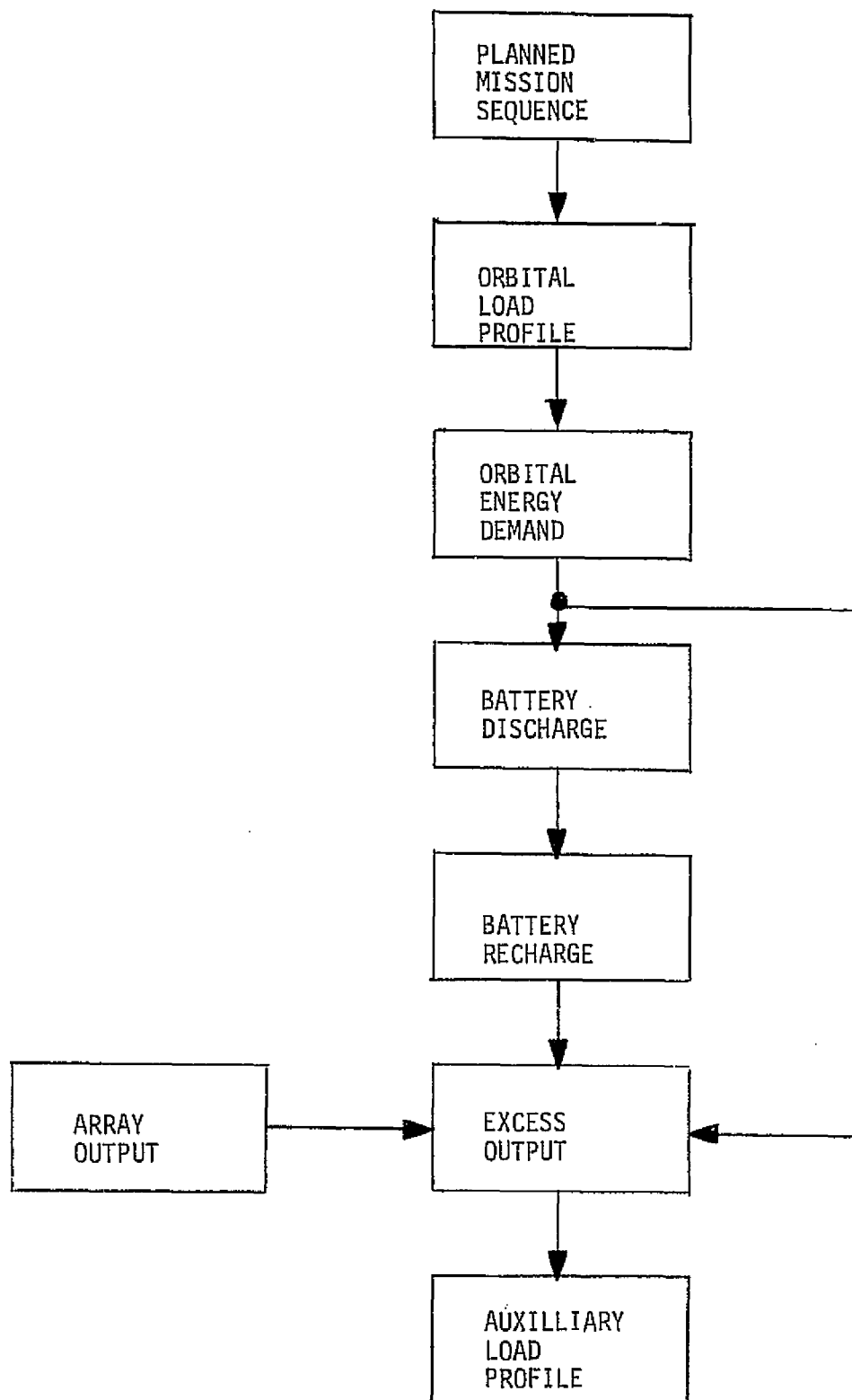


Figure E-30 Power Management Flow Diagram

cloud cover predictions for the orbital tracks to be covered in the next 24 hours, selects his picture making mission based on user requests and priorities. His output results in a spacecraft activity file (SCAT) defining "on" and "off" times of payload operation. They include realtime coverage of imaging payloads and wideband video tape recorder operations of record, re-wind and playback. It also includes scheduling of narrow band tape records and playback (containing full orbit sampled telemetry) and its associated USB down-link. On an orbital basis, this planned sequence of events is converted to a profile of load demands which, in turn, results in an orbital energy demand. With power system losses included, this demand is that reflected at the solar array/battery unregulated bus.

Battery discharge is determined by that portion of the loads occurring during spacecraft night and for certain cases during spacecraft day when the loads exceed the output of the solar array. Thus far on ERTS-1 the discharge during such cases has been negligible.

Battery recharge energy is determined on the basis of the observed ampere-hour charge/discharge (C/D) ratio. The ampere-hour C/D ratio is about 1.15 to 1.2.

The excess output of the solar array is determined by deducting the recharge requirement and the remaining portion of the orbital energy demand from the array output profile. The available solar array energy is determined directly from flight measurements and is updated on a continuous basis.

Auxiliary loads are programmed to absorb the expected excess array output. Thus, on an overall basis, the power management of ERTS-1 responds to a pro-

posed mission sequence by designating the levels and sequence for applying auxiliary loads.

The effect of these designated loads is evaluated on an orbit-to-orbit basis. A proper value of auxiliary load is considered to exist when a C/D ratio of 1.2 is achieved. A range of 1.195 to 1.215 is considered acceptable. Telemetry is monitored for proper end-of-day and end-of-night voltage, maximum battery temperatures and the spread of temperature among all batteries. Appropriate adjustments in the level of auxiliary loads are made as indicated by specific symptoms or trends.



## REFERENCES

## REFERENCES

1. Modeling and Analysis of Power Processing Systems Task 3 Report, Modeling and Analysis Techniques, dated 26 March 1974. Available from the General Electric Company, PO Box 8555, Philadelphia, Pa., 19101, Attention J. H. Hayden.
2. Study of Aircraft Electrical Power Systems, NASA CR-120939, June 1972.
3. Mariner Jupiter/Saturn 1977 Mission Requirements Document, JPL Project Document No. 618-4.
4. Mariner Jupiter/Saturn 1977 Spacecraft Description, Jet Propulsion Laboratory, 12 July 1972.